Forschungszentrum Karlsruhe
in der Helmholtz-Gemeinschaft
Wissenschaftliche Berichte
FZKA 7517

Post irradiation examination of RAF/M steels after fast reactor irradiation up to 33 dpa and <340 °C (ARBOR 1)

RAFM Steels: Metallurgical and Mechanical Characterisation

Final Report for TW2-TTMS-001b, D9

C. Petersen

Institut für Materialforschung II
Programm Kernfusion
Association Forschungszentrum Kalrsruhe/EURATOM

November 2010

Forschungszentrum Karlsruhe

in der Helmholtz-Gemeinschaft

Wissenschaftliche Berichte

FZKA 7517

Fusion 304

Post irradiation examination of RAF/M steels after fast reactor irradiation up to 33 dpa and < 340°C (ARBOR 1)

RAFM Steels: Metallurgical and Mechanical Characterisation

Final Report for
TW2-TTMS-001b, D 9

C. Petersen

Institut für Materialforschung II
Programm Kernfusion
Association Forschungszentrum Karlsruhe / EURATOM

Forschungszentrum Karlsruhe GmbH, Karlsruhe

2010

Für diesen Bericht behalten wir uns alle Rechte vor

Forschungszentrum Karlsruhe GmbH
Postfach 3640, 76021 Karlsruhe

Mitglied der Hermann von Helmholtz-Gemeinschaft
Deutscher Forschungszentren (HGF)

ISSN 0947-8620

urn:nbn:de:0005-075178

The results obtained within the studies performed under this task did not yield any specific innovation or intellectual property.

This work, supported by the European Communities under the contract of Association between EURATOM and Forschungszentrum Karlsruhe, was carried out within the framework of the European Fusion Development Agreement. The views and opinions expressed herein do not necessarily reflect those of the European Commission.

Abstract

In an energy generating fusion reactor structural materials will be exposed to very high dpa-levels of about 100 dpa. Due to this fact and because fast reactor irradiation facilities in Europe are not available anymore, a reactor irradiation at the State Scientific Center of the Russian Federation with its Research Institute of Atomic Reactors (SSC RIAR), Dimitrovgrad, had been performed in the fast reactor BOR 60 with an instrumented test rig. This test rig contained tensile, impact and Low Cycle Fatigue type specimens used at FZK since many years. Samples of actual Reduced Activation Ferritic/Martensitic (RAF/M) -steels (e.g. EUROFER 97) had been irradiated in this reactor at a lower temperature (< 340°C) up to a damage of 33 dpa. This irradiation campaign was called ARBOR 1.

Starting in 2003 one half of these irradiated samples were post irradiation examined (PIE) by tensile testing, low cycle fatigue testing and impact testing under the ISTC Partner Contract #2781p in the hot cells of SSC RIAR.

In the post irradiation instrumented impact tests a significant increase in the Ductile to Brittle Transition Temperature as an effect of irradiation has been detected. During tensile testing the strength values are increasing and the strain values reduced due to substantial irradiation hardening. The hardening rate is decreasing with increasing damage level, but it does not show saturation.

The low cycle fatigue behaviour of all examined RAF/M - steels show at total strain amplitudes below 1 % an increase of number of cycles to failure, due to irradiation hardening.

From these post irradiation experiments, like tensile, low cycle fatigue and impact tests, radiation induced design data, e.g. for verification of design codes, can be generated.

Nachbestrahlungsuntersuchung von RAF/M Stählen aus der Bestrahlung in einem Schnellen Reaktor bis zu 33 dpa und < 340°C, (ARBOR 1)

Zusammenfassung

In einem energieerzeugenden Fusionsreaktor werden Strukturmaterialien sehr hohen Bestrahlungen ausgesetzt, die bis zu 100 dpa betragen können. Deswegen und weil Bestrahlungseinrichtungen mit schnellen Neutronen in Europa derzeit nicht zur Verfügung stehen, wurde eine Reaktorbestrahlung am State Scientific Center der Russischen Föderation mit seinem Research Institute of Atomic Reactors (SSC RIAR), Dimitrovgrad, in deren schnellen Reaktor BOR 60 in einer instrumentierten Bestrahlungskapsel durchgeführt. Diese Bestrahlungskapsel enthielt Zug-, Kerbschlag- und Ermüdungsproben in Abmessungen wie sie schon seit Jahren im FZK gebräuchlich sind. Proben aus niedrig aktivierbaren (engl. Reduced Activation Ferritic/Martensitic (RAF/M)) - Stählen (z.B. EUROFER 97) waren in diesem Reaktor bei niedrigerer Temperatur (< 340°C) bis zu einer Strahlenschädigung von 33 dpa bestrahlt worden. Diese Bestrahlungskampagne wurde mit ARBOR 1 bezeichnet.

Beginnend im Jahr 2003 wurden an einer Hälfte der bestrahlten Proben Nachbestrahlungsversuche (engl. post irradiation examinations (PIE)) in Form von Zug-, Kerbschlag- und Ermüdungsversuchen unter dem ISTC Partner Contract #2781p in den Heißen Zellen von SSC RIAR durchgeführt.

Bei den Nachbestrahlungsversuchen wurde in instrumentierten Kerbschlagversuchen eine starke Zunahme der Übergangstemperatur vom duktilen zum spröden Zustand als Auswirkung der Bestrahlung festgestellt. Bei den Zugversuchsergebnissen bestrahlter Proben wurde eine Erhöhung der Festigkeitswerte bei gleichzeitiger Abnahme der Dehnungswerte durch die Strahlenverfestigung beobachtet. Dieser Festigkeitsanstieg nimmt mit zunehmender Strahlenschädigung ab, erreicht aber noch keine Sättigung.

Im Ermüdungsverhalten zeigten alle geprüften RAF/M – Stähle bei Gesamtdehnungsamplituden unterhalb 1 % wegen der Strahlenverfestigung eine Zunahme der Versagenszyklenzahlen.

Von diesen Nachbestrahlungsversuchen in Form von Zug-, Kerbschlag- und Ermüdungsversuchen können Datensätze mit Strahlenschädigung erzeugt werden, die zur Verifizierung von Design Codes verwendet werden können.

TABLE OF CONTENTS

LIST OF TABLES

LIST OF FIGURES

1 Introduction

In an energy generating fusion reactor, structural materials will be exposed to very high levels of irradiation damage of about 100 dpa. A simulation facility - like IFMIF - is not available in the nearer future, to study the materials behaviour under fusion relevant irradiation conditions, e.g. specific He/dpa-ratio. Therefore these irradiation damage conditions can be realised in fast reactors only. Due to the fact that fast reactor irradiation facilities in Europe are not available anymore, a cooperation between Forschungszentrum Karlsruhe (FZK) and State Scientific Centre of Russian Federation Research Institute of Atomic Reactors (SSC RF RIAR) had been implemented. The irradiation project "Associated Reactor Irradiation in BOR 60" is named "ARBOR" (Latin for tree).

The problem of irradiation-induced embrittlement of possible martensitic alloy candidates still is unsolved. Following the evaluation of precursor irradiation programmes, however, a clear tendency is recognisable [1] [2] [3] [4] [5] [6].

The ARBOR 1 irradiation programme mainly concentrates on the reduced activation ferritic/martensitic (RAF/M) alloy EUROFER 97, a result of FZK's development from OPTIFER I to OPTIFER VII. It will be investigated in different variations. Regarding the EUROFER 97 steel, an embrittlement behaviour comparable to that of the best alloys investigated in former irradiation programmes is expected, keeping its good mechanical properties. The higher irradiation dose of 33 dpa is a step towards fusion-relevant doses.

The preparation of the project started in 1999, the irradiation on 25. November 2000, the target dose of 30 dpa had been reached on 15. October 2002. The ARBOR 1 project includes 150 mini-tensile/low cycle fatigue specimens and 150 mini-impact (KLST) specimens of 9 different RAF/M steels. Specimens irradiation had been performed in an especially designed irradiation rig of BOR 60, in a fast neutron flux (> 0.1 MeV) of 1,8 10^{15} n/cm²s and with direct sodium cooling at a temperature less than 340°C. For more details the reader is referred to .[7].

2 Irradiation conditions

2.1 BOR 60

In December 1969 the BOR 60, Fig. 2-1, experimental fast reactor started operation. Initially designed for solving physical and technical problems of fast power reactors with sodium coolant, it is nowadays also widely used as irradiation facility for material science purposes. With a reactor core dimension of 450 mm height and 550 mm in equivalent diameter, different irradiation positions are available. The cell D-23 has been selected for the first campaign, because in this position a direct temperature measurement by thermocouple during irradiation is possible.

Fig. 2-1 Reactor building of BOR 60.

2.2 Irradiation assembly

The design of the ARBOR 1 irradiation device is shown in Fig. 2-2 (outer hexagon size, 45 mm, and specimen capsule diameter, 39 mm) and was based on a previously used design with heat insulation against the surrounding fuel assemblies to provide relatively low irradiation temperatures. The irradiation device is heated by the coolant from the reactor high-pressure chamber, which allows a sufficiently large coolant flow rate (of the order of 7 m^3/ h) and a relatively low gamma heating rate of approximately 5 watts/gm (i.e. an increase of about 10-15^{o}C over the length of the capsule).

Each capsule has a height of 30 mm and contains either 30 LCF-, tensile-specimens or 30 impact specimens. Therefore 300 specimens, 150 LCF-, tensile-specimens and 150 impact specimens are irradiated.

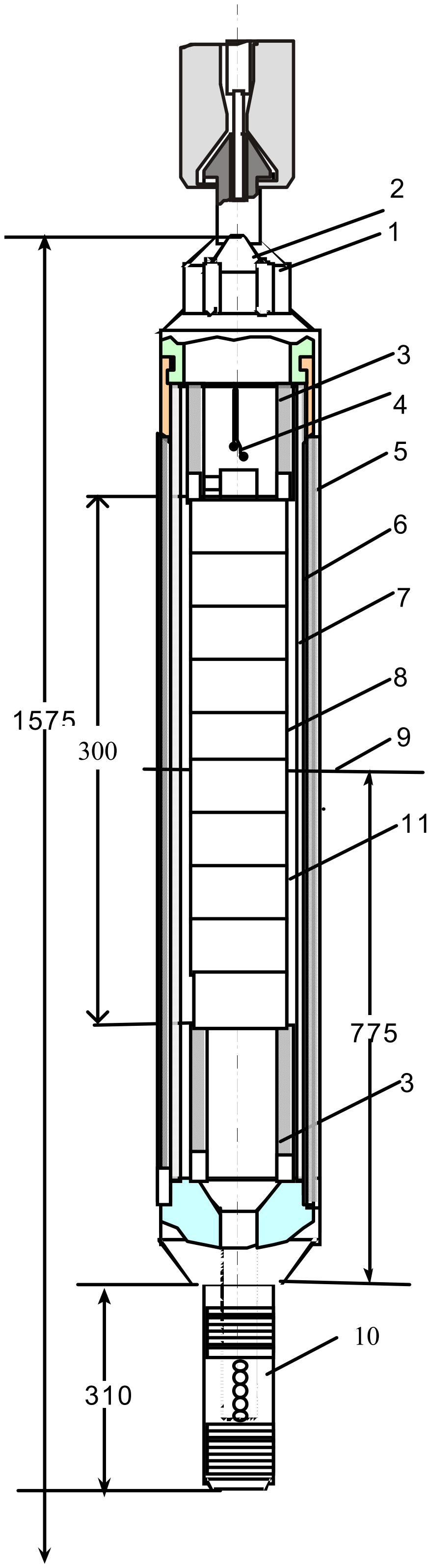

1- thermometric probe;
2- detachable head;
3- spacer tubes;
4- probe thermocouples;
5- wrapper;
6- gas gap;
7- internal tube;
8- ampoule assembly;
9- core center;
10- tail;
11- annular gap

Fig. 2-2 Dismountable assembly with a thermocouple. (Detail: Capsule 6 from above, filled with KLST mini impact specimens)

2.3 Dosimetry

The irradiation rig is instrumented with neutron monitors, as indicated in Fig. 2-3 schematically, they are arranged in the central tube and on three of ten levels of specimen positions as well as with three temperature detectors also on three of ten levels.

During special reactor spectrometry experiments a large number of different material foils (about 50) were irradiated, their activity was measured and the spectrum was unfolded by using MIXER computer code [8].

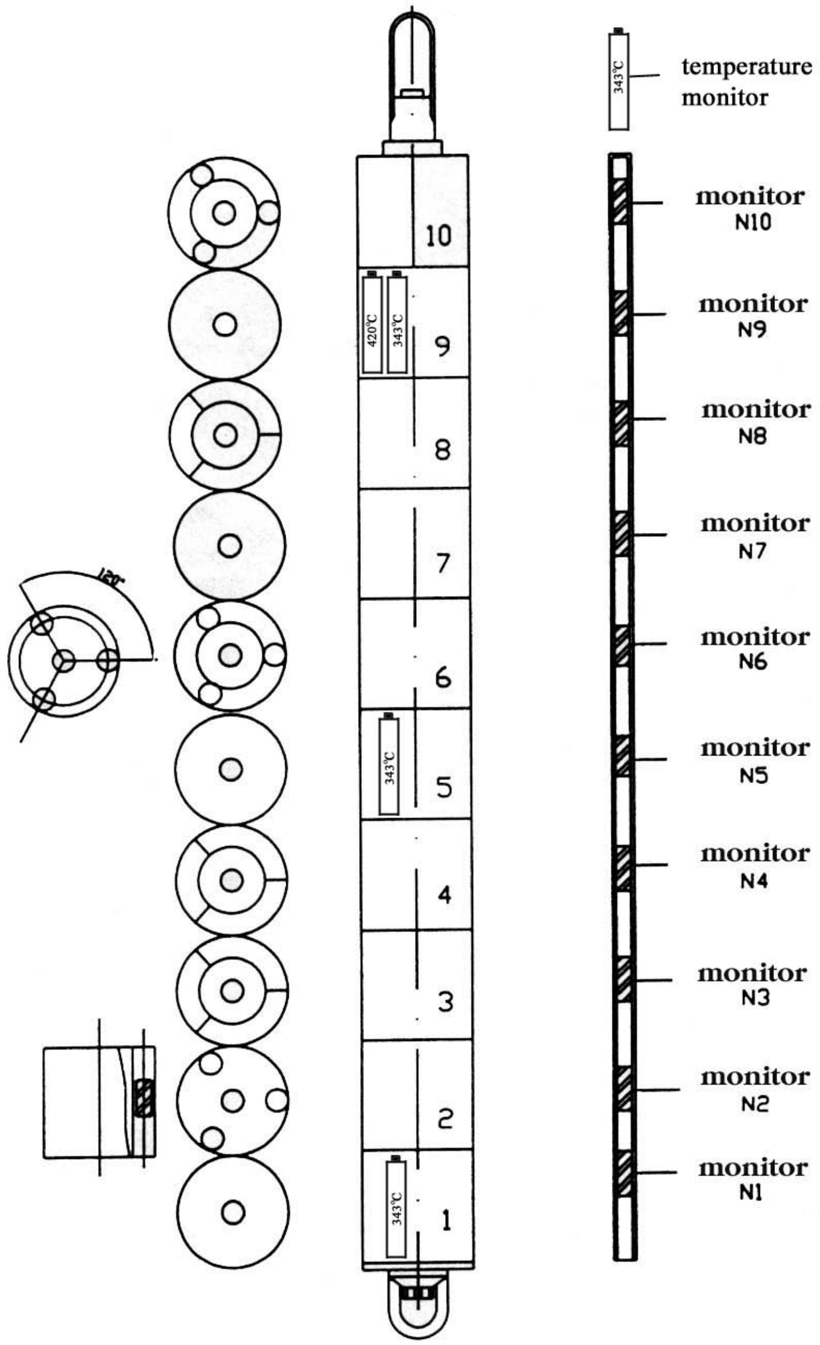

Fig. 2-3 Scheme of the neutron and temperature monitors location in the suspensor.

The calculation of the damage dose values for ferritic steel specimens was conducted using SPECTER code [9]. In this case a neutron energy spectrum in cell D-23 was used that had been measured in the previously performed dosimetry experiments and normalised for measured neutron fluence values with energies higher than 3, 4.6 and 7 MeV.

Metal foils with 0.1 mm thickness were used for the neutron monitor production. They were cut into discs having 1.0 mm diameter. All detectors were washed in a weak solution of nitric acid, in alcohol and then they were weighed with a "Sartorius" balance. The monitor sets were placed into labelled quartz ampoules having 3 mm diameter and 13 mm height. After irradiation the absolute measurement of γ-ray activity was performed.

Tab. 2-1 Calculation results of damage dose during material science experiment for steel EUROFER 97

Level	Distance from the core central plane, mm	Damage dose, dpa			
		Normalization for fluence above 3 MeV	Normalization for fluence above 4.6 MeV	Normalization for fluence above 7 MeV	Average value
1	-113	3.37	3.75	3.37	3.50
2	-89	3.59	3.99	3.66	3.74
3	-59	3.70	4.08	3.77	3.85
4	-29	3.81	4.06	3.74	3.87
5	1	3.74	3.92	3.99	3.88
6	31	3.69	3.96	3.85	3.83
7	61	3.65	3.76	3.74	3.72
8	91	3.32	3.48	3.40	3.40
9	121	3.09	3.36	3.15	3.20
10	151	2.77	2.94	2.95	2.89

During material science experiments only few different material foils (usually natural iron, niobium and titanium as well as of enriched copper: ^{63}Cu – 99.6 %,) are irradiated and measured. Damage dose calculation results for steel EUROFER 97 are given in Table 2-1, where these three normalisations and also average damage dose values for normalizations were listed.

In Fig. 2-4, the average damage dose is plotted versus core level. The damage dose values of other types of ferritic steels under irradiation differ from those given in Table 2-1 less than 0.5% [8]. Sure, there is a difference in the uncertainty estimations of each dosimetry result. But nevertheless the used simple averaging method is sufficient to estimate the damage dose. It was done because both the dosimetry results and the uncertainty estimations for different neutron energy ranges are close enough together. Using the most accurate weights for averaging one could obtain a different value of 1-3%, but it is not better then the result of simple averaging.

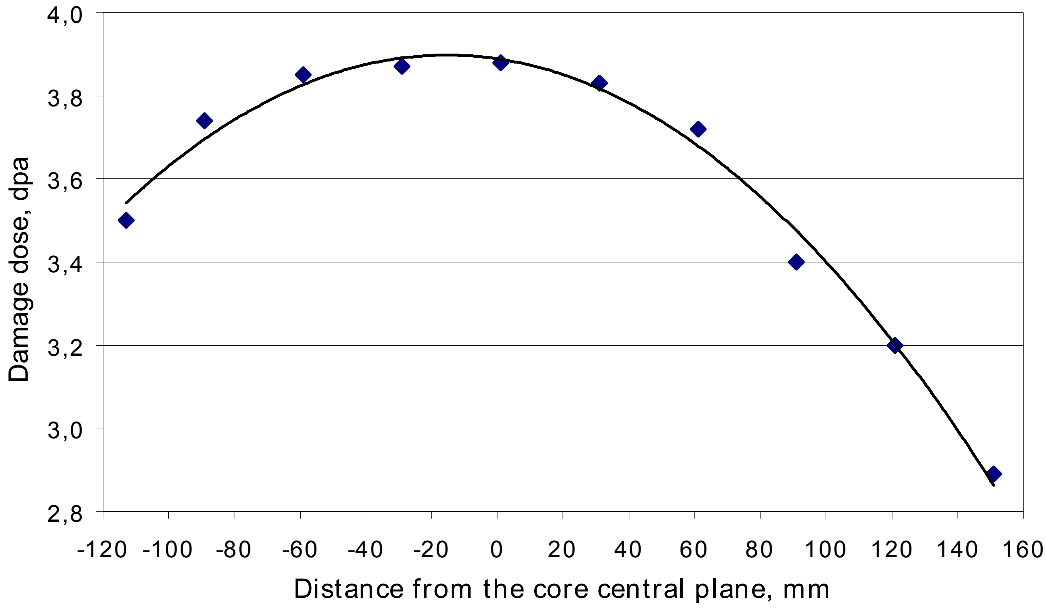

Fig. 2-4 The damage dose distribution during material science experiment for steel EUROFER 97 along the core plane.

Tab. 2-2 Irradiation conditions during the ARBOR 1 irradiation (capsules 1, 3, 4, 7 and 10 for PIE 1 are shaded and indicated by bold letters)

Capsule Nr.	**1**	**2**	**3**	**4**	**5**
Capsule	**1. LCF**	**1. Tensile**	**1. Impact**	**2. Impact**	**2. LCF**
position from center [mm]	**-150 to -120**	-120 to -90	**-90 to -60**	**-60 to -30**	-30 to 0
mean position [mm]	**-135**	-105	**-75**	**-45**	-15
amount of specimen	**30**	30	**30**	**30**	30
calculated mean damage [dpa]	**24,50**	26,00	**27,60**	**29,10**	29,90
measured central values [dpa]	**31**	31,7	**31,8**	**32,3**	32,1
mean temperature [°C]	**331,00**	331,50	**332,30**	**333,20**	334,00

Capsule Nr.	**6**	**7**	**8**	**9**	**10**
Capsule	**3. Impact**	**2. Tensile**	**4. Impact**	**3. LCF**	**5. Impact**
position from center [mm]	0 to +30	**+30 to +60**	+60 to +90	+90 to +120	**+120 to +150**
mean position [mm]	15	**45**	75	105	**135**
amount of specimen	30	**30**	30	30	**30**
calculated mean damage [dpa]	30,00	**29,80**	28,70	26,70	**23,10**
measured central values [dpa]	30,7	**30,2**	27,6	25,7	**22,4**
mean temperature [°C]	334,90	**335,80**	336,80	337,50	**338,40**

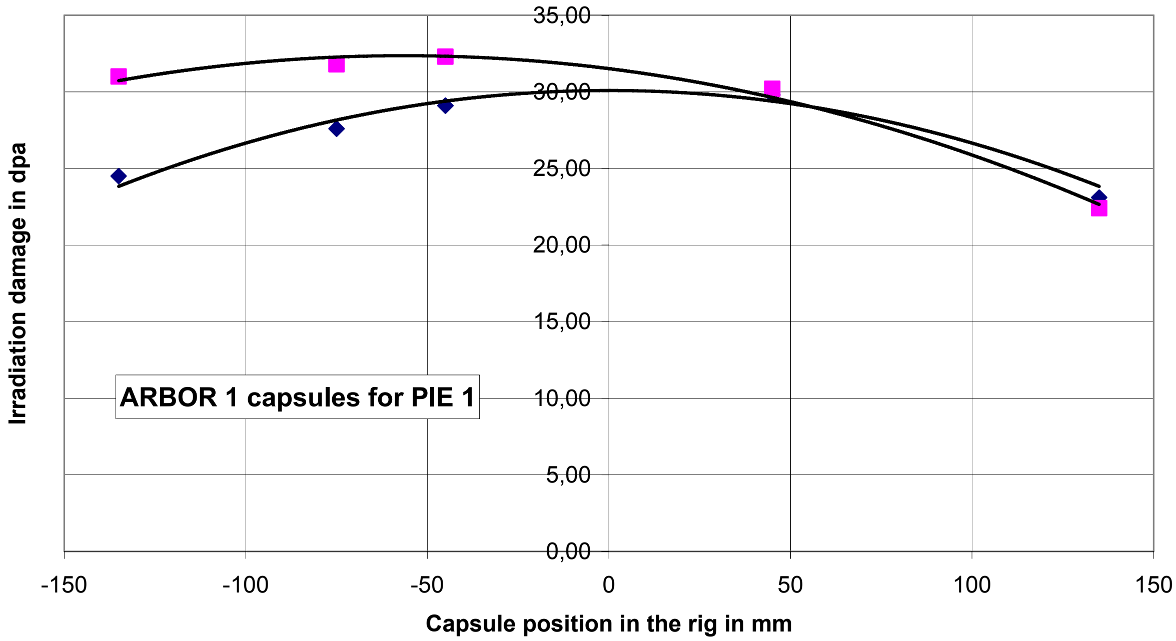

Fig. 2-5 Calculated damage dose distribution of capsules 1, 3, 4, 7 and 10 during the ARBOR 1 irradiation for EUROFER 97 along the core plane (the magenta squares are the measured values from central neutron detectors).

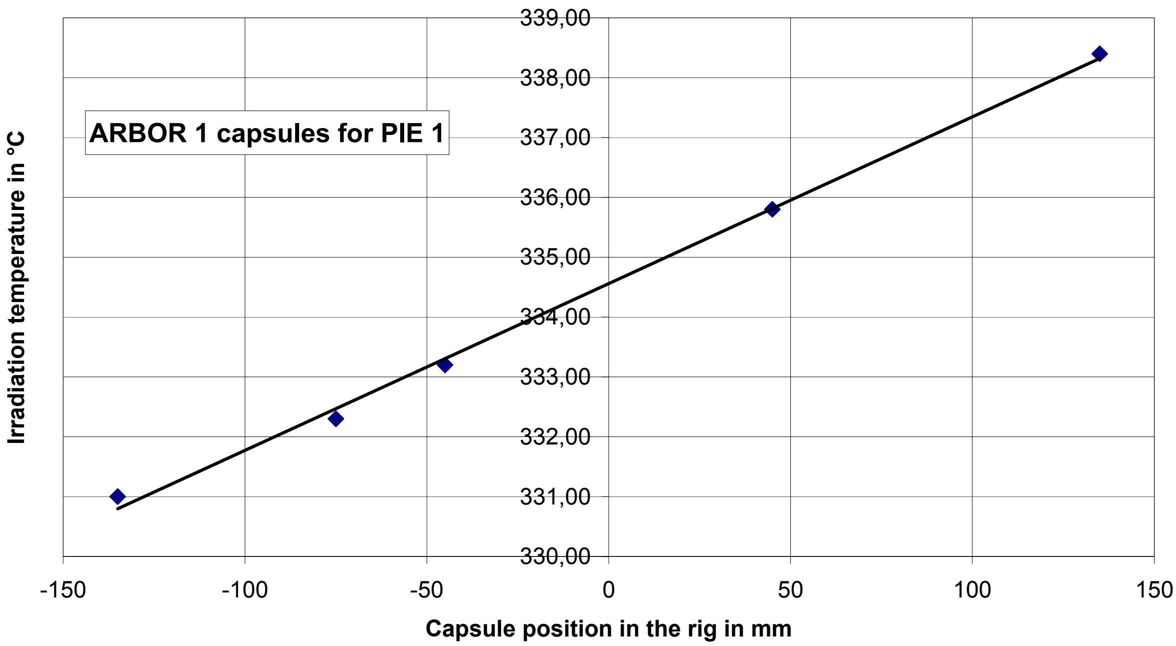

Fig. 2-6 Calculated temperature distribution of capsules 1, 3, 4, 7 and 10 during the ARBOR 1 irradiation for EUROFER 97 along the core plane

The damage dose distribution from Fig. 2-5 shows the higher values for the calculated distribution and the real distribution from the measured values of the central neutron detectors together with the averaged values of the three outer neutron detectors from capsules 2, 6 and 10. These values had been used as the damage dose of the irradiated specimens.

The temperature distributions from Fig. 2-6 are calculated values. But in no case the temperature melting detectors of the lowest temperature of 343°C situated in the top of the central tube and in the outer positions of capsules 1, 5 and 9 had been indicated any reaction.

2.4 Irradiated materials

Small size cylindrical specimen for tensile and low cycle fatigue testing and the KLST specimen for impact testing were utilised to investigate the mechanical properties after irradiation of the materials shown in Table 2-2 together with their heat denomination and chemical composition. The ARBOR 1 irradiation rig contains 150 mini-tensile/low cycle fatigue specimens and 150 mini-impact (KLST) specimens of the 9 different RAFM steels.

The European RAF/M heat EUROFER 97 is included in two annealing conditions. EUROF 1: EUROFER 97 (as received: 980°C 31 min/air cooled + 760°C 90 min/ air cooled), EUROF 2: EUROFER 97 (1040°C 31 min/ air cooled + 760°C 90 min/ air cooled). Whereas EUROF 1 is optimised for good fatigue resistance and EUROF 2 for good impact ductile to brittle behaviour. The Japanese RAF/M steel F82H mod. is implemented as international reference steel: F82H mod. (as received: 1040°C 38 min/ air cooled + 750°C 2h/ air cooled). The German development OPTIFER IVc, OPT IVc: (950°C 30 min/ air cooled + 750°C 2h/ air cooled), is included as reference material to be compared to data from the HFR-irradiations. The following three materials ADS 2, ADS 3 and ADS 4, based on EUROFER 97, are experimental heats to study the He influence on RAF/M-steels. ADS 2 is an EUROFER 97-steel with 82 wppm nat. B (1040°C 31 min/ air cooled + 760°C 90 min/ air cooled), ADS 3 an EUROFER 97-steel with 83 wppm B10 (1040°C 31 min/ air cooled + 760°C 90 min/ air cooled) and ADS 4 an EUROFER 97-steel with 1160 wppm B10 (1040°C 31 min/ air cooled + 760°C 90 min/ air cooled).

A real feature of this ARBOR 1 irradiation was the implementation of specimens of mechanically alloyed EUROFER 97 with 0,5% Y_2O_3 as the recent development of higher heat resistant RAF/M-steels. The specimen denomination is EURODShip: as received: 980°C 31 min/ air cooled + 760°C 90 min/ air cooled.

The NRG, Petten, contribution covers technological questions with a British Steel batch of EUROFER 97, called BS-EUROF: as received (1050°C 60 min/ air cooled + 760°C 120 min/ air cooled), as reference material for electron beam welded EUROFER 97, called EUROF-EB: as received (980°C 31 min/ air cooled + 760°C 90 min/ air cooled), then EB welded with a post weld heat treatment at 730°C 120 min/ air cooled

Tab. 2-3 Chemical composition of irradiated materials

Material	**Heat**	**C**	**Si**	**Mn**	**P**	**S**	**Cr**	**Mo**	**Ni**	**Al**	**B**	**Cu**	**N**	**Nb**	**Ti**	**V**	**W**	**Ta**
EUROF 1	E83697	0,12	0,06	0,47	<0,005	0,004	8,93	0,0015	0,022	0,008	<0,001	0,0036	0,018	0,0022	0,009	0,2	1,07	0,14
EUROF 2	E83697	0,12	0,06	0,47	<0,005	0,004	8,93	0,0015	0,022	0,008	<0,001	0,0036	0,018	0,0022	0,009	0,2	1,07	0,14
F82H mod.	9753	0,09	0,08	0,1	0,003	0,001	7,89	0,003	0,02	0,001	0,0002	0,01	0,006	0,0002	0,004	0,19	1,99	0,02
OPT IVc	986779	0,12	0,022	0,54	0,004	0,003	9,35	<0,002	0,0073	<0,0005	<0,004	0,0019	0,05	<0,0006	<0,0004	0,26	1,03	0,07
ADS 2 = EUROF 1 + 82 wppm B	806	0,109	0,02	0,602	0,0035	0,003	9,31	0,002	0,005	0,001	0,0082	0,005	0,021	0,005	0,001	0,19	1,27	0,055
ADS 3 = EUROF 1 + 83 wppm B	826	0,095	0,031	0,395	0,0024	0,003	8,8	0,046	0,008	0,004	0,0083	0,006	0,028	0,005	0,001	0,193	1,125	0,088
ADS 4 = EUROF 1 + 1160 wppm B	825	0,1	0,03	0,38	0,001	0,0025	9,0	0,028	0,006	0,004	0,112	0,005	0,0255	0,002	0,001	0,197	1,06	0,08
EURODShip = EUROF 1 + 0,5% Y_2O_3	HXN 958/3	0,11	0,08	0,37	0,007	0,004	8,94	0,007	0,03	0,01	<0,001	0,018	0,027	0,001	0,006	0,19	1,07	0,87
BS-EUROF	VS3102	0,094	0,05	0,42	<0,005	0,005	9,03	<0,02	<0,02	0,009	<0,001	<0,02	0,027	<0,02	<0,02	0,19	1,14	0,08
EUROF-EB = EUROF 1 EB welded	E83697	0,12	0,06	0,47	<0,005	0,004	8,93	0,0015	0,022	0,008	<0,001	0,0036	0,018	0,0022	0,009	0,2	1,07	0,14

2.5 Specimens

Based on the knowledge gained from earlier fatigue experiments a tensile/low cycle fatigue specimen geometry (Fig. 2-7) has been developed and optimised by finite element calculations using different material models. Special emphasis has been put on the radius of curvature at the end of the gauge length to achieve throughout the gauge volume homogeneous stress-strain fields under uniaxial push-pull fatigue testing conditions [5]. The surface quality after the radial grinding procedure is R_{max} = 2.5 µm.

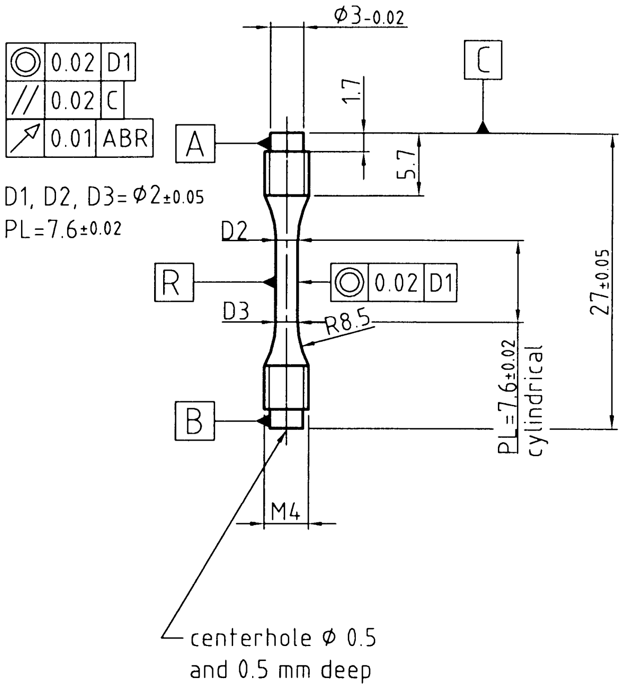

Fig. 2-7 Tensile/Low Cycle Fatigue specimen

The miniaturised tensile and LCF specimen geometry exactly fits in length and thickness to the geometrical dimensions of the KLST specimen: 27 mm x M4 with a weight of: 1,2991 g. The dimensions of the gauge length are 7.6 mm x Ø2 mm. It has been developed specially for use in irradiation programmes. 30 specimens are irradiated on each level (i.e. capsule) of the irradiation rig. The LCF/Tensile-specimens have one laser made engraving on one top side. A set of at least 5 specimens is needed for generating a convenient set of fatigue data.

The KLST mini impact specimen geometry is according to DIN 50115: 27 x 3 x 4 mm³ with 1 mm notch depth and has a weight of: 2,4744 g. It was already used in former irradiation programmes (MANITU, SIENA and SPICE [a]), as a result of which a wide data base is available on this geometry. In the ARBOR 1 irradiation 30 specimens are irradiated on each level (i.e. capsule) of the irradiation rig. The KLST-specimens have two mechanically made engravings left and right on the top side. For determining the Ductile to Brittle Transition Temperature (DTTB), a set of at least 6 specimens is necessary [5].

I50 Specimens are to be irradiated. They are labelled by a four-sign code, consisting of one or two letters for the material and two or three digits for the serial number. The KLST mini impact specimen is depicted in Fig. 2-8.

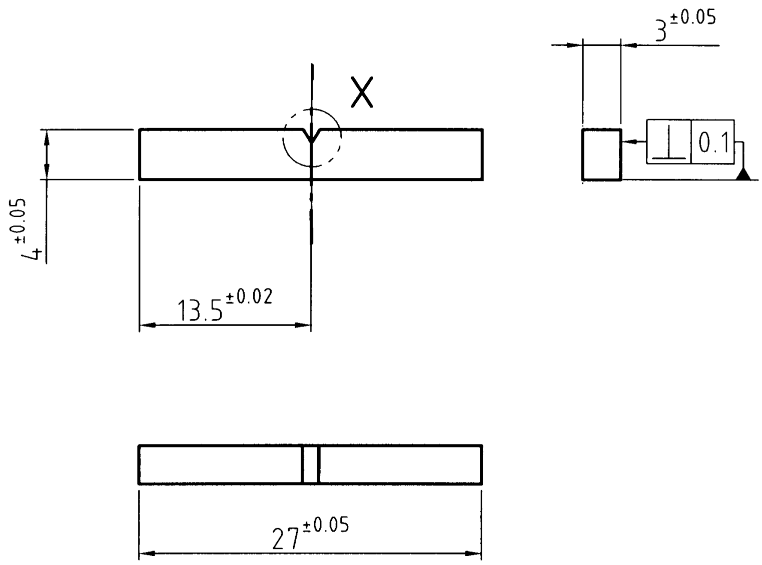

Fig. 2-8 KLST impact specimen

The specimens have been fabricated at FZK's central workshop. All specimens have been measured and comply with the tolerance dimensions indicated in the drawings. The complete dimension tables for the different materials are reported in a technical report. All KLST-specimens and LCF/Tensile-specimens have been cleaned in the following way:

- 10 minutes in ultrasonic bath with acetone and dried.
- cleaned with isopropyl alcohol.
- 5 minutes in ultrasonic bath with isopropyl alcohol and dried with hot air from fan.

This procedure has been performed on 20.9.2000 by D. Rodrian. All KLST-specimens and LCF/Tensile-specimens have been packed in packages of 10 in 3 segments of a plastic box in the right sequence of numbering to be implemented in one capsule of the BOR 60-irradiation rig. This procedure has been performed on 22.9.2000 by D. Rodrian and C. Petersen.

The specimens were handed over to SSC RIAR on 17. October 2000. An associated technical documentation was delivered as well [4]. The specific position foreseen for each separate specimen in the sample holder is documented.

2.6 Performance of the irradiation experiment ARBOR 1:

After the first negotiations between the State Scientific Center of the Russian Federation with its Research Institute of Atomic Reactors (SSC RIAR), Dimitrovgrad, and FZK, IMF II, the irradiation procedure has been defined in different Memoranda and a contract had been signed between both partners.

The assembly of the irradiation device at SSC RIAR had been prepared from mid 2001 on. After thermal physical calculations, the manufacturing and implementation of neutron monitors as well as the loading of the samples, hydraulic testing of complete irradiation device has been performed. When the irradiation rig was installed in the core of the reactor BOR 60 and the irradiation started, SSC RIAR delivered after each reactor cycle a so called Technical Report that described the specific conditions of the cycle and the damage dose reached. The first irradiation campaign was as scheduled in position D-23 i.e. the instrumented cell located in the 5th row of the BOR 60 reactor, to specify the required irradiations parameters. The start of the irradiation was in cycle 72, i.e. 25.11.2000. To reach the target damage dose of 30 dpa, 5 cycles were needed, first in the instrumented position D-23, than in an identical position G-23 in the 5th row of the core. The irradiation ended with cycle 75a on 15.10.2002.

The final analysis of the neutron monitors had been available in May 2003 after the end of the analysis period [4].

In the following tables are listed the identifications of all 10 materials of the ARBOR 1 irradiation (Tab. 2-4), the identification of heats, thermal treatments and amount of specimens of the 10 materials irradiated in the ARBOR 1 irradiation (Tab. 2-5), the identification of specimens of the ARBOR 1 irradiation (Tab. 2-6) and the correlation of materials to the identifications numbers of the ARBOR 1 irradiation (Tab. 2-7).

In a next step, that has been negotiated between EFDA and FZK in 2002, it was decided to select 50 % of the irradiated samples to be mechanically postirradiation examined (PIE 1) by tensile testing, low cycle fatigue testing and in impact tests in the hot cells of the material science laboratory of SSC RIAR. The remaining 50 % of the specimens were irradiated in the ARBOR 2 irradiation [4].

Tab. 2-4 Identification of materials of the ARBOR 1 irradiation

capsule 1	capsule 2	capsule 3	capsule 4	capsule 5	capsule 6	capsule 7	capsule 8	capsule 9	capsule 10
1. LCF	1. Tensile	1. Impact	2. Impact	2. LCF	3. Impact	2. Tensile	4. Impact	3. LCF	5. Impact
EUROF 1	EUROF 1	EUROF 1	F82Hmod.	EUROF 1	EUROF 1	EUROF 1	EUROF 1	EUROF 1	ADS 2
EUROF 1	EUROF 1	EUROF 1	F82Hmod.	EUROF 1	EUROF 1	EUROF 1	EUROF 1	EUROF 1	ADS 2
EUROF 1	EUROF 1	EUROF 1	F82Hmod.	EUROF 1	EUROF 1	EUROF 1	EUROF 1	EUROF 1	ADS 2
EUROF 1	EUROF 1	EUROF 1	F82Hmod.	EUROF 1	EUROF 1	EUROF 1	EUROF 1	EUROF 1	ADS 2
EUROF 1	EUROF 2	EUROF 1	F82Hmod.	EUROF 1	EUROF 1	EUROF 2	EUROF 1	EUROF 1	ADS 2
EUROF 2	EUROF 2	EUROF 1	F82Hmod.	EUROF 2	EUROF 1	EUROF 2	EUROF 1	EUROF 2	ADS 2
EUROF 2	EUROF 2	EUROF 1	F82Hmod.	EUROF 2	EUROF 1	EUROF 2	EUROF 1	EUROF 2	ADS 2
EUROF 2	EUROF 2	EUROF 2	ADS 4	EUROF 2	EUROF 1	EUROF 2	EUROF 2	EUROF 2	ADS 2
EUROF 2	F82Hmod.	EUROF 2	ADS 4	EUROF 2	EUROF 2	ADS 2	EUROF 2	EUROF 2	ADS 3
EUROF 2	F82Hmod.	EUROF 2	ADS 4	EUROF 2	EUROF 2	ADS 2	EUROF 2	EUROF 2	ADS 3
F82Hmod.	F82Hmod.	EUROF 2	ADS 4	ADS 2	EUROF 2	ADS 2	EUROF 2	F82Hmod.	ADS 3
F82Hmod.	F82Hmod.	EUROF 2	ADS 4	ADS 2	EUROF 2	ADS 2	EUROF 2	F82Hmod.	ADS 3
F82Hmod.	EURODShip	EUROF 2	ADS 4	ADS 2	EUROF 2	ADS 3	EUROF 2	F82Hmod.	ADS 3
F82Hmod.	EURODShip	EUROF 2	ADS 4	ADS 2	EUROF 2	ADS 3	EUROF 2	F82Hmod.	ADS 3
F82Hmod.	EURODShip	EUROF 2	OPT IVc	ADS 2	EUROF 2	ADS 3	EUROF 2	F82Hmod.	ADS 3
EURODShip	EURODShip	EURODShip	OPT IVc	ADS 3	EUROF 2	ADS 3	F82Hmod.	ADS 4	ADS 3
EURODShip	ADS 2	EURODShip	OPT IVc	ADS 3	ADS 2	OPT IVc	F82Hmod.	ADS 4	BS-EUROF
EURODShip	ADS 2	EURODShip	OPT IVc	ADS 3	ADS 2	OPT IVc	F82Hmod.	ADS 4	BS-EUROF
EURODShip	ADS 2	EURODShip	OPT IVc	ADS 3	ADS 2	OPT IVc	F82Hmod.	ADS 4	BS-EUROF
EURODShip	ADS 3	EURODShip	OPT IVc	ADS 3	ADS 2	OPT IVc	F82Hmod.	ADS 4	BS-EUROF
EUROF-EB	ADS 3	EURODShip	OPT IVc	OPT IVc	ADS 2	EURODShip	F82Hmod.	BS-EUROF	BS-EUROF
EUROF-EB	ADS 3	EURODShip	BS-EUROF	OPT IVc	ADS 2	EURODShip	F82Hmod.	BS-EUROF	BS-EUROF
EUROF-EB	EUROF-EB	EUROF-EB	EUROF-EB	OPT IVc	ADS 2	EURODShip	EURODShip	BS-EUROF	BS-EUROF
EUROF-EB	EUROF-EB	EUROF-EB	EUROF-EB	OPT IVc	ADS 3	EURODShip	EURODShip	BS-EUROF	BS-EUROF
EUROF-EB	EUROF-EB	EUROF-EB	EUROF-EB	OPT IVc	ADS 3	F82Hmod.	EURODShip	BS-EUROF	BS-EUROF
EUROF-EB	EUROF-EB	EUROF-EB	EUROF-EB	BS-EUROF	ADS 3	F82Hmod.	EURODShip	EURODShip	BS-EUROF
BS-EUROF	EUROF-EB	EUROF-EB	EUROF-EB	BS-EUROF	ADS 3	F82Hmod.	EURODShip	EURODShip	BS-EUROF
BS-EUROF	EUROF-EB	EUROF-EB	EUROF-EB	BS-EUROF	ADS 3	ADS 4	EURODShip	EURODShip	BS-EUROF
BS-EUROF	EUROF-EB	EUROF-EB	EUROF-EB	BS-EUROF	ADS 3	ADS 4	EURODShip	EURODShip	BS-EUROF
BS-EUROF	EUROF-EB	EUROF-EB	EUROF-EB	BS-EUROF	ADS 3	ADS 4	EURODShip	EURODShip	BS-EUROF

Tab. 2-5 Identification of heats, thermal treatments and amount of specimens of the 10 materials irradiated in the ARBOR 1 irradiation

Heat	Material	LCF + Tensile	Impact
E83697	EUROF 1 = EUROFER 97 (980°C 31 min/air + 760°C 90 min/air)	15 + 8	22
E83697	EUROF 2 = EUROFER 97 (1040°C 31 min/air + 760°C 90 min/air)	15 + 8	24
9753	F82H mod. = F82H mod. (1040°C 38 min/air + 750°C 2h/air)	10 + 7	14
986779	OPT IVc = OPTIFER IVc (950°C 30 min/air + 750°C 2h/air)	5 + 4	7
806	ADS 2 = EUROFER 97-Steel with 82 wppm nat. B (1040°C ...)	5 + 7	15
826	ADS 3 = EUROFER 97-Steel with 83 wppm B10 (1040°C ...)	5 + 7	15
825	ADS 4 = EUROFER 97-Steel with 1160 wppm B10 (1040°C ...)	5 + 3	7
HXN 958/3	EURODShip = EUROFER 97 with ODS (980°C 31 min/air + 760°C 90 min/air)	10 + 8	15
VS3102	BS-EUROF = EUROFER 97 (1050°C 1hr/AC + 750°C 2hrs/AC)	14 + 0	15
E83697	EUROF-EB = EUROFER 97, EB welded (post weld heat treatment 730°C 2h/AC)	6 + 8	16

Tab. 2-6 Identification of specimens of the ARBOR 1 irradiation

capsule 1	capsule 2	capsule 3	capsule 4	capsule 5	capsule 6	capsule 7	capsule 8	capsule 9	capsule 10
1. LCF	1. Tensile	1. Impact	2. Impact	2. LCF	3. Impact	2. Tensile	4. Impact	3. LCF	5. Impact
E 1 01	E 1 06	E 1 01	F 01	E 1 10	E 1 08	E 1 15	E 1 16	E 1 19	A 2 08
E 1 02	E 1 07	E 1 02	F 02	E 1 11	E 1 09	E 1 16	E 1 17	E 1 20	A 2 09
E 1 03	E 1 08	E 1 03	F 03	E 1 12	E 1 10	E 1 17	E 1 18	E 1 21	A 2 10
E 1 04	E 1 09	E 1 04	F 04	E 1 13	E 1 11	E 1 18	E 1 19	E 1 22	A 2 11
E 1 05	E 2 06	E 1 05	F 05	E 1 14	E 1 12	E 2 15	E 1 20	E 1 23	A 2 12
E 2 01	E 2 07	E 1 06	F 06	E 2 10	E 1 13	E 2 16	E 1 21	E 2 19	A 2 13
E 2 02	E 2 08	E 1 07	F 07	E 2 11	E 1 14	E 2 17	E 1 22	E 2 20	A 2 14
E 2 03	E 2 09	E 2 01	A 4 01	E 2 12	E 1 15	E 2 18	E 2 17	E 2 21	A 2 15
E 2 04	F 06	E 2 02	A 4 02	E 2 13	E 2 09	A 2 09	E 2 18	E 2 22	A 3 08
E 2 05	F 07	E 2 03	A 4 03	E 2 14	E 2 10	A 2 10	E 2 19	E 2 23	A 3 09
F 01	F 08	E 2 04	A 4 04	A 2 04	E 2 11	A 2 11	E 2 20	F 13	A 3 10
F 02	F 09	E 2 05	A 4 05	A 2 05	E 2 12	A 2 12	E 2 21	F 14	A 3 11
F 03	E O 02	E 2 06	A 4 06	A 2 06	E 2 13	A 3 09	E 2 22	F 15	A 3 12
F 04	E O 04	E 2 07	A 4 07	A 2 07	E 2 14	A 3 10	E 2 23	F 16	A 3 13
F 05	E O 07	E 2 08	OT 01	A 2 08	E 2 15	A 3 11	E 2 24	F 17	A 3 14
E O 01	E O 09	E O 01	OT 02	A 3 04	E 2 16	A 3 12	F 08	A 4 04	A 3 15
E O 03	A 2 01	E O 02	OT 03	A 3 05	A 2 01	OT 06	F 09	A 4 05	H 143
E O 05	A 2 02	E O 03	OT 04	A 3 06	A 2 02	OT 07	F 10	A 4 06	H 144
E O 06	A 2 03	E O 04	OT 05	A 3 07	A 2 03	OT 08	F 11	A 4 07	H 145
E O 08	A 3 01	E O 05	OT 06	A 3 08	A 2 04	OT 09	F 12	A 4 08	H 146
C 087	A 3 02	E O 06	OT 07	OT 01	A 2 05	E O 10	F 13	A 910	H 147
C 088	A 3 03	E O 07	H 142	OT 02	A 2 06	E O 12	F 14	A 911	H 148
C 089	C 093	C 165	C 173	OT 03	A 2 07	E O 15	E O 08	A 912	H 149
C 090	C 094	C 166	C 174	OT 04	A 3 01	E O 17	E O 09	A 913	H 150
C 091	C 095	C 167	C 175	OT 05	A 3 02	F 10	E O 10	A 914	H 151
C 092	C 096	C 168	C 176	A 905	A 3 03	F 11	E O 11	E O 11	H 152
A 901	C 097	C 169	C 177	A 906	A 3 04	F 12	E O 12	E O 13	H 153
A 902	C 098	C 170	C 178	A 907	A 3 05	A 4 01	E O 13	E O 14	H 154
A 903	C 099	C 171	C 179	A 908	A 3 06	A 4 02	E O 14	E O 16	H 155
A 904	C 100	C 172	C 180	A 909	A 3 07	A 4 03	E O 15	E O 18	H 156

Tab. 2-7 Correlation of materials to the identifications numbers of the ARBOR 1 irradiation

Material	Kind of specimen: LCF + Tensile	Identification of specimen	Kind of specimen: Impact (KLST)	Identification of specimen
EUROF 1 = EUROFER 97 (980°C)	23	**E 1 01 - E 1 23**	22	**E 1 01 - E 1 22**
EUROF 2 = EUROFER 97 (1040°C)	23	**E 2 01 - E 2 23**	24	**E 2 01 - E 2 24**
F82H mod. = F82H mod. (1040°C)	17	**F 01 - F 17**	14	**F 01 - F 14**
OPT IVc = OPTIFER IVc (950°C)	9	**OT 01 - OT 09**	7	**OT 01 - OT 07**
ADS 2 = EUROFER 97 (82 wppm nat. B)	12	**A 2 01 - A 2 12**	15	**A 2 01 - A 2 15**
ADS 3 = EUROFER 97 (83 wppm B10)	12	**A 3 01 - A 3 12**	15	**A 3 01 - A 3 15**
ADS 4 = EUROFER 97 (1160 wppm B10)	8	**A 4 01 - A 4 08**	7	**A 4 01 - A 4 07**
EURODShip = EUROFER 97 with ODS	18	**E O 01 - E O 18**	15	**E O 01 - E O 15**
BS-EUROF = EUROFER 97	14	**A 901 - A 914**	15	**H 142 - H 156**
EUROF-EB = EUROFER 97, EB welded	14	**C 087 - C 100**	16	**C 165 - C 180**
Number of specimen	**LCF + Tensile:**	**150**	**Impact (KLST):**	**150**

3 Postirradiation examination

3.1 Test conditions

The post irradiation mechanical testing of the selected specimens of the ARBOR 1 irradiation (Tables 3-1 and 3-2) is performed at the material science laboratory of SSC RIAR under the ISTC Partner Project #2781p.

After dismantling, transportation and decontamination of the specimens the post-irradiation experiments had been planned to be started in mid of 2004. Difficulties evolved from the delivery of both - from FZK - contributed testing facilities to be implemented in the hot cells of SSC RIAR delayed the planned start PIE 1 at SSC RIAR. Therefore the cold check out of both facilities was finished in June 2004 and the first PIE 1 test started in August 2004.

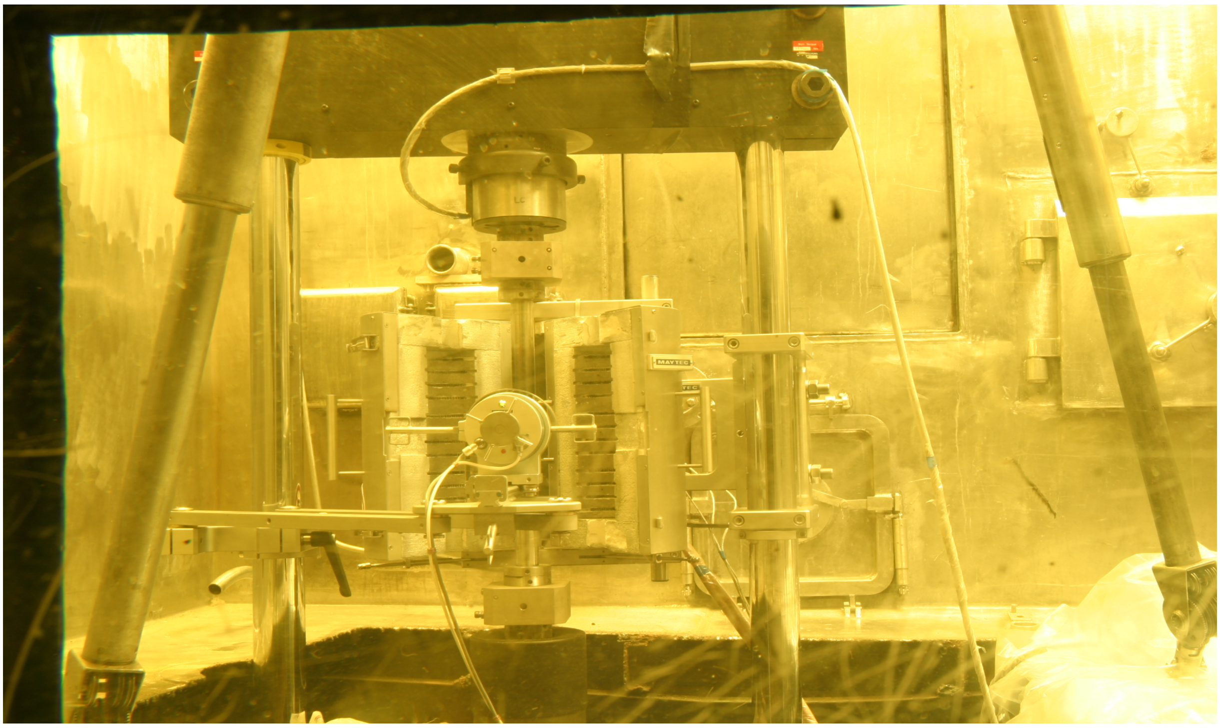

Fig. 3-1 Electro-mechanical testing machine with three zone furnace and high temperature extensometer in the hot cells of RIAR

Tensile and LCF tests are performed with an electro-mechanical testing machine INSTRON 1362 DOLI, Fig. 3-1, equipped with a three-zone furnace up to 1000°C and a high-temperature MAYTEC extensometer [4]. Tensile specimens are tested under static (tensile) loading at different temperatures (250, 300 and 350 °C) with a strain rate of $3x10^{-3}$ s^{-1}. From the load-displacement curves, strength and strain quantities like the 0.2% yield stress ($R_{p0.2}$), ultimate tensile strength (R_m), uniform strain (A_g) and total strain (A) are calculated. Reduction of area (Z) was measured from photos of the broken specimens taken after testing.

The LCF loading was performed at a constant temperature of 330 °C with different total strain ranges ($\Delta\varepsilon_{tot}$) between 0.8% and 1.2% with a strain rate of $3x10^{-3}$ s^{-1}. The number of cycles to failure (N_f) was defined at a point where a peak tensile stress decreased by 30% from its value at point marking the termination of the linear dependence of peak tensile stress on the number of cycles (N_D).

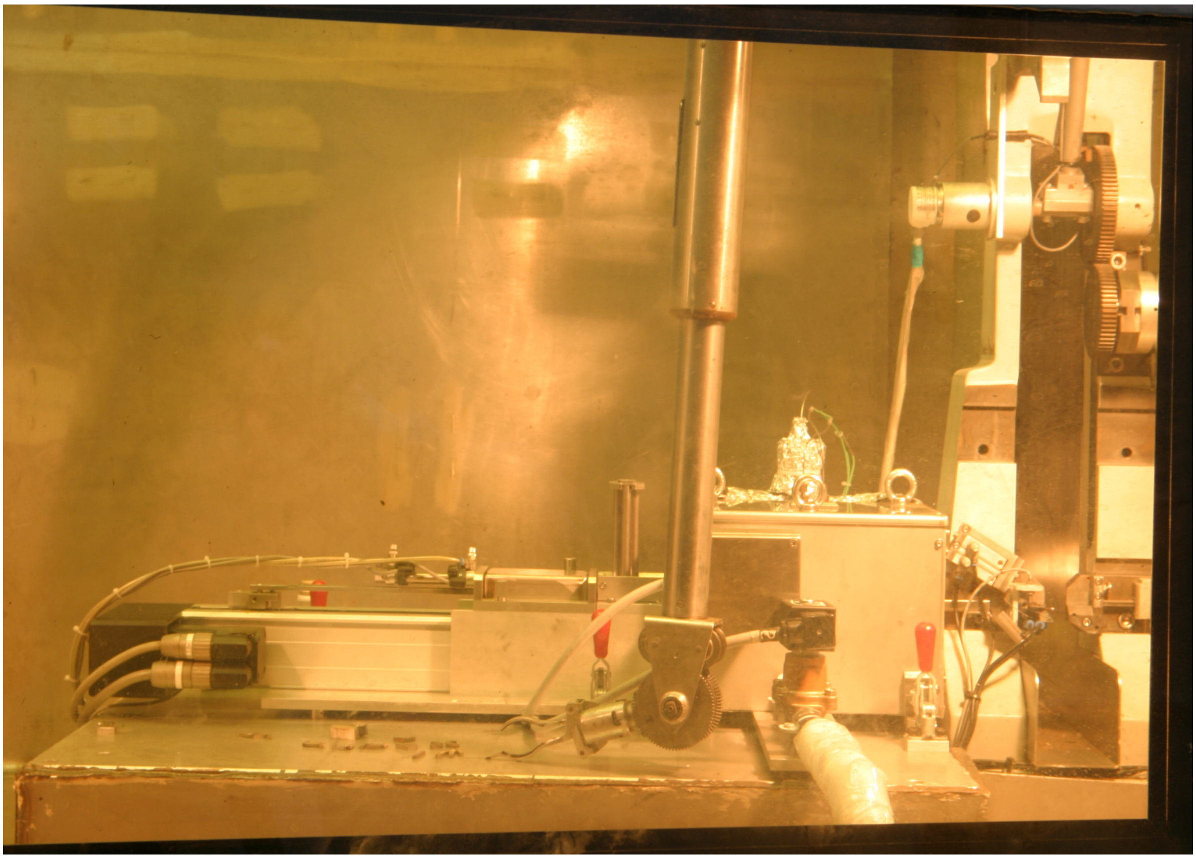

Fig. 3-2 Instrumented impact testing facility with transporting system, cooling facility/furnace and specimen positioning system implemented in the hot cells of RIAR

Impact tests were performed with a ZWICK 5113-HKE instrumented impact testing facility, Fig. 3-2, equipped with a pendulum hammer of 25 J impact energy, an impact velocity of 3.85 m/s and a test temperature range of -180°C to 600°C [4]. The impact energies (E) vs. test temperature (T) curves were analyzed with respect to the upper shelf energy (USE) and the ductile-to-brittle transition temperature (DBTT), see e.g. [4] for the test and evaluation procedures.

Tab. 3-1 Specimens selected for PIE 1 after the ARBOR 1 irradiation with irradiation conditions on the bottom of the table

capsule 1	capsule 2	capsule 3	capsule 4	capsule 5	capsule 6	capsule 7	capsule 8	capsule 9	capsule 10
1. LCF	1. Tensile	1. Impact	2. Impact	2. LCF	3. Impact	2. Tensile	4. Impact	3. LCF	5. Impact
E 1 01		E 1 01	F 01			E 1 15			A 2 08
E 1 02		E 1 02	F 02			E 1 16			A 2 09
E 1 03		E 1 03	F 03			E 1 17			A 2 10
E 1 04		E 1 04	F 04			E 1 18			A 2 11
E 1 05		E 1 05	F 05			E 2 15			A 2 12
E 2 01		E 1 06	F 06			E 2 16			A 2 13
E 2 02		E 1 07	F 07			E 2 17			A 2 14
E 2 03		E 2 01	A 4 01			E 2 18			A 2 15
E 2 04		E 2 02	A 4 02			A 2 09			A 3 08
E 2 05		E 2 03	A 4 03			A 2 10			A 3 09
F 01		E 2 04	A 4 04			A 2 11			A 3 10
F 02		E 2 05	A 4 05			A 2 12			A 3 11
F 03		E 2 06	A 4 06			A 3 09			A 3 12
F 04		E 2 07	A 4 07			A 3 10			A 3 13
F 05		E 2 08	OT 01			A 3 11			A 3 14
E O 01		E O 01	OT 02			A 3 12			A 3 15
E O 03		E O 02	OT 03			OT 06			H 143
E O 05		E O 03	OT 04			OT 07			H 144
E O 06		E O 04	OT 05			OT 08			H 145
E O 08		E O 05	OT 06			OT 09			H 146
C 087		E O 06	OT 07			E O 10			H 147
C 088		E O 07	H 142			E O 12			H 148
C 089		C 165	C 173			E O 15			H 149
C 090		C 166	C 174			E O 17			H 150
C 091		C 167	C 175			F 10			H 151
C 092		C 168	C 176			F 11			H 152
A 901		C 169	C 177			F 12			H 153
A 902		C 170	C 178			A 4 01			H 154
A 903		C 171	C 179			A 4 02			H 155
A 904		C 172	C 180			A 4 03			H 156
331,0 °C		**332,3 °C**	**333,2 °C**			**335,8 °C**			**338,4 °C**
31,0 dpa		**31,8 dpa**	**32,3 dpa**			**30,2 dpa**			**22,4 dpa**

Tab. 3-2 Correlation of test condition to specimen number during PIE 1 after the ARBOR 1 irradiation

capsule 1	Test Cond.	capsule 3	Test Temp.	capsule 4	Test Temp.	capsule 7	Test Temp.	capsule 10	Test Temp.
1. LCF	°C / %	1. Impact	°C	2. Impact	°C/%	2. Tensile	°C	5. Impact	°C
E 1 01	330 / 1.2	E 1 01	110	F 01	120	E 1 15	250	A 2 08	150
E 1 02	330 / 1.0	E 1 02	130	F 02	160	E 1 16	300	A 2 09	180
E 1 03	330 / 0.8	E 1 03	160	F 03	330	E 1 17	350	A 2 10	300
E 1 04	330 / 0.9	E 1 04	145	F 04	140	E 1 18	no test	A 2 11	210
E 1 05	330 / 0.9	E 1 05	138	F 05	150	E 2 15	250	A 2 12	165
E 2 01	330 / 1.0	E 1 06	200	F 06	145	E 2 16	300	A 2 13	no test
E 2 02	330 / 0.8	E 1 07	330	F 07	no test	E 2 17	350	A 2 14	no test
E 2 03	330 / 1.2	E 2 01	70	A 4 01	180	E 2 18	no test	A 2 15	no test
E 2 04	330 / 0.9	E 2 02	120	A 4 02	240	A 2 09	250	A 3 08	150
E 2 05	no test	E 2 03	90	A 4 03	330	A 2 10	300	A 3 09	180
F 01	330 / 1.2	E 2 04	105	A 4 04	450	A 2 11	350	A 3 10	300
F 02	330 / 1.0	E 2 05	115	A 4 05	no test	A 2 12	no test	A 3 11	210
F 03	no test	E 2 06	110	A 4 06	no test	A 3 09	250	A 3 12	165
F 04	330 / 0.9	E 2 07	330	A 4 07	no test	A 3 10	300	A 3 13	no test
F 05	330 / 0.8	E 2 08	no test	OT 01	150	A 3 11	350	A 3 14	no test
E O 01	330 / 1.2	E O 01	330	OT 02	100	A 3 12	no test	A 3 15	no test
E O 03	330 / 1.0	E O 02	400	OT 03	20	OT 06	250	H 143	100
E O 05	no test	E O 03	450	OT 04	60	OT 07	300	H 144	200
E O 06	330 / 0.8	E O 04	500	OT 05	40	OT 08	350	H 145	250
E O 08	330 / 0.9	E O 05	no test	OT 06	330	OT 09	no test	H 146	125
C 087	330 / 1.2	E O 06	no test	OT 07	no test	E O 10	250	H 147	150
C 088	330 / 1.0	E O 07	no test	H 142	no test	E O 12	300	H 148	175
C 089	330 / 0.9	C 165	140	C 173	failed	E O 15	350	H 149	115
C 090	330 / 0.8	C 166	200	C 174	180	E O 17	no test	H 150	100
C 091	no test	C 167	130	C 175	330	F 10	250	H 151	50
C 092	no test	C 168	330	C 176	no test	F 11	300	H 152	80
A 901	330 / 1.0	C 169	150	C 177	200	F 12	350	H 153	65
A 902	330 / 1.2	C 170	140	C 178	no test	A 4 01	250	H 154	72
A 903	330 / 0.9	C 171	160	C 179	no test	A 4 02	300	H 155	65
A 904	330 / 0.8	C 172	160	C 180	no test	A 4 03	350	H 156	no test

Tab. 3-3 Correlation of materials to the identification numbers of the PIE 1 of the ARBOR 1 irradiation

	Kind of specimen:		Identification	Kind of specimen:		Identification
	LCF		**of specimen**	impact (KLST)		**of specimen**
	Tensile					
EUROF 1 = EUROFER 97 (980°C)	5		**E 101-E 105**	7		**E101-E107**
	4		**E 115-E 118**			
EUROF 2 = EUROFER 97 (1040°C)	5		**E 201-E 205**	8		**E201-E208**
	4		**E 215-E 218**			
F82H mod. = F82H mod. (1040°C)	5		**F 01-F 05**	7		**F01-F07**
	3		**F 10-F 12**			
OPT IVc = OPTIFER IVc (950°C)				7		**OT01-OT07**
	4		**OT06-OT09**			
ADS 2 = EUROFER 97 (82 wppm nat. B)				8		**A208-A215**
	4		**A 209-A212**			
ADS 3 = EUROFER 97 (83 wppm B10)				8		**A308-A315**
	4		**A 309-A312**			
ADS 4 = EUROFER 97 (1160 wppm B10)				7		**A401-A407**
	3		**A 401-A403**			
EURODShip = EUROFER 97 with ODS	5		**EO01,EO03,EO05,EO06,EO08**	7		**EO01-EO07**
	4		**EO10,EO12,EO15,EO17**			
BS-EUROF = EUROFER 97	4		**A901-A904**	15		**H142-H156**
EUROF-EB = EUROFER 97, EB welded	6		**C087-C092**	16		**C165-C180**

Number of specimen LCF + Tensile: 60 Impact (KLST): 90

From specimens of these post irradiation experiments, like tensile, fatigue and impact tests, especially selected parts of deformed and undeformed areas had been transported for fractographic and micro structural investigations to FZK's Fusion Materials Laboratory, FML, in 2007.

Tab. 3-4 Specimens of the PIE 1 of the ARBOR 1 irradiation selected for transport to FZK

Material	Quantity of samples *)	Sample type	Sample numbers	Comments
EUROF 1	2,5	KLST	One half of E 1 01 - E 1 05,	Charpy samples
EUROF 1	2,5	FZK-type	One half of E 1 15 - E 1 17, one full of E 1 18	Tensile/Fatigue samples
EUROF 2	4	KLST	One half of E 2 01 - E 2 06, one full of E 2 08	Charpy samples
EUROF 2	2,5	FZK-type	One half of E 2 15 - E 2 17, one full of E 2 18	Tensile/Fatigue samples
F82 H mod.	4	KLST	One half of F 01 - F 06, one full of F 07	Charpy samples
F82 H mod.	1,5	FZK-type	One half of F 10 - F 12	Tensile/Fatigue samples
OPTIFER 4	3	KLST	One half of OT 01 and OT 03 - OT 05, one full of OT 07	Charpy samples
OPTIFER 4	2,5	FZK-type	One half of OT 06 - OT 08, one full of OT 09	Tensile/Fatigue samples
ADS 2	3	KLST	Three full of A 2 13 – A 2 15	Charpy samples
ADS 2	2,5	FZK-type	One half of A 2 09 - A 2 11, one full of A 2 12	Tensile/Fatigue samples
ADS 3	3	KLST	Three full of A 3 13 – A 3 15	Charpy samples
ADS 3	2,5	FZK-type	One half of A 3 09 - A 3 11, one full of A 3 12	Tensile/Fatigue samples
ADS 4	3	KLST	Three full of A 4 05 – A 4 07	Charpy samples
ADS 4	1,5	FZK-type	One half of A 4 01 - A 4 03	Tensile/Fatigue samples
EUROFER-ODS HIP (0.5% Y_2O_3)	2,5	FZK-type	One half of E O 10, E O 12, E O 15 and one full of E O 17	Tensile/Fatigue samples

*) Quantity of samples is the sum of halves of samples and full samples

Remark: Tensile and Charpy specimens contributed by NRG are still at the hot cells of RIAR.

4 Testing results

4.1 Impact testing

The instrumented impact tests on irradiated KLST specimens have been performed the instrumented ZWICK 5113-HKE impact testing facility in hot cell VK-39of the materials department of RIAR. This facility is identical with that one at FZK used for testing the unirradiated reference specimens. Both facilities have 25 J pendulum impact hammers with strikers implemented with strain gauges and a radius of 2 mm. The specimen support has a distance of 22 mm and the impact velocity was 3.85 m/s. The test execution with automatic cooling or heating of the specimen, between – 180°C and 600°C, as well as transporting to the striking position is controlled by PC. Data were recorded with a sampling rate of 1 MHz.

From the recorded force vs. time curve of each test the oscillatory part of the system was filtered out by a fast Fourier transformation. The deflection was calculated from the filtered force vs. time curves by solving the pendulum equation of motion and the impact velocity. After integration of the force vs. deflection curve, the impact energy, E, was received and has been plotted vs. test temperature, T, as is shown in the following figures

Characteristic values of these curves are the Upper Shelf Energy, USE, which is the maximum in the E vs. T-diagram and the Ductile to Brittle Transition Temperature, DBTT. For the determination of DBTT in most cases the temperature at USE/2 is used. These values are listed in Table 4-1 and 4-2 together with the ΔDBTT- and ΔUSE-values.

Tab. 4-1 Results of impact tests on FZK's KLST specimens from the ARBOR 1 irradiation experiment (31.8 dpa, 332°C)

Materials, Irradiation conditions	DBTT unirr. [°C]	DBTT irr. [°C]	ΔDBTT [°C]	USE unirr. [J]	USE irr. [J]	ΔUSE [J]
EUROFER 97 as received, 332 °C, 31.8 dpa	- 81	137	218	9.84	7.01	- 2.83
EUROFER 97 heat treated, 332 °C, 31.8 dpa	- 90	107	197	9.84	6.76	- 3.08
F82H mod., 333 °C, 32.3 dpa	- 72	148	220	9.41	5.03	- 4.38
OPT IVc, 333 °C, 32.3 dpa	- 105	48	153	9.12	5.84	- 3.28
ADS 2 = EUROF 1 + 82 wppm natural B, 338 °C, 22.4 dpa	- 74	174	248	8.81	5.60	- 3.21
ADS 3 = EUROF 1 + 83 wppm ^{10}B, 338 °C, 22.4 dpa	- 100	174	274	8.92	5.78	- 3.14
ADS 4 = EUROF 1 + 1160 wppm ^{10}B, 333 °C, 32.3 dpa	- 12	260	272	5.50	0.67	- 4.83
EURODShip = EUROF 1 + 0.5% Y_2O_3, 332 °C, 31.8 dpa	135	382	247	2.54	1.51	- 1.03

Tab. 4-2 Results of impact tests on NRG's KLST specimens from the ARBOR 1 irradiation experiment

Materials, Irradiation conditions	DBTT unirr. [°C]	DBTT irr. [°C]	ΔDBTT [°C]	USE unirr. [J]	USE irr. [J]	ΔUSE [J]
BS-EUROFER, 338 °C, 22.4 dpa	- 87	70	157	9.16	6.26	- 2.90
EUROFER 97, EB welded, 332 °C, 31.8 dpa	- 88	145	233	11.15	5.49	- 5.66

The impact testing results of irradiated EUROFER 97 in two conditions show a remarkable shift in DBTT towards temperatures above 100°C. As can be seen from Fig. 4-1 there is no difference of both EUROFER 97 modifications in the unirradiated reference conditions. But after the irradiation of 31.8 dpa the increase in DBTT is 21 °C higher for the as received EUROFER 97. Whereas the reduction of USE for both irradiated conditions is very similar. Both tendencies had been found already in the post irradiation of the SPICE irradiation [18].

In Figs. 8-1 to 8-4 of the Annex the original Force (Kraft) vs. Time (Zeit) curves and the analysis of RIAR are shown for as received EUROFER 97 and annealed EUROFER 97, respectively. In addition to the curves are depicted in Figs. 8-21 to 8-26 of the Annex macro graphic views of the tested specimens of as received EUROFER 97 and annealed EUROFER 97, respectively.

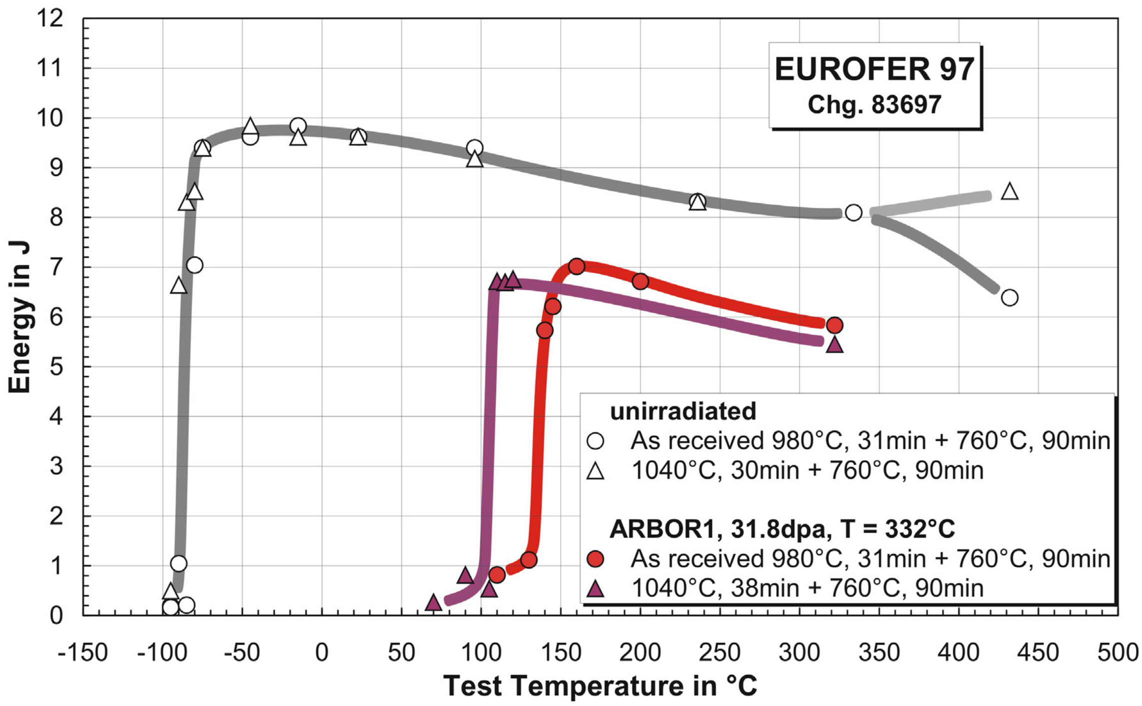

Fig. 4-1 Impact energy vs. test temperature for unirradiated and 31.8 dpa, 332.2°C, irradiated EUROFER 97 in the as received (980°C) and heat treated (1040°C) condition.

For F82H mod., depicted in Fig. 4-2, the DBTT after the 31.8 dpa irradiation is with 148°C much higher than that of EUROFER 97. But the ΔDBTT of 220 °C is comparable to as received EUROFER 97. Also the USE is with 5 J much lower. It shows with a ΔUSE of – 4.38 J the greatest reduction in upper shelf energy of all tested base materials.

In Figs. 8-5 and 8-6 of the Annex the original Force (Kraft) vs. Time (Zeit) curves and the analysis of RIAR are shown for as received F82H mod.. In addition to the curves are depicted in Figs. 8-27 and 8-28 of the Annex macro graphic views of the tested specimens of as received F82H mod..

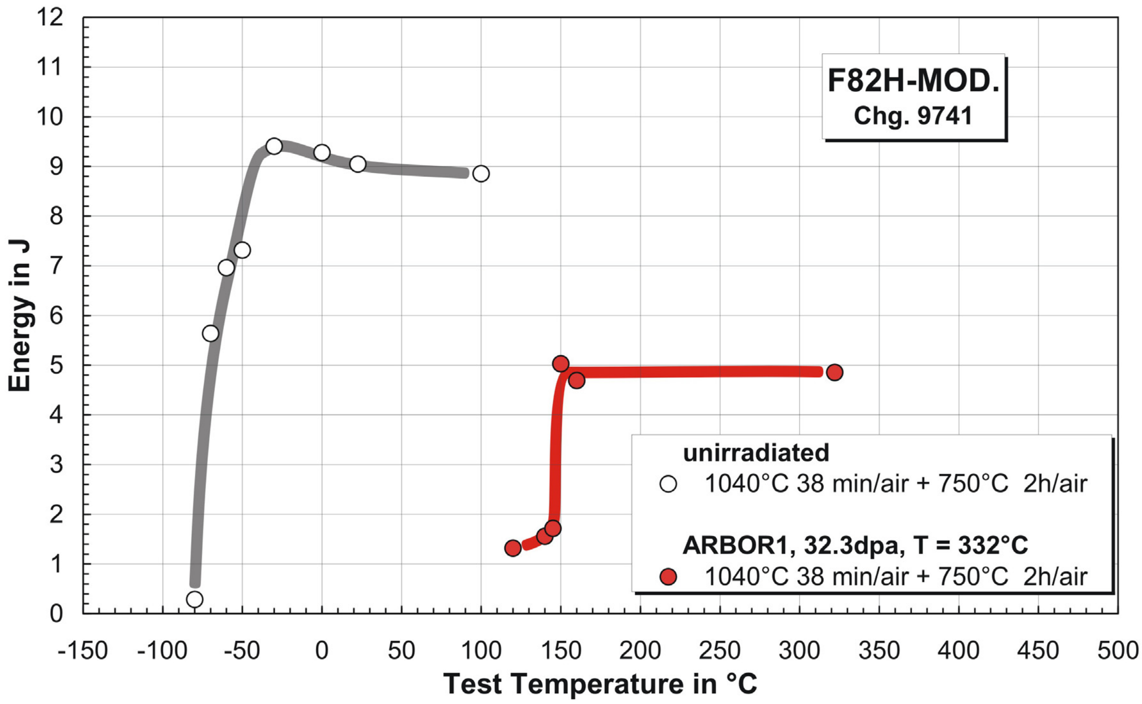

Fig. 4-2 Impact energy vs. test temperature for unirradiated and 32.3 dpa, 333.2°C, irradiated F82H mod. in the as received condition.

The best results of all irradiated ferritic/martensitic materials had been received for 32.3 dpa irradiated OPTIFER IVc with a DBTT of 48°C and an USE near 6 J, as can be seen from Fig. 4-3.

In Figs. 8-7 and 8-8 of the Annex the original Force (Kraft) vs. Time (Zeit) curves and the analysis of RIAR are shown for OPTIFER IVc. In addition to the curves are depicted in Figs. 8-29 and 8-30 of the Annex macro graphic views of the tested specimens of OPTIFER IVc.

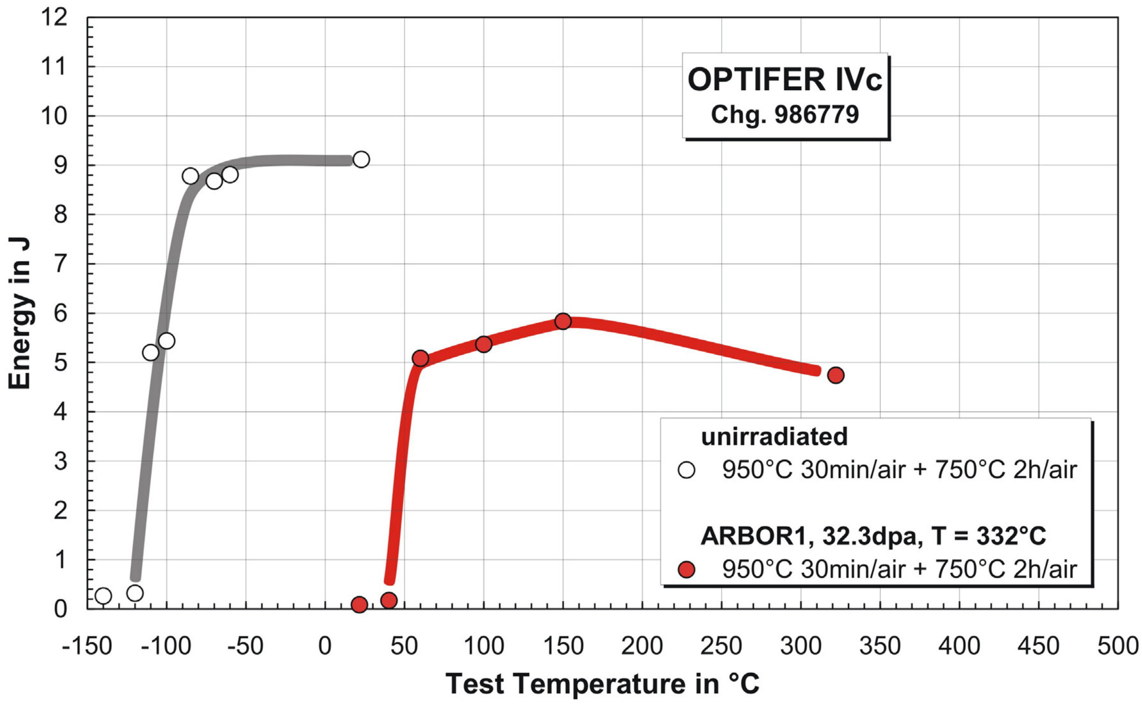

Fig. 4-3 Impact energy vs. test temperature for unirradiated and 32.3 dpa, 333.2°C, irradiated OPTIFER IVc in the as received condition.

USE of the 82 wppm natural Boron steel (ADS 2, Fig. 4-4) and the 83 wppm ^{10}B isotope steel (ADS 3, Fig. 4-5) in the unirradiated reference condition results in a slightly lower value (ca. 0.9 J) than the USE of unirradiated, heat treated EUROFER 97. Therefore the alloying effect of Boron on impact properties can be neglected.

In Figs. 8-9 and 8-10 of the Annex the original Force (Kraft) vs. Time (Zeit) curves and the analysis of RIAR are shown for ADS 2. And in Figs. 8-11 and 8-12 of the Annex the original Force (Kraft) vs. Time (Zeit) curves and the analysis of RIAR are shown for ADS 3. In addition to the curves are depicted in Figs. 8-31 to 8-34 of the Annex macro graphic views of the tested specimens of ADS 2 and ADS 3, respectively.

Whereas the Boron doped model alloys ADS 2 and ADS 3 of EUROFER 97 show a degraded neutron irradiation resistance in the USE compared to 32.3 dpa irradiated, as received EUROFER 97 by ca. 15 %, even if the irradiation damage was about 10 dpa lower.

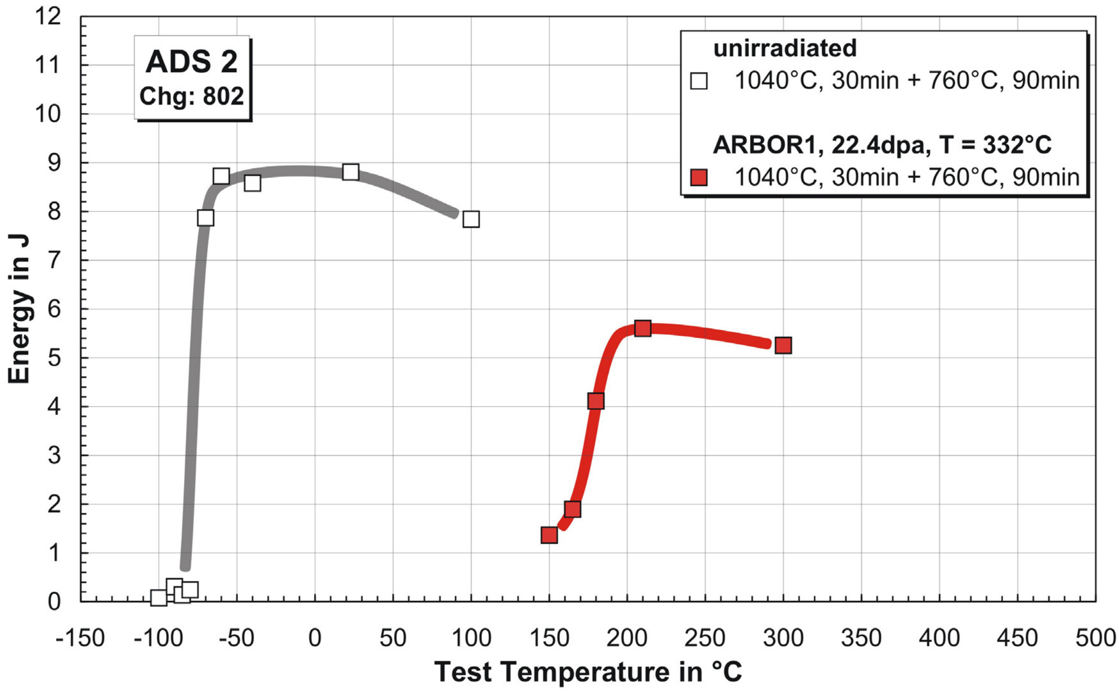

Fig. 4-4 Impact energy vs. test temperature for unirradiated and 22.4 dpa, 338.4°C, irradiated ADS 2 in the as received condition.

DBTT's of the 82 wppm natural Boron steel (ADS 2, Fig. 4-4) and the 83 wppm ^{10}B isotope steel (ADS 3, Fig. 4-5) in the unirradiated reference condition result in a similar range than the DBTT of unirradiated, heat treated EUROFER 97. But the shift of this quantity at 22.4 dpa irradiation damage is about + 65°C compared to 32.3 dpa irradiated EUROFER 97.

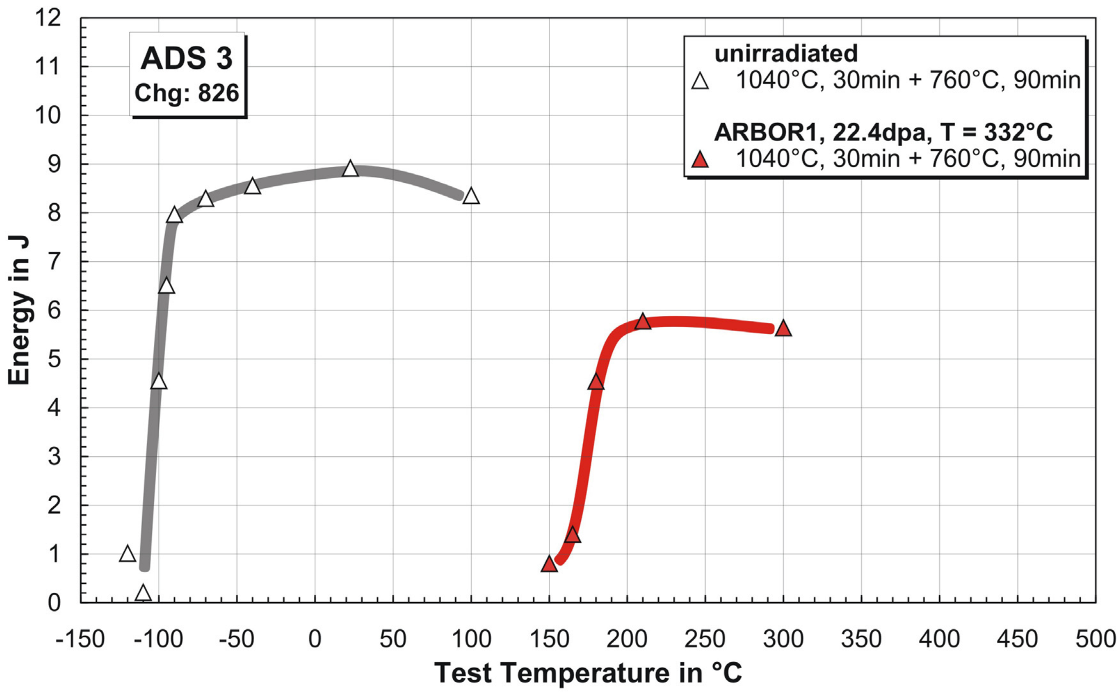

Fig. 4-5 Impact energy vs. test temperature for unirradiated and 22.4 dpa, 338.4°C, irradiated ADS 3 in the as received condition.

The 1120 wppm ^{10}B isotope steel (ADS 4, Fig. 4-6) results in the unirradiated reference condition with an USE of 5.5 J and a DBTT of – 12°C already in such a low range that it can be assumed this high alloying by Boron influences impact properties dramatically.

In Fig. 8-13 of the Annex the original Force (Kraft) vs. Time (Zeit) curves are shown for ADS 4. In addition to the curves are depicted in Figs. 8-35 and 8-36 of the Annex macro graphic views of the tested specimens of ADS 4.

Under irradiation with 32.3 dpa at 333.2°C ADS 4 shows extremely brittle behaviour in the tested temperature area between 170°C and 450°C. A better understanding of this behaviour is expected after the micro structural examination performed at the hot cells of FZK later.

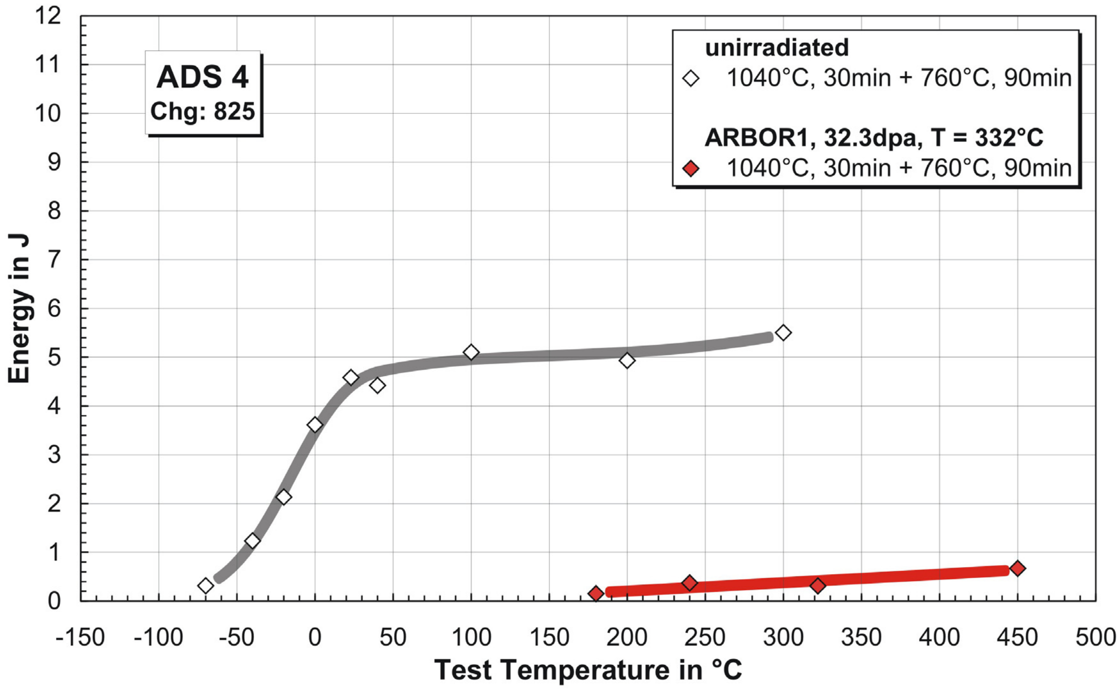

Fig. 4-6 Impact energy vs. test temperature for unirradiated and 32.3 dpa, 333.2°C, irradiated ADS 4 in the as received condition.

DBTT of the ODS EUROFER with 0.3 % Y_2O_3 (Fig. 4-7) in the unirradiated reference condition results in a value of 132 °C and an USE of 2.54 J which is in a range that is out of technical relevance, because the material is brittle. Also the shift of these quantities after 31.8 dpa irradiation damage with a DBTT of 382 °C and an USE of 1.51 J is far from a material that can be used for the construction of a fusion reactor. For further development and a better understanding of this behaviour the micro structural examination performed at FZK later will serve new information.

In Figs. 8-14 and 8-15 of the Annex the original Force (Kraft) vs. Time (Zeit) curves and the analysis of RIAR are shown for ODS EUROFER with 0.3 % Y_2O_3. In addition to the curves are depicted in Fig. 8-37 of the Annex macro graphic views of the tested specimens of ODS EUROFER with 0.3 % Y_2O_3.

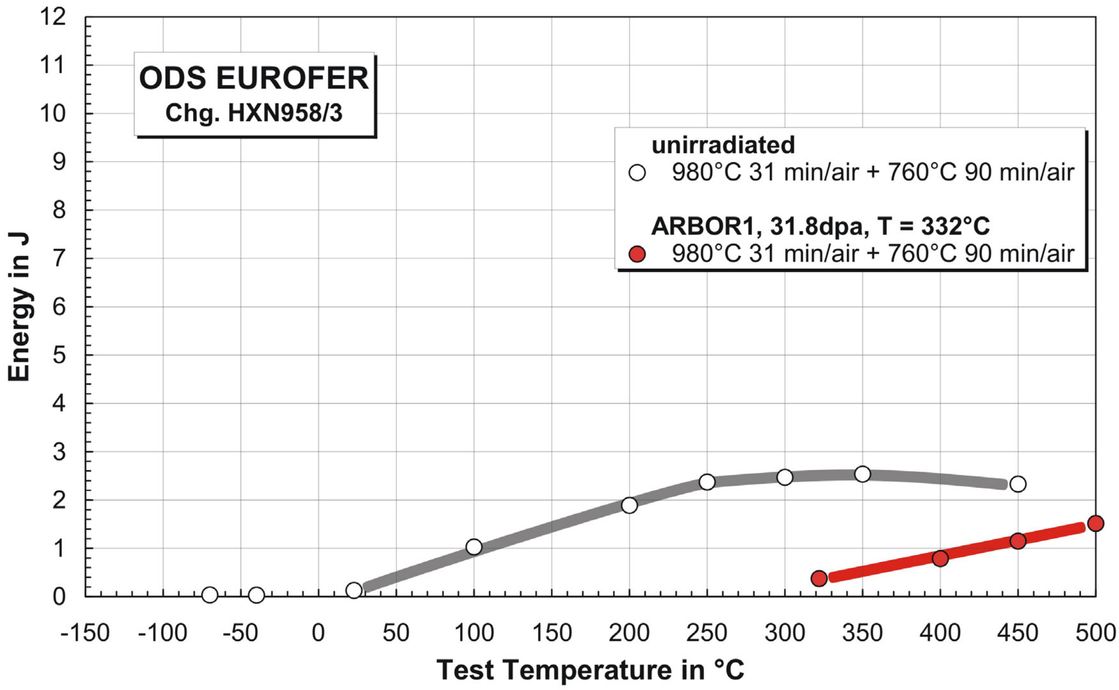

Fig. 4-7 Impact energy vs. test temperature for unirradiated and 31.8 dpa, 332.3°C, irradiated ODS EUROFER in the as received condition.

The BS EUROFER steel (Fig. 4-8) results in the unirradiated reference condition with a DBTT of – 87 °C and an USE of 9.16 J in a similar range as the as received EUROFER 97. After the 22.4 dpa irradiation damage it reacts with a DBTT of 70 °C better than the 31.8 dpa irradiation damaged, as received EUROFER 97 and with an USE of 9.16 J in a similar range.

In Figs. 8-16 to 8-18 of the Annex the original Force (Kraft) vs. Time (Zeit) curves and the analysis of RIAR are shown for BS EUROFER. In addition to the curves are depicted in Figs. 8-38 to 8-41 of the Annex scanning electron micrographic and macro graphic views of the tested specimens of BS EUROFER.

For the electron beam welded EUROFER of NRG (Fig. 4-9) we received in the reference impact experiments of the unirradiated material with a DBTT value of – 88 °C and an USE of 11.19 J similar or even better results than the as received EUROFER 97. But the scatter of data was higher than with the base material.

In Figs. 8-19 and 8-20 of the Annex the original Force (Kraft) vs. Time (Zeit) curves and the analysis of RIAR are shown for EUROFER EB welded. In addition to the curves are depicted in Figs. 8-42 to 8-45 of the Annex macro graphic views of the tested specimens of EUROFER EB welded.

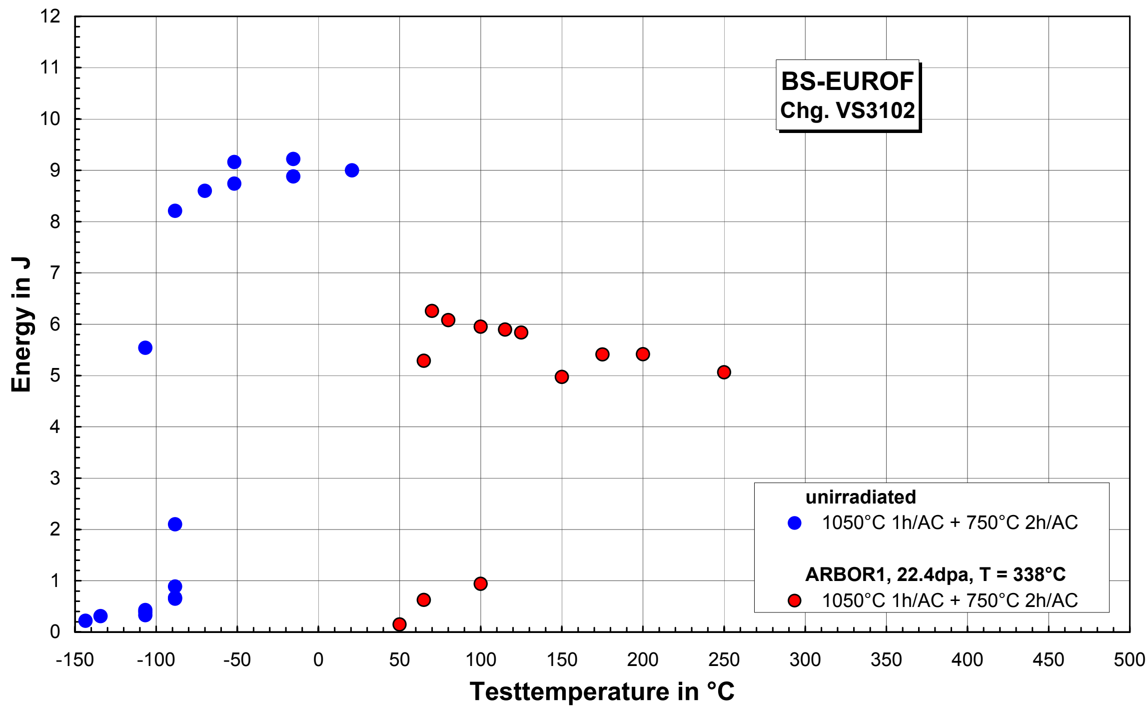

Fig. 4-8 Impact energy vs. test temperature for unirradiated and 22.4 dpa, 338.4°C, irradiated BS EUROFER in the as received condition.

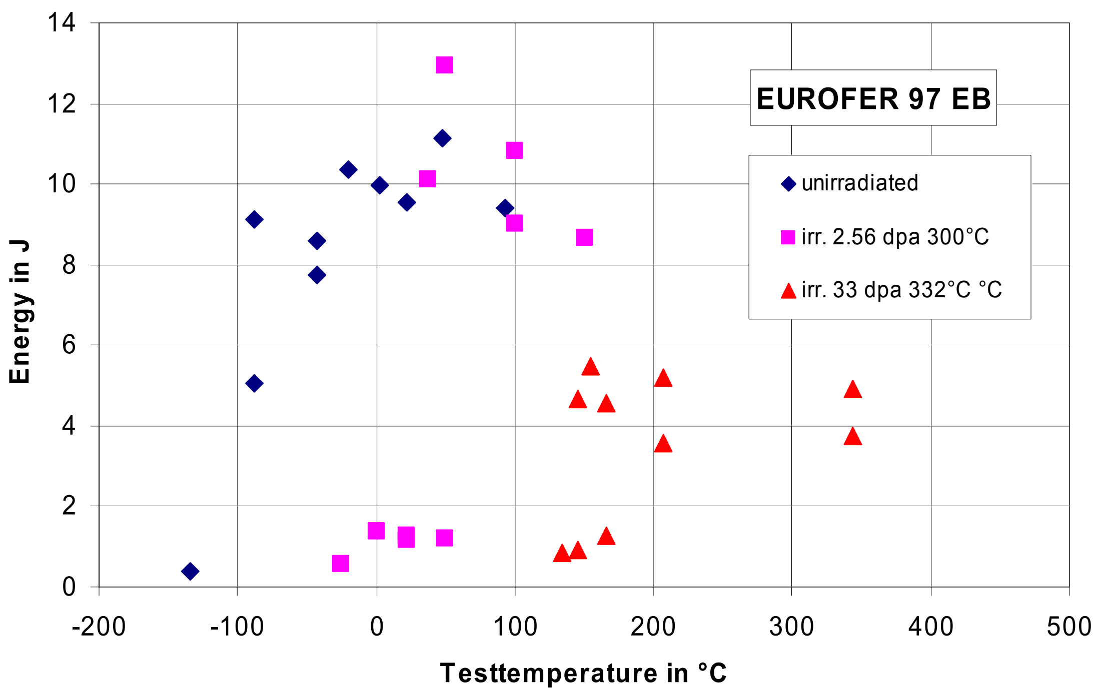

Fig. 4-9 Impact energy vs. test temperature for unirradiated and 33 dpa, 332°C, irradiated EUROFER 97 EB in the post weld heat treated condition. For comparison also data of a 2.56 dpa, 300°C, HFR irradiation is shown.

Fig. 4-10 shows the evolution of the embrittlement due to neutron irradiation, i.e. DBTT, as function of the irradiation damage up to 30 dpa for the materials irradiated in the ARBOR 1 irradiation. Impact data had been taken from irradiations with irradiation temperatures between 300 and 338 °C. For comparison literature results from MANET-I, F82H, OPTIFER 1a and OPTIFER-V are also included. In case of EUROFER 97 a differentiation is made between specimens from as received material (Anl., 980 °C) and specimens subjected to pre-irradiation heat treatment (WB, 1040 °C). The pre-irradiation heat treatment of EUROFER 97 leads to a considerable improvement of the irradiation resistance at doses up to 30 dpa. All three steels show steep increase in the DBTT with dose below 10 dpa. At the achieved doses a clear tendency to saturation of embrittlement is identified. Indeed, for 31.8 dpa at 332 °C irradiation the DBTT of EUROFER 97 is found to be = 137 °C.

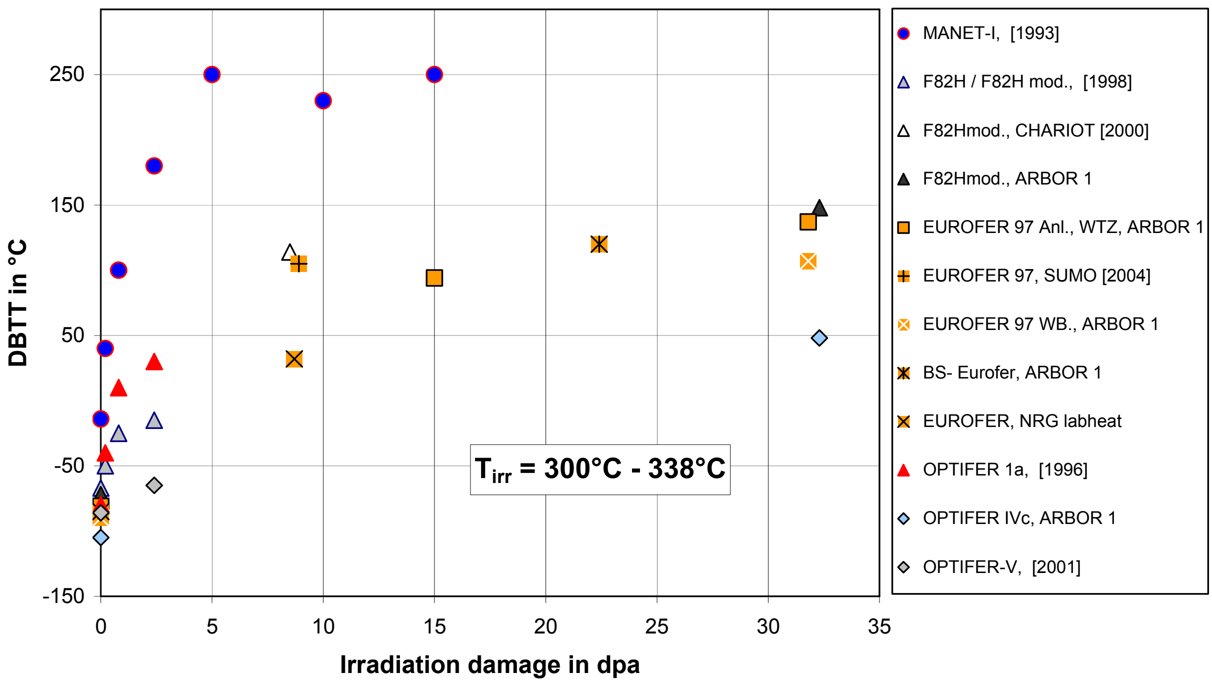

Fig. 4-10 Comparison of irradiation dependence on the Ductile to Brittle Transition Temperature behavior for different technically relevant RAF/M steels compared to conventional 12% Cr steel MANET-I

The evolution of the increase of irradiation embrittlement with the dose in Fig. 4-11 is qualitatively similar to the evolution of the irradiation hardening of tensile testing results. This similarity makes it reasonable to use an equation of the form: $\Delta DBTT = \Delta DBTT_s(1-\exp(-\Phi/\Phi_0))^{1/2}$, with $\Delta DBTT_s$ as the saturation embrittlement, for phenomenological description of the dose dependence of the embrittlement. For further information see [19].

From the knowledge of these results of the PIE of ARBOR 1 a saturation embrittlement seems to be reached, but a better understanding will be achieved after PIE of ARBOR 2 where an irradiation damage of ca. 70 dpa is obtained.

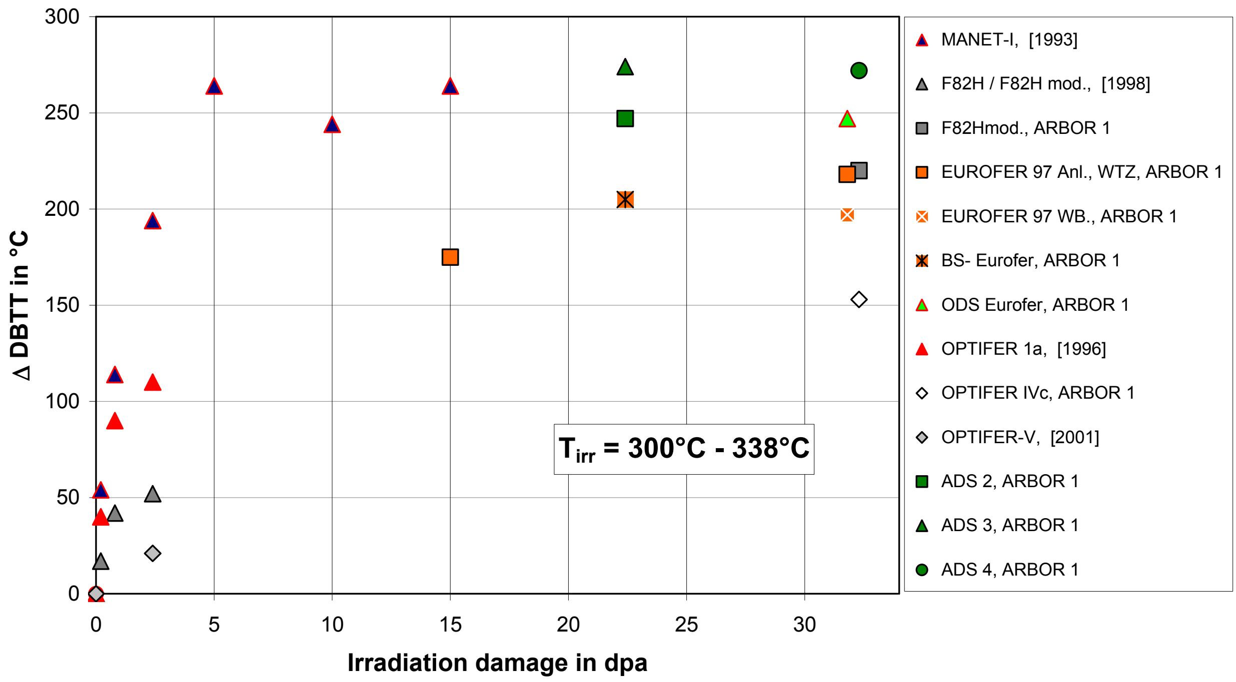

Fig. 4-11 Comparison of irradiation dependence on the irradiation induced increase of the Ductile to Brittle Transition Temperature behavior for different technically relevant RAF/M steels compared to conventional 12% Cr steel MANET-I

4.2 Tensile testing

The tensile tests are performed with a tensile/LCF testing facility of INSTRON-DOLI 1362 type, equipped with a 100 KN load cell, a high temperature furnace and a strain measurement system (details in Annex B, Fig. 9-1), installed in the K-12 hot cell of the SSC RF RIAR. For comparison results from other recently published irradiation campaigns are included. But these results were generated on different specimen shapes and under different tensile testing conditions. Tensile tests have been performed on four different kinds of specimens types utilized in the different irradiations. NRG (SIWAS-04, SUMO-02) irradiated cylindrical specimens of 20 mm gauge length and 4 mm diameter and performed the tests with a strain rate of $5x10^{-4}$ s^{-1} [22]. In the SPICE irradiation cylindrical specimens of 18 mm gauge length and 3 mm diameter are tensile tested under vacuum with a strain rate of $1x10^{-4}$ s^{-1} [23]. In the 15 dpa WTZ 01/577 irradiation cylindrical specimens of 15 mm gauge length and 3 mm diameter are tensile tested with a strain rate of $3x10^{-3}$ s^{-1}[24].
Even if one takes into account the slightly different tensile testing conditions, a continuous increase of the Yield Stress is detectable with increasing irradiation damage.

Considerable changes due to irradiation hardening are found in the $R_{p0,2}$- and R_m-values, Figs. 4-12 and 4-13. from tensile data of EUROFER 97.

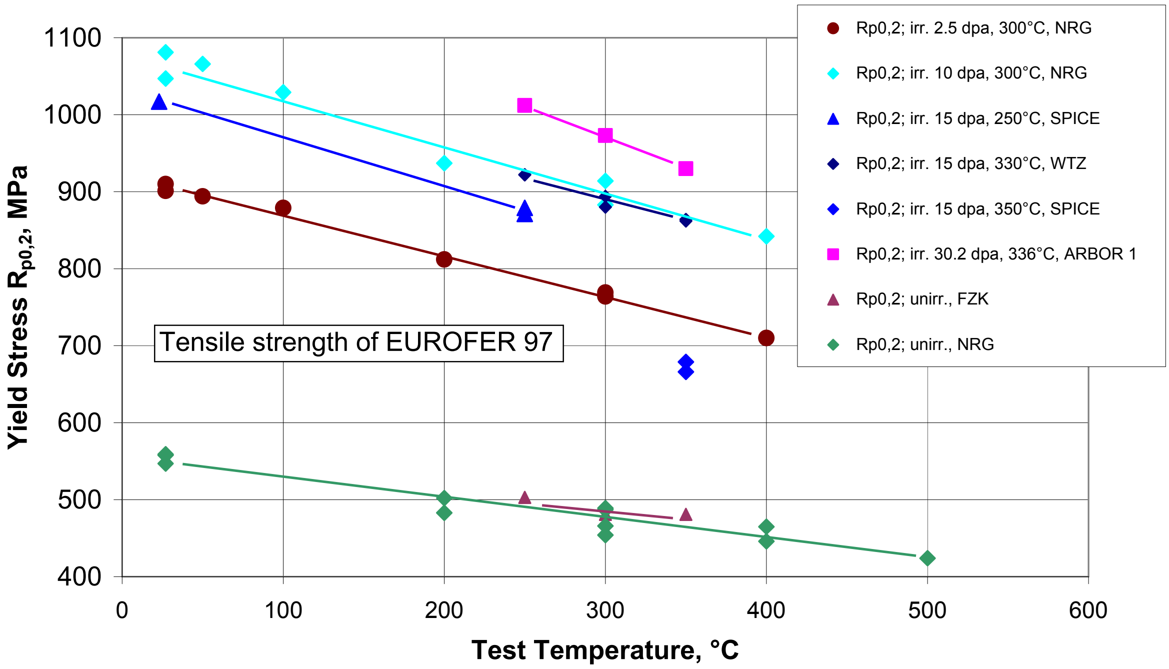

Fig. 4-12 Yield Stress ($R_{p0,2}$) behaviour of 30,2 dpa irradiated EUROFER 97 as a function of test temperature compared to other irradiated and unirradiated data (the temperature in the legend indicates the irradiation temperature)

The reference tensile test performed at NRG and FZK (Fig. 4-12) concerning the stresses are in a close scatter band and give a good basis for the interpretation of the tensile results. With increasing irradiation damage (2.5, 10, 15 and 30 dpa) stress values of as received EUROFER 97 are increasing continuously.

So in Fig. 4-12 the 2.5 dpa damage (SIWAS-04) has the lowest increase of around 300 MPa in Yield Stress and the 30.2 dpa damage (ARBOR 1) the highest increase of around 460 MPa in Yield Stress, that is nearly a duplication of the unirradiated quantity.

But irradiation temperature plays a big role as the 15 dpa value of the SPICE irradiation at a temperature level of 350°C shows. At this higher temperature the irradiation hardening is more than 100 MPa lower in Yield Stress ($R_{p0,2}$) compared to the 300 and 250°C values.

The same influence has the irradiation hardening on the Ultimate Tensile Strength (R_m) of EUROFER 97. But the stress increase from $R_{p0,2}$ to R_m of unirradiated material is much higher than after irradiation. Therefore in Fig. 4-13 the 2.5 dpa damage (SIWAS-04) has the lowest increase of around 200 MPa in Ultimate Tensile Strength and the 30.2 dpa damage (ARBOR 1) the highest increase of around 410 MPa in Ultimate Tensile Strength that is nearly a duplication of the unirradiated quantity.

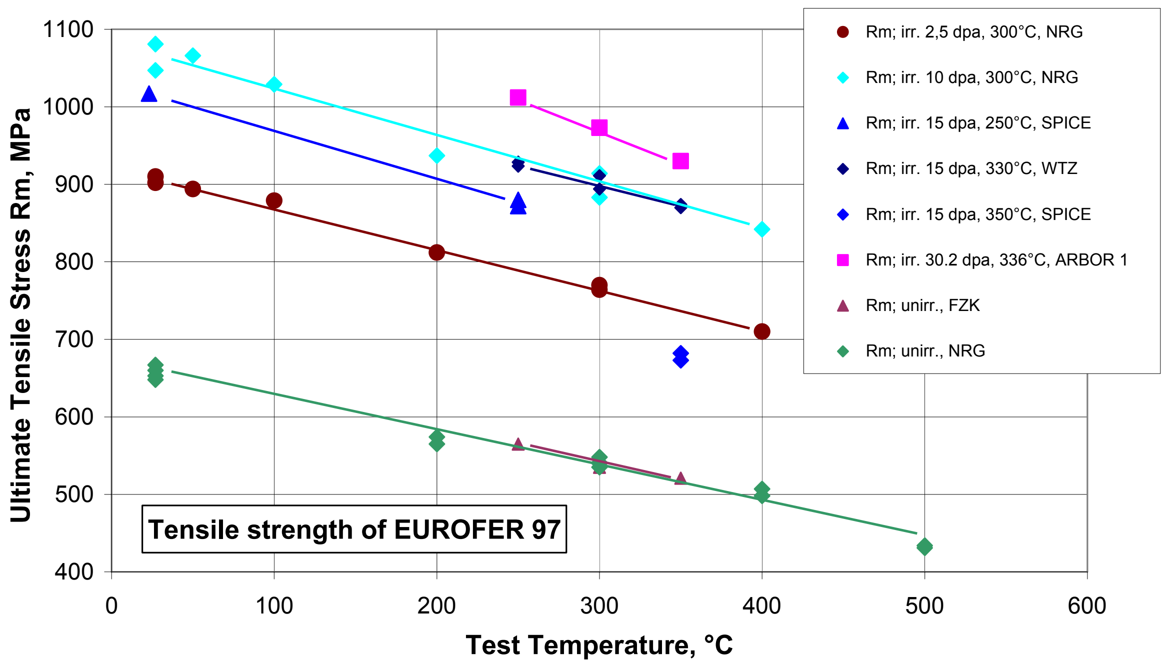

Fig. 4-13 Ultimate Tensile Strength (R_m) behaviour of 30,2 dpa irradiated EUROFER 97 as a function of test temperature compared to other irradiated and unirradiated data (the temperature in the legend indicates the irradiation temperature)

The reference tensile test performed at NRG and FZK (Fig. 4-14) concerning the strains are in a certain scatter band but also give a good basis for the interpretation of the tensile results. With increasing irradiation damage (2.5, 10, 15 and 30 dpa) strain values of as received EUROFER 97 are decreasing.

The effect of the irradiation damage on the Uniform Strain is also considerable - mostly A_g-values below 0.5 % are reached - but does not depend so much of the damage dose as the stress values.

So in Fig. 4-14 the 2.5 dpa damage (SIWAS-04) until the 30.2 dpa damage (ARBOR 1) the decrease in Uniform Strain is very similar.

Irradiation temperature plays again a role as the 15 dpa value of the SPICE irradiation at a temperature level of 350°C shows. At this higher temperature the reduction in A_g is not of that quantity as with the lower temperatures but higher irradiation damages.

The influence of irradiation on the Uniform Strain (A_g) of EUROFER 97 leads to a situation where technically not relevant strain values are reached. The Total Strain values in Fig. 4-15 do not show a consistent picture, because the reduction in Total Strain (A) do not follow a sequence.

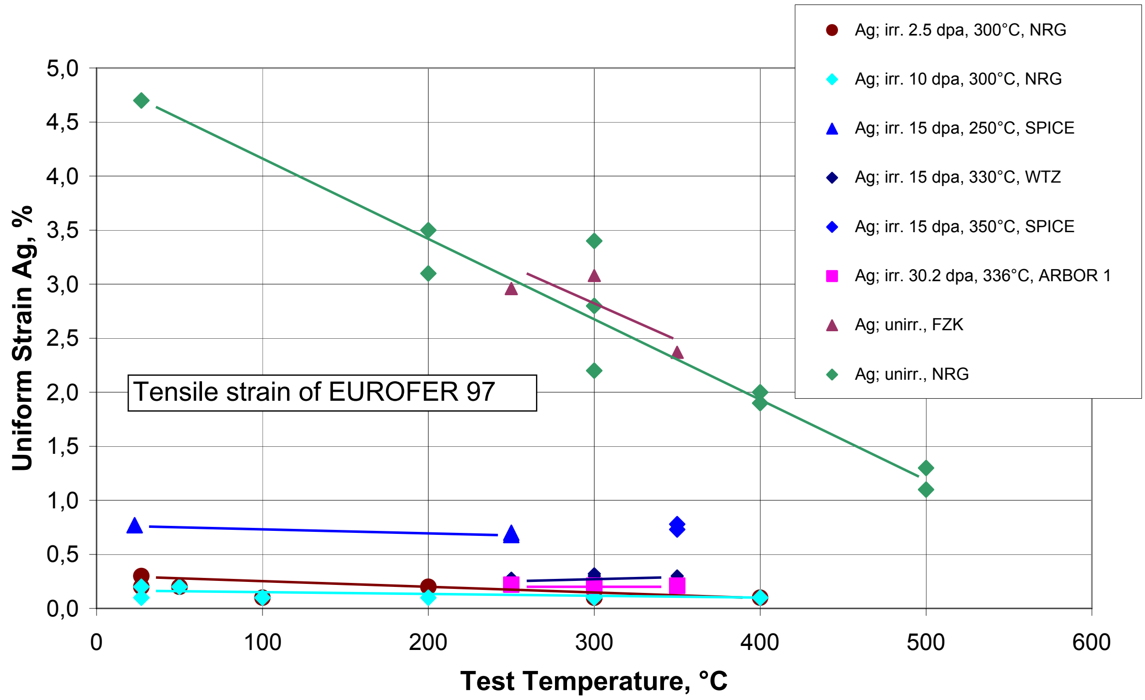

Fig. 4-14 Uniform Strain (A_g) behaviour of 30,2 dpa irradiated EUROFER 97 as a function of test temperature compared to other irradiated and unirradiated data (the temperature in the legend indicates the irradiation temperature)

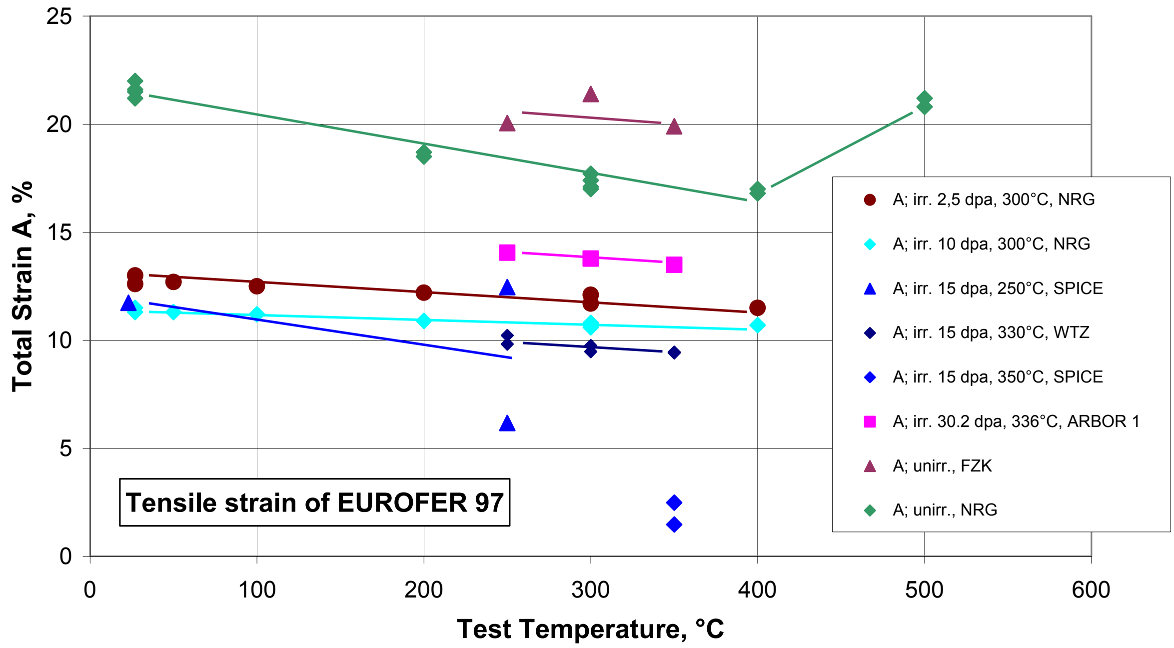

Fig. 4-15 Total Strain (A) behaviour of 30,2 dpa irradiated EUROFER 97 as a function of test temperature compared to other irradiated and unirradiated data (the temperature in the legend indicates the irradiation temperature)

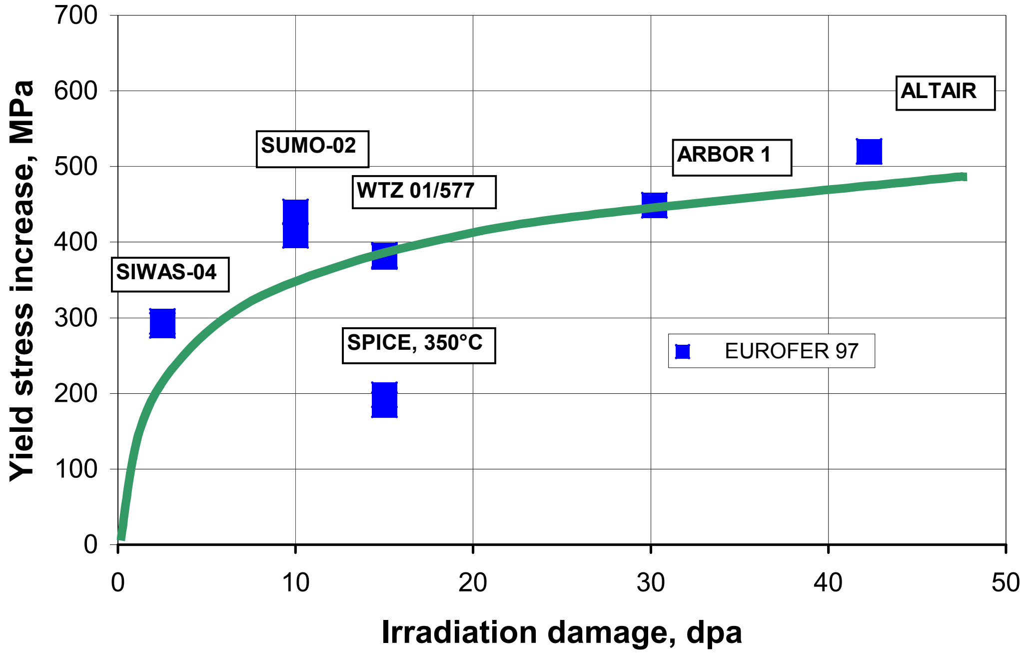

Fig. 4-16 Yield stress increase due to irradiation damage compared to data of other irradiations (Test temperatures close to irradiation temperatures)

In Fig. 4-16 the yield stress increase is plotted in dependence of the irradiation damage for irradiations performed around 300°C. Only the yield stress increase of specimens irradiated at 350°C to 15 dpa damage (SPICE), that is not included in the fit, is much lower and demonstrates the strong influence of irradiation temperatures in this temperature range between 300 and 350°C.

The radiation defects are acting as obstacles for the dislocations and lead to strong material hardening which can be evaluated according to the following relationship

$$\Delta\sigma = M\alpha\mu b\sqrt{Nd} \qquad (1)$$

with *M* being the Taylor factor, α – an average obstacle strength, μ – the shear modulus of the steel, *b* – the Burgers vector of the moving dislocation, *N* – the volume density of the obstacles and *d* – their average diameter. For the case when different obstacle types contribute to the hardening the resulting total hardening can be evaluated by $\Delta\sigma_{total} = \sum\Delta\sigma_i$, with the summation over all obstacle types i [20].
The curve in Fig. 4-16 describes a phenomenological approach for the evolution of the radiation defect density with irradiation dose that was given by Whapham and Makin in [21].

Within this model the defect density *N* increases with dose at the initial stage of irradiation, but as their concentration increases the newly formed defects become captured by the already existing ones leading to a decrease of the number of newly formed defects during a given increment of dose as the dose increases. Hence, the increase in *N* and the achievement of a saturation value N_s is expected:

$$N = N_s \left[1 - \exp\left(-\frac{\Phi}{\Phi_0} \right) \right] \qquad (2)$$

here Φ denotes the irradiation dose and Φ_0 is the scaling dose characterizing how fast the saturation of *N* sets in. For irradiation hardening dominated by a single obstacle type, combination of Eq. (2) with Eq. (1) yields the following relationship for the evolution of the irradiation hardening with dose:

$$\Delta\sigma = \Delta\sigma_s \sqrt{1 - \exp\left(-\frac{\Phi}{\Phi_0} \right)} \qquad (3)$$

where $\Delta\sigma_s$ is the saturation value of hardening.

The solid line in Fig. 4-16 is a description of the irradiation hardening according to Eq. (3) with $\Delta\sigma_s$ =492 MPa and Φ_0 =7.3 dpa. In spite of (i) differences in the irradiation conditions, e.g. irradiation temperature and neutron flux density, (ii) differences in test conditions *e.g.* specimen geometry, strain rate and (iii) scatter of experimental data, Eq. (3) describes qualitatively the evolution of hardening with dose. Furthermore, the hardening rate appears to be significantly decreased at the achieved damage doses. Planned quantitative analysis of the radiation defects and their evolution with damage dose will shed more light on the hardening mechanism.

More detailed tensile results of EUROFER 97, F82H mod., OPTIFER IVc, EUROFER 97 with different boron contents and ODS-EUROFER 97 are compared in the following tables and figures. The gripping of the tensile specimen is given in Fig. 9-1 of Annex B. Tensile curves also from the other tested temperatures of 250°C and 300°C with the analysis of RIAR (Figs. 9-2 to 9-9) and a series of macro photos from each tested specimen (Figs. 9-10 to 9-17) are given in the Annex B.

Tab. 4-3 Results of tensile tests on specimens from the ARBOR 1 irradiation experiment at 30.2 dpa and 336°C.

Material	**T_{test}**	**$R_{p0.2}$**	**R_m**	**A_g**	**A**	**Z**
	°C	MPa	MPa	%	%	%
EUROFER 97 980°C	350	929,90	929,90	0,20	11,93	63,70
EUROFER 97 1040°C	350	916,00	916,10	0,18	9,85	65,70
F82Hmod.	350	913,00	915,00	0,22	5,69	38,20
OPTIFER IVc	350	932,30	939,40	0,16	11,47	56,30
ADS 2	350	888,60	891,90	0,37	8,76	47,60
ADS 3	350	918,10	924,30	0,34	8,42	11,72
ADS 4	350	1041,50	1058,70	0,42	2,52	14,20
EURODShip 0.5%Y_2O_3	350	1047,10	1081,90	1,34	9,36	20,60

Tab. 4-4 Results of cold reference tensile tests at 350°C for the ARBOR 1 irradiation experiment (mean values of two experiments).

Material	$R_{p0.2}$	R_m	A_g	A	Z
	MPa	MPa	%	%	%
EUROFER 97 980°C	471,95	515,76	2,27	20,81	88,42
EUROFER 97 1040°C	445,26	502,26	2,89	20,71	95,48
F82Hmod.	487,85	536,20	2,79	20,12	95,23
OPTIFER IVc	429,50	506,65	3,74	22,04	94,84
ADS 2	411,85	459,83	2,77	20,07	94,16
ADS 3	409,81	480,79	3,44	20,80	94,07
ADS 4	372,96	456,10	3,68	16,90	90,31
EURODShip 0.5%Y_2O_3	709,66	833,95	6,72	14,04	84,82

Tab. 4-5 Results of irradiation influence on tensile tests at 350°C from the ARBOR 1 irradiation experiment.

	Delta values for ARBOR 1 tensile tests				
Material	Δ $R_{p0.2}$	Δ R_m	Δ A_g	Δ A	Δ Z
	MPa	MPa	%	%	%
EUROFER 97 980°C	457,96	414,14	-2,07	-8,88	-24,72
EUROFER 97 1040°C	470,75	413,84	-2,71	-10,86	-29,78
F82Hmod.	425,15	378,80	-2,57	-14,43	-57,03
OPTIFER IVc	502,80	432,75	-3,58	-10,57	-38,54
ADS 2	476,75	432,07	-2,40	-11,31	-46,56
ADS 3	508,29	443,51	-3,10	-12,38	-82,35
ADS 4	668,55	602,61	-3,26	-14,38	-76,11
EURODShip 0.5%Y_2O_3	337,44	247,96	-5,38	-4,68	-64,22

In Tab. 4-3 are listed the ARBOR 1 irradiation damaged stress and strain values of EUROFER 97 as received (980°C), EUROFER 97 annealed (1040°C), F82H mod., OPTIFER IVc, three EUROFER 97 with different boron contents (ADS 2, ADS 3 and ADS 4) and ODS-EUROFER 97 (EURODShip 0.5%Y_2O_3) tested at 350°C and with a strain rate of $3x10^{-3}$ s^{-1}. Tab. 4-4 show cold reference values of the same materials under similar testing conditions. Whereas in Tab. 4-5 the increases in stresses and the decreases in strains are depicted.

In Fig. 4-17 are depicted Yield Stress ($R_{p0,2}$) and Ultimate Tensile Strength (R_m) behaviour of 30,2 dpa, 336°C irradiated RAF/M materials tested at 350°C. The irradiation hardening results in a high stress level between 890 and 930 MPa for EUROFER 97 (980°C), EUROFER 97 (1040°C), F82H mod., OPTIFER IVc, ADS 2 and ADS 3. Whereas ADS 4 and EURODShip with 0.5%Y_2O_3 result in values above 1040 MPa. Characteristic for the strong irradiation hardening is also the small stress increase between $R_{p0,2}$ and R_m.

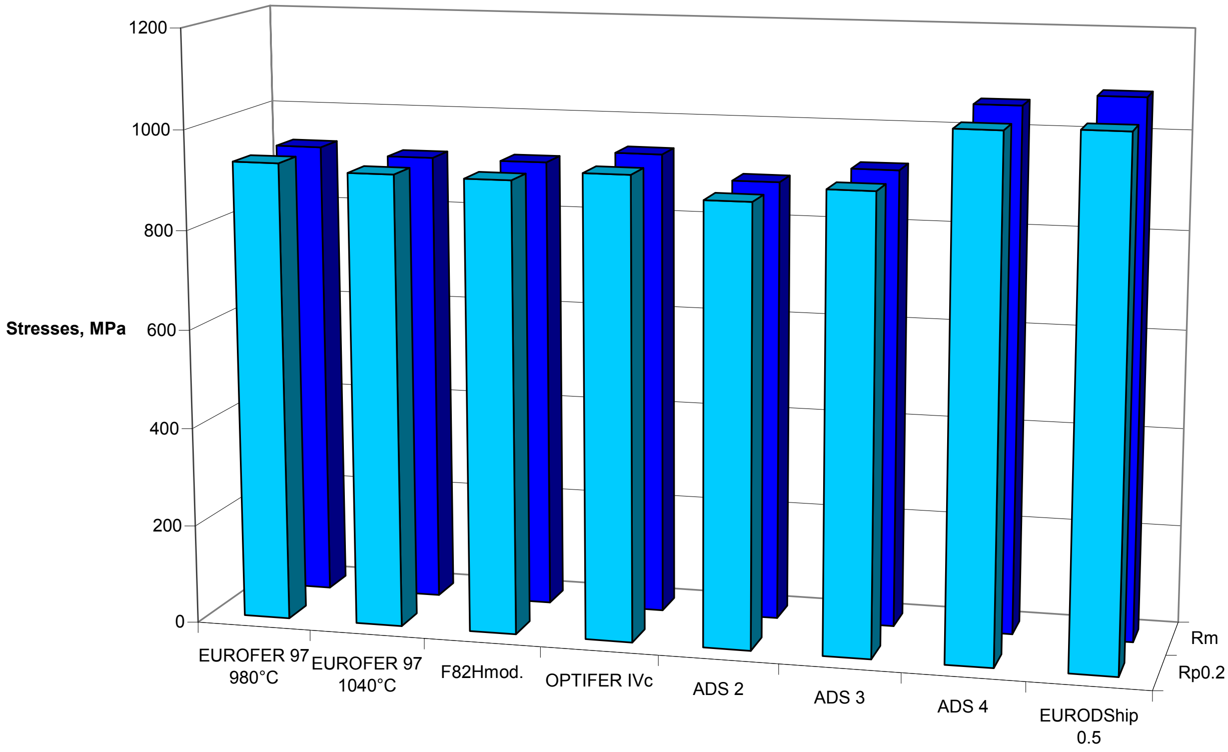

Fig. 4-17 Comparison of Yield Stress ($R_{p0,2}$) and Ultimate Tensile Strength (R_m) behaviour of 30,2 dpa, 336°C irradiated RAF/M materials tested at 350°C.

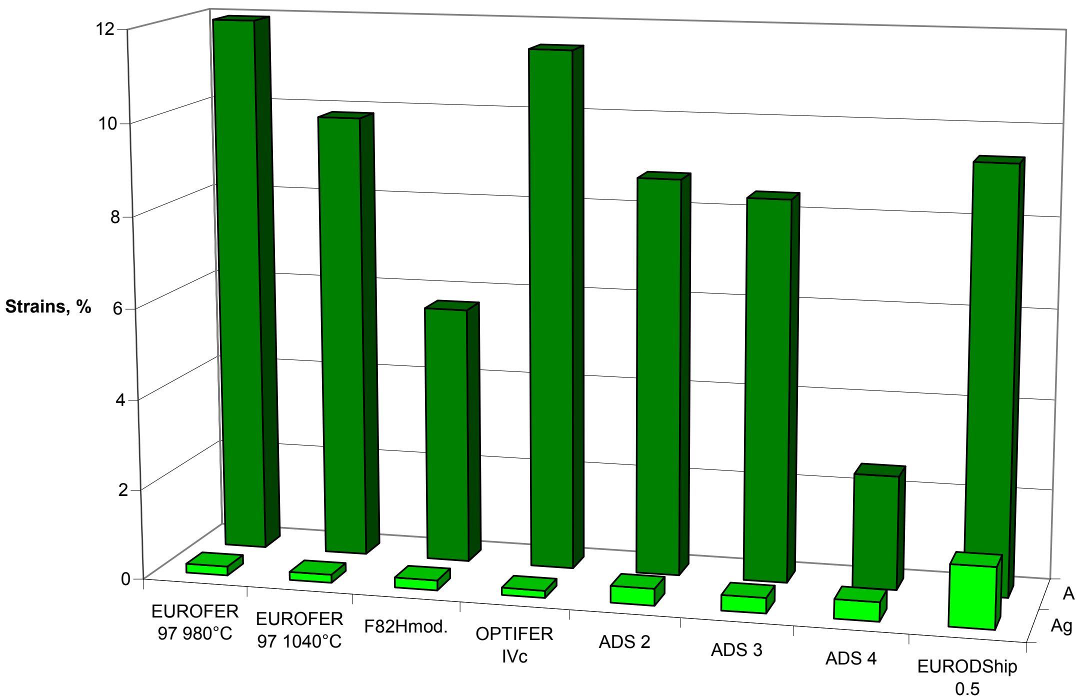

Fig. 4-18 Comparison of Uniform Strain (A_g) and Total Strain (A) behaviour of 30,2 dpa, 336°C irradiated RAF/M materials tested at 350°C

The Uniform Strain (A_g) and Total Strain (A) behaviour of 30,2 dpa, 336°C irradiated RAF/M materials tested at 350°C in Fig. 4-18 show the dramatic reduction of A_g after irradiation. The A-values of EUROFER 97 (980°C), OPTIFER IVc, ADS 2 and ADS 3 as well as EURODShip with 0.5%Y_2O_3, instead remain after irradiation above 8 % Total Strain. F82H mod. and ADS 4 remain on values of 5.7 % and 2.5 %, respectively.

The Reduction of Area (Z) behaviour of 30,2 dpa, 336°C irradiated RAF/M materials tested at 350°C in Fig. 4-19 gives with Z-values of above 40 % for EUROFER 97 (980°C and 1040°C), OPTIFER IVc and ADS 2 a result of good ductility, but for F82H mod., ADS 3, ADS 4 and EURODShip with 0.5%Y_2O_3, a real brittle behaviour.

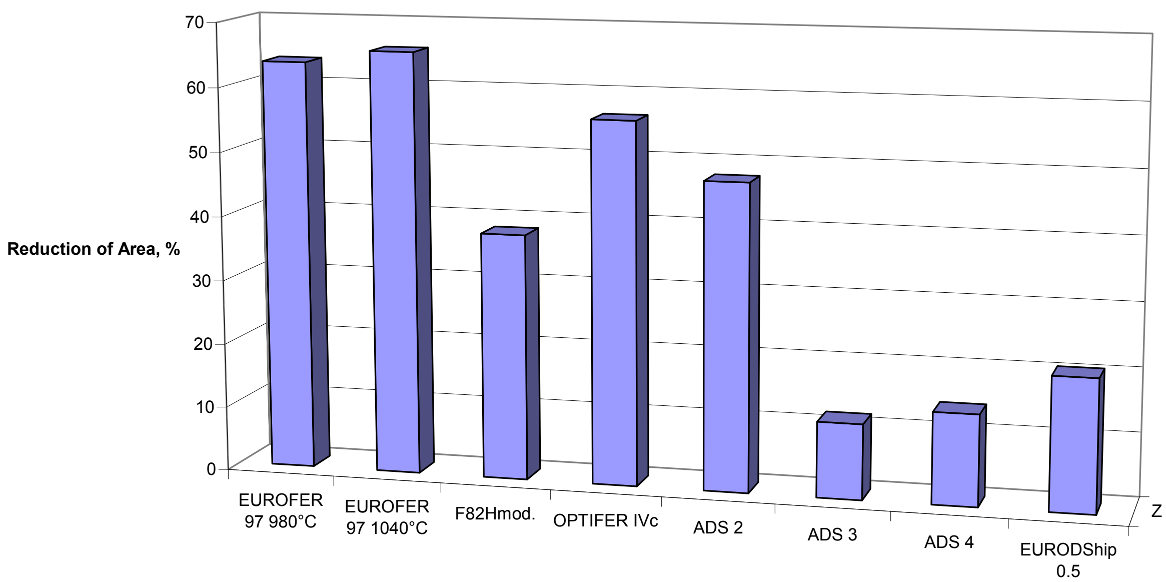

Fig. 4-19 Reduction of Area (Z) behaviour of 30,2 dpa, 336°C irradiated RAF/M materials tested at 350°C

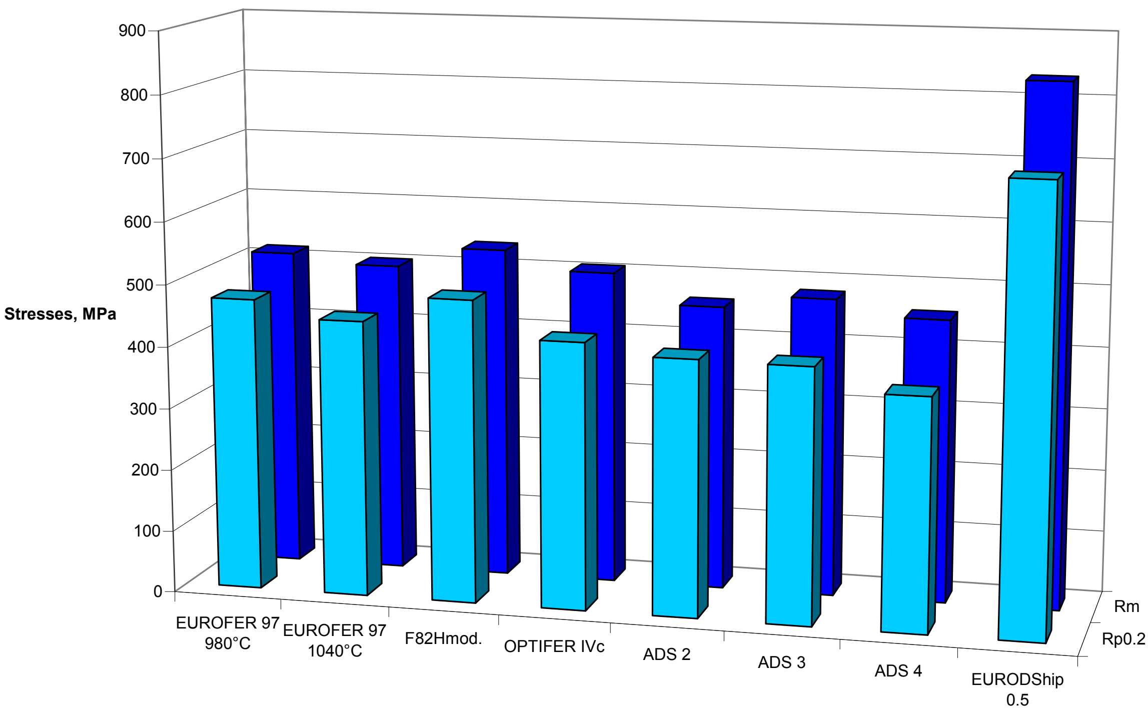

Fig. 4-20 Comparison of Yield Stress ($R_{p0,2}$) and Ultimate Tensile Strength (R_m) behaviour of unirradiated RAF/M materials tested at 350°C.

In Fig. 4-20 are displayed Yield Stress ($R_{p0,2}$) and Ultimate Tensile Strength (R_m) behaviour of cold reference materials tested at 350°C. The basic material results in a stress level around 500 MPa for EUROFER 97 (980°C), EUROFER 97 (1040°C), F82H mod., OPTIFER IVc, ADS 2, ADS 3 and ADS 4. Whereas for EURODShip with 0.5%Y_2O_3 had been measured values above 700 MPa. The stress increase between $R_{p0,2}$ and R_m is for all tested materials very similar in the cold reference state.

The Uniform Strain (A_g) and Total Strain (A) behaviour of cold reference materials tested at 350°C in Fig. 4-21 show for EUROFER 97 (980°C), EUROFER 97 (1040°C), F82H mod., OPTIFER IVc, ADS 2, ADS 3 and ADS 4, A_g–values between 2 % and 4 % strain, that is a good mean value for ferritic martensitic steels. The A_g–values of EURODShip with 0.5%Y_2O_3, reach values above 6 % strain.

In Fig. 4-21 the EUROFER 97 (980°C), EUROFER 97 (1040°C), F82H mod., OPTIFER IVc, ADS 2 and ADS 3 show with A-values above 20 % strain a high ductility. Total Strain values of ADS 4 and EURODShip with 0.5%Y_2O_3, remain slightly lover between 17 and 14 % strain, respectively.

The Reduction of Area (Z) behaviour of unirradiated RAF/M materials tested at 350°C show in Fig. 4-22 Z-values of around 90 % for EUROFER 97 (980°C) and ADS 4. Whereas EUROFER 97 (1040°C), F82H mod., OPTIFER IVc, ADS 2 and ADS 3 result around 95 % that demonstrate good ductility. Only EURODShip with 0.5%Y_2O_3, is with Z-values of 85 % a little bit less ductile.

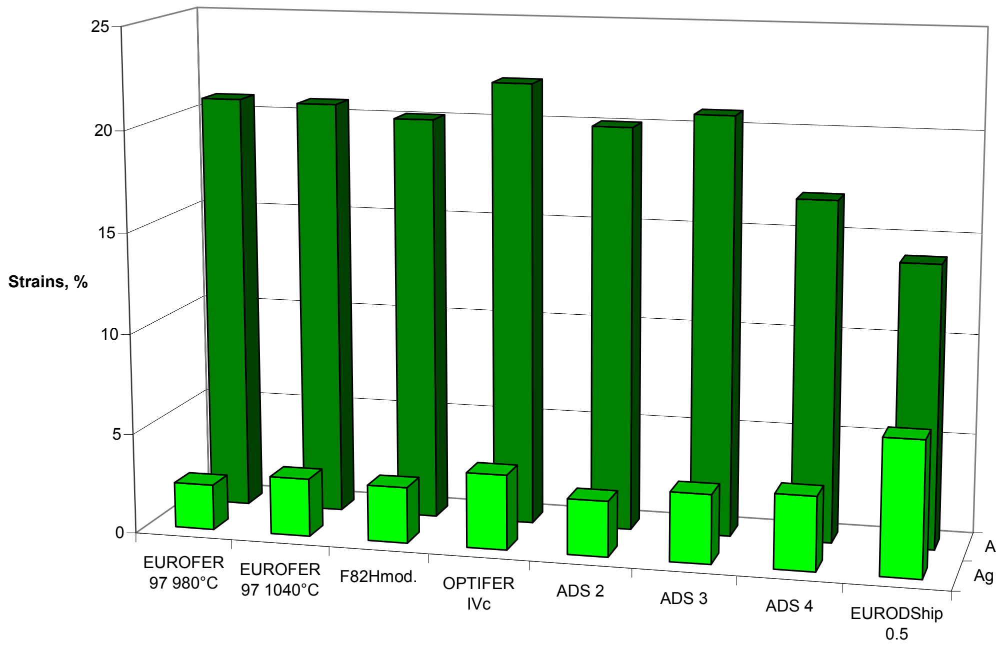

Fig. 4-21 Comparison of Uniform Strain (A_g) and Total Strain (A) behaviour of unirradiated RAF/M materials tested at 350°C.

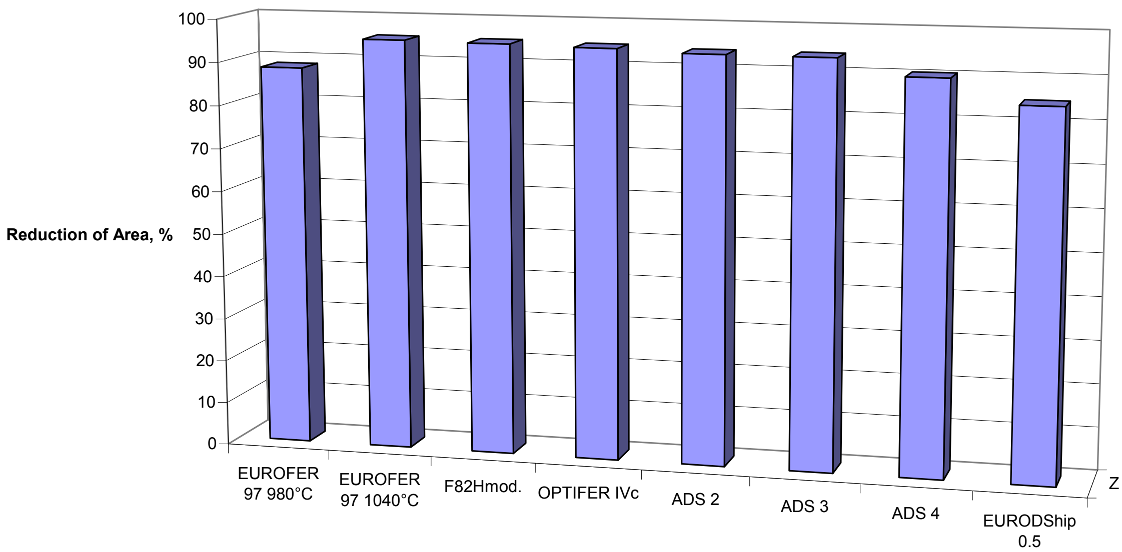

Fig. 4-22 Reduction of area (Z) behaviour of unirradiated RAF/M materials tested at 350°C.

In Fig. 4-23 are displayed ratios of Yield Stress ($\Delta R_{p0,2}$) and Ultimate Tensile Strength (ΔR_m) of cold reference materials to 30,2 dpa, 336°C irradiated material tested at 350°C. EUROFER 97 (980°C), is hardening in respect to $\Delta R_{p0,2}$ by 458 MPa and EUROFER 97 (1040°C) a little bit higher by 471 MPa, whereas F82H mod. reaches only an $\Delta R_{p0,2}$-value of 425 MPa. OPTIFER IVc however, increase in Yield Stress by 503 MPa. The influence of the increasing Boron doping in ADS 2, ADS 3 and ADS 4 is found in increasing $\Delta R_{p0,2}$-values of 477, 508 and 669 MPa, respectively. Whereas for EURODShip with 0.5%Y_2O_3 hardens in $\Delta R_{p0,2}$-only by 337 MPa.

The ratio of Ultimate Tensile Strength (ΔR_m) of cold reference materials to 30,2 dpa, 336°C irradiated material tested at 350°C (Fig. 4-23) is for EUROFER 97 (980°C) and EUROFER 97 (1040°C) very similar by 414 MPa, whereas F82H mod. reaches only an ΔR_m-value of 379 MPa. OPTIFER IVc and ADS 2 are very similar in this quantity with ΔR_m-values of 432 MPa. ADS 3 and ADS 4 instead show increasing ΔR_m-values of 444 and 603 MPa, respectively. Whereas for EURODShip with 0.5%Y_2O_3 hardens in ΔR_m-only by 248 MPa. The reason is the very high R_m-value of 834 MPa of the unirradiated material.

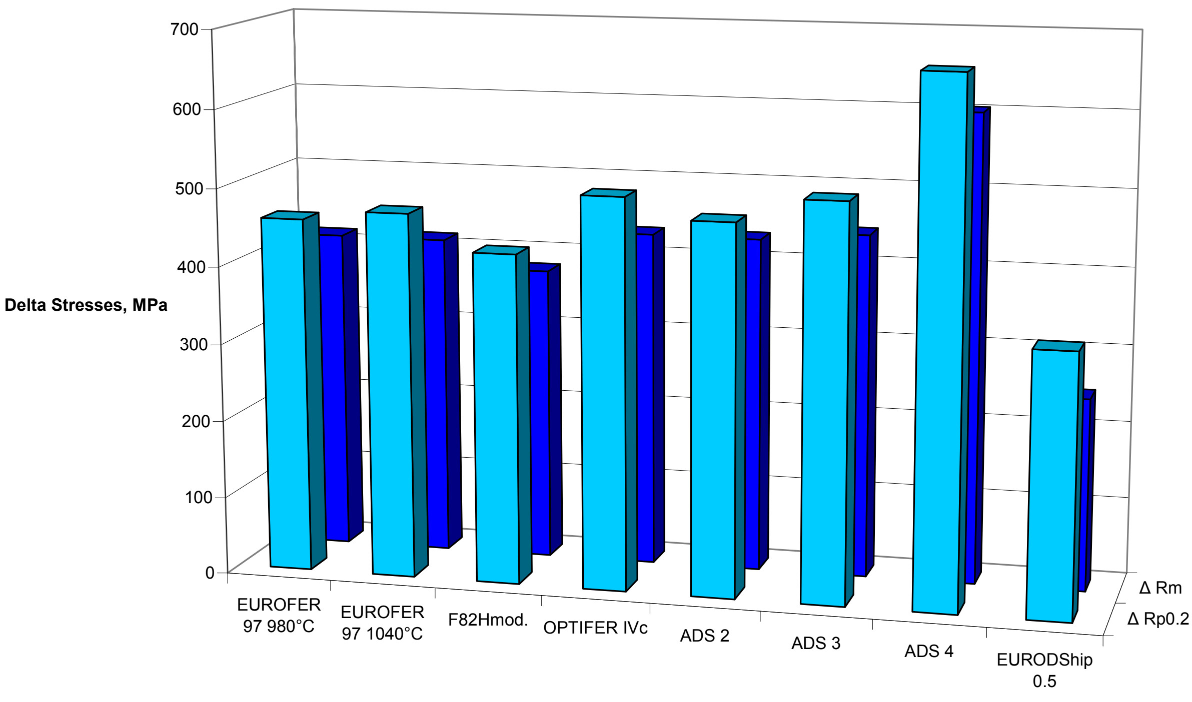

Fig. 4-23 Irradiation induced increase of Yield Stress ($\Delta R_{p0,2}$) and Ultimate Tensile Strength (ΔR_m) behaviour of 30,2 dpa, 336°C irradiated RAF/M materials tested at 350°C.

In Fig. 4-24 are displayed ratios of Uniform Strain (ΔA_g) and Total Strain (ΔA) of cold reference materials to 30,2 dpa, 336°C irradiated material tested at 350°C. Uniform Strain of EUROFER 97 (980°C), is reduced to ΔA_g by – 2.07 % and of EUROFER 97 (1040°C) a little bit lower by – 2.71 %, whereas F82H mod. reaches only an ΔA_g-value of – 2.57 %. OPTIFER IVc however, has a higher reduction of ΔA_g by – 3.58 %. The influence of the increasing Boron doping in ADS 2, ADS 3 and ADS 4 is found in regular ΔA_g-values between – 2.40 and –

3.26 %, respectively. Whereas for EURODShip with 0.5%Y_2O_3 has the highest reduction of ΔA_g by – 5.38 %.

The ratio of Total Strain (ΔA) of cold reference materials to 30,2 dpa, 336°C irradiated material tested at 350°C (Fig. 4-24) is for EUROFER 97 (980°C) reduced to ΔA by – 8.88 % and of EUROFER 97 (1040°C) a little bit lower by – 10.86 %, whereas F82H mod. reaches the lowest ΔA-value of – 14.43 %. OPTIFER IVc however, has a similar reduction of ΔA as EUROFER 97 (1040°C) by – 10.57 %. The influence of the increasing Boron doping in ADS 2, ADS 3 and ADS 4 is found in a continuous reduction of ΔA-values between – 11.31 and – 14.38 %, respectively. Whereas for EURODShip with 0.5%Y_2O_3 has the lowest reduction of ΔA by – 4.68 %.

The ratio of Reduction of Area (ΔZ) of unirradiated RAF/M materials tested at 350°C show in Fig. 4-25 ΔZ-values of around – 25 to - 30 % for EUROFER 97 (980°C) and EUROFER 97 (1040°C). Whereas, F82H mod. has a much higher reduced value of ΔZ-values of – 57.03 %. With OPTIFER IVc we received a ΔZ-value of – 38.54 %, In the ADS 2, ADS 3 and ADS 4 series ΔZ-values are much lower and reach at ADS 3 with ΔZ of – 82.35 % the lowest amount of ductility. Also EURODShip with 0.5%Y_2O_3, is with a ΔZ-value of – 64.22 % a little bit less ductile.

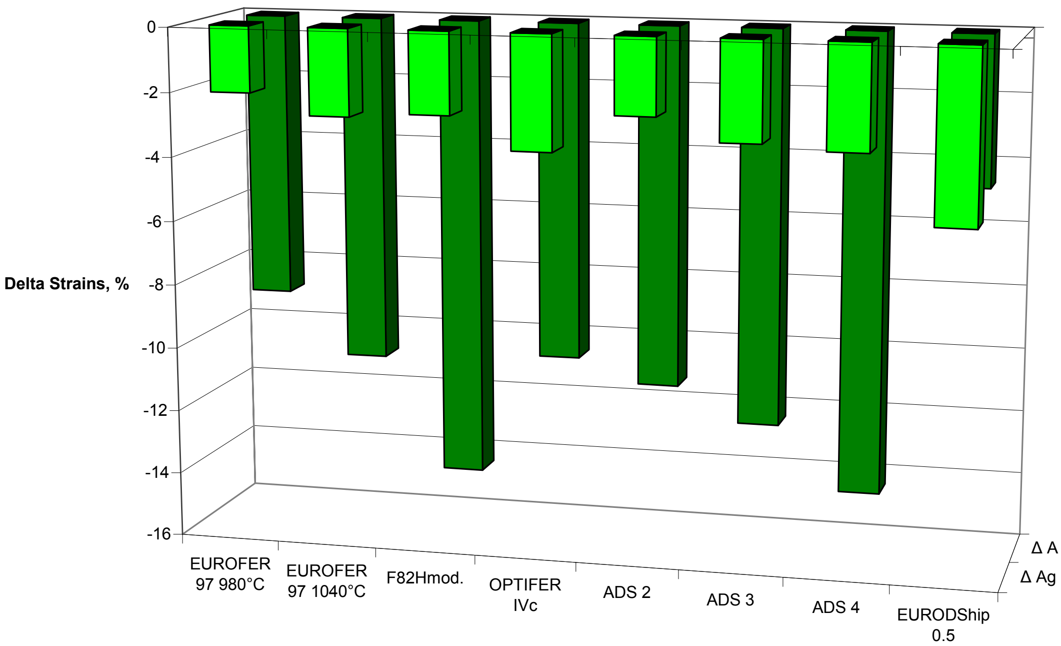

Fig. 4-24 Irradiation induced decrease of Uniform Strain (ΔA_g) and Total Strain (ΔA) behaviour of 30,2 dpa, 336°C irradiated RAF/M materials tested at 350°C

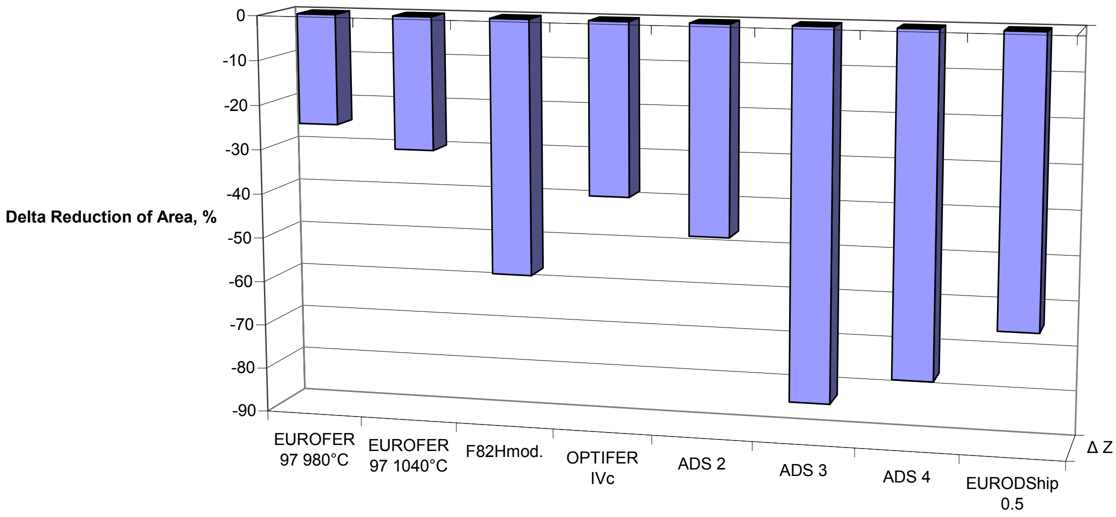

Fig. 4-25 Irradiation induced decrease of Reduction of area (ΔZ) behaviour of 30,2 dpa, 336°C irradiated RAF/M materials tested at 350°C

4.3 Low Cycle Fatigue Testing

The Low Cycle Fatigue (LCF) behaviour of RAFM steels irradiated to a displacement damage doses up to 31 dpa at 331 °C in the ARBOR 1 irradiation programme are reported and compared to other literature values, if available. The gripping of the LCF specimen is shown in Fig. 10-1 of Annex C. The RIAR analysis is shown in Annex C for EUROFER 97 (980°C) in the Figs. 10-2 to 10-11 of chapter 10.1, for EUROFER 97 (1040°C) in the Figs. 10-12 to 10-19 of chapter 10.2, for F82H mod. in the Figs. 10-20, 10-21 and 10-24 to 10-29 of chapter 10.3, for EURODShip with 0.5%Y_2O_3 in the Figs. 10-30, 10-31 and 10-34 to 10-39 of chapter 10.4, for electron beam welded EUROFER 97, EB in the Figs. 10-40 to 10-47 of chapter 10.5 and for BS-EUROFER in the Figs. 10-48 to 10-55 of chapter 10.6. Selected SEM micrographs of broken specimens of F82H mod. (Figs. 10-22 and 10-23) and EURODShip with 0.5%Y_2O_3 (Figs. 10-32 and 10-33) are found there.

The RIAR criterion to determine Nf was defined at a point where peak tensile stress of a cycle decreased by 10% from an extrapolation line of peak tensile stresses vs. number of cycles (N). Therefore the Nf results differ between our analysis and that of RIAR. Another difference is in the amount of irradiation damage, because RIAR took the calculated model value and we the mean value of neutron detectors.

The comparison with the corresponding results in the unirradiated reference state was performed with data of experiments in total strain control.

Small size cylindrical specimens of 7.0 mm gauge length and 2 mm diameter were used for the investigation of LCF properties. The strain controlled Low Cycling Fatigue loading was performed at a constant temperature of 330 °C with different total strain ranges ($\Delta\varepsilon_{tot}$) between 0.6 and 1.2% and a strain rate of $3x10^{-3}$ s^{-1}. The number of cycles to failure (N_f) was defined at a point where peak tensile stress of a cycle decreased by 30% from an extrapolation line of peak tensile stresses vs. number of cycles (N).

In the upper half of Tabs. 4-6 to 4-11 are listed the reference results of unirradiated specimens - in most cases - two tests per total strain range. The lower half of the Tables contain test results of the irradiated specimens, where only one test per parameter was possible.

EUROF 1 980°C, 31 min/air + 760°C, 90 min/air

Strain rate: 3x10 -3 [1/s].

EUROFER 97, 980°C (EUROF 1), unirr.

Specimen	Temp,°C	delta epsilon,%	$N_{f\ unirr}$, -
1	330	0,8	1324
2	330	0,9	1258
3	330	1,0	907
4	330	1,2	763
5	330	0,8	1556
6	330	0,9	1470
7	330	1,0	736
8	330	1,2	572
10	330	0,6	2400
11	330	0,6	2250

EUROFER 97, 980°C (EUROF 1) irr., 31 dpa, 331°C,

Specimen, Test	Temp,°C	delta epsilon,%	$N_{f\ irr}$, -	
E 103 , 1_747-1_753	330	0,81	20102	
E 104 , 1_773	330	0,91	2526	
E 102 , 1_741	330	1,01	769	
E 101 , 1_736	330	1,21	14	
E 105 , 1_759	330	0,90	3	not valid

Tab. 4-6 LCF data of unirradiated and irradiated EUROFER 97, as received.

The comparison of irradiated and unirradiated cyclically loaded specimens of EUROFER 97 (980°C), shown in Tab. 4-6 and Fig. 4-26, leads after LCF testing to an ambiguous behaviour. The results of the 31 dpa irradiation damage at 331°C can be described by two effects. The first one occurs at high total strain ranges, $\Delta\varepsilon_{tot}$ > 1 % where the material is loaded remarkably over the yield stress point. Therefore in the second cycle no additional strain hardening takes place and thus the numbers of cycles to failure are smaller than under unirradiated conditions. Furthermore this effect should increase with increasing irradiation damage.

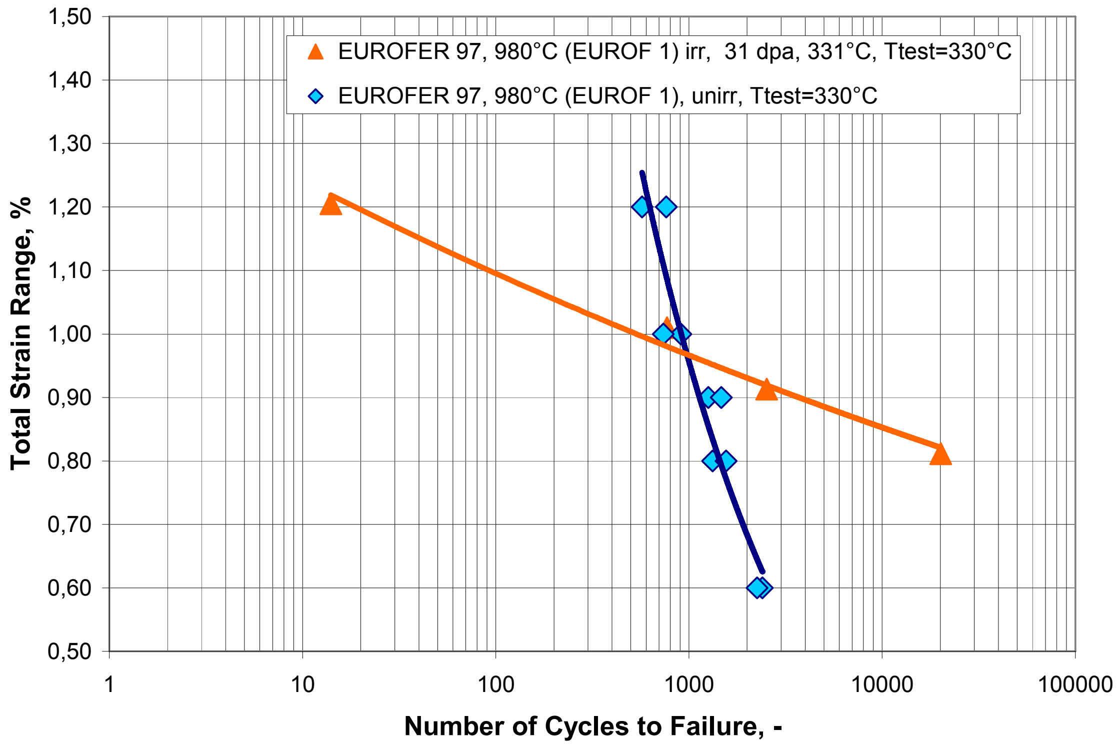

Fig. 4-26 Effect of irradiation on the LCF behaviour of EUROFER 97, as received.

The second effect occurs at low total strain ranges, $\Delta\varepsilon_{tot} < 1$ % where the numbers of cycles to failure of irradiated specimens are increasing. Analysing the hysteresis loops, very narrow loops are recorded with little plastic strain contribution only. This is due to the irradiation induced damage, which raised the yield stress point above the elastic strain range with increasing irradiation damage.

Also for the 31 dpa irradiated EUROFER 97 (1040°C), shown in Tab. 4-7 and Fig. 4-27 a similar tendency was found in LCF testing, but the increase in numbers of cycles to failure for lower total stain ranges is not as high as for EUROFER 97 (980°C).

EUROF 2 1040°C, 31 min/air + 760°C, 90 min/air

Strain rate: 3x10 -3 [1/s].

EUROFER 97, 1040°C (EUROF 2), unirr.

Specimen	Temp,°C	delta epsilon,%	$N_{f\ unirr}$, -
1	330	0,8	1438
2	330	0,9	1574
3	330	1,0	1172
4	330	1,2	750
5	330	0,8	1623
6	330	0,9	1137
7	330	1,0	1285
8	330	1,2	582

EUROFER 97, 1040°C (EUROF 2) irr., 31 dpa, 331°C,

Specimen, Test	Temp,°C	delta epsilon,%	$N_{f\ irr}$, -
E 202 , 1_581-1_586	330	0,81	7993
E 204 , 1_597-1_606	330	0,92	1634
E 201 , 1_569-1_573	330	1,01	1437
E 203 , 1_591	330	1,21	906

Tab. 4-7 LCF data of unirradiated and irradiated EUROFER 97, heat treated.

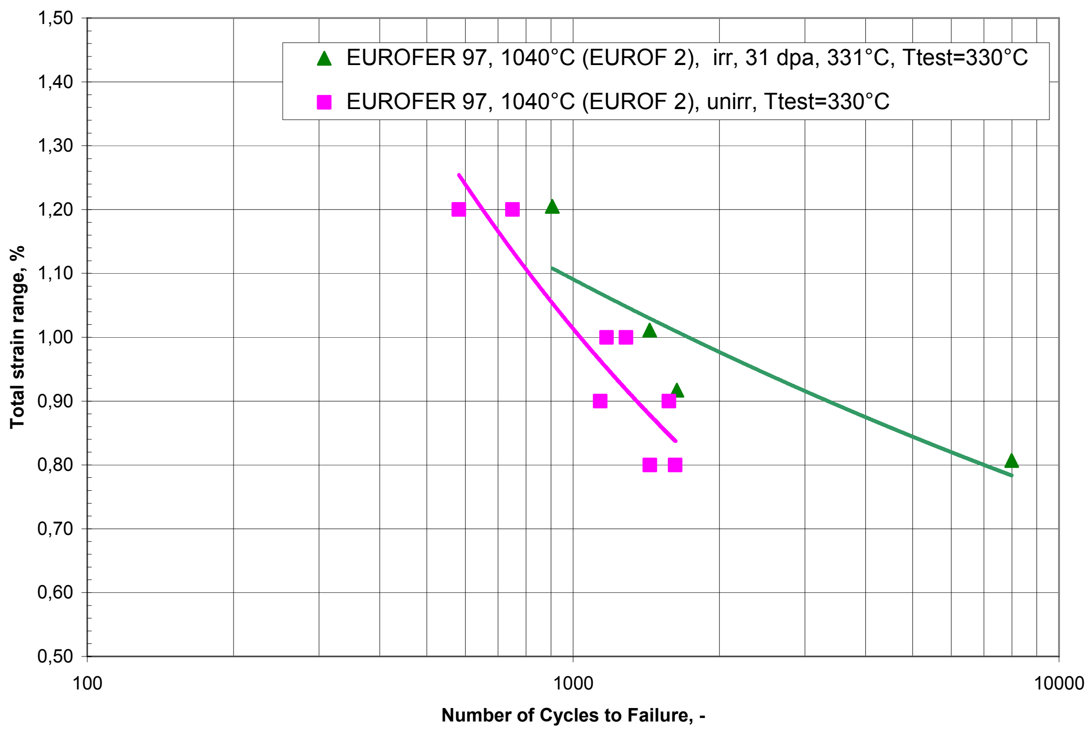

Fig. 4-27 Effect of irradiation on the LCF behaviour of EUROFER 97, heat treated.

F82H mod. 1040°C, 38 min/air + 750°C, 2h/air
Strain rate: 3x10 -3 [1/s].
F82H mod., 1040°C, unirr.

Specimen	Temp,°C	delta epsilon,%	$N_{f\ unirr}$, -
1	330	0,8	1430
2	330	0,9	1232
3	330	1,0	1293
4	330	1,2	768
5	330	0,8	1763
6	330	0,9	1668
7	330	1,0	1181
8	330	1,2	627
10	330	0,6	3500
11	330	0,6	2400

F82H mod., 1040°C irr., 31 dpa, 331°C,

Specimen, Test	Temp,°C	delta epsilon,%	$N_{f\ irr}$, -
F05 , 1_697	330	0,8020	4757
F04 , 1_691	330	0,9050	1222
F02 , 1_685	330	1,0070	1324
F01 , 1_678	330	1,2090	806

Tab. 4-8 LCF data of unirradiated and irradiated F82H mod., as received.

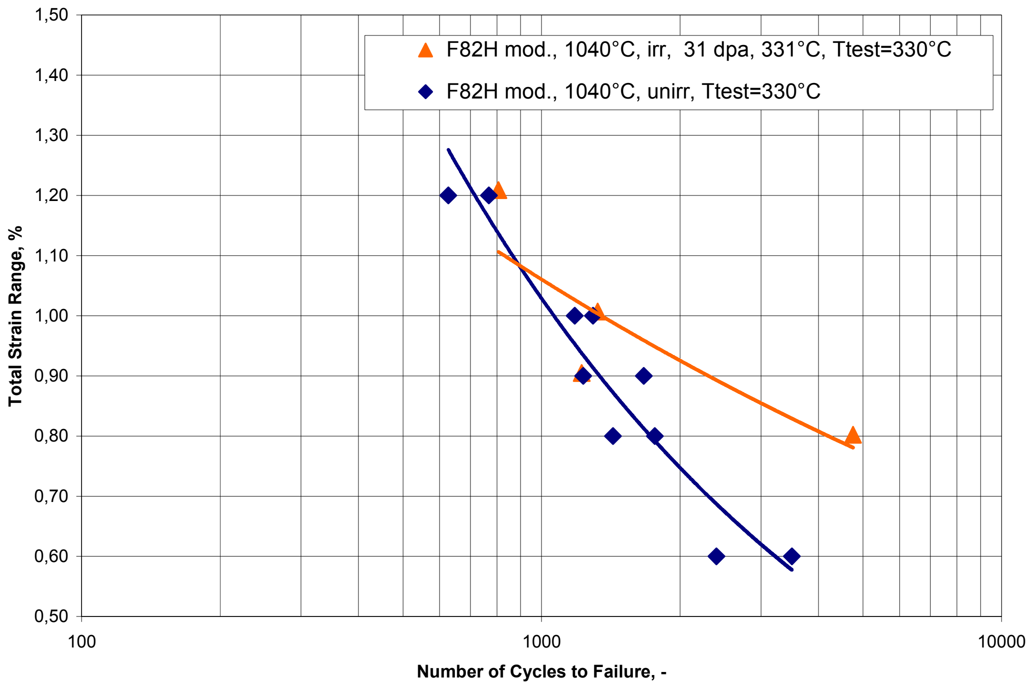

Fig. 4-28 Effect of irradiation on the LCF behaviour of F82H mod.

Also for the 31 dpa irradiated F82H mod., shown in Tab. 4-8 and Fig. 4-28 a similar tendency was found in LCF testing, but the increase in numbers of cycles to failure for lower total stain ranges is not as high as for EUROFER 97 (1040°C).

In Figs. 10-22 and 10-23 of chapter 10.3 of Annex C scanning electron beam micrographs of broken specimens of the fife LCF experiments on F82H mod. are shown. The cracks are starting from the surface and damaging the specimen in each loading cycle as can be detected on the cleavage appearance of the fracture surface. Which role the detected surface change is playing, that is supposed to be generated during the sodium contact of the specimen during irradiation campaign, should be analysed in more detail during microstructural analysis at FZK.

EURDShip 980°C, 31 min/air + 760°C, 90 min/air
Strain rate: 3x10 -3 [1/s].
EURODShip, 980°C, unirr,

Specimen	Temp,°C	delta epsilon,%	$N_{f\ unirr}$, -
1	330	0,8	1931
2	330	0,9	1850
3	330	1,0	551
4	330	1,2	325
5	330	0,8	1358
6	330	0,9	941
7	330	1,0	1112
8	330	1,2	339
9	330	0,6	9250
12	330	0,6	9250

EURODShip, 980°C, irr, 31 dpa, 331°C

Specimen, Test	Temp,°C	delta epsilon,%	$N_{f\ irr}$, -
E O06 , 1_722-1_729	330	0,7950	8398
E O08 , 1_709	330	0,8980	2144
E O03 , 1_704	330	1,0050	388
E O01 , 1_716	330	1,2040	295

Tab. 4-9 LCF data of unirradiated and irradiated EUROFER 97 with 0.3 % Y_2O_3, heat treated.

As ODS-EUROFER 97 with 0,5 % Y_2O_3 had also been included in the ARBOR 1 irradiation, the results of LCF testing of these specimens after irradiation to 31 dpa damage at 331°C seems really encouraging. In Tab. 4-9 and Fig. 4-29 the LCF behaviour after irradiation is compared to that of unirradiated specimens. Even if the material reaches in the unirradiated state at higher total strain ranges, $\Delta\varepsilon_{tot} > 1$ %, the lowest numbers of cycles to failure, compared to EUROFER 97 (980 and 1040°C) and F82H mod., the increase of numbers of cycles to failure in the lower total strain ranges, $\Delta\varepsilon_{tot} < 1$ %, is remarkable. At low total strain ranges a higher number of cycles to failure could be achieved on irradiated ODS-EUROFER 97 with 0,5 % Y_2O_3, than for F82H mod.. The above mentioned influence of irradiation on LCF behaviour was found also on this material.

In Figs. 10-32 and 10-33 scanning electron beam micrographs of broken specimens are shown. The crack appearance is completely changed compared to conventional ferritic/martensitic steels and the broken surface is very fine structured and flat. Which role the detected surface change is playing, that is supposed to be generated during the sodium contact of the specimen during irradiation campaign, should be analysed in more detail during microstructural analysis at FZK.

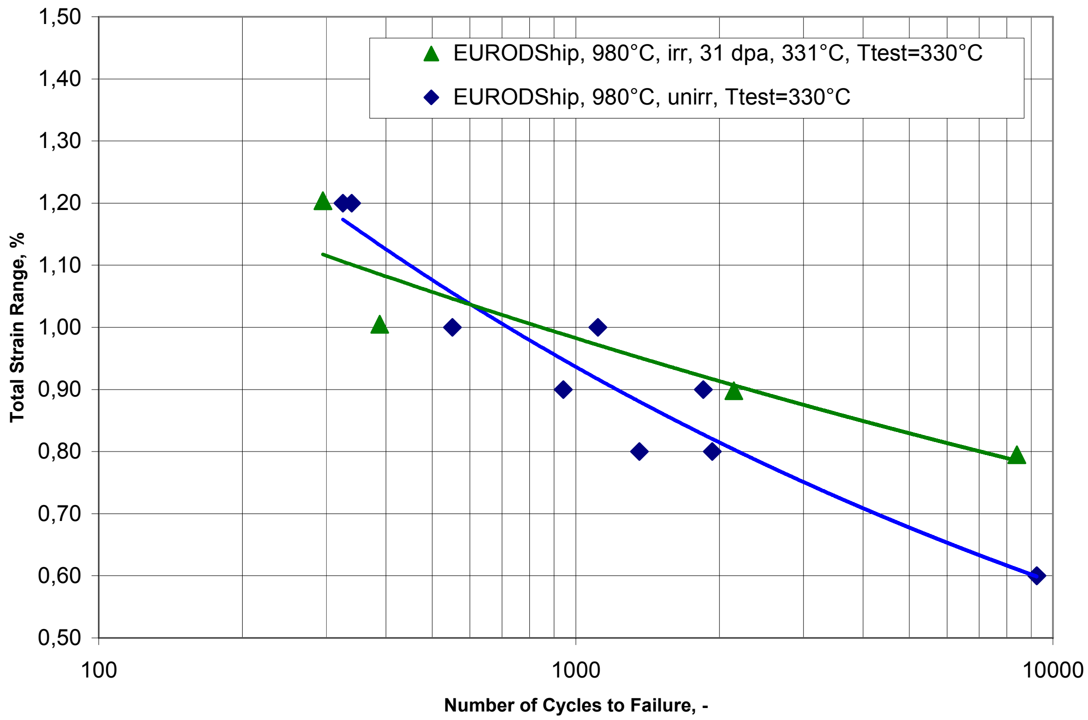

Fig. 4-29 Effect of irradiation on the LCF behaviour of ODS-EUROFER with 0,5 % Y_2O_3

To compare the LCF behaviour of EUROFER 97-NRG only reference data of the NRG report [22] where available and even if specimen sizes and raw materials for specimens preparation are different the findings are similar. For comparison also NRG results of a 2 dpa irradiation at 300°C had been taken from the same report.

All tests at NRG were performed at 300°C, to avoid effects of creep. The applied total strain ranges are from 0.6 to 1.4 %. All tests were continued until complete separation occurred, but the N_f-values reported from NRG followed the criterion of 50 % of the first stress cycle. The strain rates were mostly $1x10^{-3}$ s^{-1}, but some tests were done at $6x10^{-4}$ s^{-1}.

In Tab. 4-10 and Fig. 4-30 the LCF behaviour of EUROFER 97-NRG after irradiation is compared to that of unirradiated specimens. The EUROFER 97-NRG material reaches in the unirradiated state for all total strain ranges higher numbers of cycles to failure, compared to EUROFER 97 (980°C). The increase of numbers of cycles to failure in the lower total strain ranges, $\Delta\varepsilon_{tot}$ < 1 %, is for the 31 dpa irradiated material not so remarkable. But compared to the results of NRG's 2 dpa data the tendency of the behaviour is similar. At higher total strain ranges, $\Delta\varepsilon_{tot}$ > 1 %, lower number of cycles to failure could be achieved for both irradiation conditions.

EUROFER 97-NRG 980°C, 31 min/air + 760°C, 90 min/air
Strain rate: 3x10 -3 [1/s].
EUROFER 97-NRG, 14 mm plate, unirr.

Specimen	Temp,°C	delta epsilon,%	$N_{f\ unirr}$, -
no info	300	0,6	4794
no info	300	0,6	5819
no info	300	1,0	2265
no info	300	1,0	1525
no info	300	1,4	804
no info	300	1,4	1047
no info	300	0,6	6066
no info	300	1,0	1706
no info	300	1,4	1080

EUROFER 97-NRG, 14 mm plate, irr., 2 dpa, Tirr = Ttest = 300°C

Specimen	Temp,°C	delta epsilon,%	$N_{f\ unirr}$, -
no info	300	0,6	16449
no info	300	0,6	9808
no info	300	1,0	1269
no info	300	1,0	1717
no info	300	1,4	482
no info	300	1,4	706

BS-EUROFER, 1050°C, irr., 31 dpa, 331°C,

Specimen, Test	Temp,°C	delta epsilon,%	$N_{f\ irr}$, -
A904 , 1_646	330	0,81	2912
A903 , 1_640	330	0,90	3024
A901 , 1_625	330	1,00	1555
A902 , 1_632	330	1,21	729

Tab. 4-10 LCF data of unirradiated and irradiated EUROFER 97-NRG.

EUROFER-EB as received, post weld heat treatment 730°C 2h/AC
Strain rate: 3x10 -3 [1/s].
EUROFER-EB, as received + PWHT, irr, 31 dpa, 331°C

Specimen, Test	Temp,°C	delta epsilon,%	$N_{f\ irr}$, -
C090 , 1_658	330	0,81	1162
C089 , 1_664-1_665	330	0,91	869
C088 , 1_672	330	1,01	512
C087 , 1_654	330	1,20	24

Tab. 4-11 LCF data of irradiated EUROFER 97-EB, PWHT.

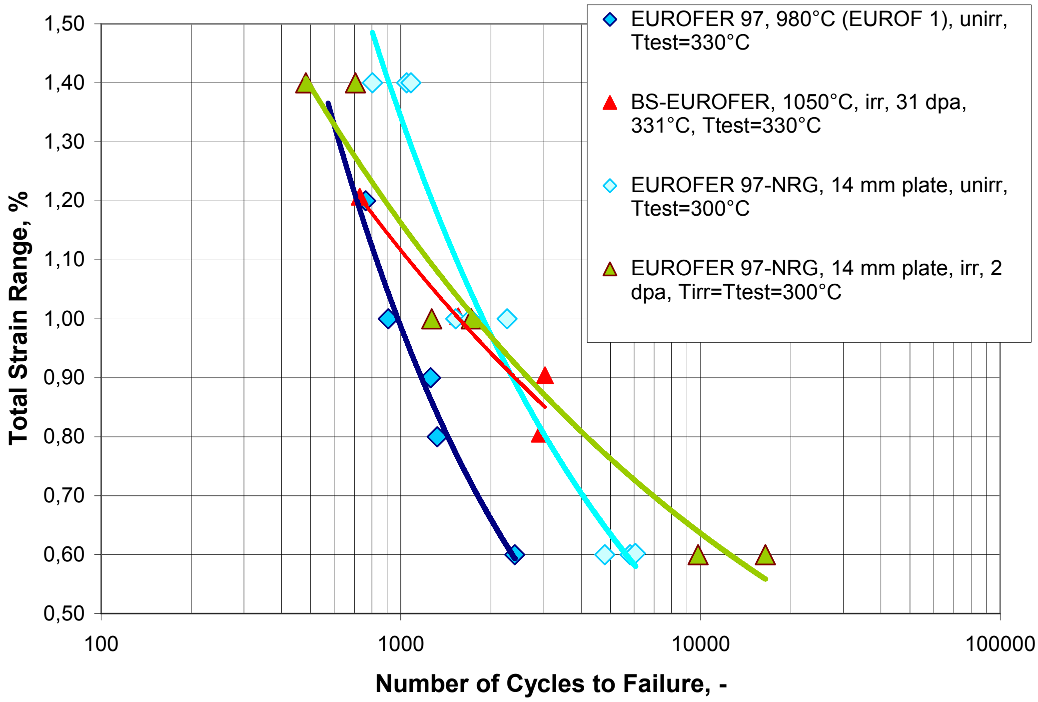

Fig. 4-30 Effect of irradiation on the LCF behaviour of BS-EUROFER and comparison to EUROFER 97, as received, unirradiated as well as to EUROFER 97-NRG results after 2 dpa.

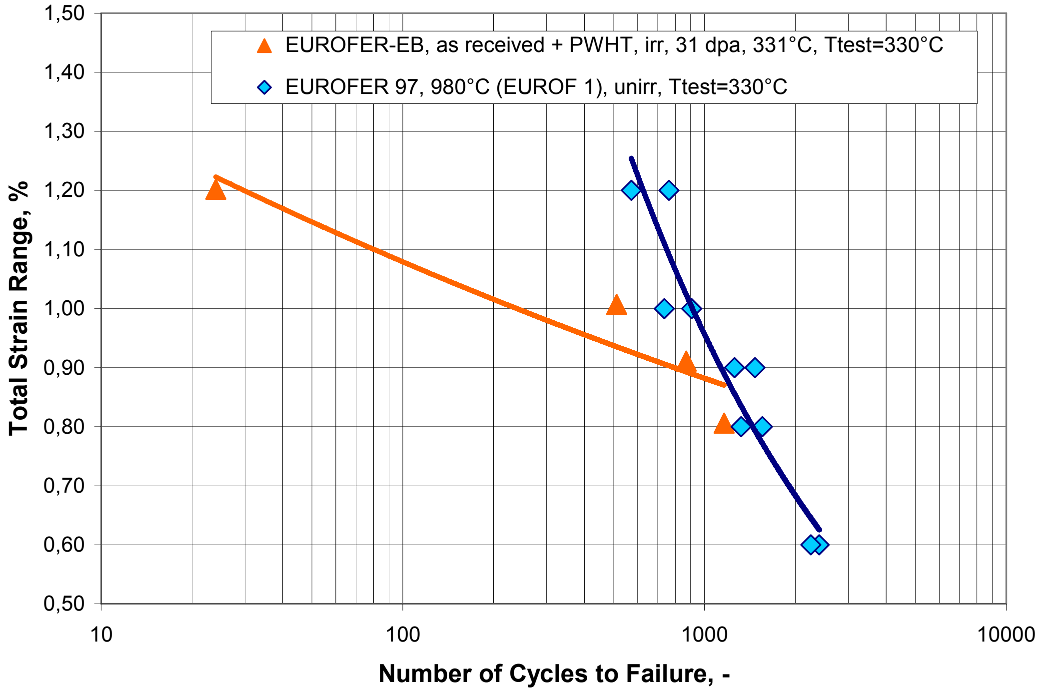

Fig. 4-31 Effect of irradiation on the LCF behaviour of EUROFER 97-EB and comparison to EUROFER 97, as received, unirradiated.

In Tab. 4-11 and Fig. 4-31 the LCF behaviour of EUROFER 97-EB specimens of NRG after irradiation is compared to that of unirradiated EUROFER 97 (980°C) specimens, because no reference data of EUROFER 97-EB had been available. The EUROFER 97-EB material reaches in the 31 dpa irradiated state for all total strain ranges lower numbers of cycles to failure, compared to unirradiated EUROFER 97 (980°C) and to 31 dpa irradiated BS-EUROFER (see Fig. 4-30). At higher total strain ranges, $\Delta\varepsilon_{tot}$ > 1 %, much lower number of cycles to failure could be achieved. But in no cases an unusual fracture due to the welding procedure was detected.

5 Conclusions

During the ARBOR 1 irradiation in the fast sodium cooled reactor BOR 60 of RIAR RAF/M steels, as EUROFER 97 (980°C), EUROFER 97 (1040°C), F82H mod., OPTIFER IVc, Boron doped EUROFER 97 with ADS 2, ADS 3 and ADS 4, EURODShip with 0.5%Y_2O_3, as well as NRG's BS-EUROFER and EUROFER-EB, had been irradiated up to 30 dpa at an irradiation temperature of 330 °C. The postirradiation examination of mechanical properties by impact, tensile and LCF testing had been performed in the hot laboratory of RIAR under the ISTC Partner contract #2781p.

All examined materials have shown in post irradiation instrumented impact tests a significant increase in the Ductile to Brittle Transition Temperature as an effect of irradiation.

During tensile testing strength values are increasing and strain values reduced due to substantial irradiation hardening. The hardening rate is decreasing with increasing damage level. Tensile hardening does not reach saturation up to 30 dpa irradiation damage at an irradiation temperature of 330 °C. A model describing radiation hardening is working well for tensile properties.

The low cycle fatigue behaviour of most examined RAF/M - steels show at total strain amplitudes below 1 % an increase of number of cycles to failure, due to irradiation hardening.

50 % of the specimens irradiated in the ARBOR 1 irradiation had been implemented in the ARBOR 2 irradiation rig to reach an irradiation damage of 70 dpa.

6 References

[1] M. Rieth, B. Dafferner, H. Ries, O. Romer, Bestrahlungsprogramm MANITU: Ergebnisse der Kerbschlagbiegeversuche mit den bis 0,8 dpa bestrahlten Werkstoffen der ersten Bestrahlungsphase, Forschungszentrum Karlsruhe, FZKA 5619, September 1995.

[2] M. Rieth, B. Dafferner, H.-D. Röhrig, Charpy impact properties of low activation alloys for fusion applications after neutron irradiation, Journal of Nuclear Materials 233 – 237 (1996) 351-355.

[3] M. Rieth, B. Dafferner, H. Ries, O. Romer, Bestrahlungsprogramm MANITU: Ergebnisse der Kerbschlagbiegeversuche mit den bis 0,2 dpa bestrahlten Werkstoffen, Forschungszentrum Karlsruhe, FZKA 5750, April 1997.

[4] M. Rieth, B. Dafferner, H.-D. Röhrig, Embrittlement behaviour of different international low activation alloys after neutron irradiation, Journal of Nuclear Materials 258 – 263 (1998) 1147-1152.

[5] H.-C. Schneider, M. Rieth, B. Dafferner, H. Ries, O. Romer, Bestrahlungsprogramm MANITU: Ergebnisse der Kerbschlagversuche mit den bis 0,8 dpa bestrahlten Werkstoffen der zweiten Bestrahlungsphase, Forschungszentrum Karlsruhe, FZKA 6519, September 2000.

[6] E. Gaganidze, B. Dafferner, H. Ries, R. Rolli, H.-C. Schneider, J. Aktaa, Irradiation Programme HFR Phase IIb – SPICE Impact testing on up to 16.3 dpa irradiated RAFM steels, Forschungszentrum Karlsruhe, FZKA 7371, April 2008.

[7] C. Petersen, D. Rodrian, BOR 60 Irradiation Programme Status Report October 2002: End of Irradiation, Forschungszentrum Karlsruhe, Internal FZKA Report FUSION 203, March 2003, Revised Edition 2007.

[8] A.I.Tellin, D.K.Ryazanov, N.V. Markina, G.I. Gadzhiev, Experimental Study of Space-Energy Neutron Distribution in the BOR-60 Reactor, Preprint RIAR-1(853), Dimitrovgrad, 1996 (in Russian).

[9] Greenwood and R. K. Smither, SPECTER: Neutron Damage Calculations for Materials Irradiations, ANL/FPP/TM-197, 1985.

[10] N. E. Holden, R. L. Martin, I. L. Barnes, Isotopic Composition of the Elements 1983, Pure Appl. Chem. 56 (1984) 675.

[11] Nuclear Data Standards for Nuclear Measurements (Ed. H. Conde), NEANC-311U/INDC(SEC)-101, 1992

[12] A. Möslang and E. Diegele, “Development of small scale specimens for creep-fatigue testing in irradiation environment”, presented at ICFRM-10, Baden-Baden, Germany, October 14-19, 2001.

[13] C. Petersen, V. Shamardin, A. Fedoseev, G. Shimansky, V. Efimov and J. Rensman: “The ARBOR irradiation project”, Journal of Nuclear Materials 307 – 311 (2002) 1655-1659.

[14] C. Petersen: “ARBOR, Technical description for irradiation in the fast reactor BOR 60 of SSC RIAR”, Internal Report, PKF 31.02.02, Sept. 2000.

[15] C. Petersen, “ARBOR 2 Irradiation Programme Status Report October 2006: End of Irradiation”, Forschungszentrum Karlsruhe, Internal Report FUSION 300, March 2010

.

[16] C. Petersen, A. Povstyanko, V. Prokhorov, A. Fedoseev, O. Makarov, M. Walter, "Tensile and low cycle fatigue properties of different ferritic/martensitic steels after the fast reactor irradiation ARBOR 1", J. Nucl. Mater. 386–388 (2009) 299–302.

[17] C. Petersen, A. Povstyanko, V. Prokhorov, A. Fedoseev, O. Makarov, B. Dafferner, "Impact property degradation of ferritic/martensitic steels after fast reactor irradiation ARBOR 1", J. Nucl. Mater. 367–370 (2007) 544-549

[18] E. Gaganidze, H.-C. Schneider, B. Dafferner, J. Aktaa, "High-dose neutron irradiation embrittlement of RAFM steels", J. Nucl. Mater. 355 (2006) 83–88

[19] E. Gaganidze, H.-C. Schneider, C. Petersen, J. Aktaa, A. Povstyanko, V. Prokhorov, R. Lindau, E. Materna-Morris, A. Möslang, E. Diegele, R. Lässer, B. van der Schaaf, E. Lucon, "Mechanical Properties of Reduced Activation Ferritic/Martensitic Steels after High Dose Neutron Irradiation", presented at 22nd IAEA Fusion Energy Conference, 13.-18. October 2008, Geneva, Switzerland

[20] J. Aktaa, C. Petersen, "Modeling the influence of high dose irradiation on the deformation and damage behavior of RAFM steels under low cycle fatigue conditions", J. Nucl. Mater. 389 (2009) 432-435.

[21] A. D. Whapham, M. J. Makin, "The hardening of lithium fluoride by electron irradiation", Phil. Mag., 5, 51 (1960) 237-250.

[22] J.W. Rensman, "NRG irradiation testing: report on 300°C and 60°C irradiated RAFM steels", Final report on the EFDA Tasks TW2-TTMS-001a D 6 and TW2-TTMS-001b D 12, NRG Report Nr. 20023/05.68497/P, August 2005.

[23] E. Materna-Morris, A. Möslang, S. Baumgärtner, B. Dafferner, J. Ehrmann, E. Gaganidze, M. Holzer, S. Lautensack, H. Ries, R. Rolli, H.-C. Schneider, and H. Zimmermann, "Irradiation Programme HFR IIb (SPICE-T), Post-Irradiation Examinations after 16.3 dpa, –Tensile Properties, –Fatigue Properties, –Fractography and Structure Analysis after Charpy and Tensile Tests", Internal FZKA Report FUSION 323, Dec. 2008.

[24] E. Lucon and W. Vandermeulen: "Overview and critical Assessment of the Tensile properties of unirradiated and irradiated EUROFER 97", Report SCK.CEN-BLG-1042 REV.(1), Oct, 2007.

[25] A. Alamo, P. Wident and V. Shamardin: "Post-Irradiation Examinations (PIE) of materials irradiated in BOR60 at 325°C up to 42 dpa", Internal CEA report, DMN/SRMA/-2005-2767/A, March 2006.

7 Acknowledgement

The author thanks A. Povstyanko, V. Prokhorov, A. Fedoseev, O Makarov and all other persons of RIAR, who had been implemented in the ISTC Partner Contract #2781p, for the highly qualified performance of the PIE at the hot laboratory of RIAR.

M. Walter, B. Dafferner and M. Klotz are acknowledged for performing the cold reference experiments.

8 Annex A: Impact Tests

In the Annexes A to C are found the measured original data of all performed impact, tensile and LCF tests together with macro photos of the tested specimens and in some cases also a selection of REM pictures. All data are stored and available at the author or his successor.

8.1 EUROFER 97, as received

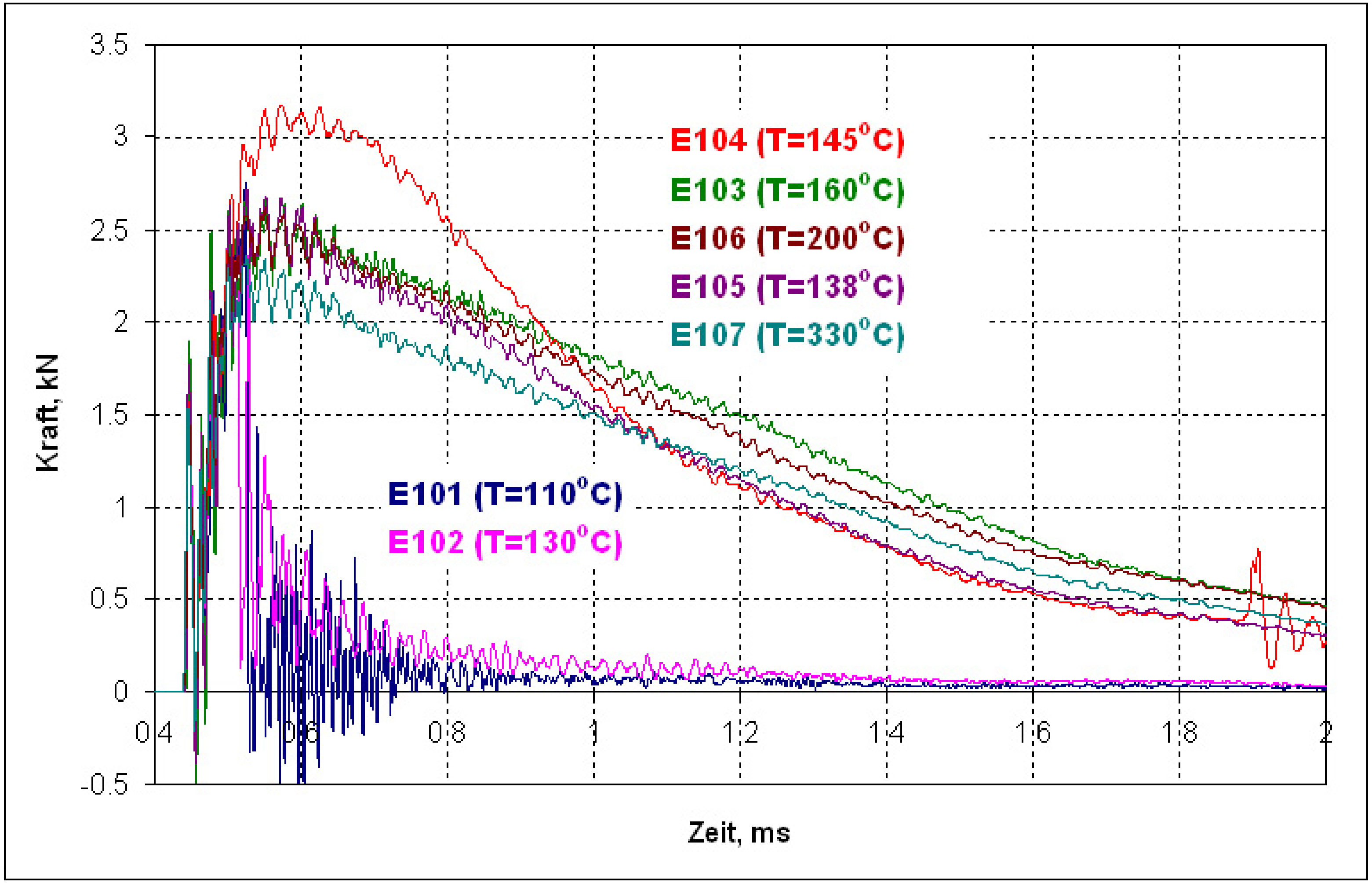

Fig. 8-1 Load-time diagrams of impact testing of E101 to E107 specimens

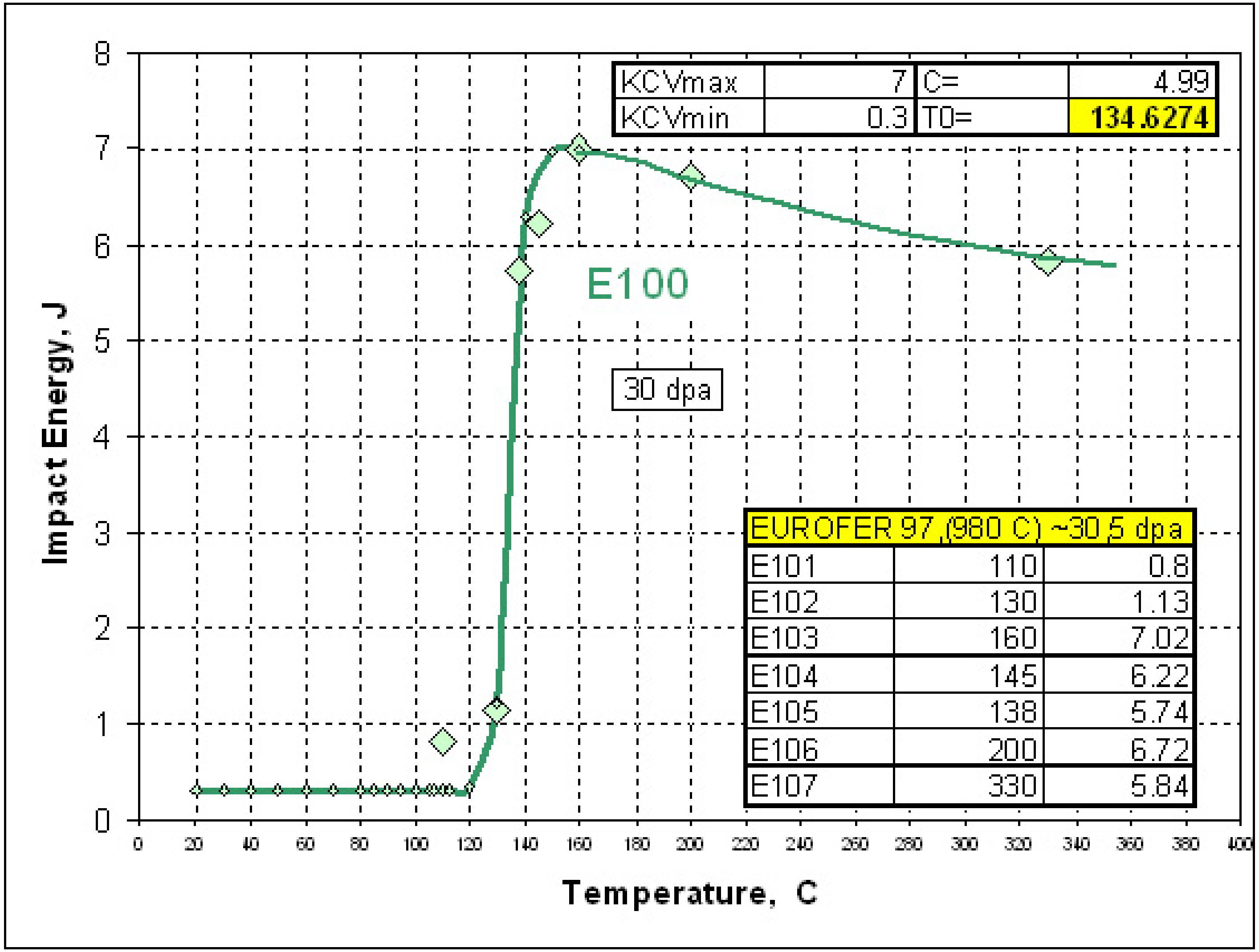

Fig. 8-2 Temperature dependence of impact toughness of E101 to E107 specimens (EUROFER 97 as received)

8.2 EUROFER 97, heat treated

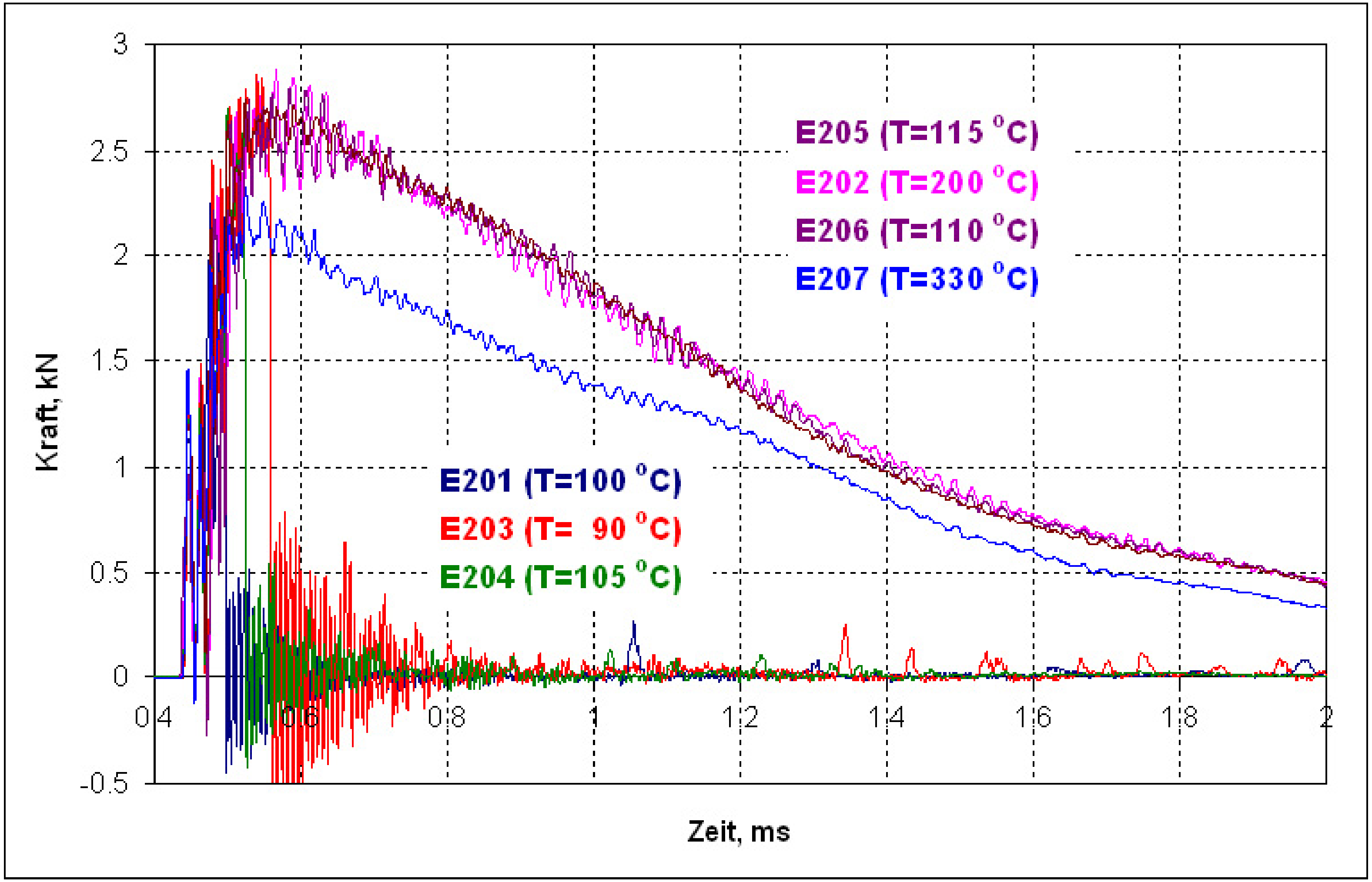

Fig. 8-3 Load-time diagrams of impact testing of E201 to E207 specimens

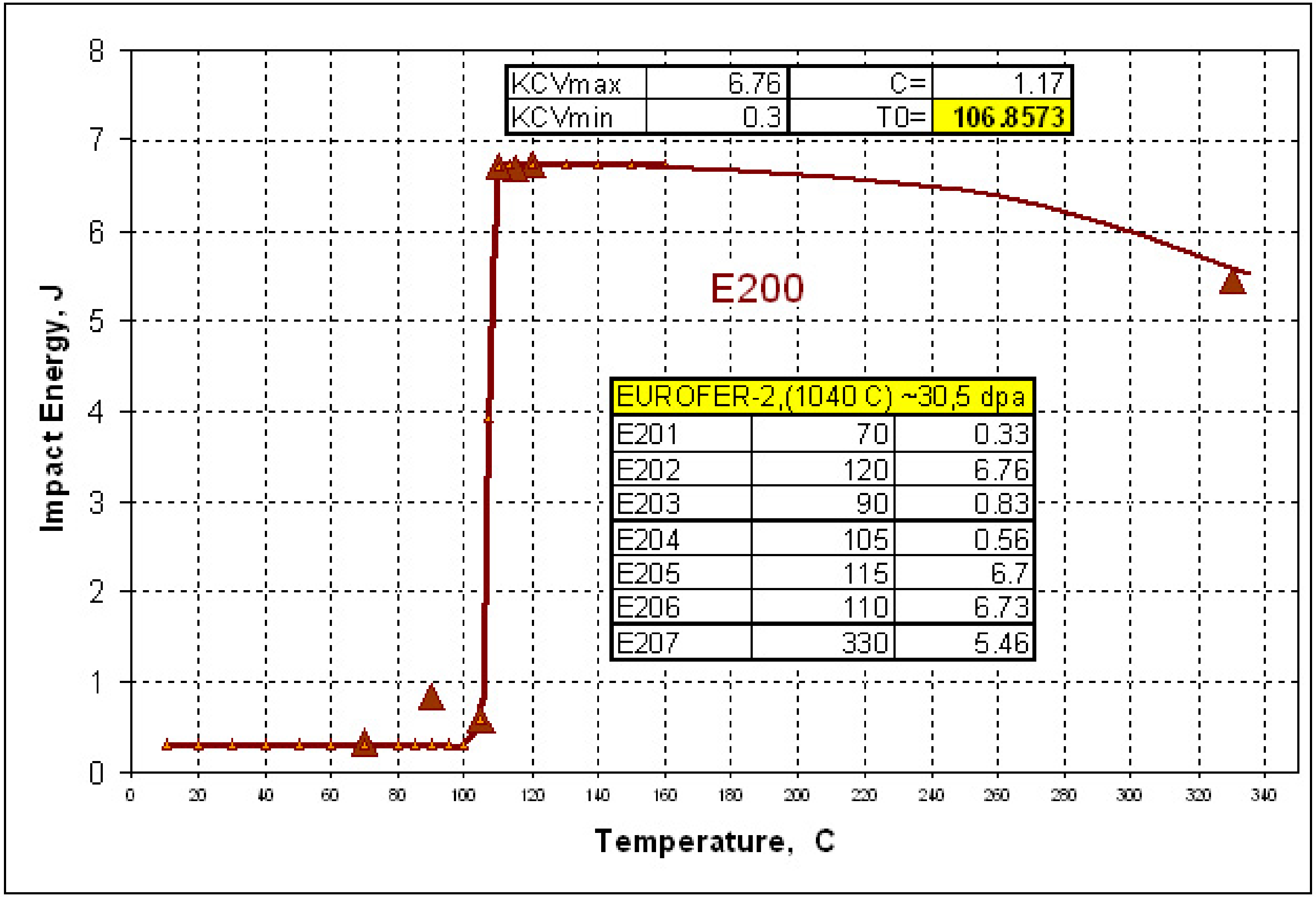

Fig. 8-4 Temperature dependence of impact toughness of E201 to E207 specimens (EUROFER 97 annealed)

8.3 F82H mod.

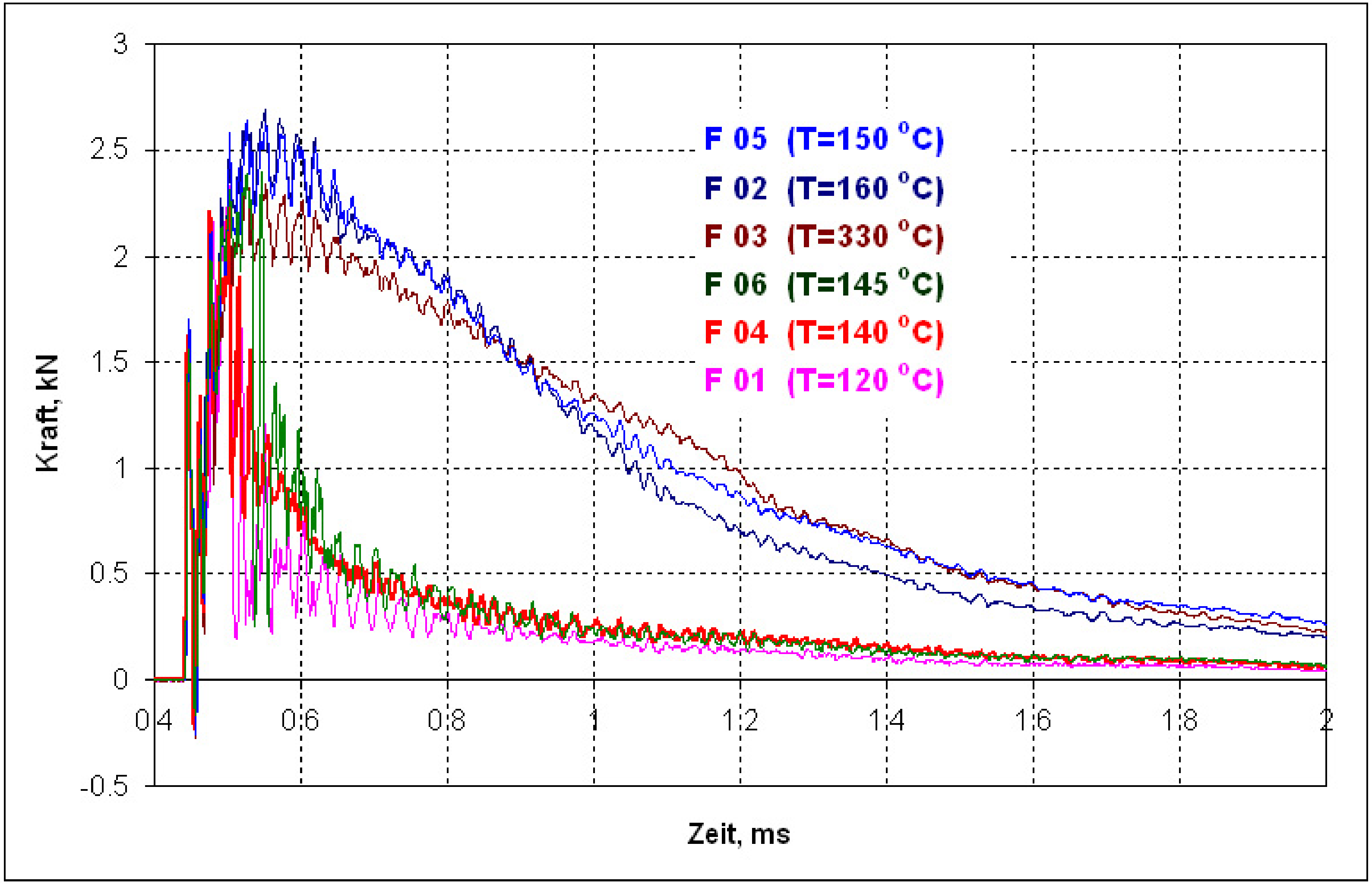

Fig. 8-5 Load-time diagrams of impact testing of F 01 to F 06 specimens (F82H mod.)

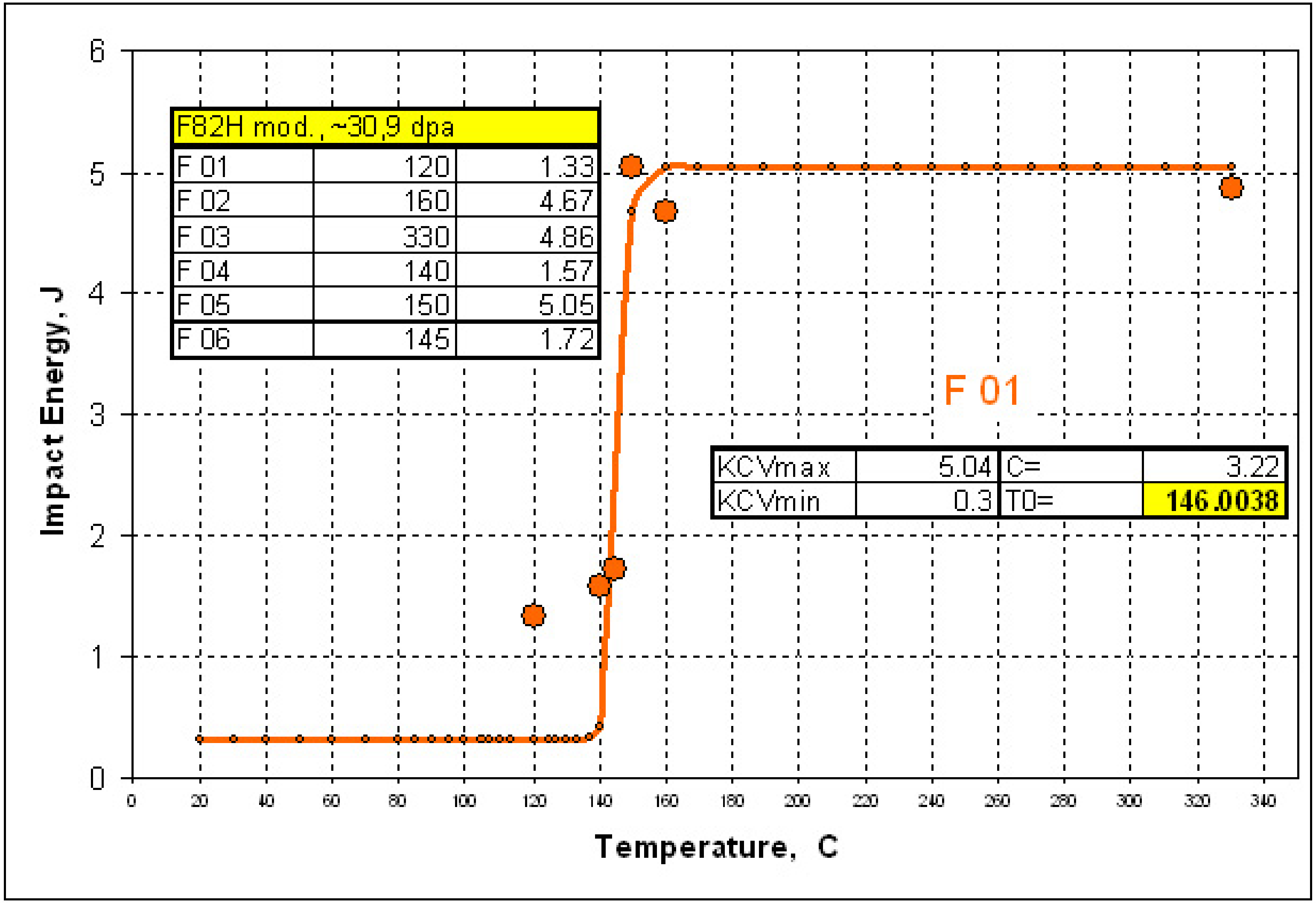

Fig. 8-6 Temperature dependence of impact toughness of F01 to F06 specimens (F82H mod.)

8.4 OPTIFER IVc

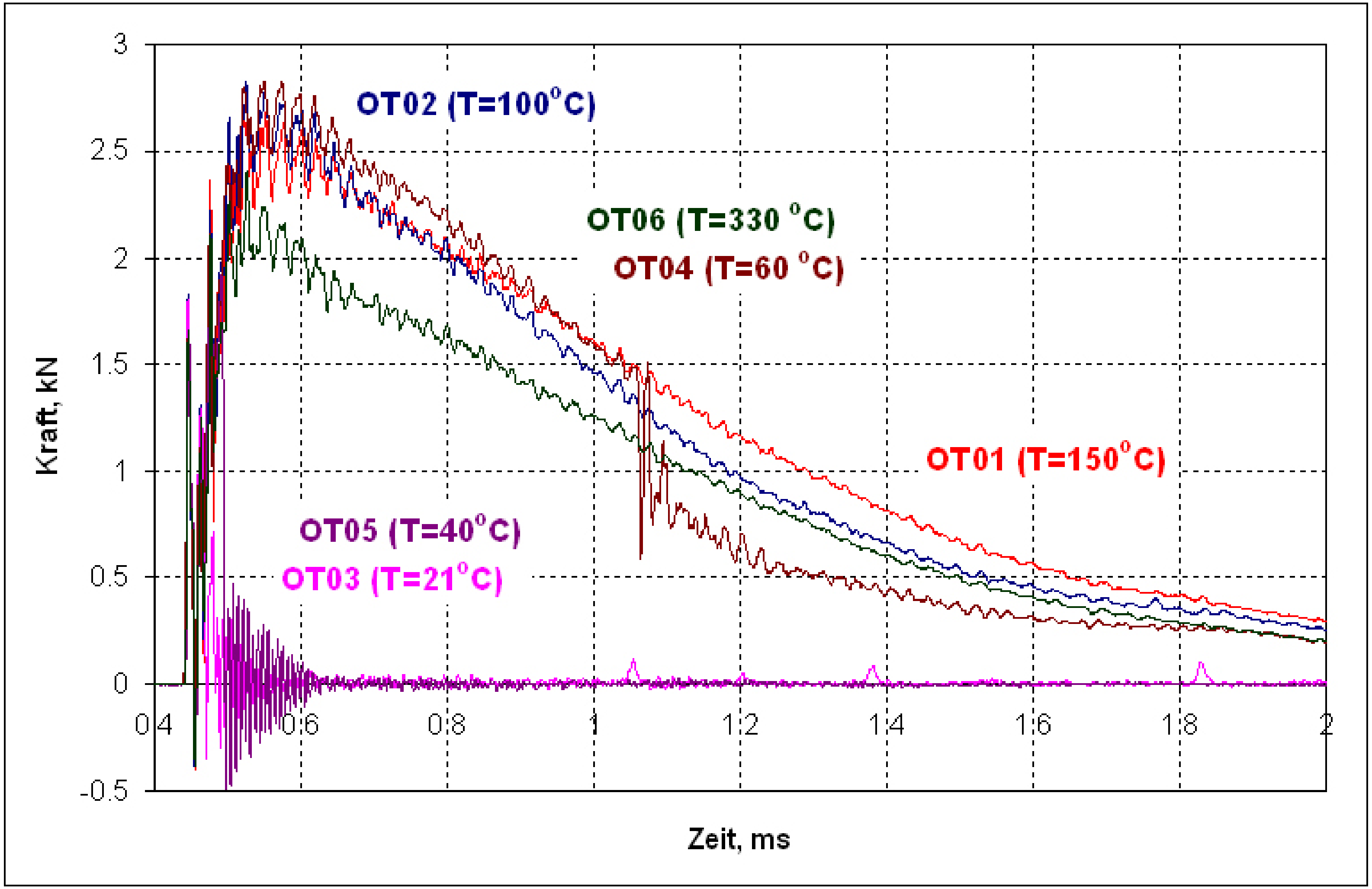

Fig. 8-7 Load-time diagrams of impact testing of OT 01 to OT 06 specimens (OPTIFER IVc)

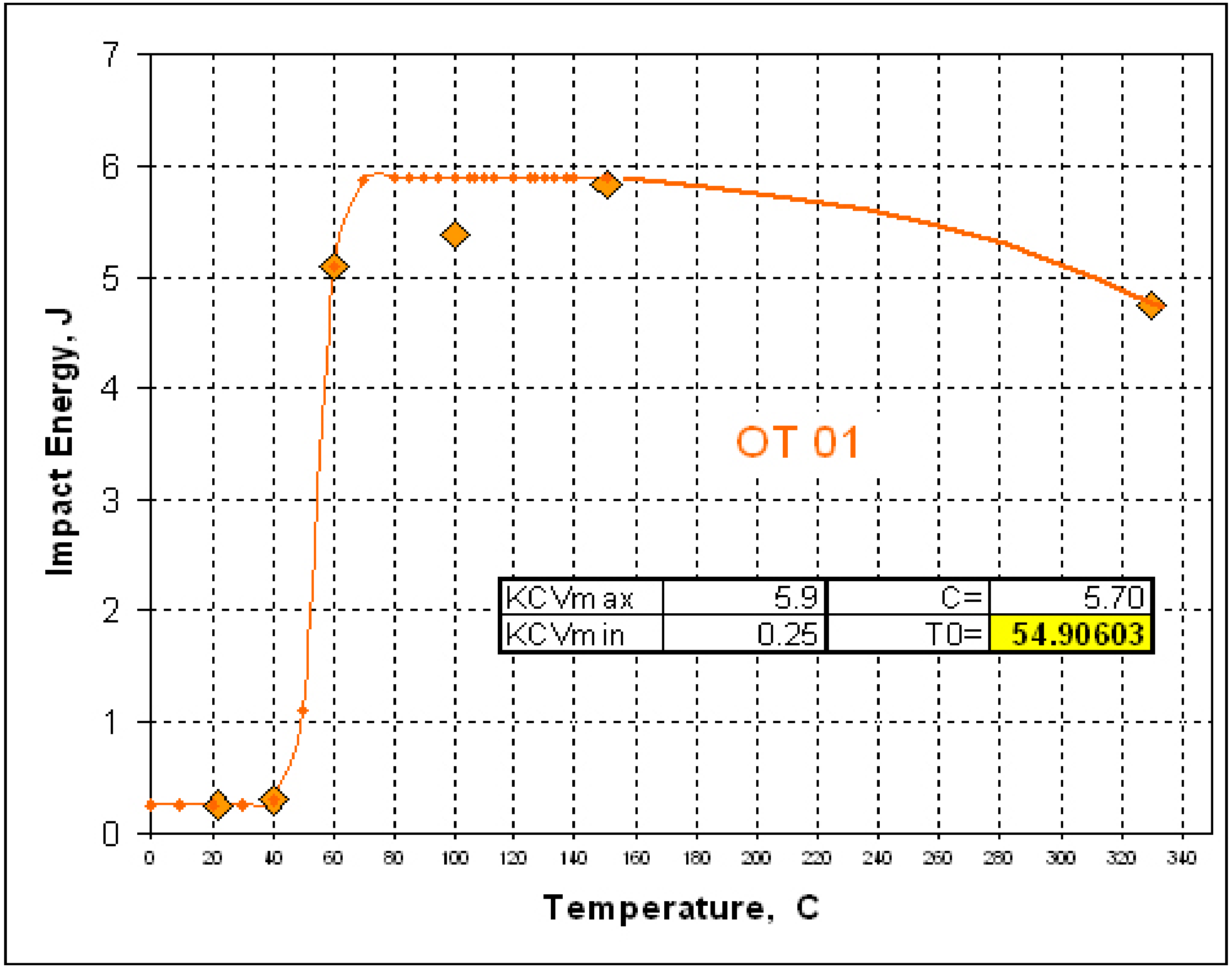

Fig. 8-8 Temperature dependence of impact toughness of OT 01 to OT 06 specimens (OPTIFER IVc)

8.5 ADS 2

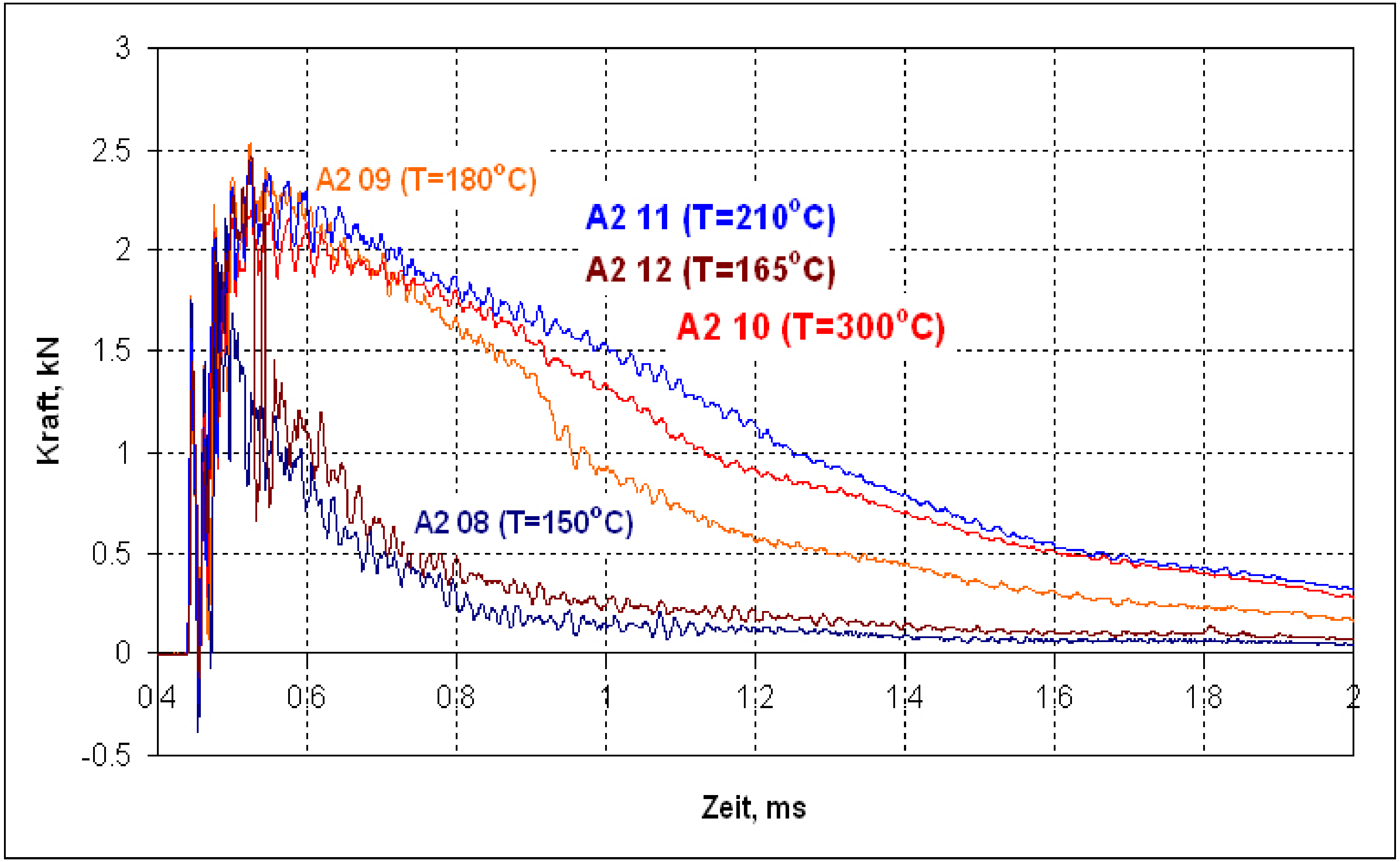

Fig. 8-9 Load-time diagrams of impact testing of A2 08, A2 09, A2 10, A2 11, A2 12 specimens (ADS 2)

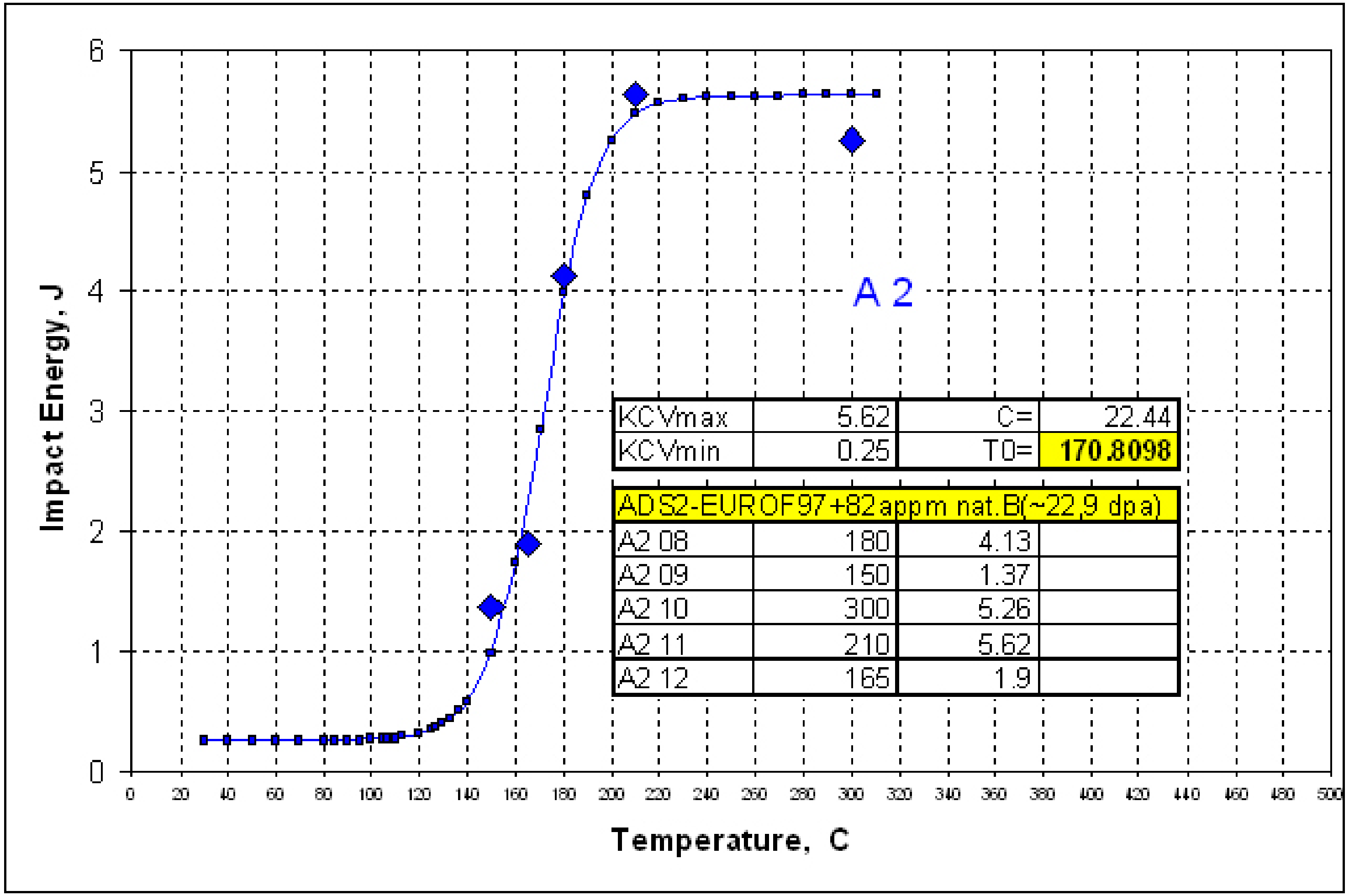

Fig. 8-10 Temperature dependence of impact toughness of A2 08, A2 09, A2 10, A2 11, A2 12 specimens (ADS 2)

8.6 ADS 3

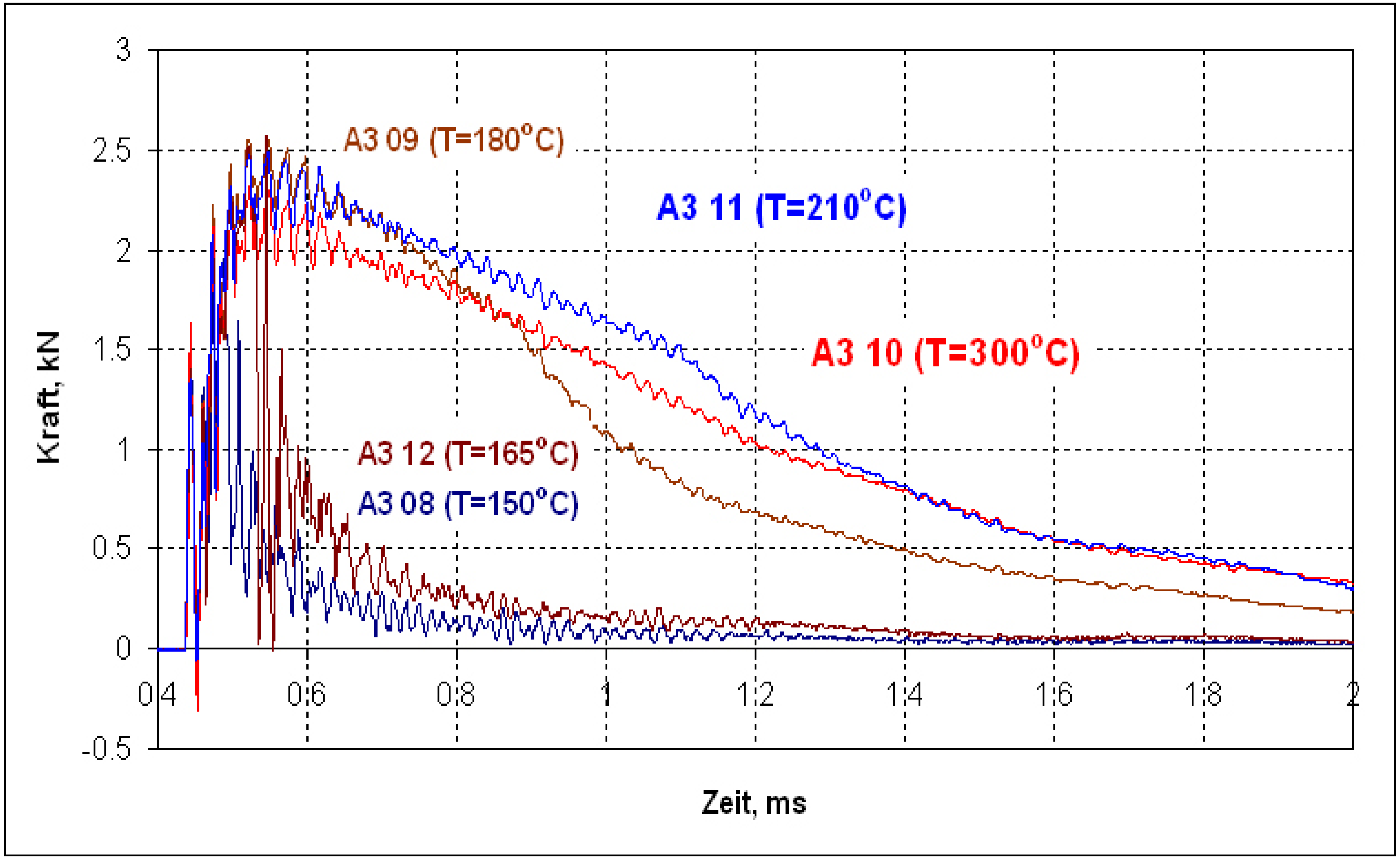

Fig. 8-11 Load-time diagrams of impact testing of A3 08, A3 09, A3 10, A3 11, A3 12 specimens (ADS 3)

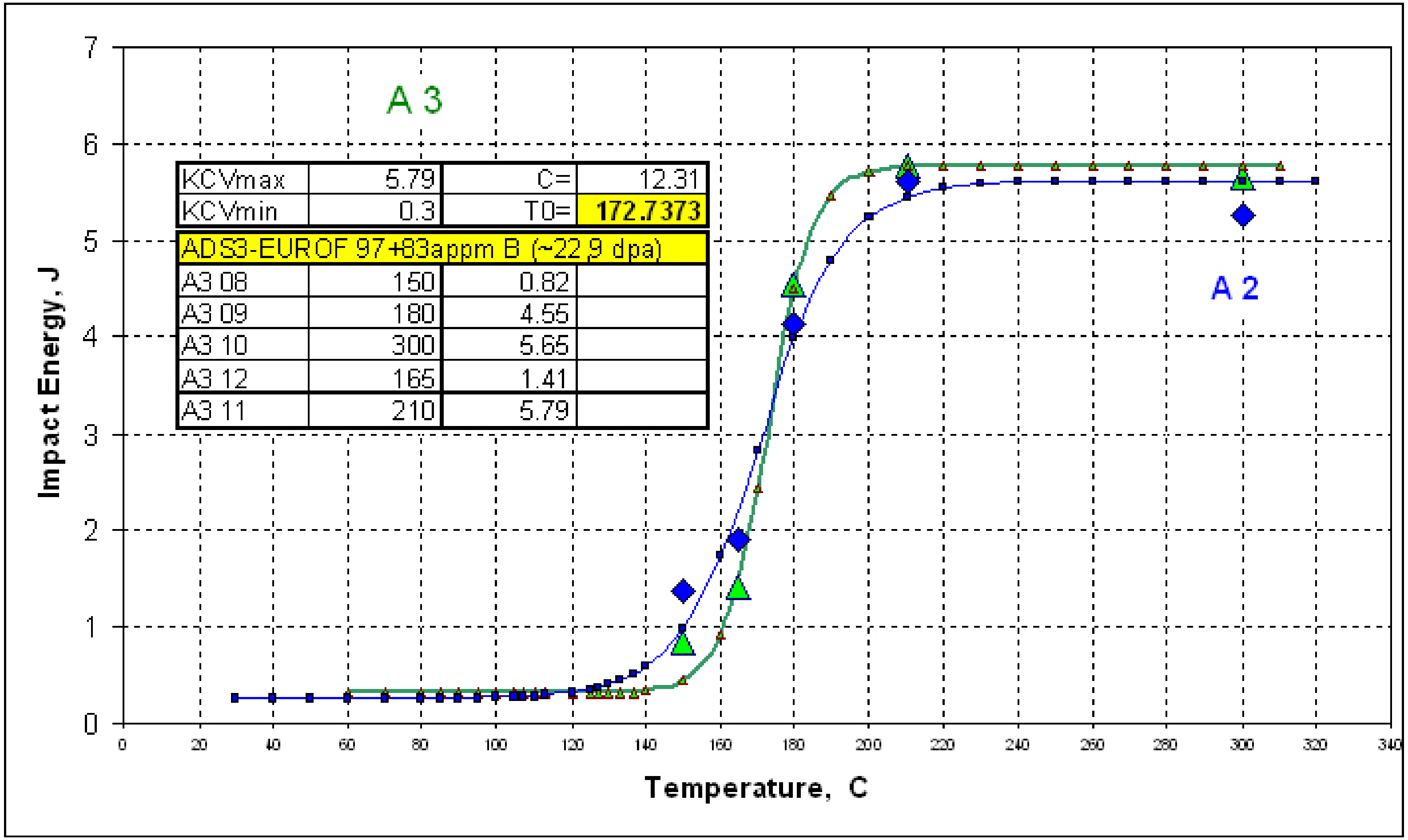

Fig. 8-12 Temperature dependence of impact toughness of A3 08, A3 09, A3 10, A3 11, A3 12 specimens (ADS 3)

8.7 ADS 4

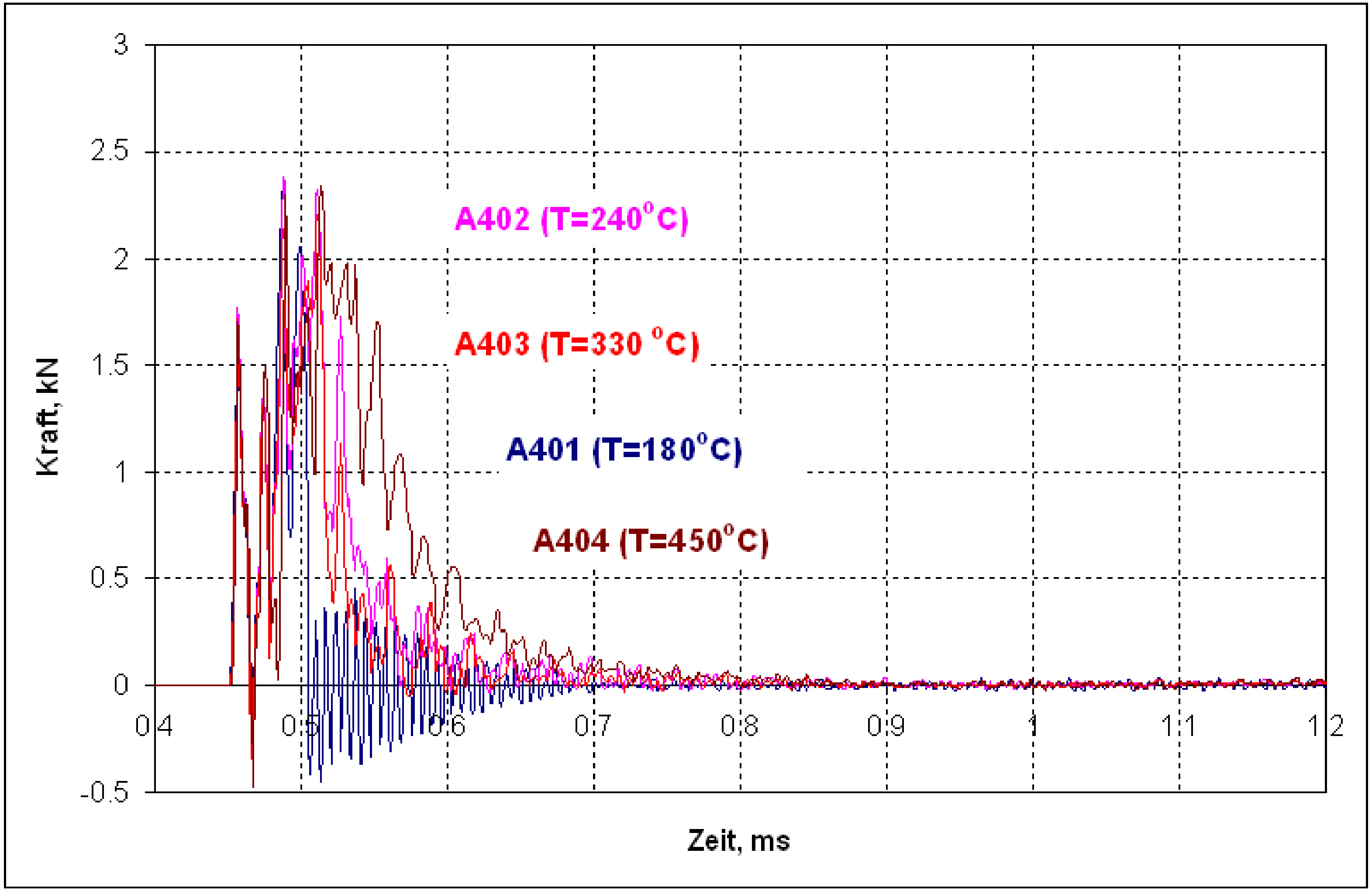

Fig. 8-13 Load-time diagrams of impact testing of A4 01, A4 02, A4 03, A4 04 specimens (ADS 4)

8.8 EURODShip, 0.3 % Y_2O_3

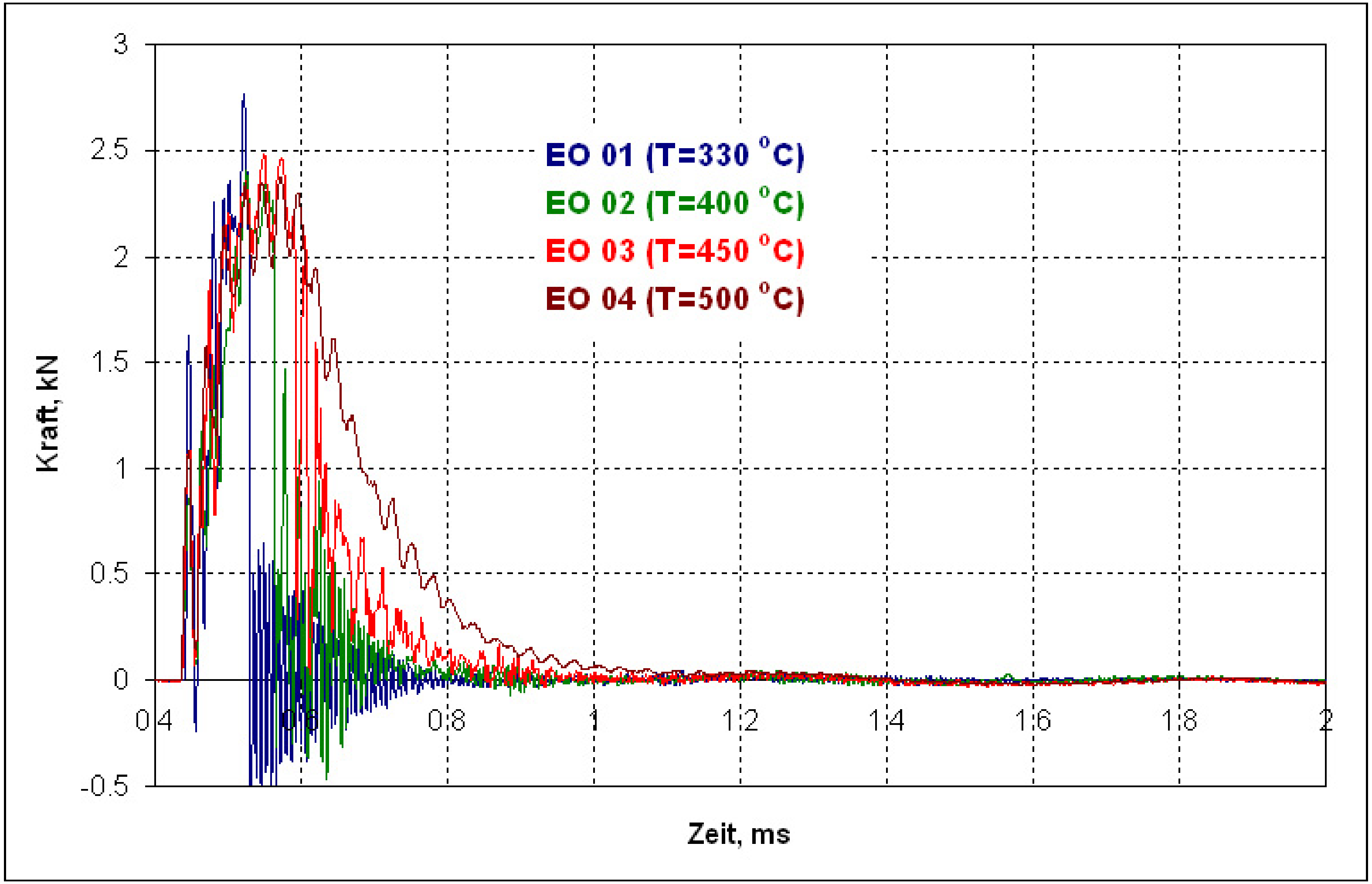

Fig. 8-14 Load-time diagrams of impact testing of EO 01, EO 02, EO 03, EO 04 specimens (EURODShip, 0.3 % Y_2O_3)

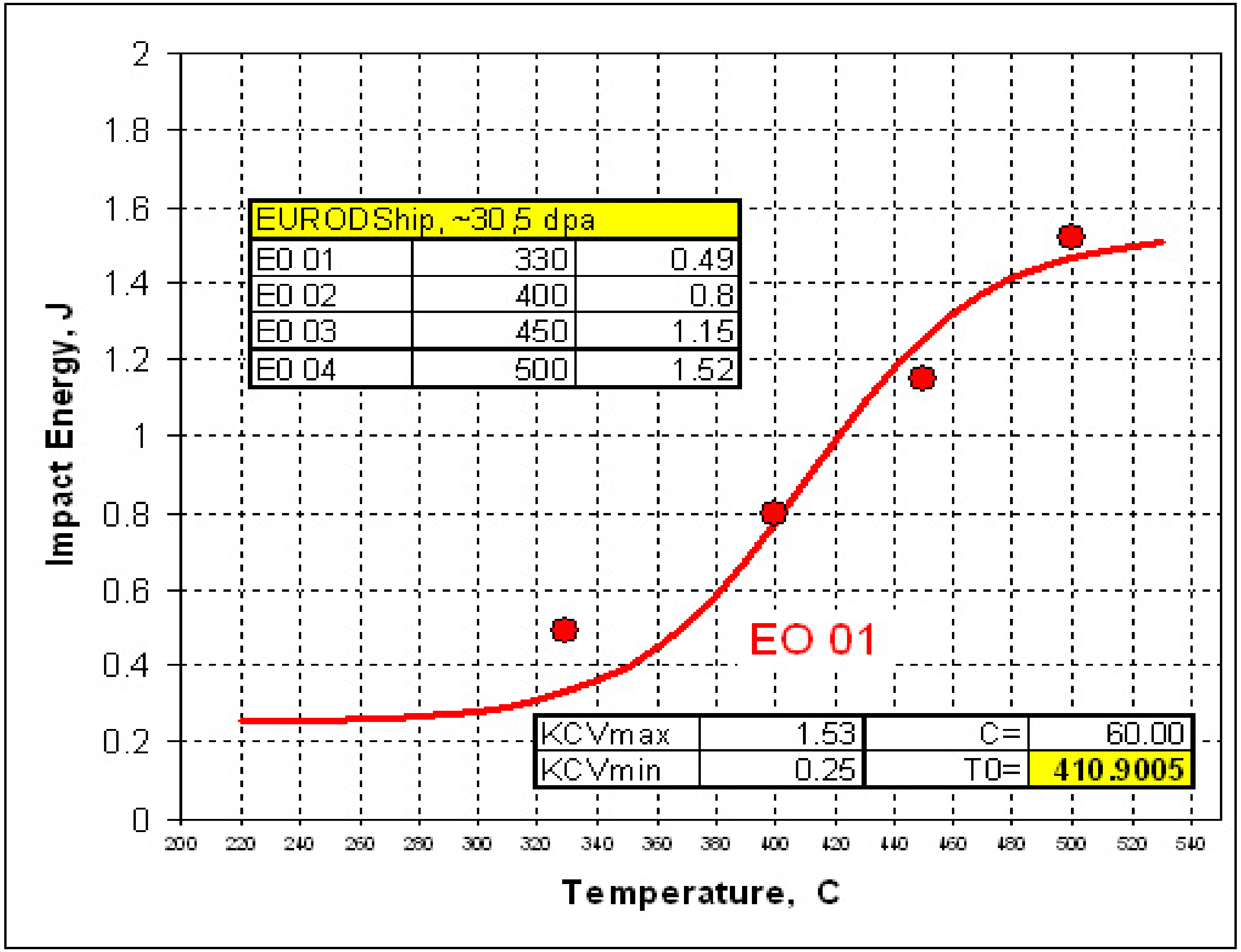

Fig. 8-15 Temperature dependence of impact toughness of EO 01, EO 02, EO 03, EO 04 specimens (EURODShip, 0.3 % Y_2O_3)

8.9 BS-EUROFER

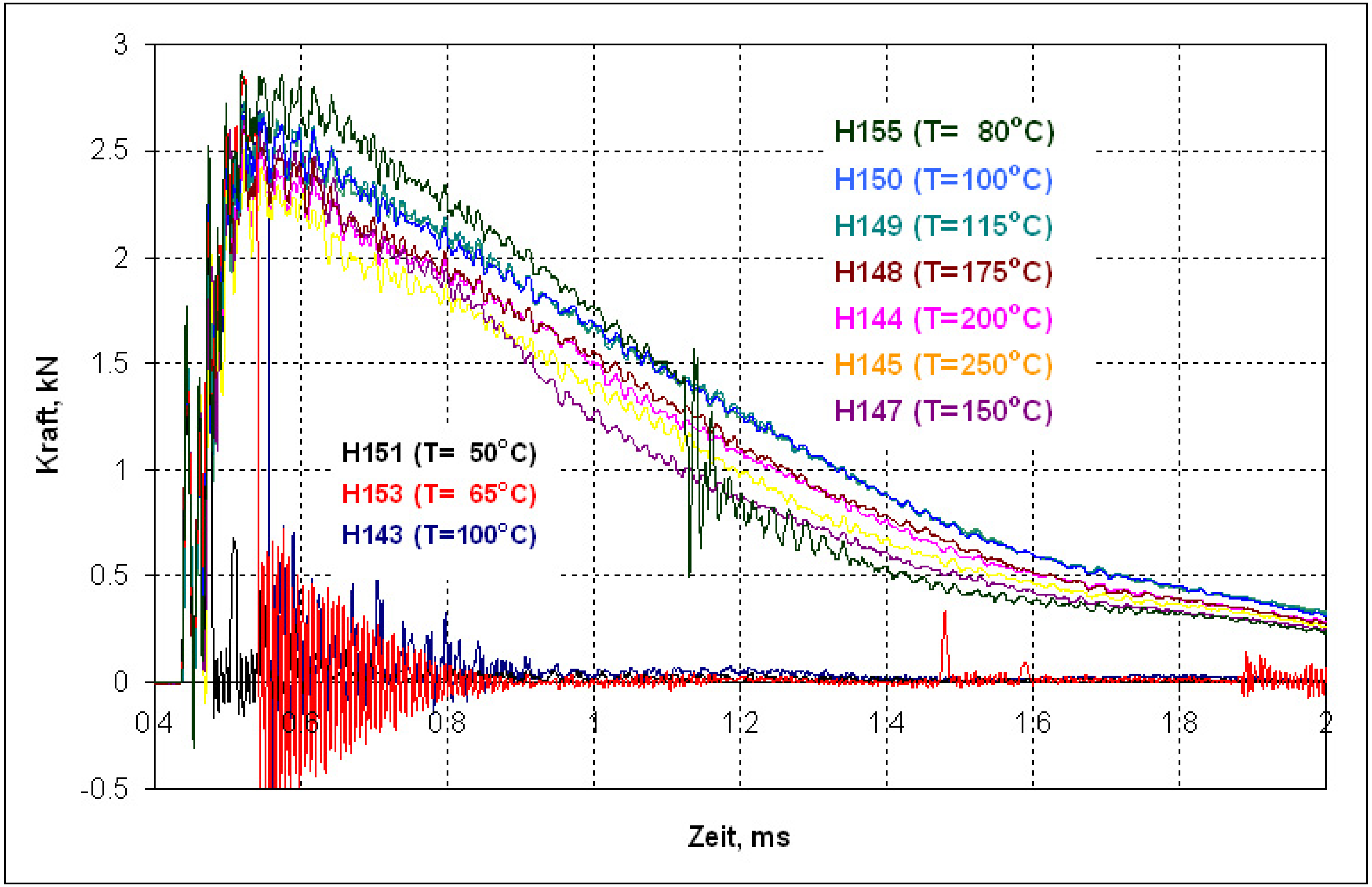

Fig. 8-16 Load-time diagrams of impact testing of H143 to H 145, H 147 to H 151, H 153 and H155 specimens (BS-EUROFER)

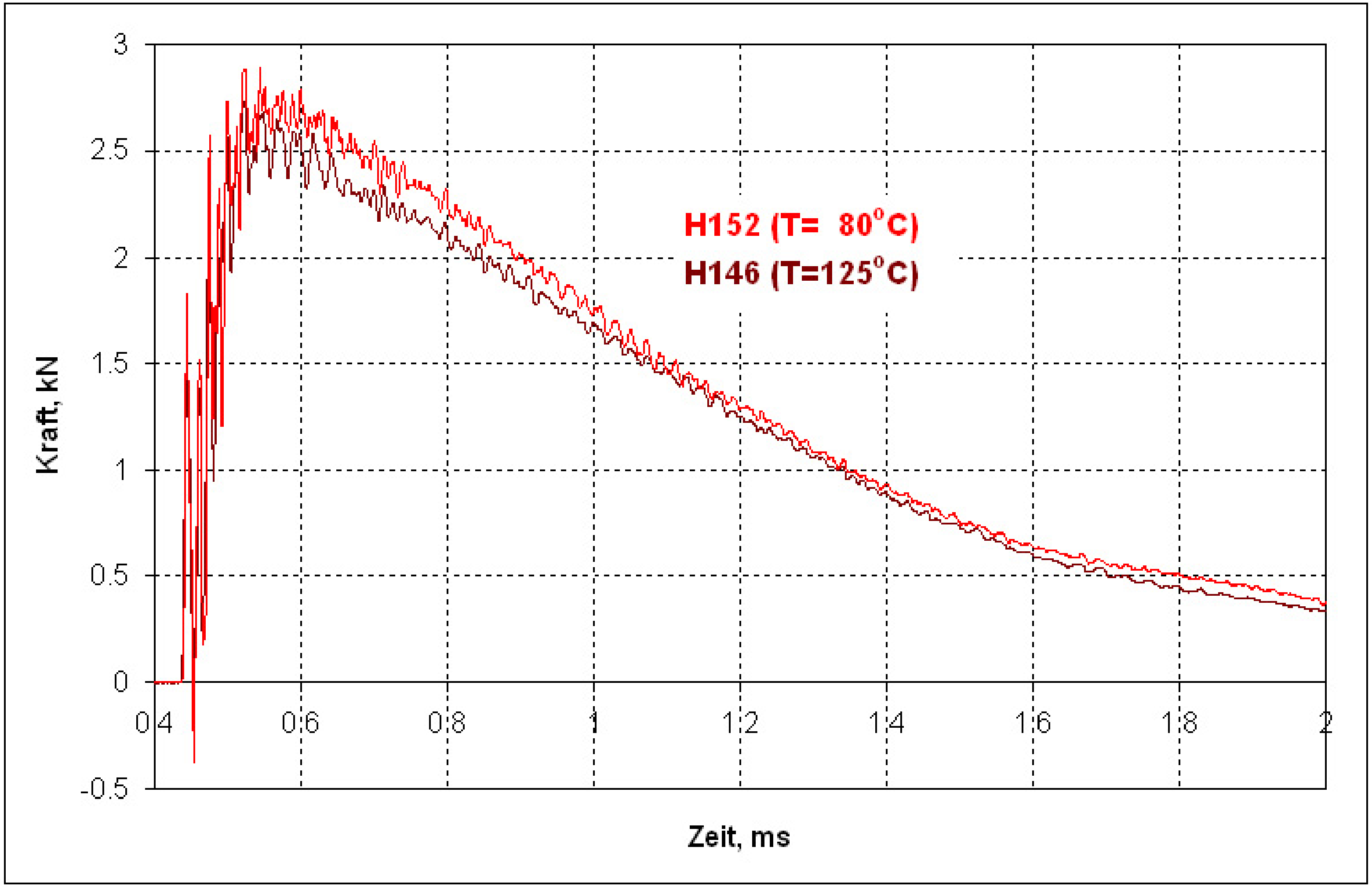

Fig. 8-17 Load-time diagrams of impact testing of H 146 and H152 specimens (BS-EUROFER)

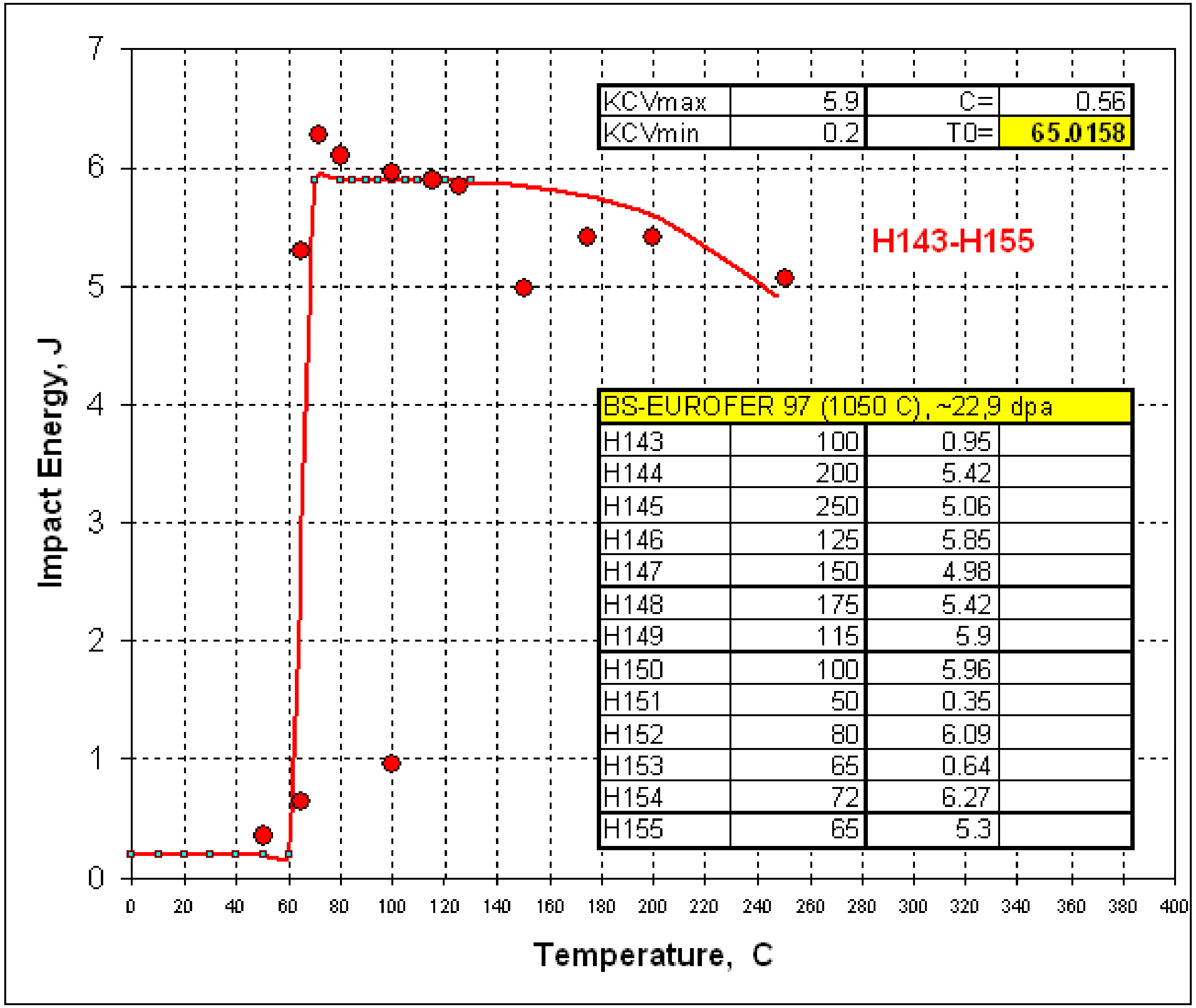

Fig. 8-18 Temperature dependence of impact toughness of H143 to H 155 specimens (BS-EUROFER)

8.10 EUROFER EB welded

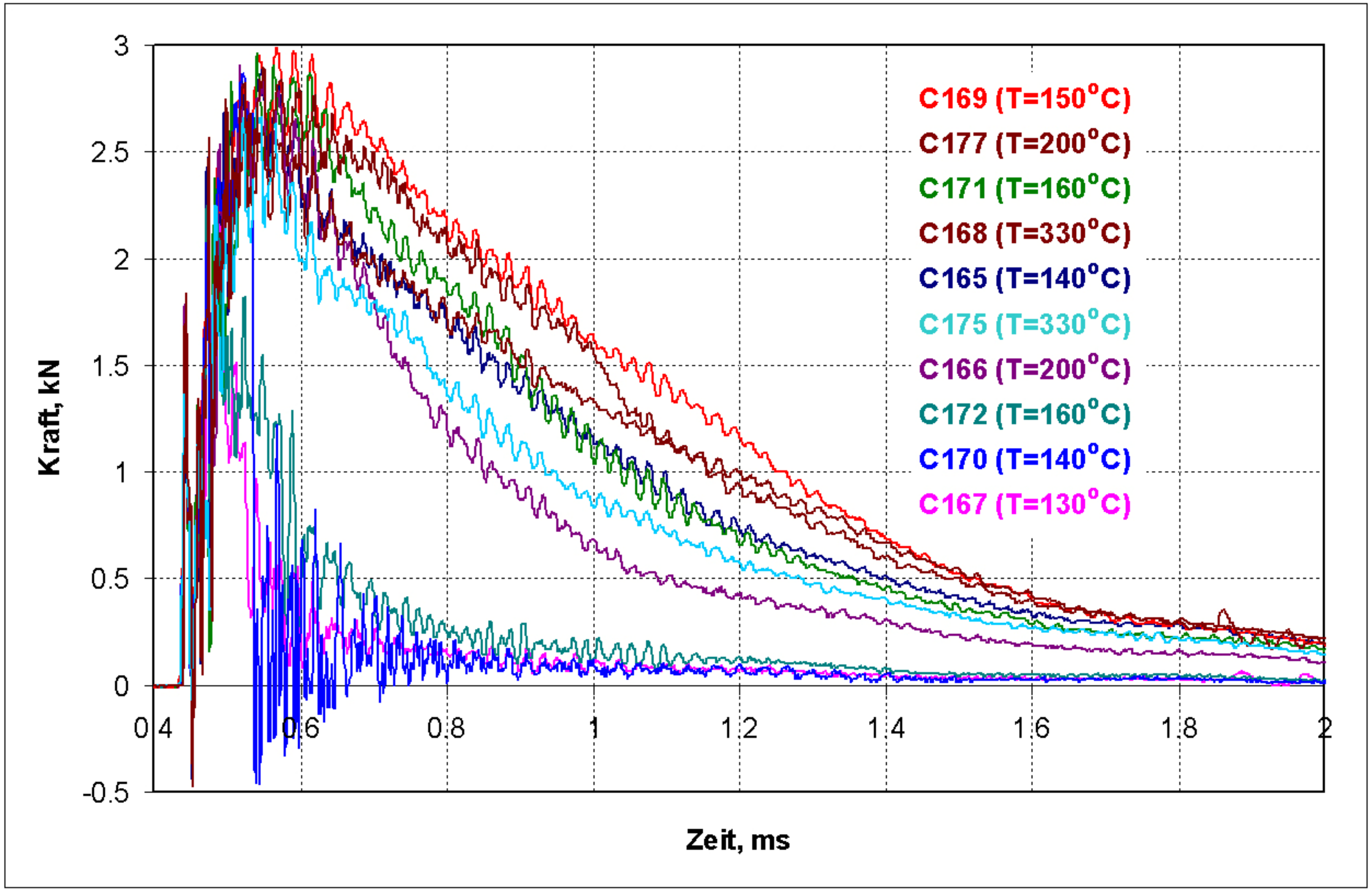

Fig. 8-19 Load-time diagrams of impact testing of C165 to C172, C175 and C177 specimens (EUROFER EB welded)

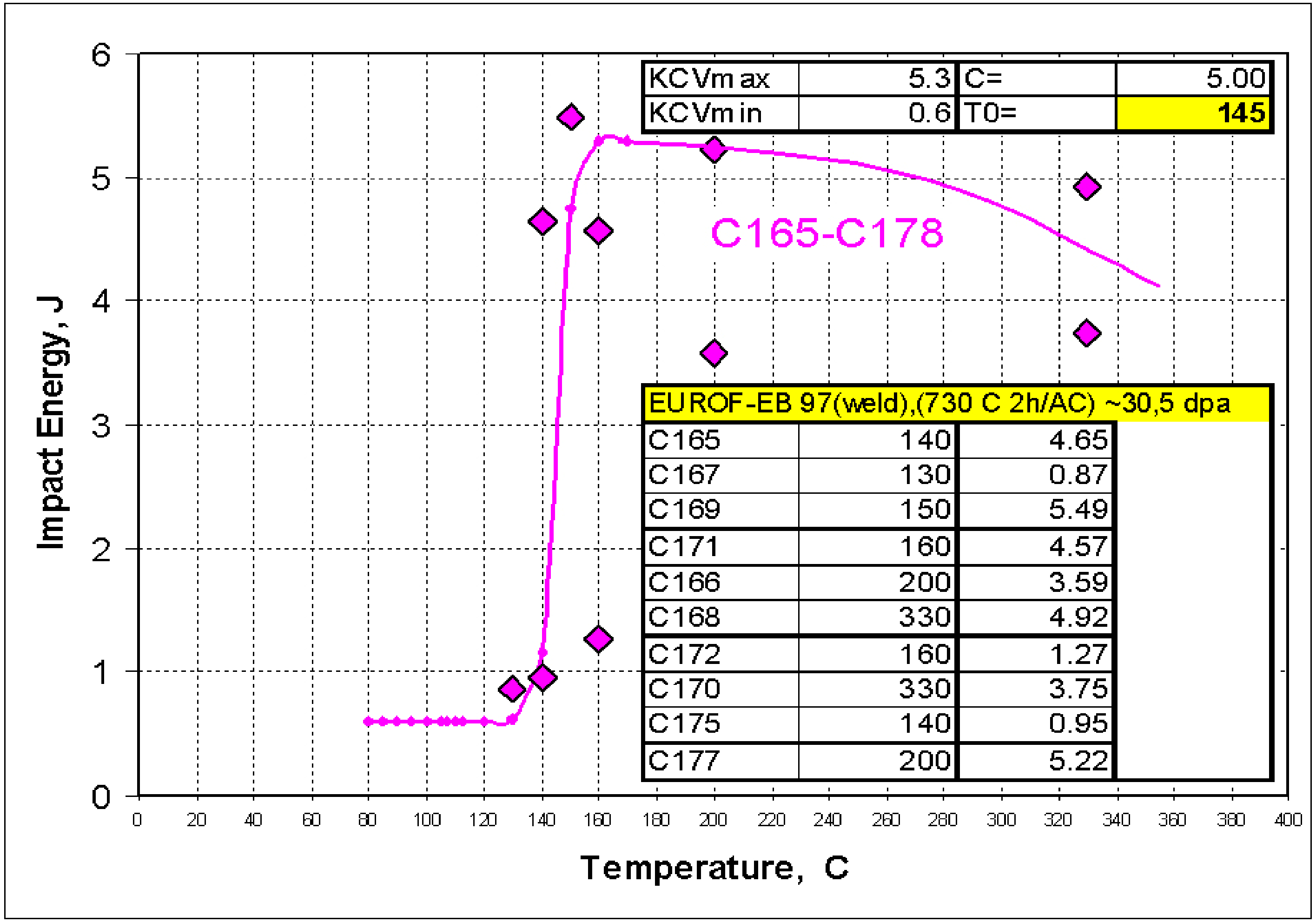

Fig. 8-20 Temperature dependence of impact toughness of C165 to C172, C175 and C177 specimens (EUROFER EB welded)

E1 01

E1 02

E1 03

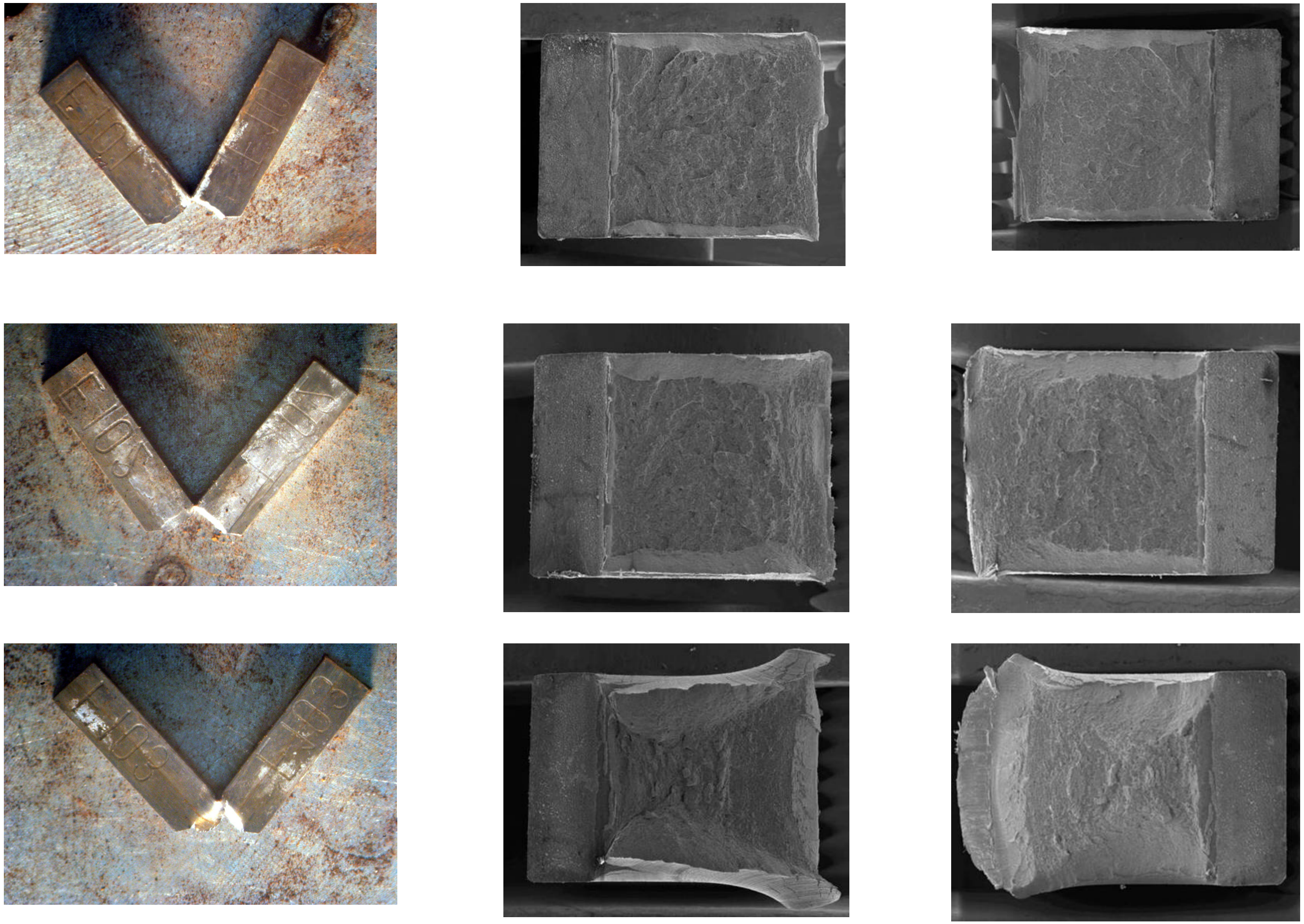

Fig. 8-21 Tested impact specimens E1 01, E1 02, E1 03 after testing (Macro) and after complete breaking (SEM)

8.11 Pictures of impact tested specimens

E1 04

E1 05

E1 06

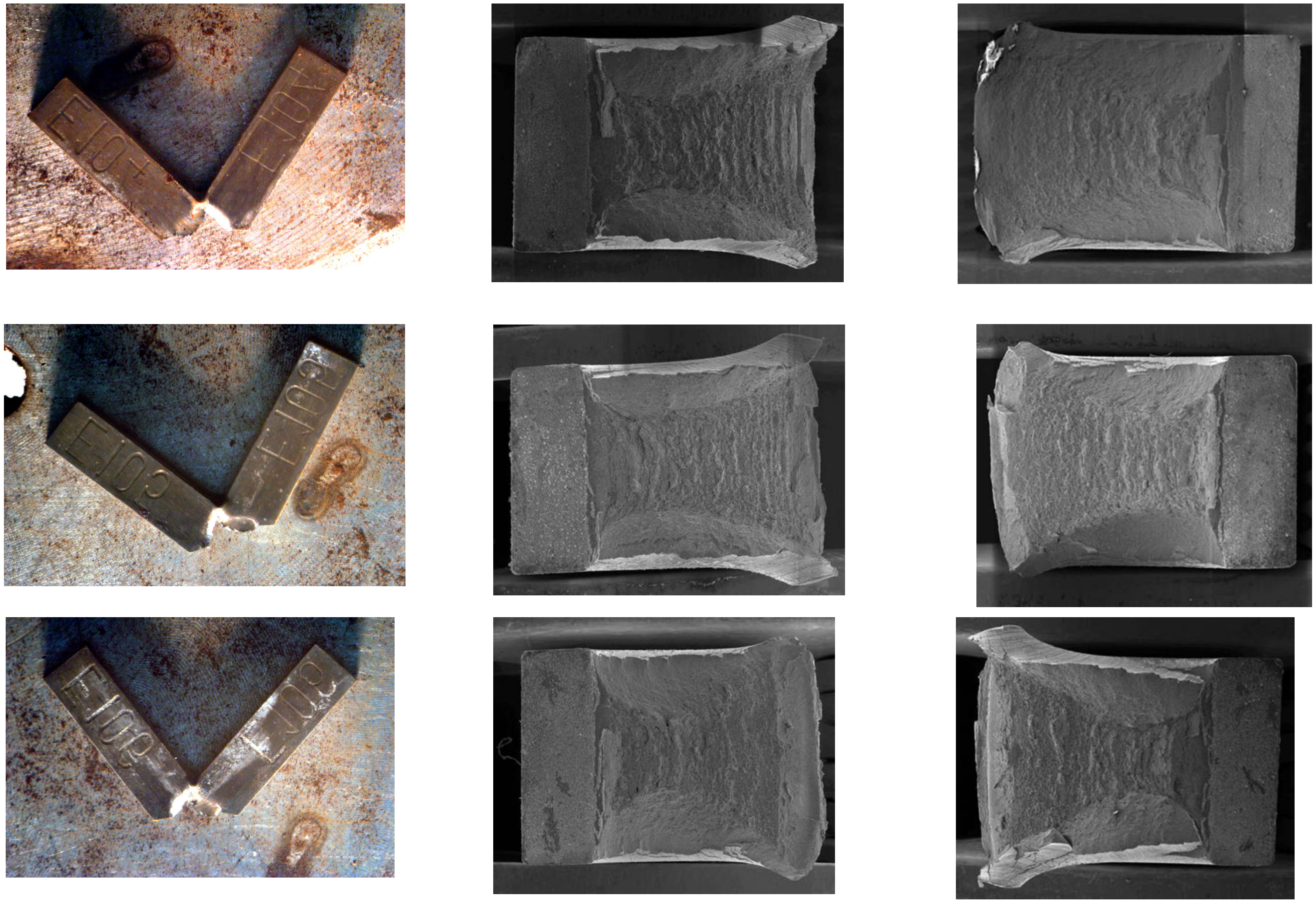

Fig. 8-22 Tested impact specimens E1 04, E1 05, E1 06 after testing (Macro) and after complete breaking (SEM)

E1 07

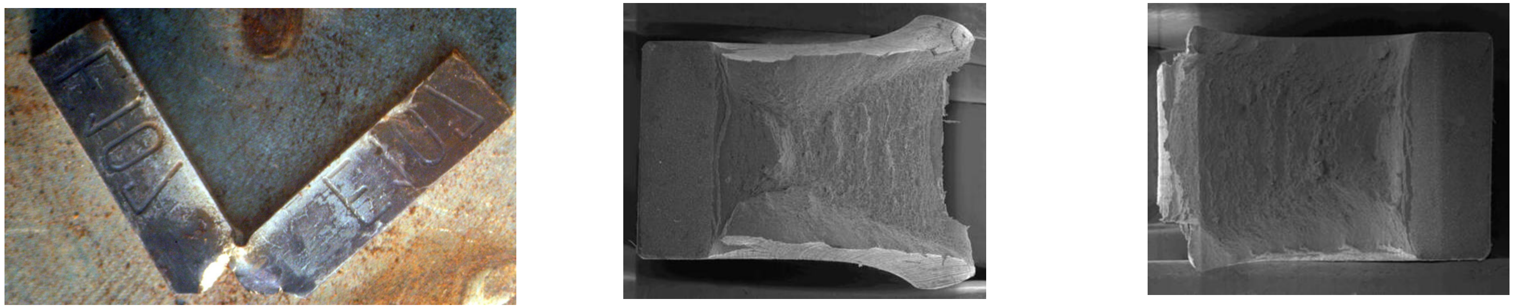

Fig. 8-23 Tested impact specimen E1 07 after testing (Macro) and after complete breaking (SEM)

E2 01

E2 02

E2 03

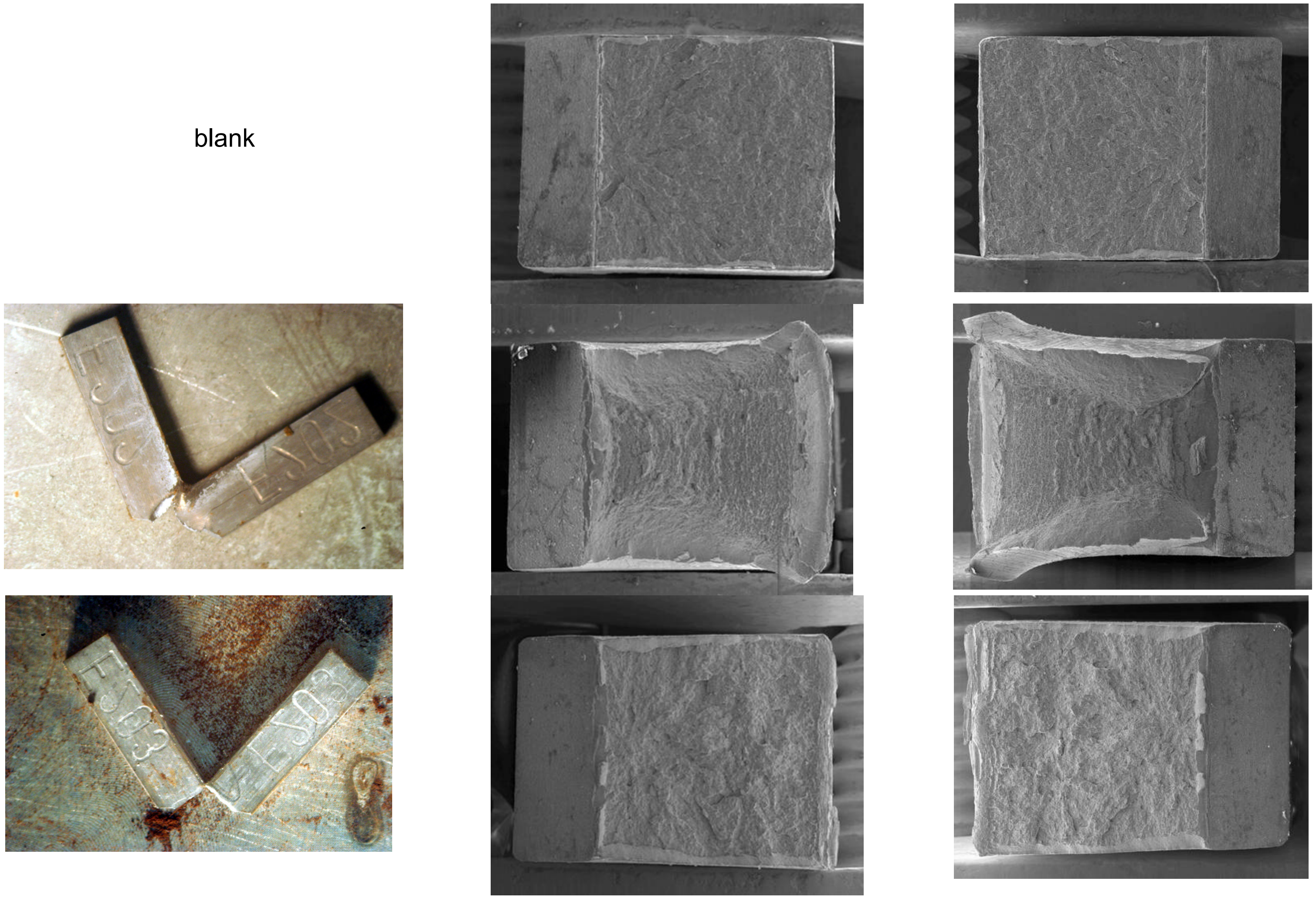

Fig. 8-24 Tested impact specimens E2 01, E2 02, E2 03 after testing (Macro) and after complete breaking (SEM)

E2 04

E2 05

E2 06

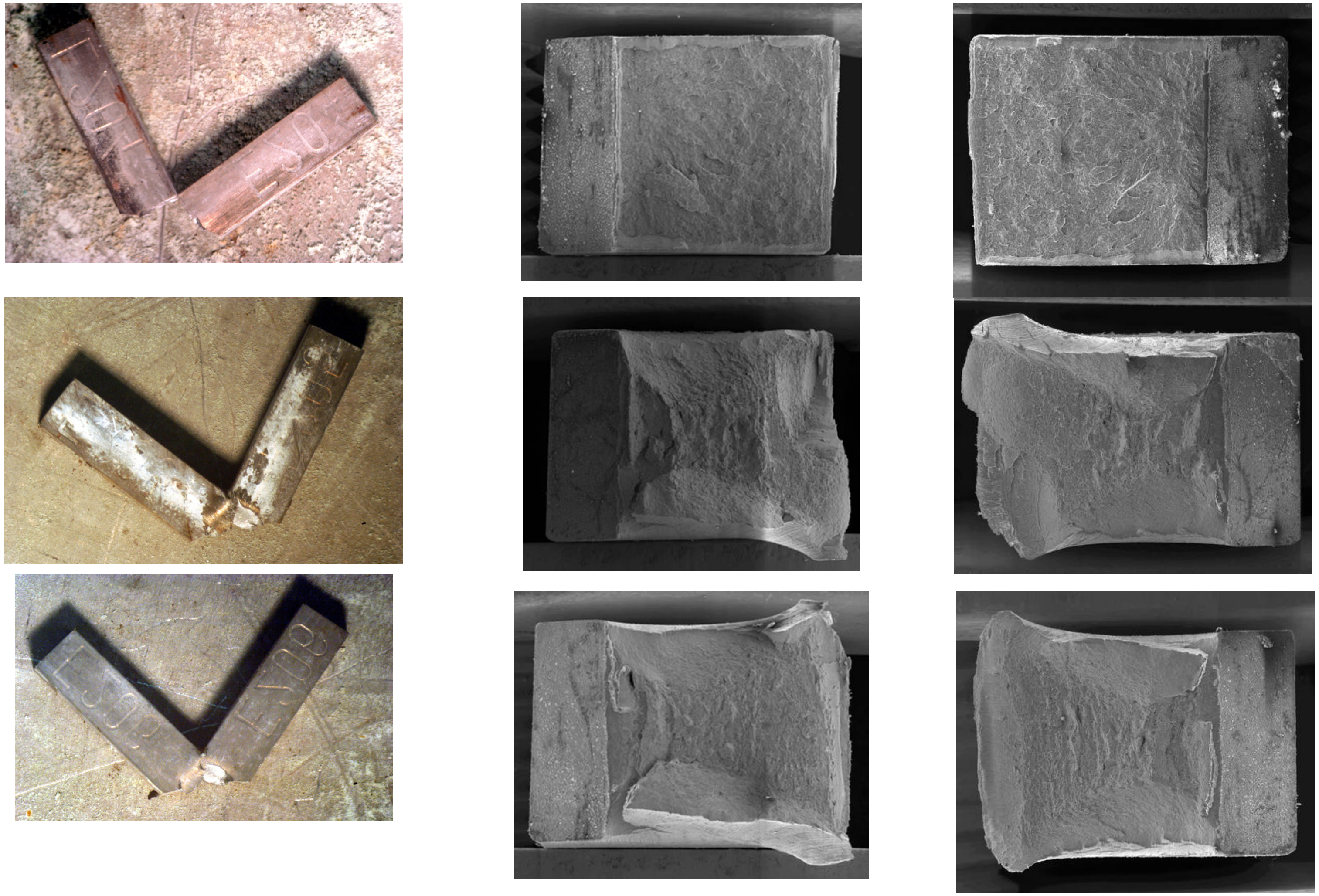

Fig. 8-25 Tested impact specimens E2 04, E2 05, E2 06 after testing (Macro) and after complete breaking (SEM)

E2 07

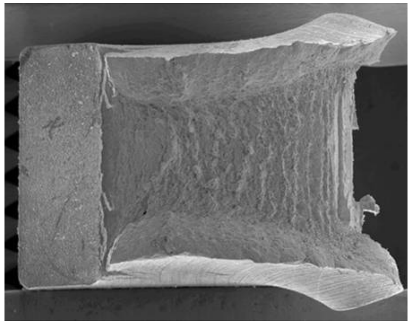

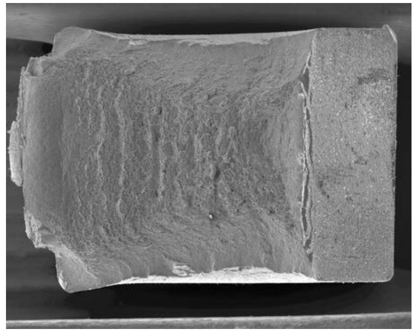

Fig. 8-26 Tested impact specimen E2 07 after testing (Macro) and after complete breaking (SEM)

F 01 **F 02** **F 03**

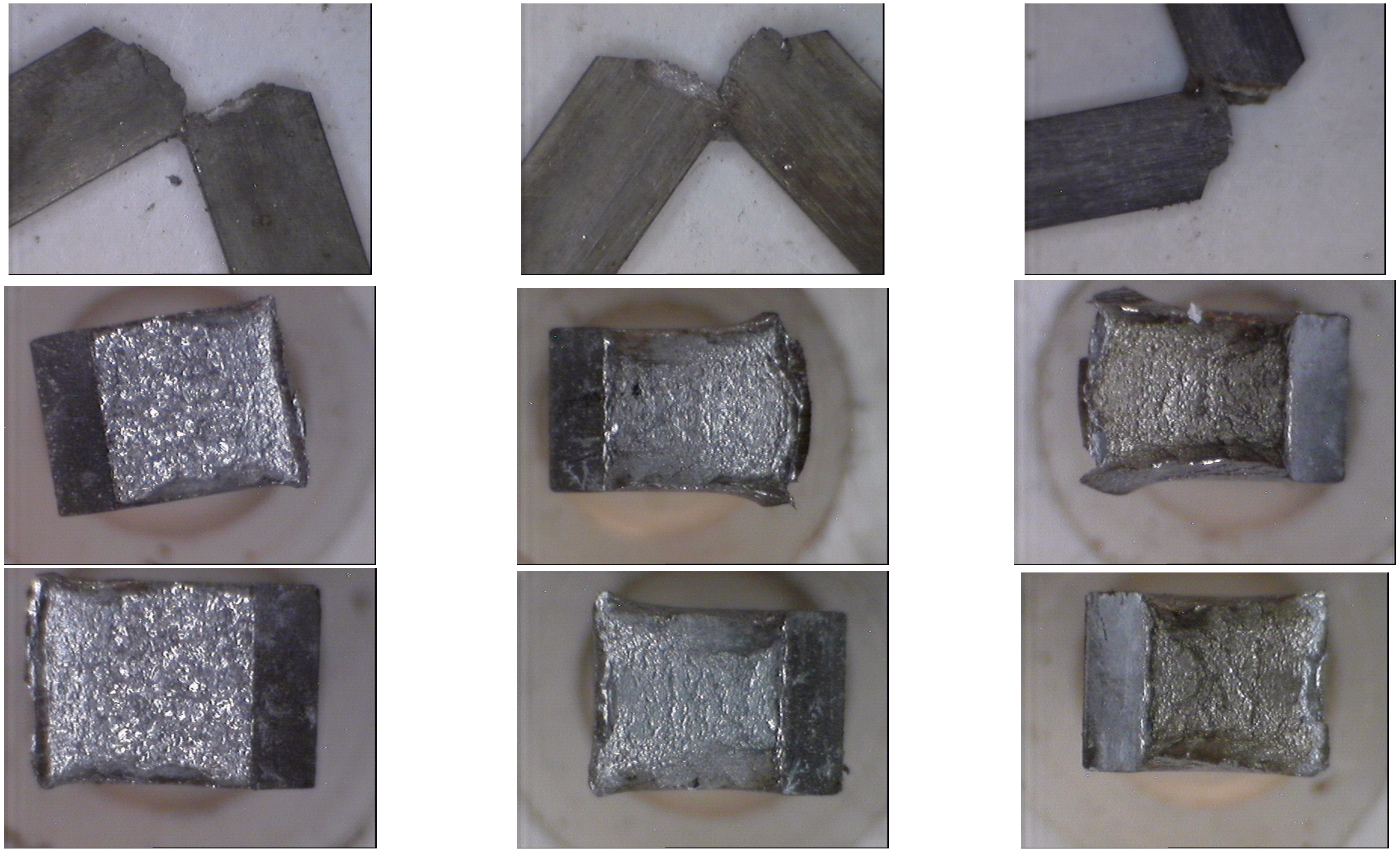

Fig. 8-27 Tested impact specimens F 01, F 02, F 03 after testing (Macro) and after complete breaking (Macro)

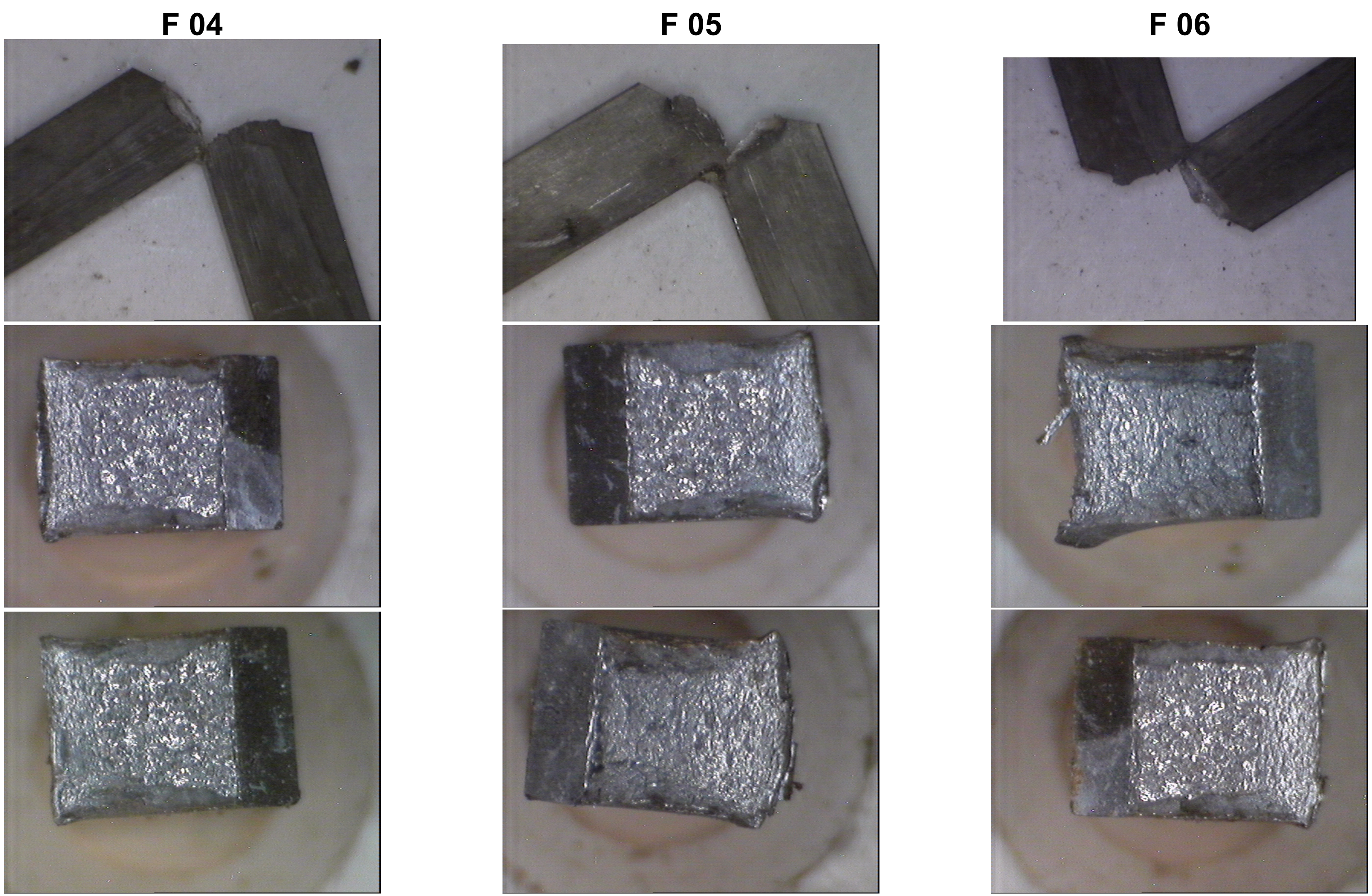

Fig. 8-28 Tested impact specimens F 04, F 05, F 06 after testing (Macro) and after complete breaking (Macro)

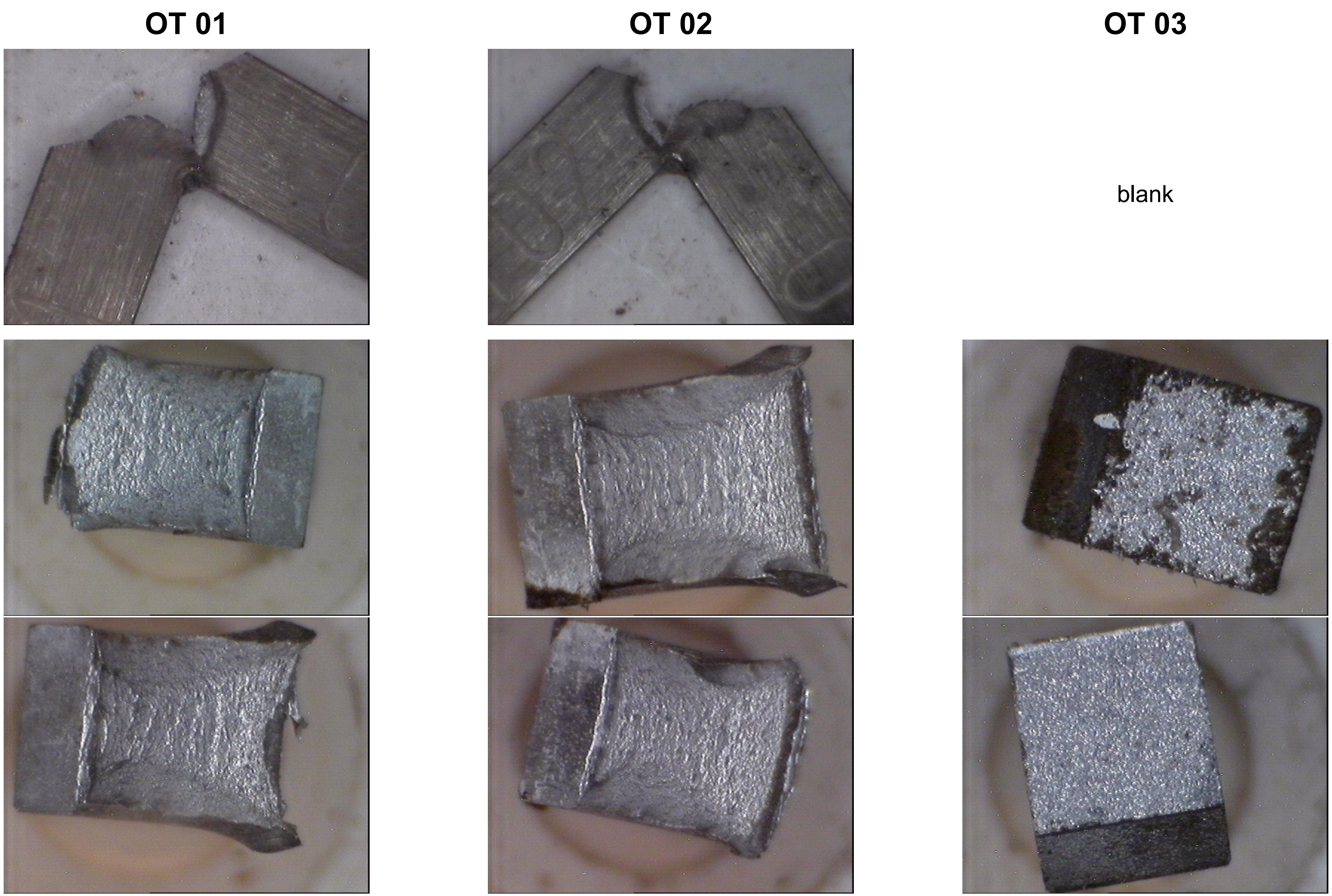

Fig. 8-29 Tested impact specimens OT 01, OT 02, OT 03 after testing (Macro) and after complete breaking (Macro)

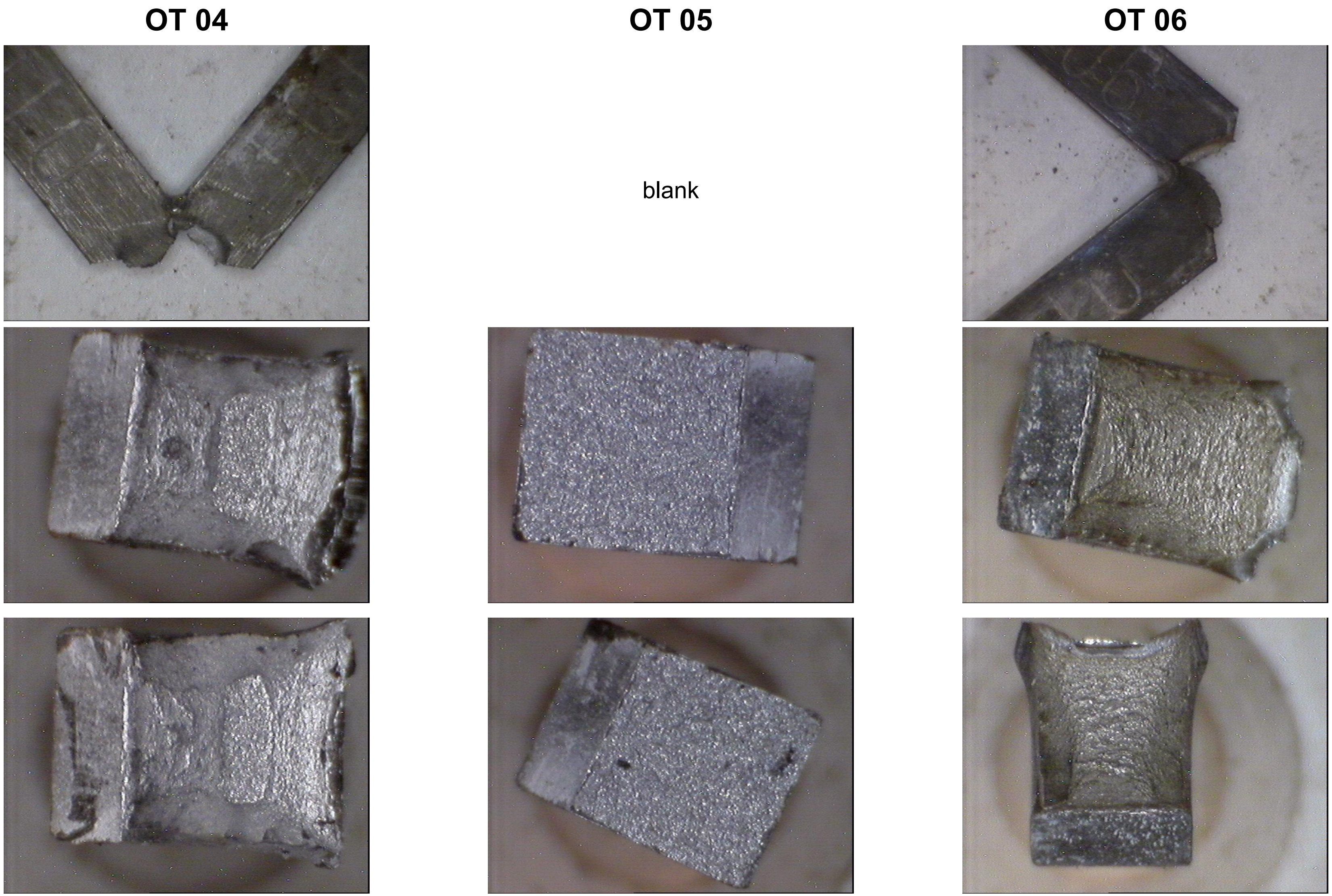

Fig. 8-30 Tested impact specimens OT 04, OT 05, OT 06 after testing (Macro) and after complete breaking (Macro)

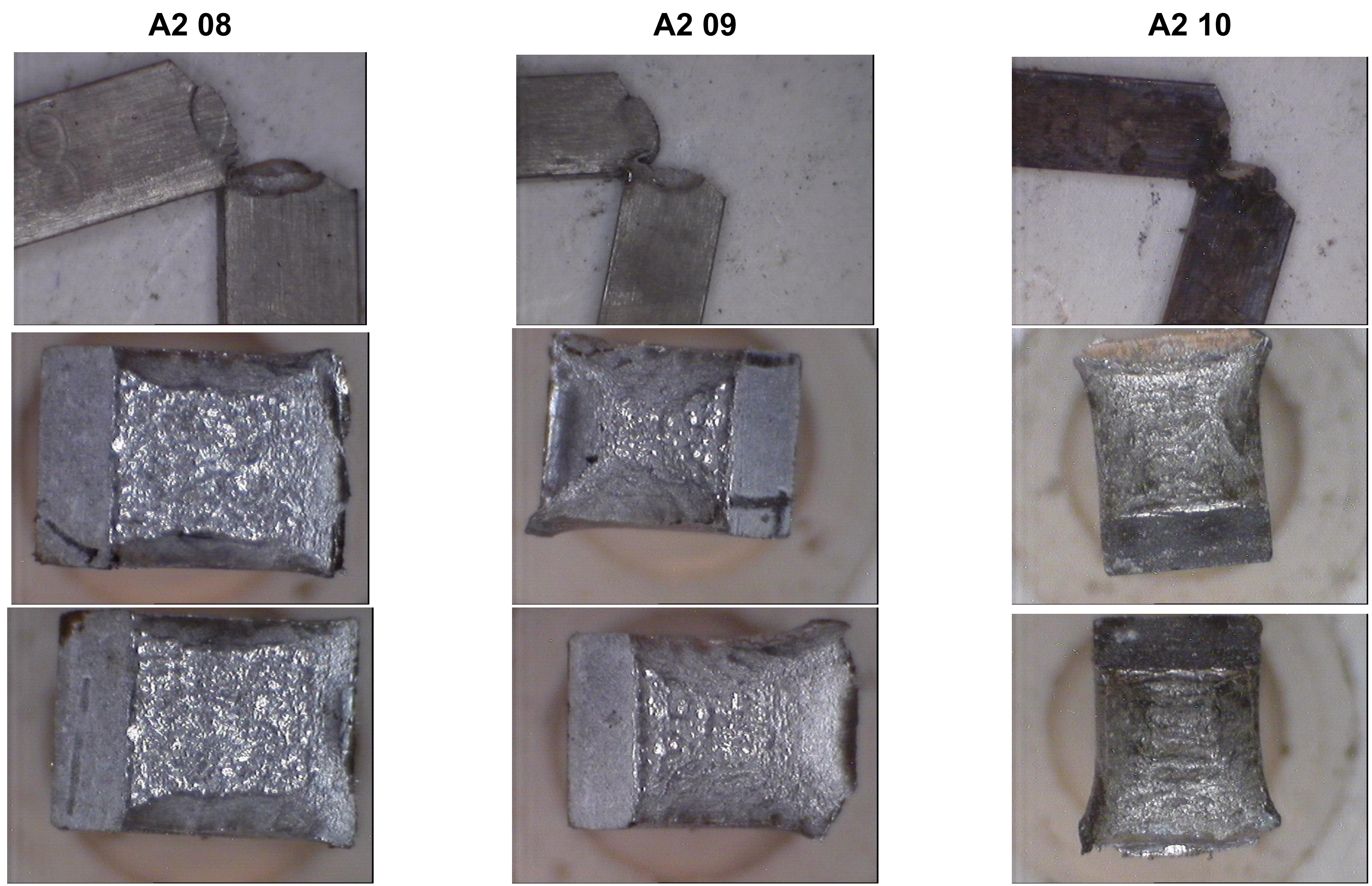

Fig. 8-31 Tested impact specimens A2 08, A2 09, A2 10 after testing (Macro) and after complete breaking (Macro)

A2 11 **A2 12**

Fig. 8-32 Tested impact specimens A2 11, A2 12 after testing (Macro) and after complete breaking (Macro)

A3 08 | A3 09 | A3 10

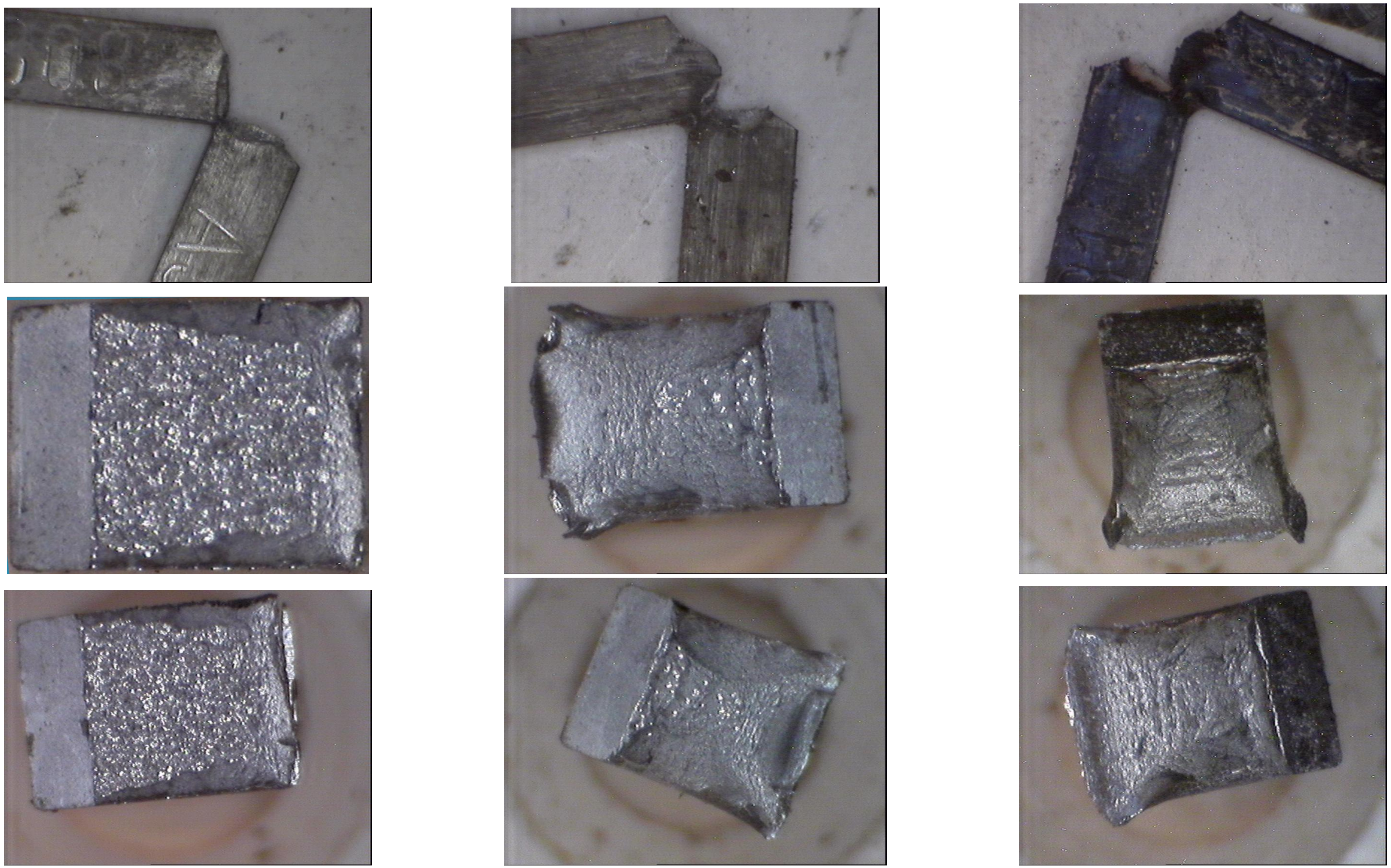

Fig. 8-33 Tested impact specimens A3 08, A3 09, A3 10 after testing (Macro) and after complete breaking (Macro)

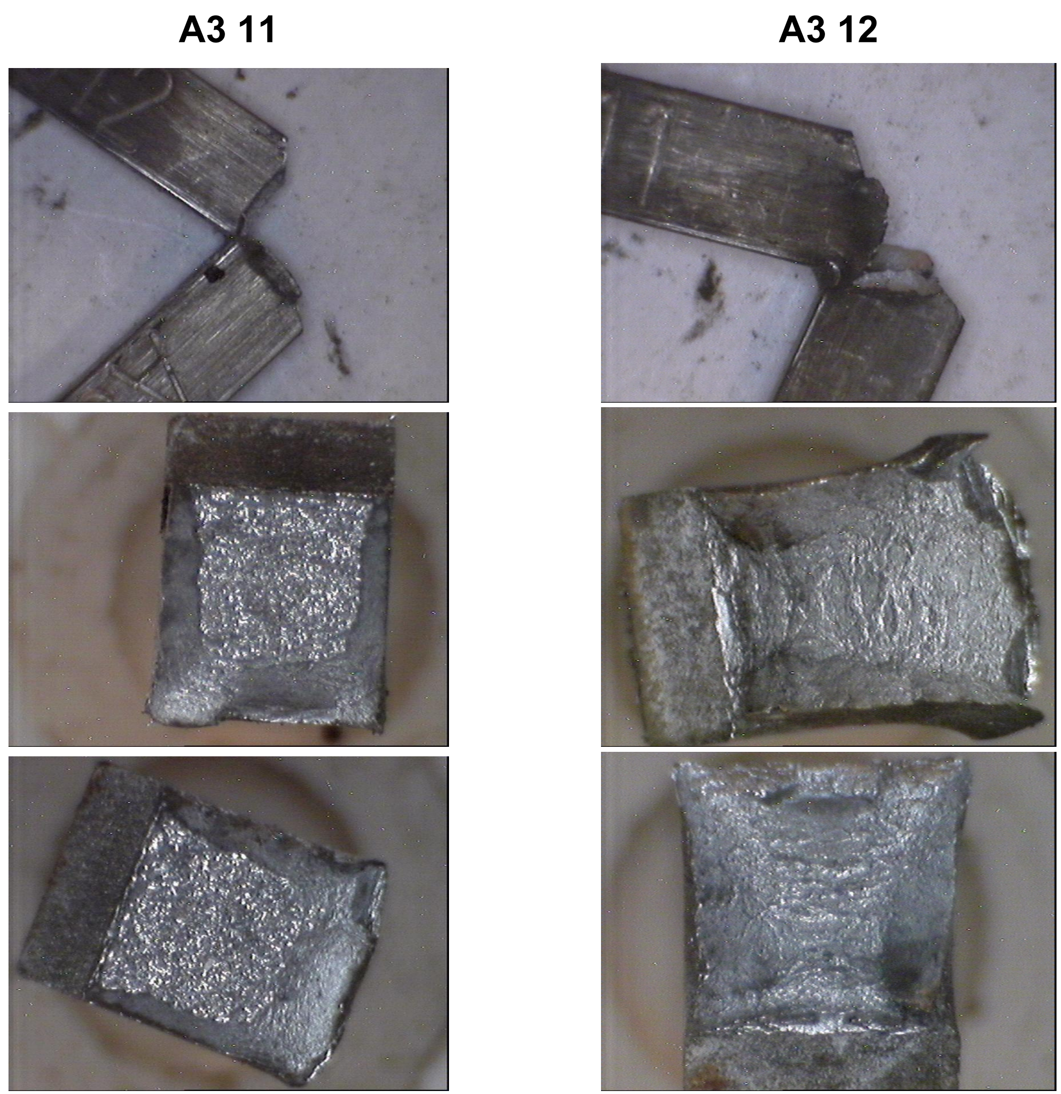

Fig. 8-34 Tested impact specimens A3 11, A3 12 after testing (Macro) and after complete breaking (Macro)

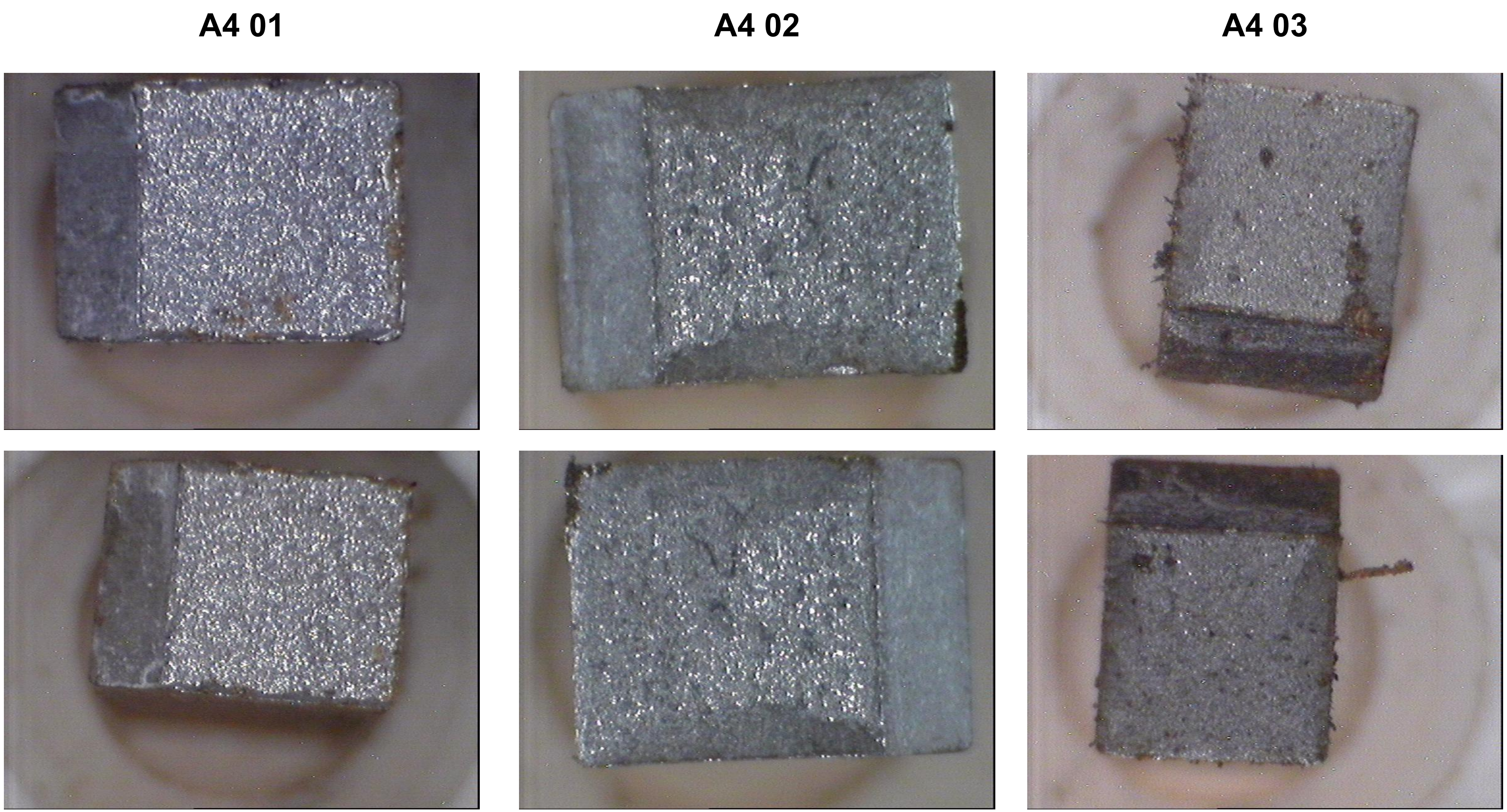

Fig. 8-35 Tested impact specimens A4 01, A4 02, A4 03 after complete breaking (Macro)

A4 04

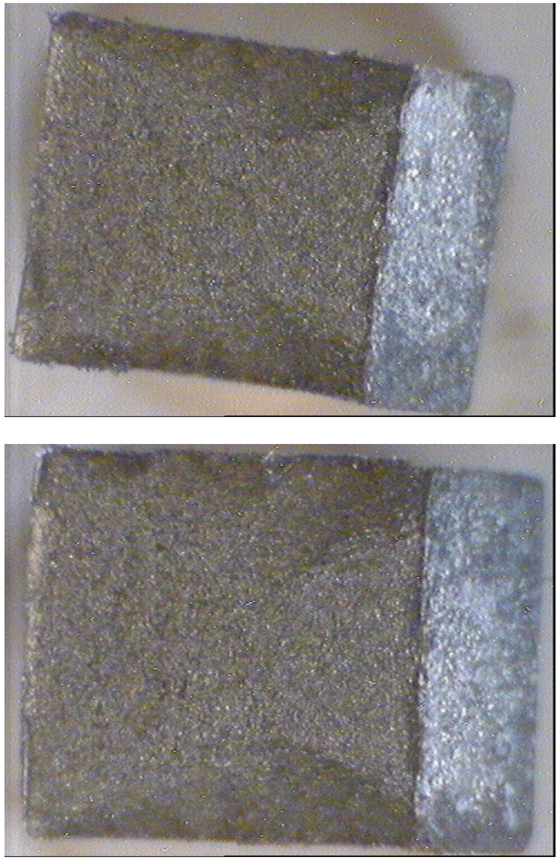

Fig. 8-36 Tested impact specimens A4 04 after complete breaking (Macro)

EO 01 **EO 02** **EO 03** **EO 04**

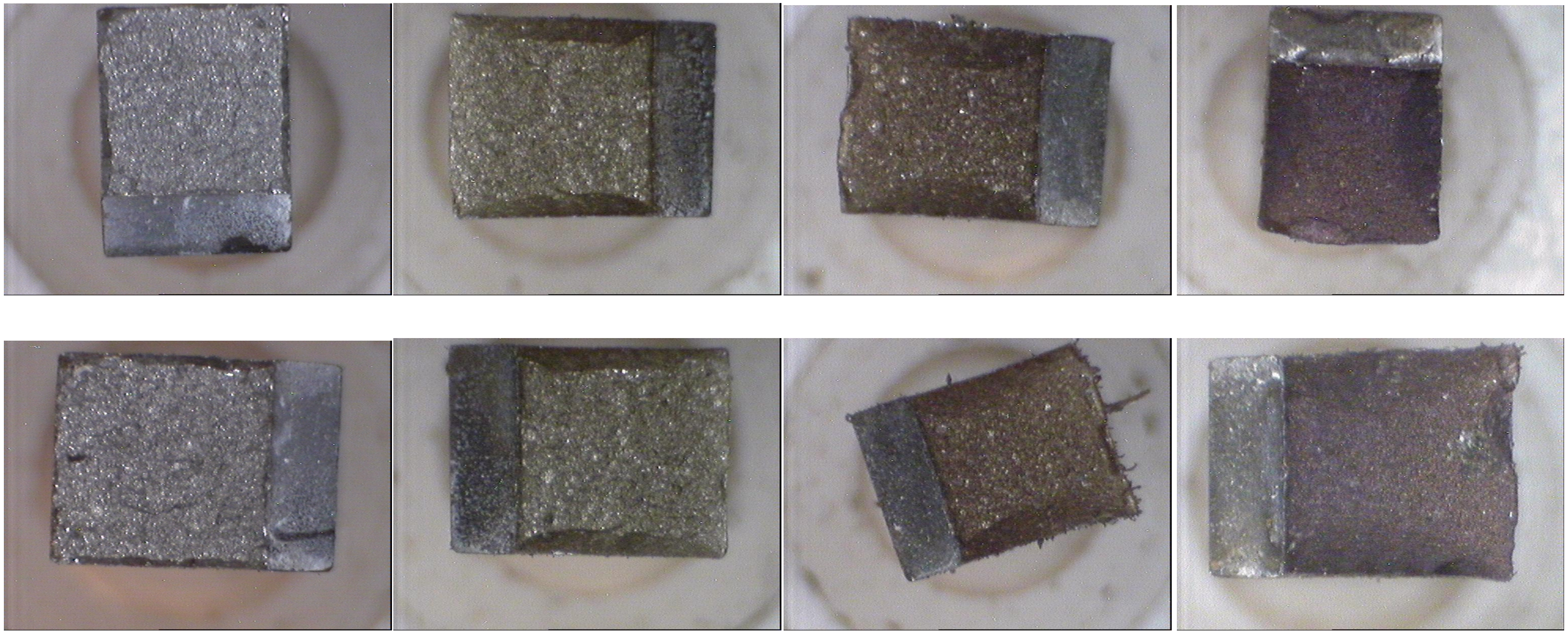

Fig. 8-37 Tested impact specimens EO 01, EO 02, EO 03, EO 04 after complete breaking (Macro)

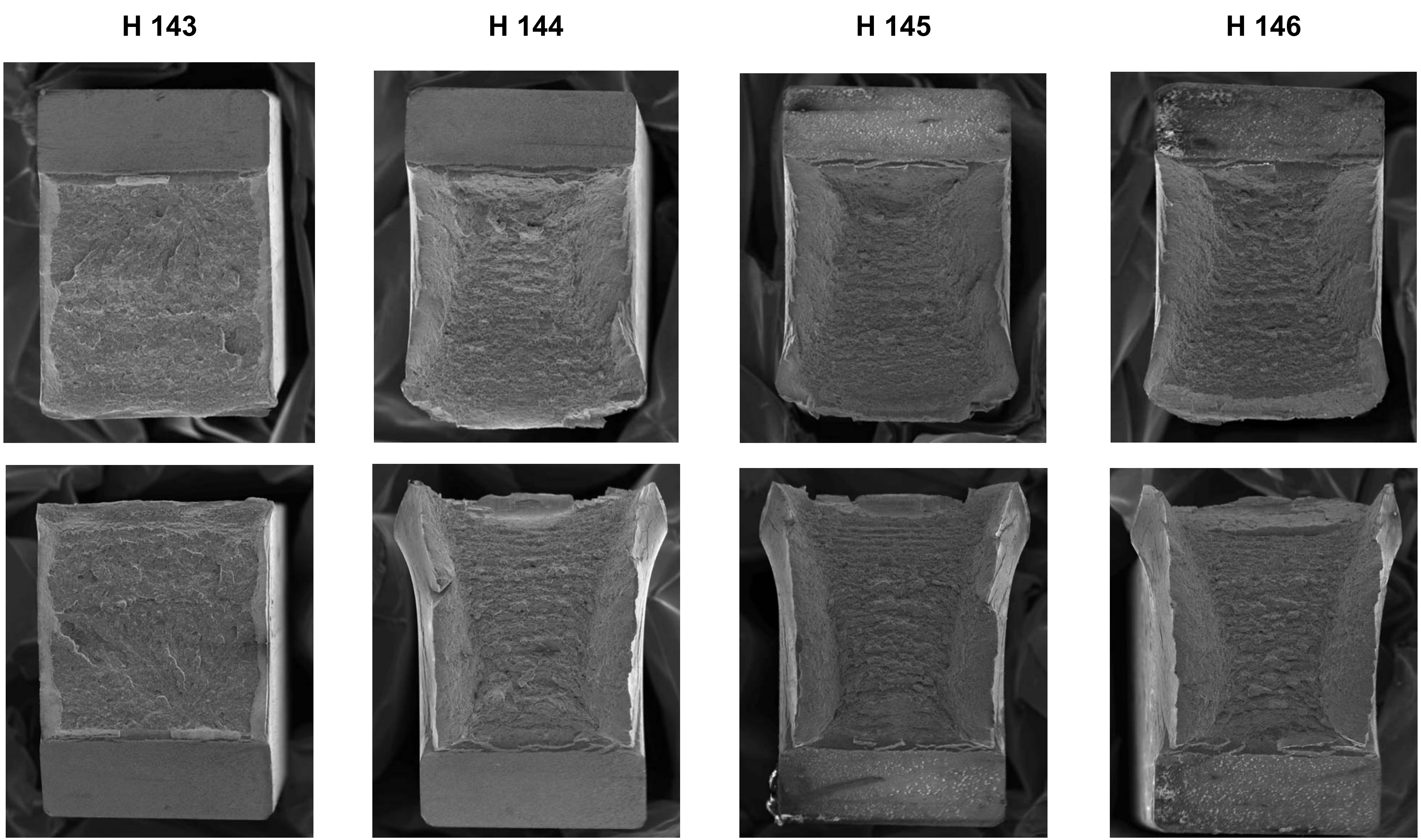

Fig. 8-38 Tested impact specimens H 143, H 144, H 145, H 146 after complete breaking (SEM)

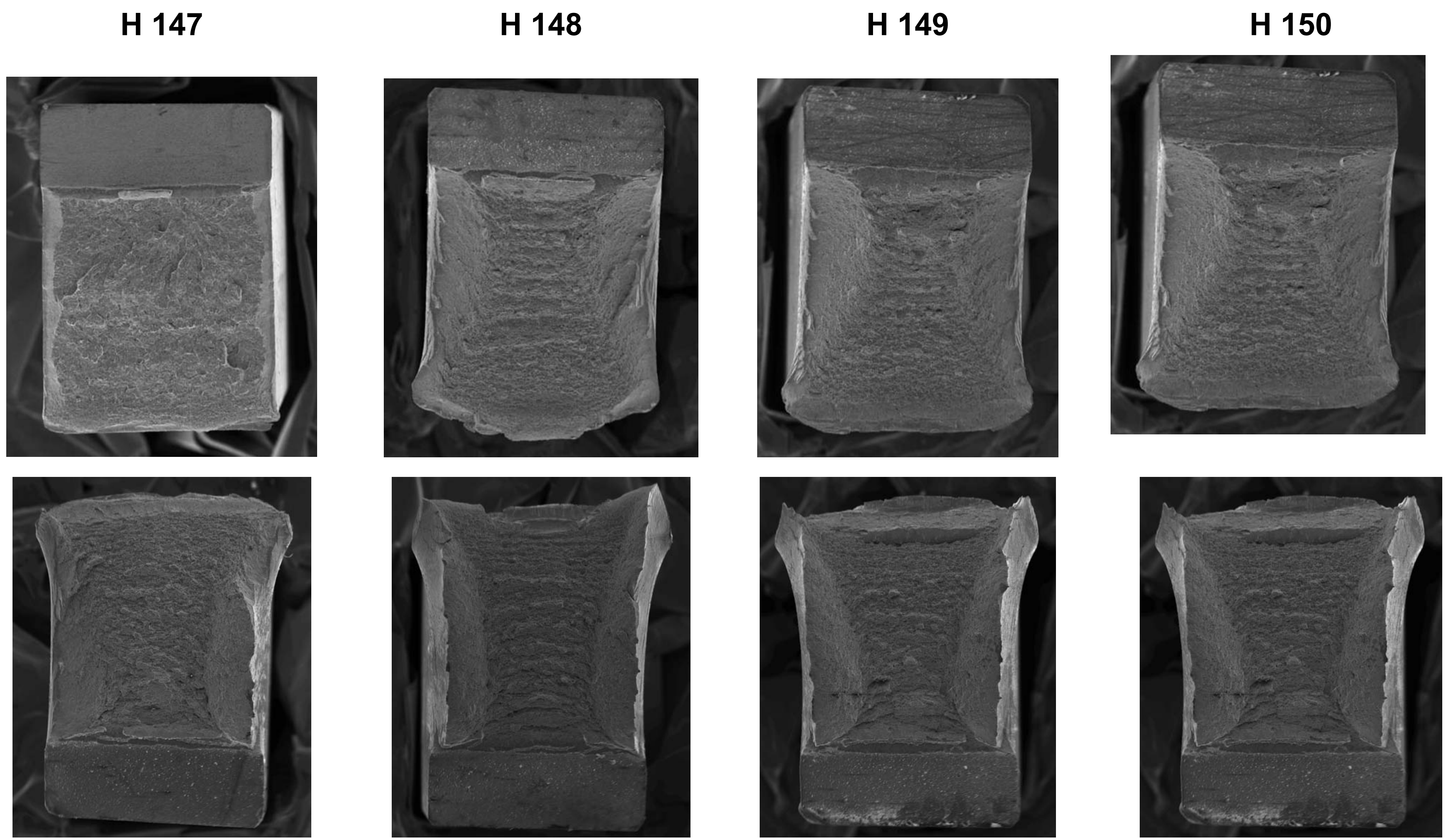

Fig. 8-39 Tested impact specimens H 147, H 148, H 149, H 150 after complete breaking (SEM)

H 151 H 152 H 153 H 154

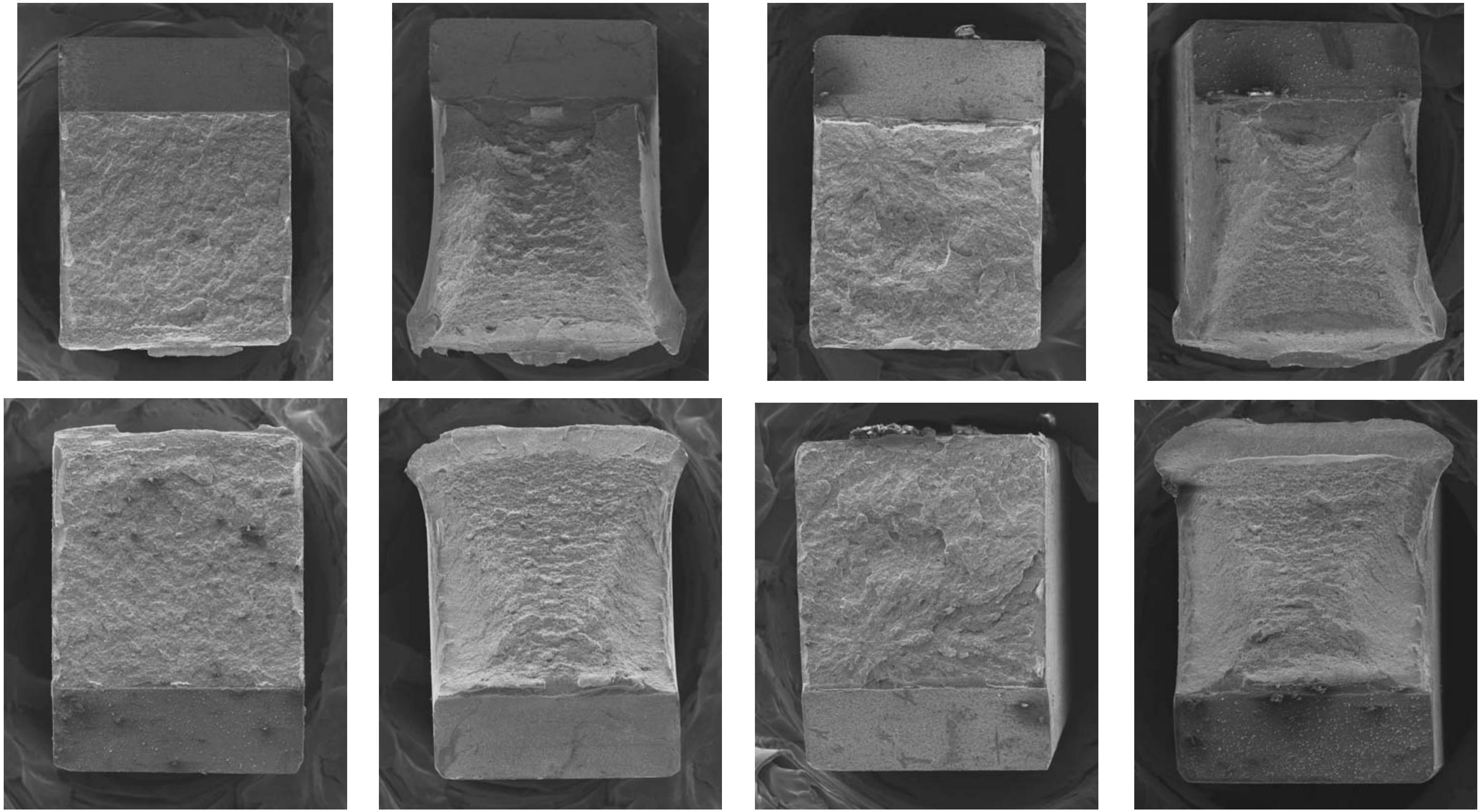

Fig. 8-40 Tested impact specimens H 151, H 152, H 153, H 154 after complete breaking (SEM)

H 155

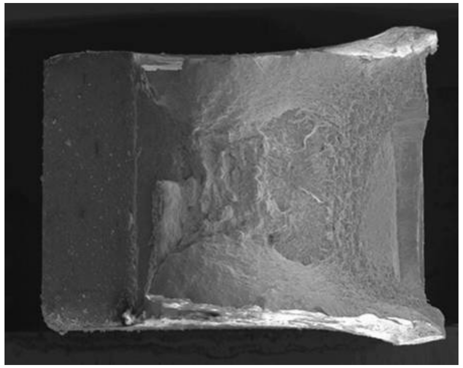

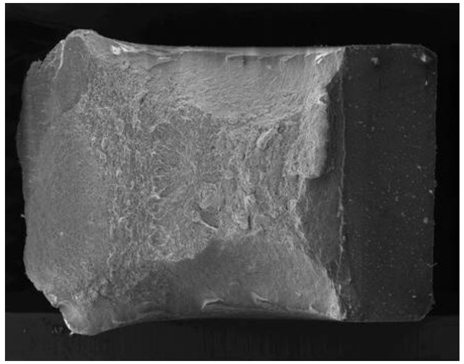

Fig. 8-41 Tested impact specimen H 155 after testing (Macro) and after complete breaking (SEM)

C 165 **C 166** **C 167**

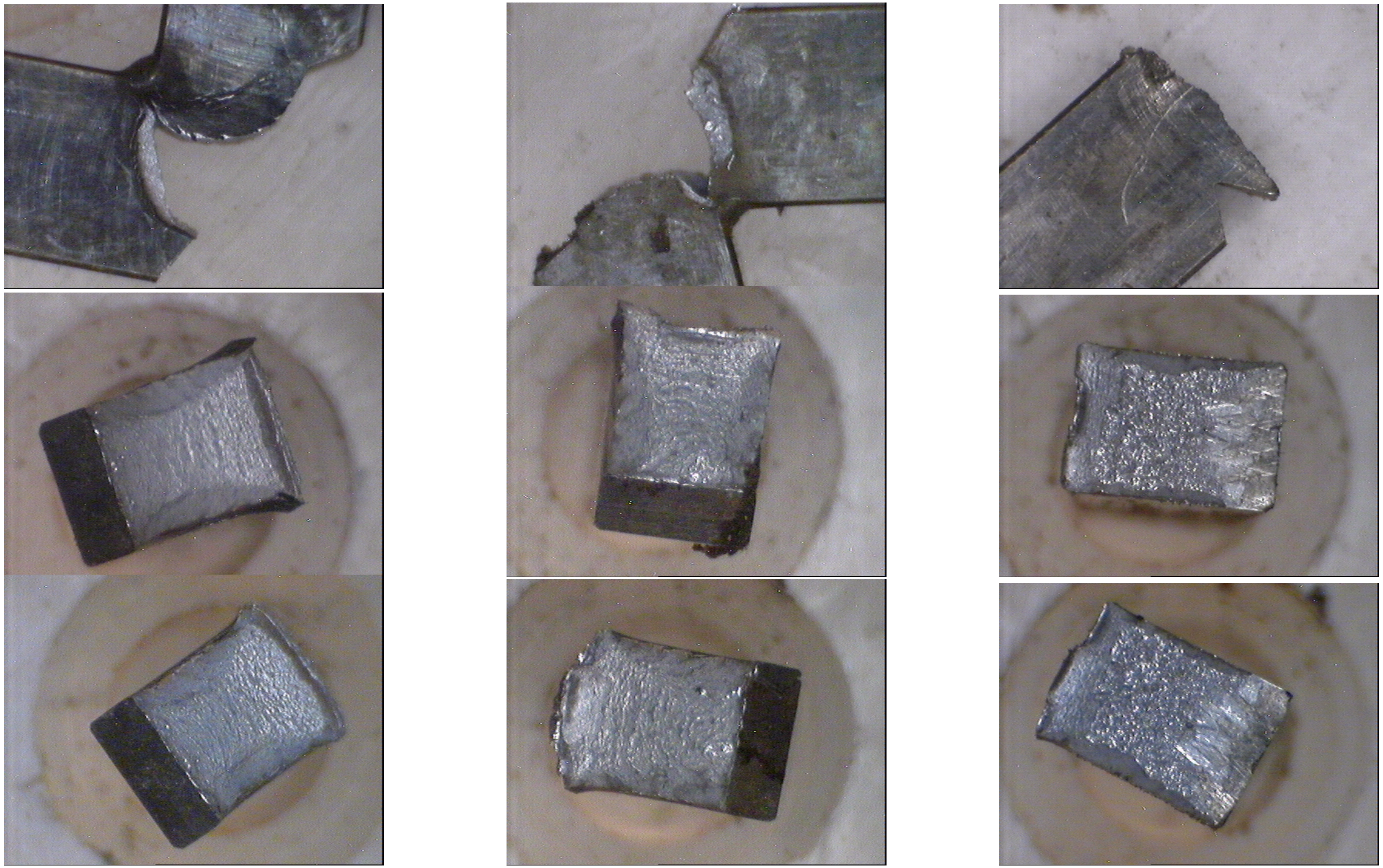

Fig. 8-42 Tested impact specimens C 165, C 166, C 167 after testing (Macro) and after complete breaking (Macro)

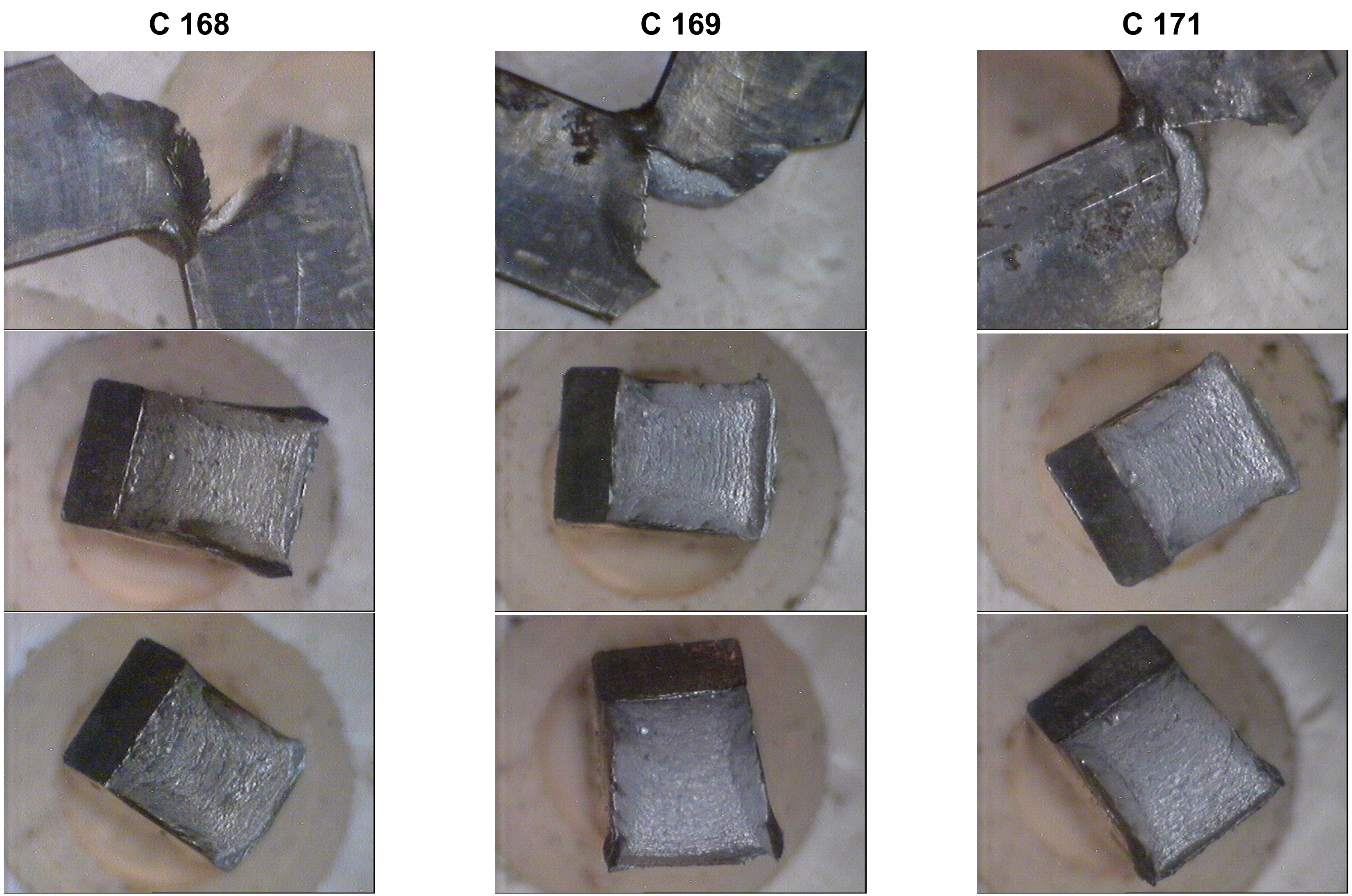

Fig. 8-43 Tested impact specimens C 168, C 169, C 171 after testing (Macro) and after complete breaking (Macro)

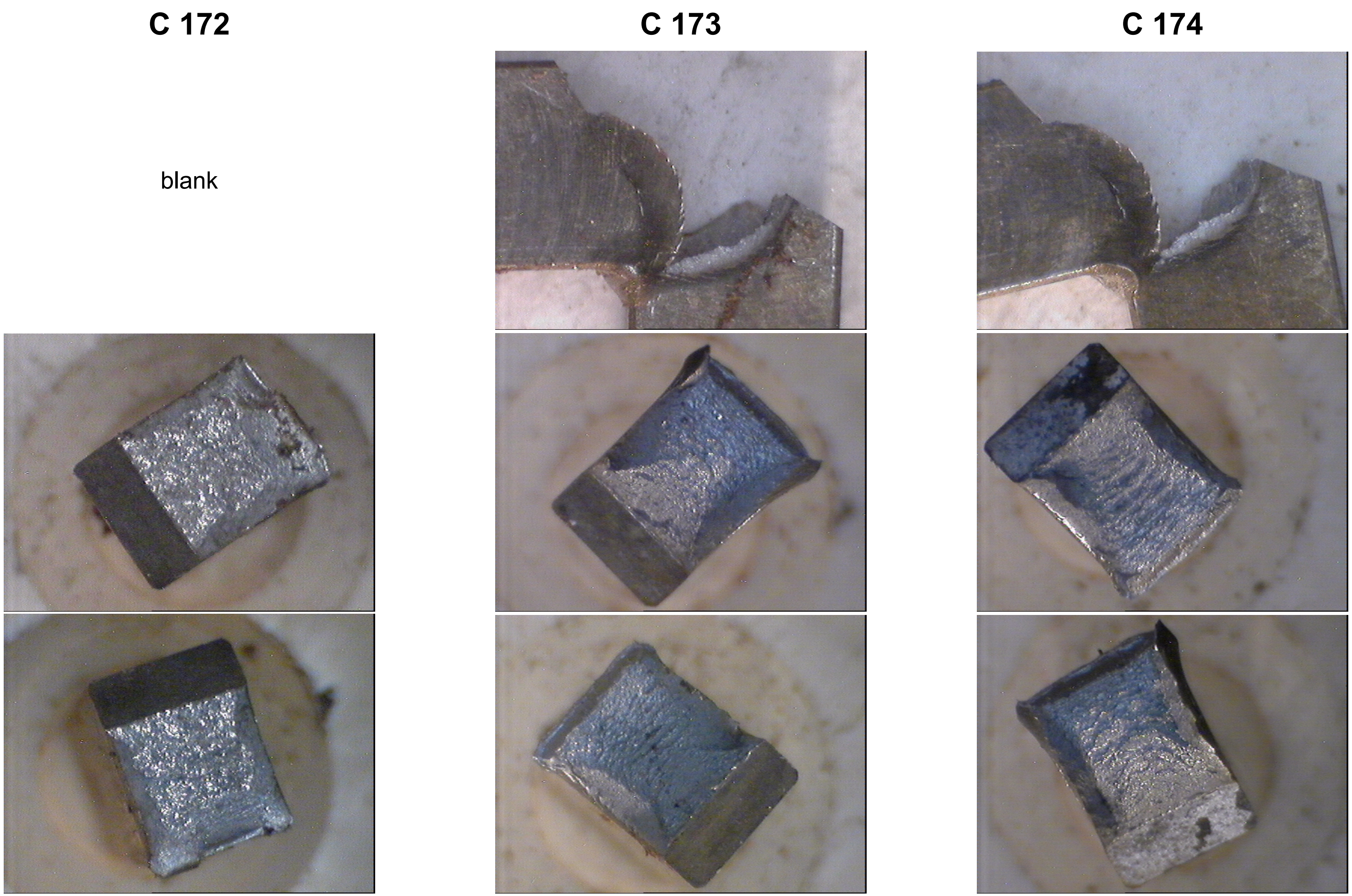

Fig. 8-44 Tested impact specimens C 172, C 173, C 174 after testing (Macro) and after complete breaking (Macro)

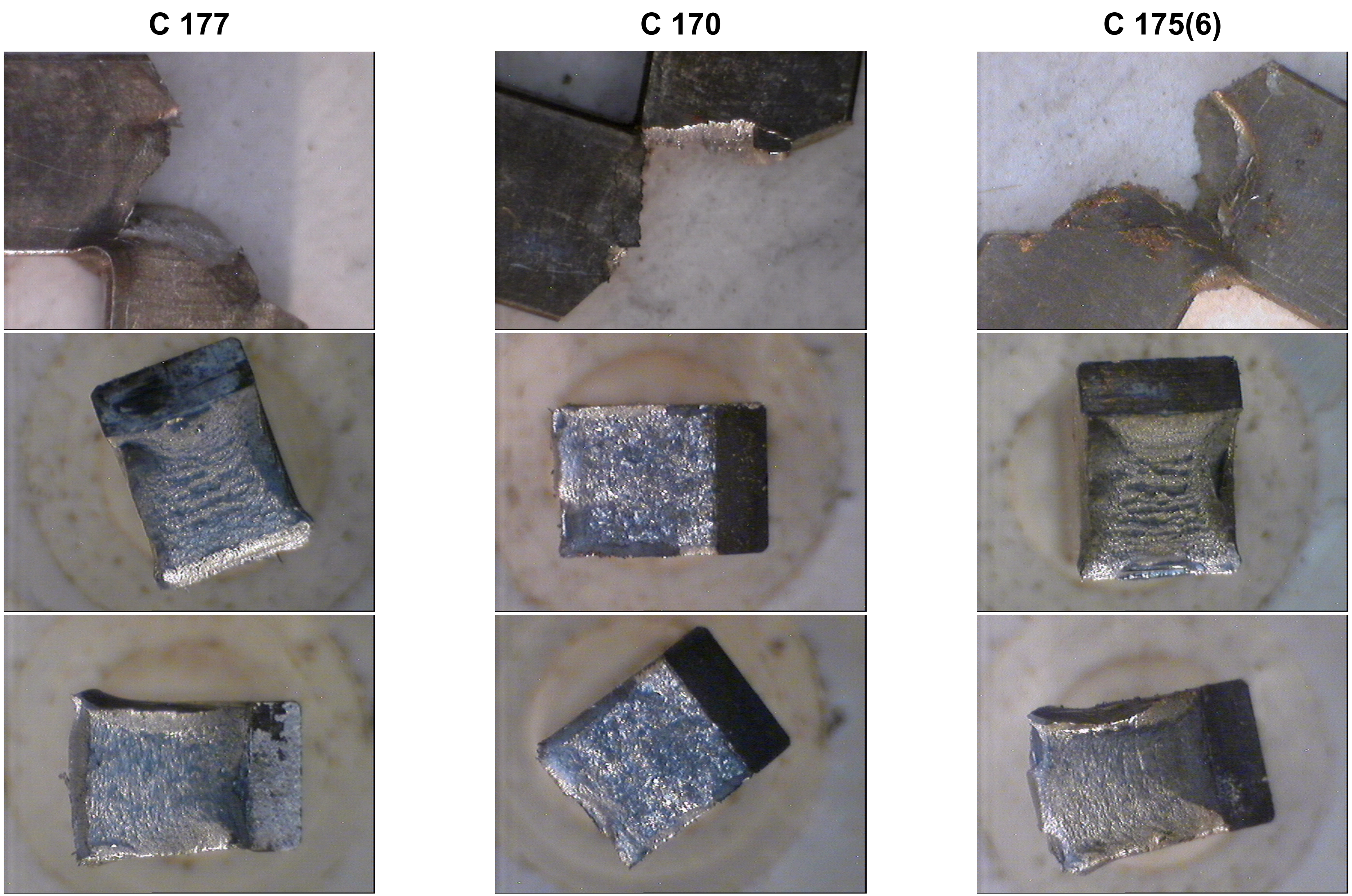

Fig. 8-45 Tested impact specimens C 177, C 170, C 175(6) after testing (Macro) and after complete breaking (Macro)

9 Annex B: Tensile Tests

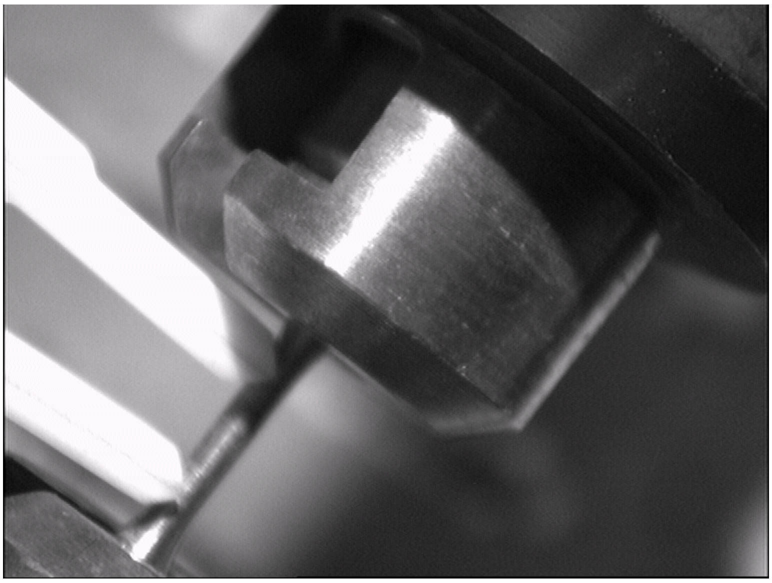

Fig. 9-1 Gripping of tensile specimen with extensometer position

9.1 EUROFER 97 as received

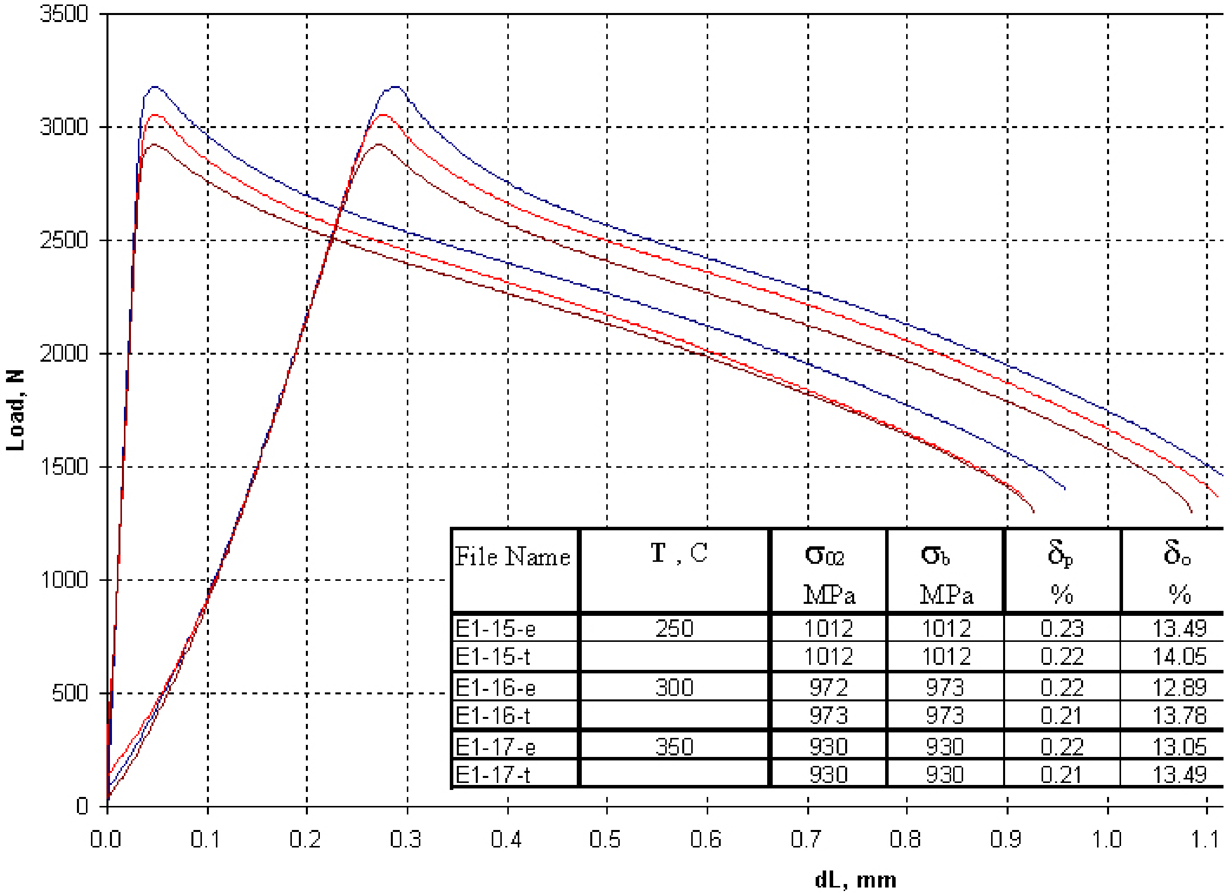

File Name	T , C	σ_{02} MPa	σ_b MPa	δ_p %	δ_o %
E1-15-e	250	1012	1012	0.23	13.49
E1-15-t		1012	1012	0.22	14.05
E1-16-e	300	972	973	0.22	12.89
E1-16-t		973	973	0.21	13.78
E1-17-e	350	930	930	0.22	13.05
E1-17-t		930	930	0.21	13.49

Fig. 9-2 Original tensile diagrams of the irradiated EUROFER 97 ANL specimens: E1 15 (T_{test} = 250°C), E1 16 (300°C), E1 17 (350°C) at 30.2 dpa, T_{irr} = 335.8°C, RIAR analysis (-e: extensometer, -t: crosshead)

9.2 EUROFER 97, heat treated

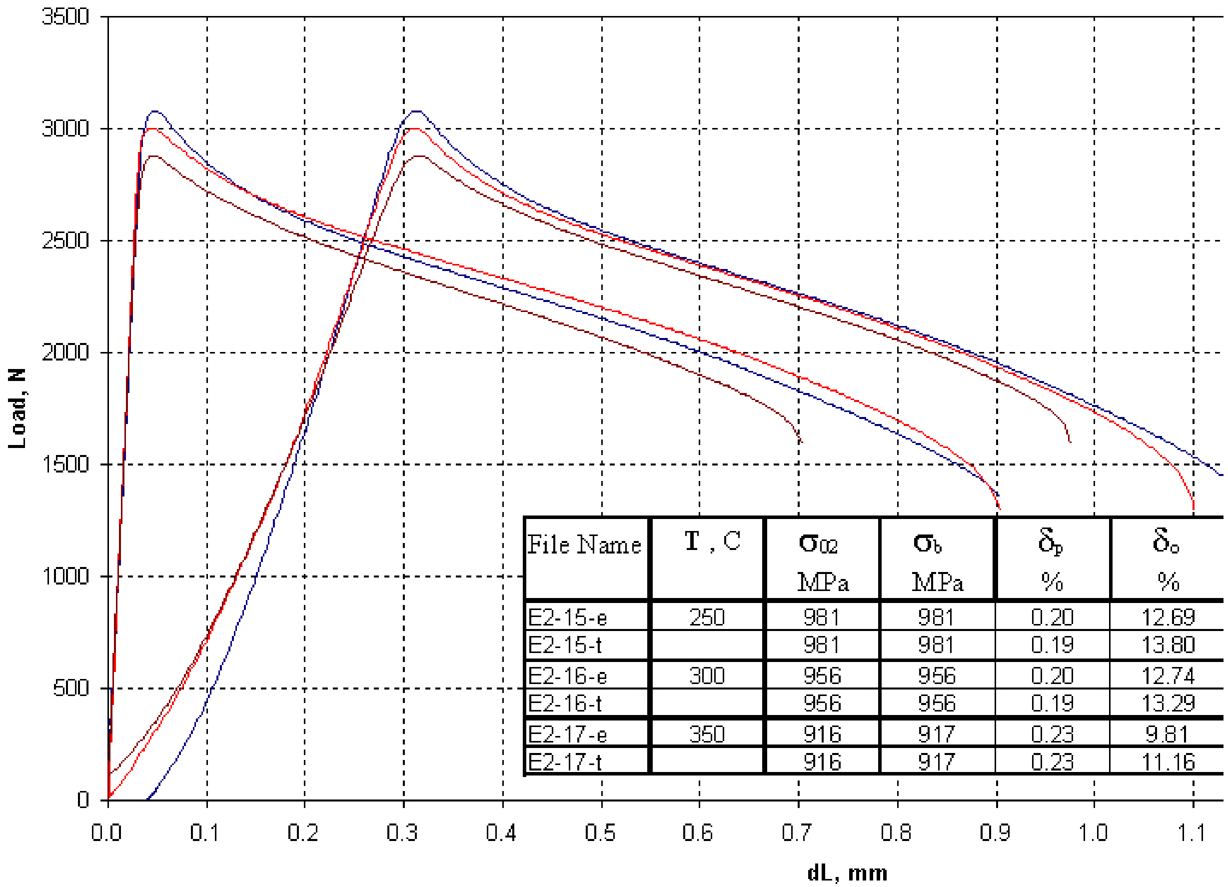

File Name	T , C	σ_{02} MPa	σ_b MPa	δ_p %	δ_o %
E2-15-e	250	981	981	0.20	12.69
E2-15-t		981	981	0.19	13.80
E2-16-e	300	956	956	0.20	12.74
E2-16-t		956	956	0.19	13.29
E2-17-e	350	916	917	0.23	9.81
E2-17-t		916	917	0.23	11.16

Fig. 9-3 Original tensile diagrams of the irradiated EUROFER 97 WB specimens: E2 15 (T_{test} = 250°C), E2 16 (300°C), E2 17 (350°C) at 30.2 dpa, T_{irr} = 335.8°C, RIAR analysis (-e: extensometer, -t: crosshead)

9.3 F82H mod.

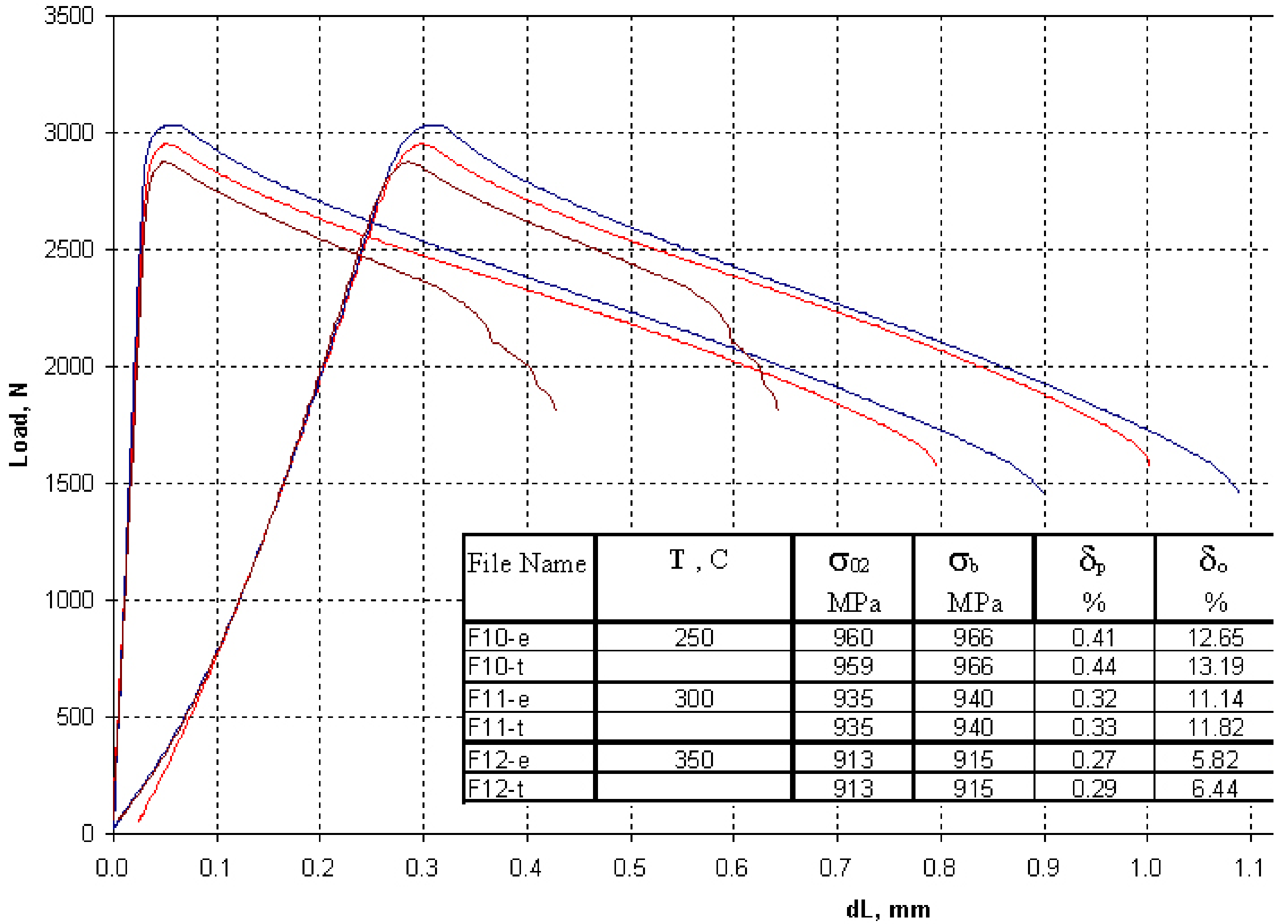

File Name	T , C	σ_{02} MPa	σ_b MPa	δ_p %	δ_o %
F10-e	250	960	966	0.41	12.65
F10-t		959	966	0.44	13.19
F11-e	300	935	940	0.32	11.14
F11-t		935	940	0.33	11.82
F12-e	350	913	915	0.27	5.82
F12-t		913	915	0.29	6.44

Fig. 9-4 Original tensile diagrams of the irradiated F82H mod. specimens: F 10 (T_{test} = 250°C), F 11 (300°C), F 12 (350°C) at 30.2 dpa, T_{irr} = 335.8°C, RIAR analysis (-e: extensometer, -t: crosshead)

9.4 OPTIFER IVc

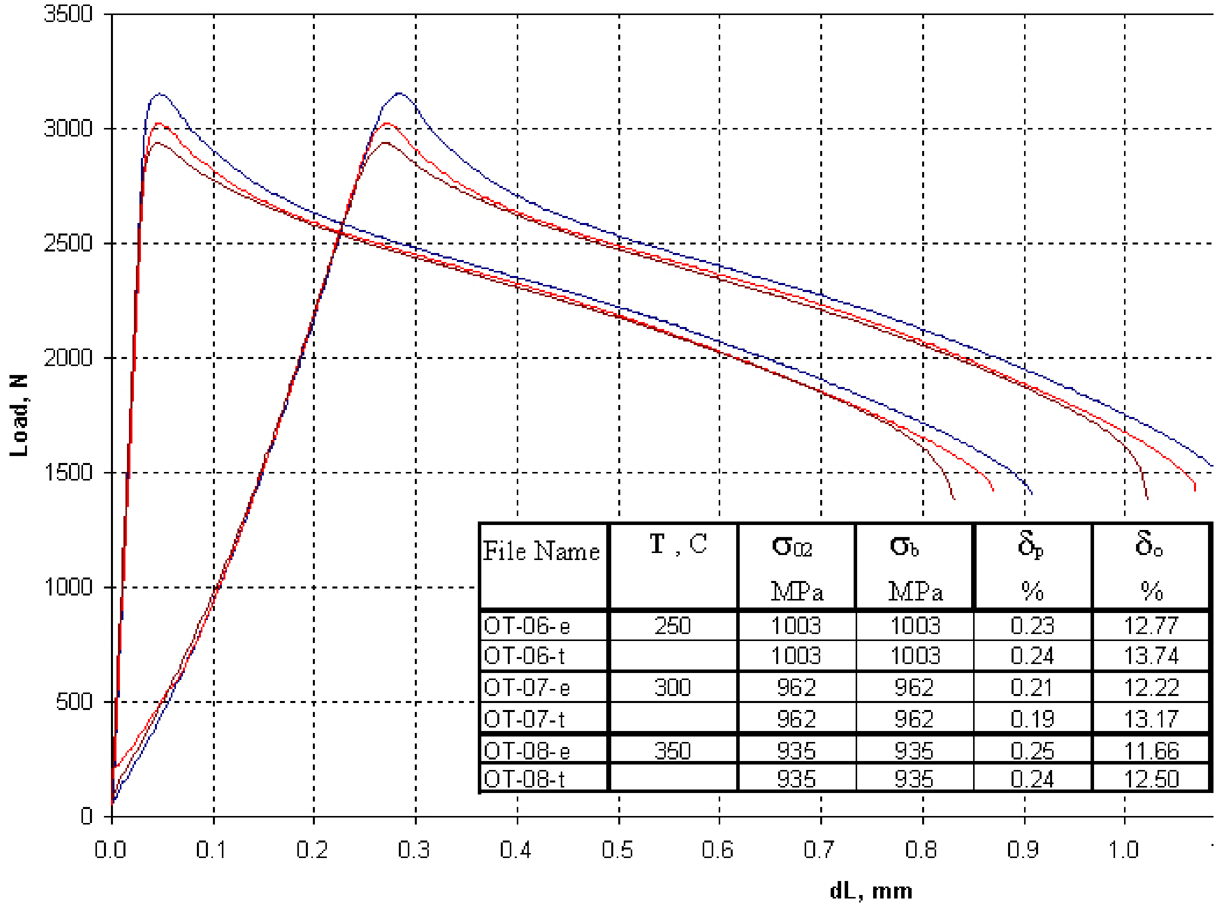

File Name	T , C	σ_{02} MPa	σ_b MPa	δ_p %	δ_o %
OT-06-e	250	1003	1003	0.23	12.77
OT-06-t		1003	1003	0.24	13.74
OT-07-e	300	962	962	0.21	12.22
OT-07-t		962	962	0.19	13.17
OT-08-e	350	935	935	0.25	11.66
OT-08-t		935	935	0.24	12.50

Fig. 9-5 Original tensile diagrams of the irradiated OPTIFER IVc specimens: OT 06 (T_{test} = 250°C), OT 07 (300°C), OT 08 (350°C) at 30.2 dpa, T_{irr} = 335.8°C, RIAR analysis (-e: extensometer, -t: crosshead)

9.5 ADS 2

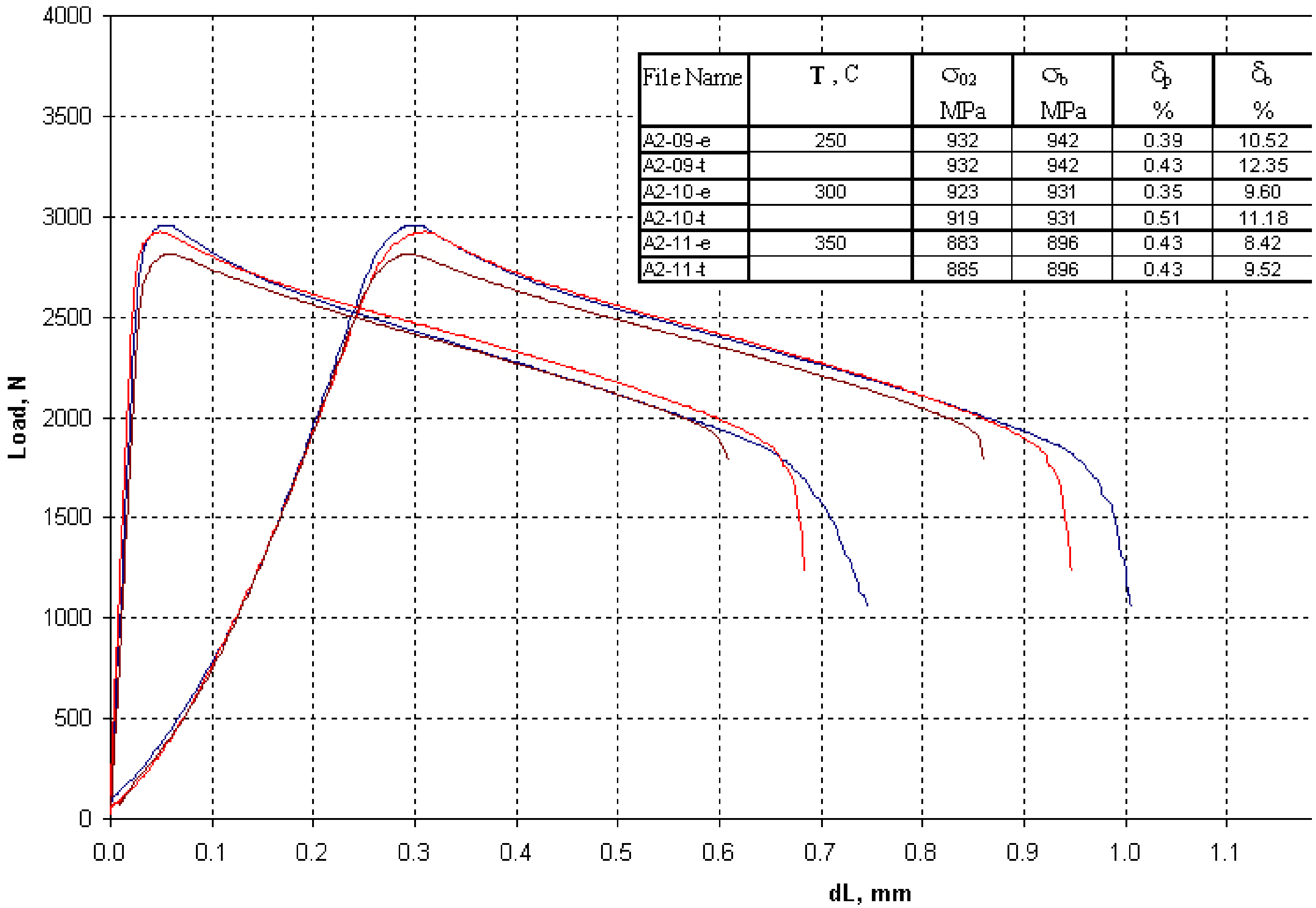

File Name	T, C	σ_{02} MPa	σ_b MPa	δ_p %	δ_o %
A2-09-e	250	932	942	0.39	10.52
A2-09-t		932	942	0.43	12.35
A2-10-e	300	923	931	0.35	9.60
A2-10-t		919	931	0.51	11.18
A2-11-e	350	883	896	0.43	8.42
A2-11-t		885	896	0.43	9.52

Fig. 9-6 Original tensile diagrams of the irradiated ADS 2 specimens: A2 09 (T_{test} = 250°C), A2 10 (300°C), A2 11 (350°C) at 30.2 dpa, T_{irr} = 335.8°C, RIAR analysis (-e: extensometer, -t: crosshead)

9.6 ADS 3

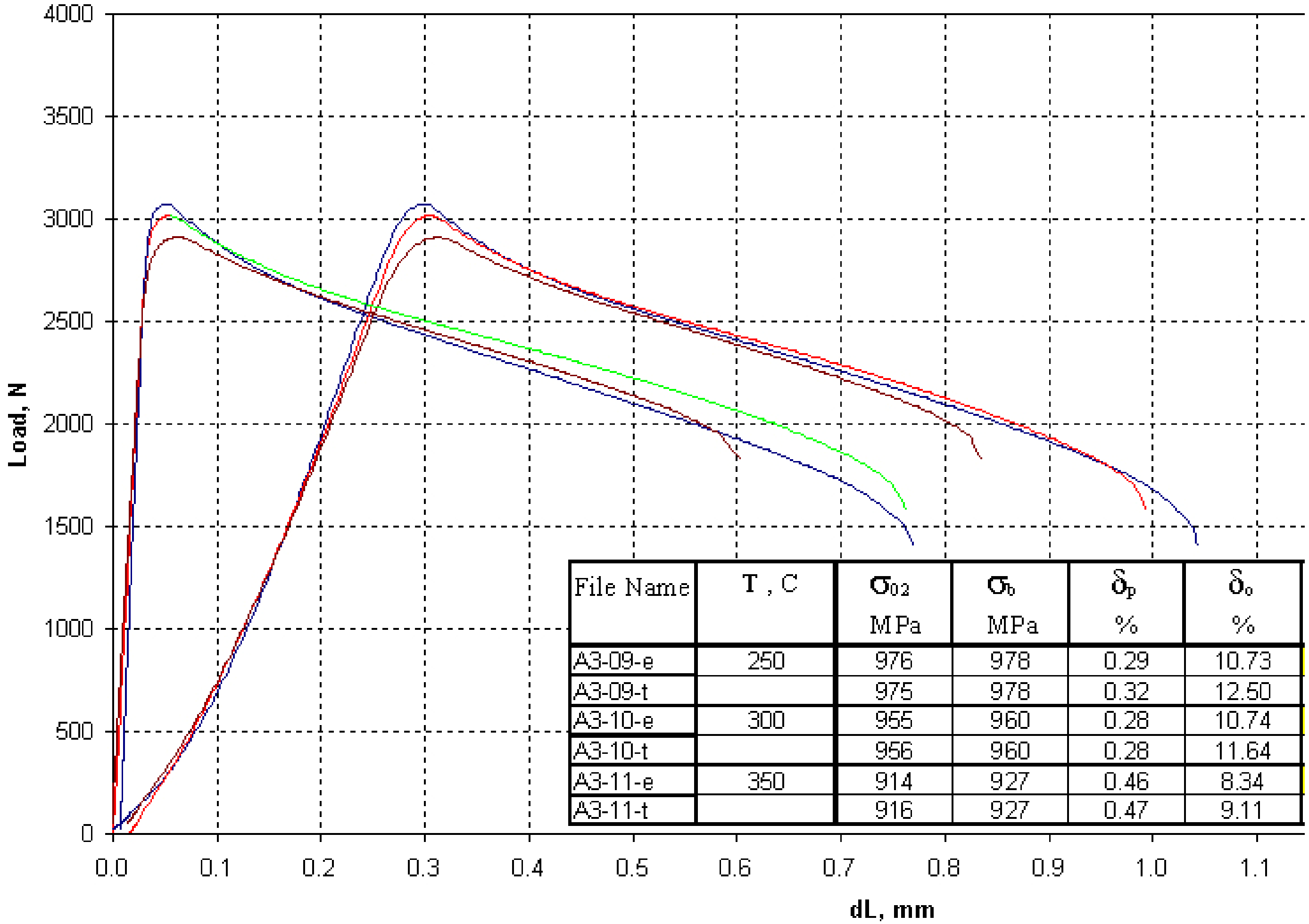

File Name	T , C	σ_{02} MPa	σ_b MPa	δ_p %	δ_o %
A3-09-e	250	976	978	0.29	10.73
A3-09-t		975	978	0.32	12.50
A3-10-e	300	955	960	0.28	10.74
A3-10-t		956	960	0.28	11.64
A3-11-e	350	914	927	0.46	8.34
A3-11-t		916	927	0.47	9.11

Fig. 9-7 Original tensile diagrams of the irradiated ADS 3 specimens: A3 09 (T_{test} = 250°C), A3 10 (300°C), A3 11 (350°C) at 30.2 dpa, T_{irr} = 335.8°C, RIAR analysis (-e: extensometer, -t: crosshead)

9.7 ADS 4

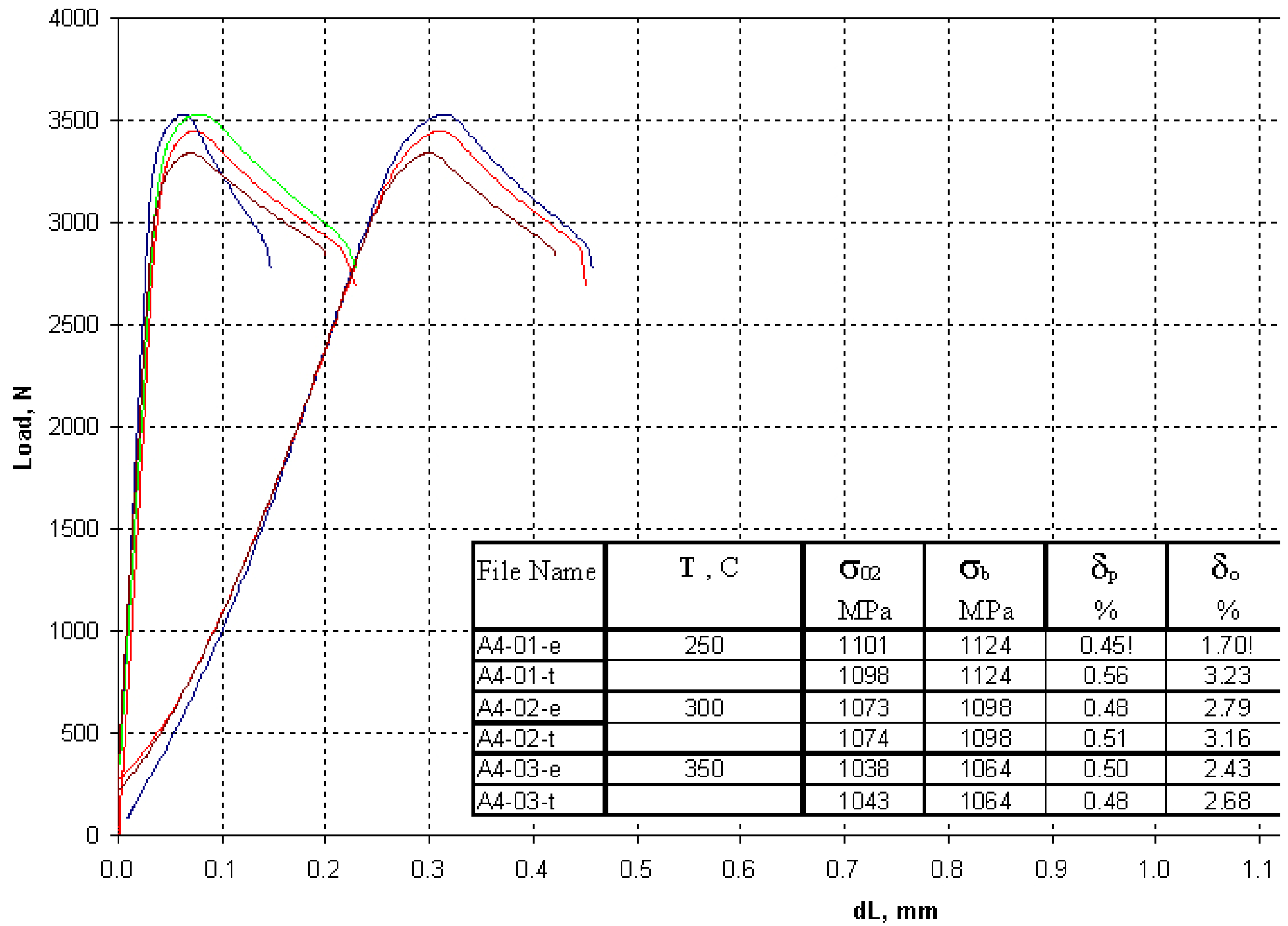

File Name	T, C	σ_{02} MPa	σ_b MPa	δ_p %	δ_o %
A4-01-e	250	1101	1124	0.45!	1.70!
A4-01-t		1098	1124	0.56	3.23
A4-02-e	300	1073	1098	0.48	2.79
A4-02-t		1074	1098	0.51	3.16
A4-03-e	350	1038	1064	0.50	2.43
A4-03-t		1043	1064	0.48	2.68

Fig. 9-8 Original tensile diagrams of the irradiated ADS 4 specimens: A4 01 (T_{test} = 250°C), A4 02 (300°C), A4 03 (350°C) at 30.2 dpa, T_{irr} = 335.8°C, RIAR analysis (-e: extensometer, -t: crosshead)

9.8 EURODShip, 0.3 % Y_2O_3

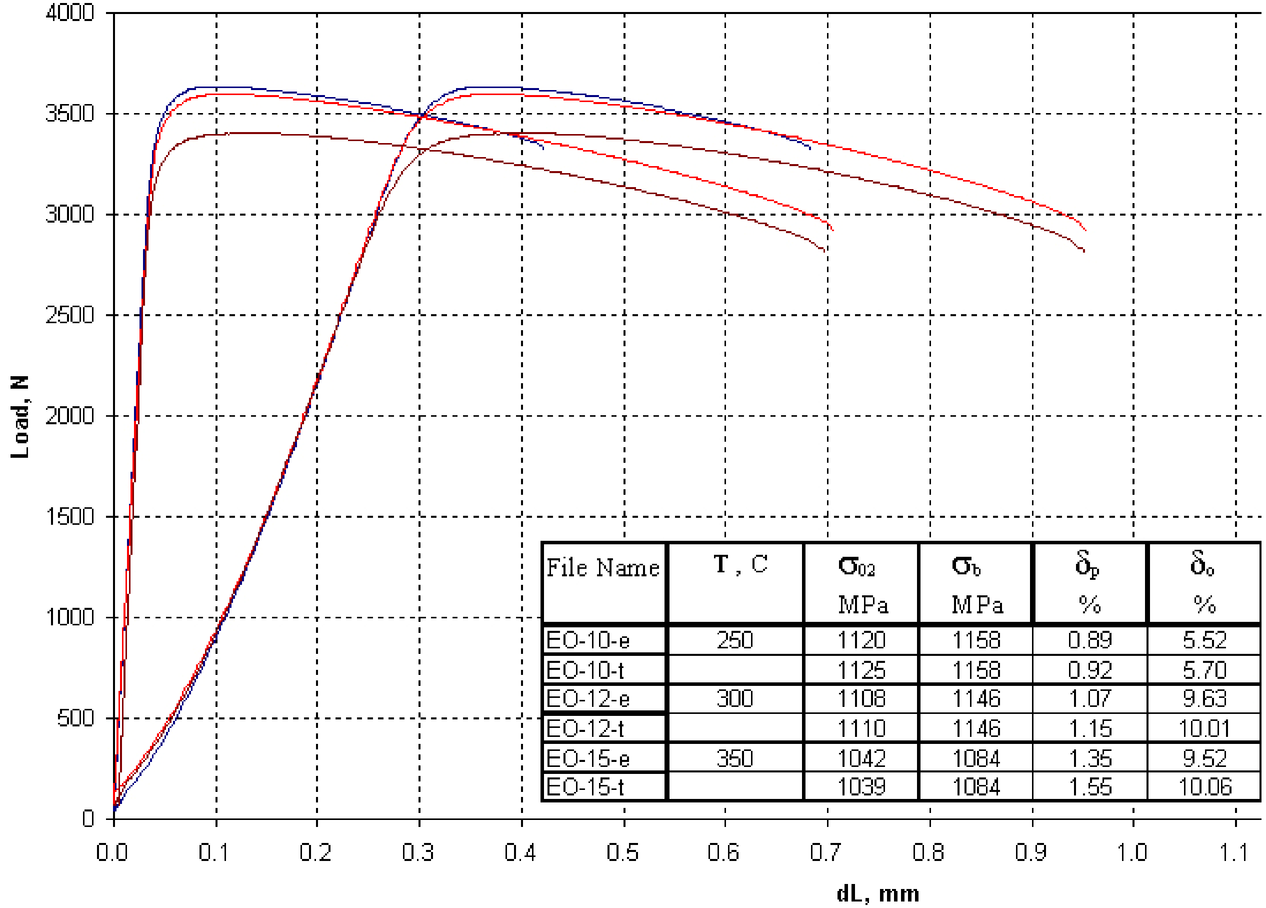

File Name	T , C	σ_{02} MPa	σ_b MPa	δ_p %	δ_o %
EO-10-e	250	1120	1158	0.89	5.52
EO-10-t		1125	1158	0.92	5.70
EO-12-e	300	1108	1146	1.07	9.63
EO-12-t		1110	1146	1.15	10.01
EO-15-e	350	1042	1084	1.35	9.52
EO-15-t		1039	1084	1.55	10.06

Fig. 9-9 Original tensile diagrams of the irradiated EURODShip specimens: EO 10 (T_{test} = 250°C), EO 12 (300°C), EO 15 (350°C) at 30.2 dpa, T_{irr} = 335.8°C, RIAR analysis (-e: extensometer, -t: crosshead)

E1 15

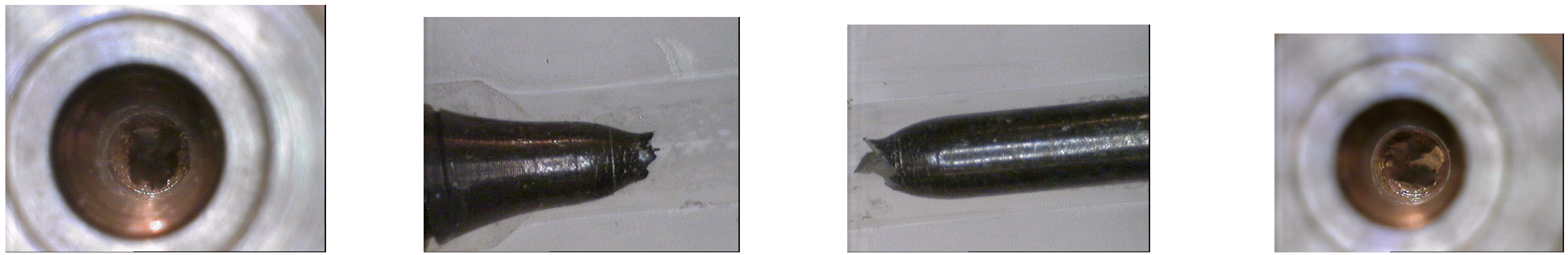

E1 16

E1 17

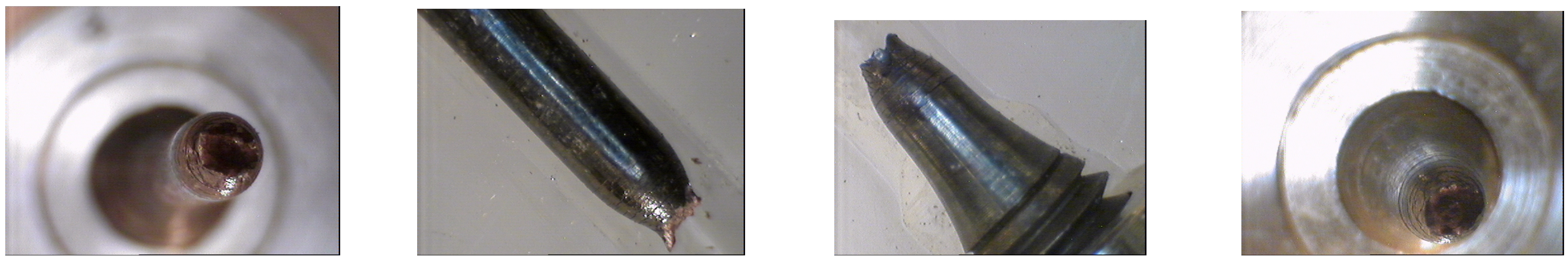

Fig. 9-10 Photographs (Macro) of the tensile tested EUROFER 97 ANL specimens: E1 15 (T_{test} = 250°C), E1 16 (300°C), E1 17 (350°C)

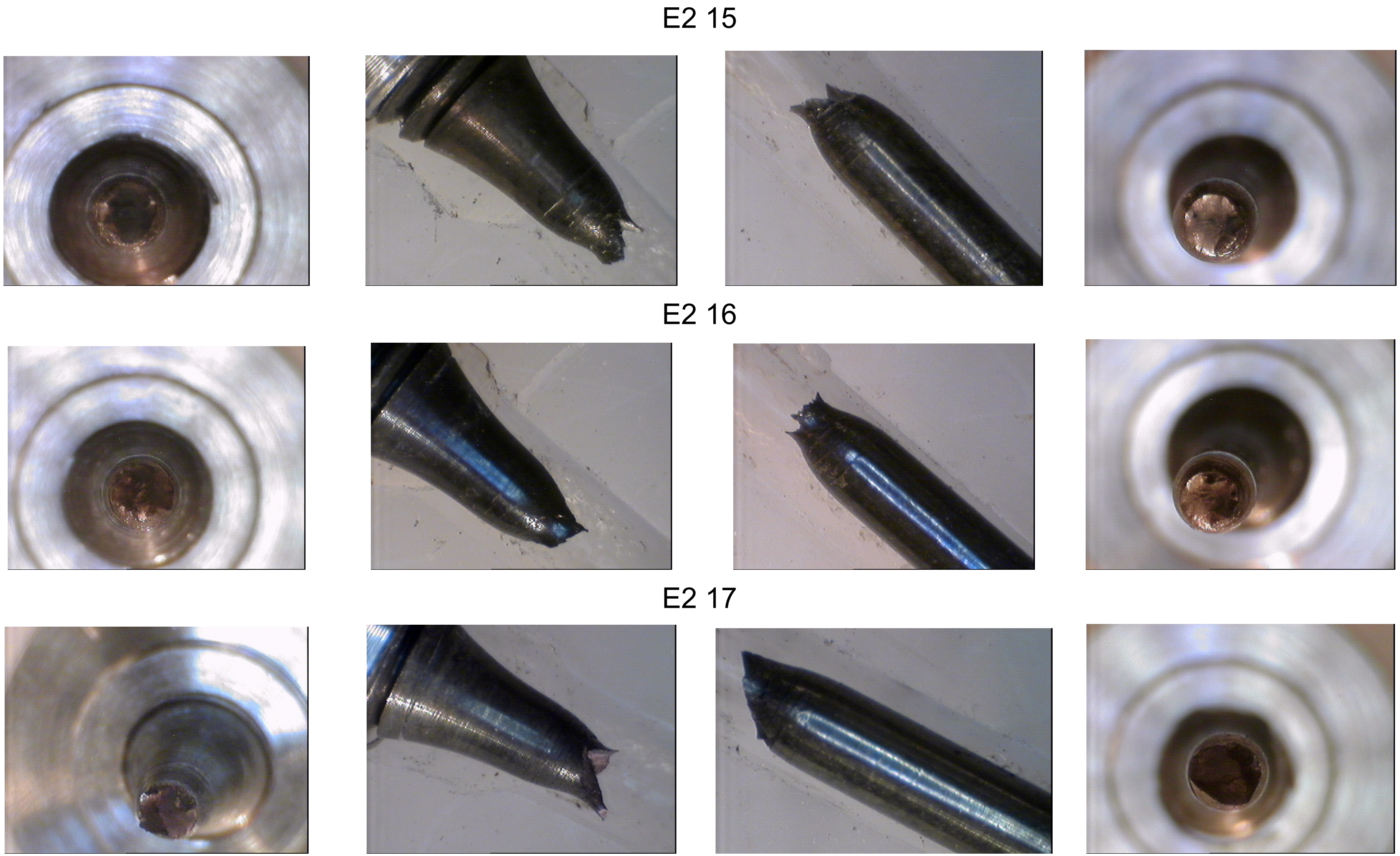

Fig. 9-11 Photographs (Macro) of the tensile tested EUROFER 97 WB specimens: E2 15 (T_{test} = 250°C), E2 16 (300°C), E2 17 (350°C)

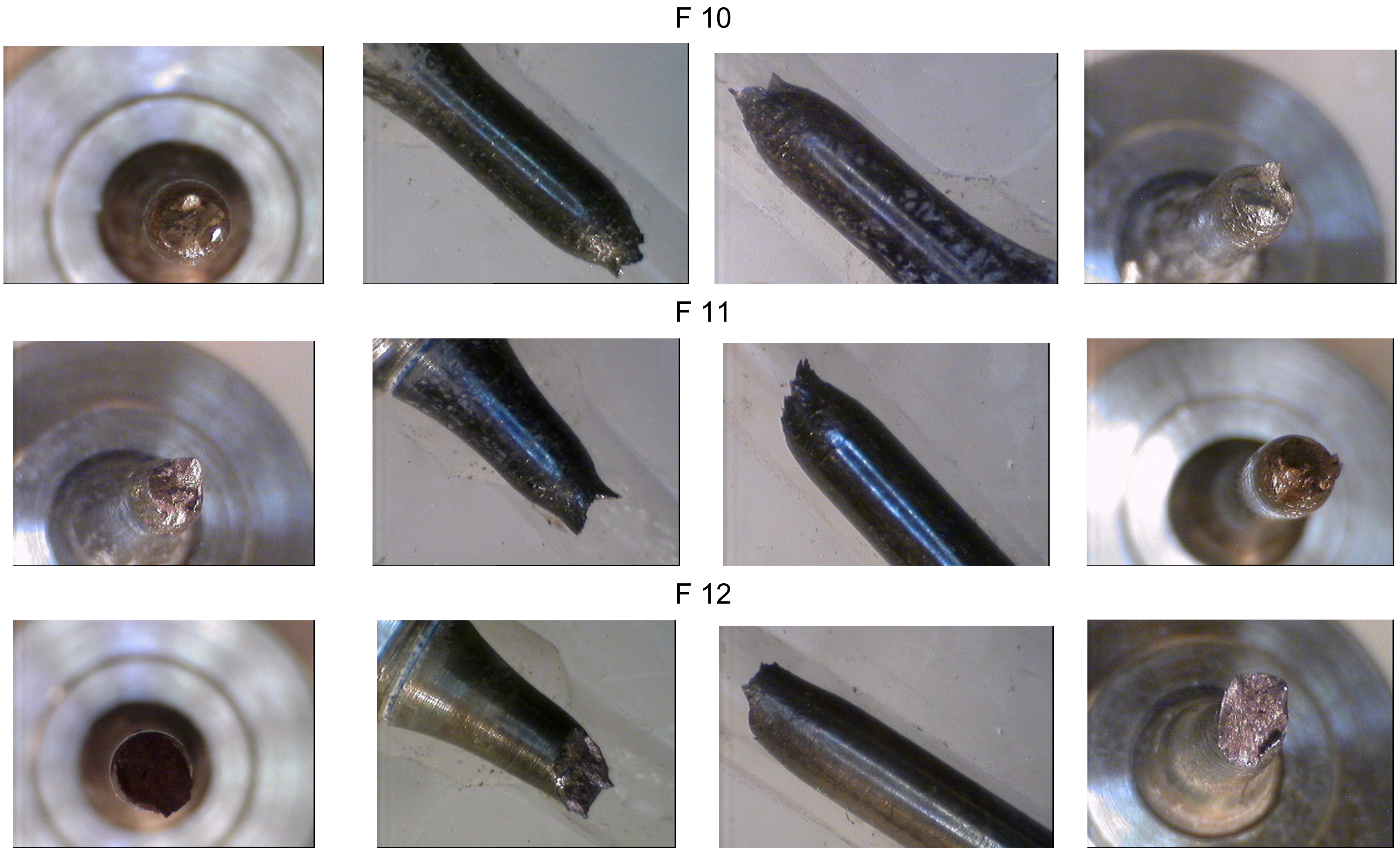

Fig. 9-12 Photographs (Macro) of the tensile tested F82H mod. specimens: F 10 (T_{test} = 250°C), F 11 (300°C), F 12 (350°C)

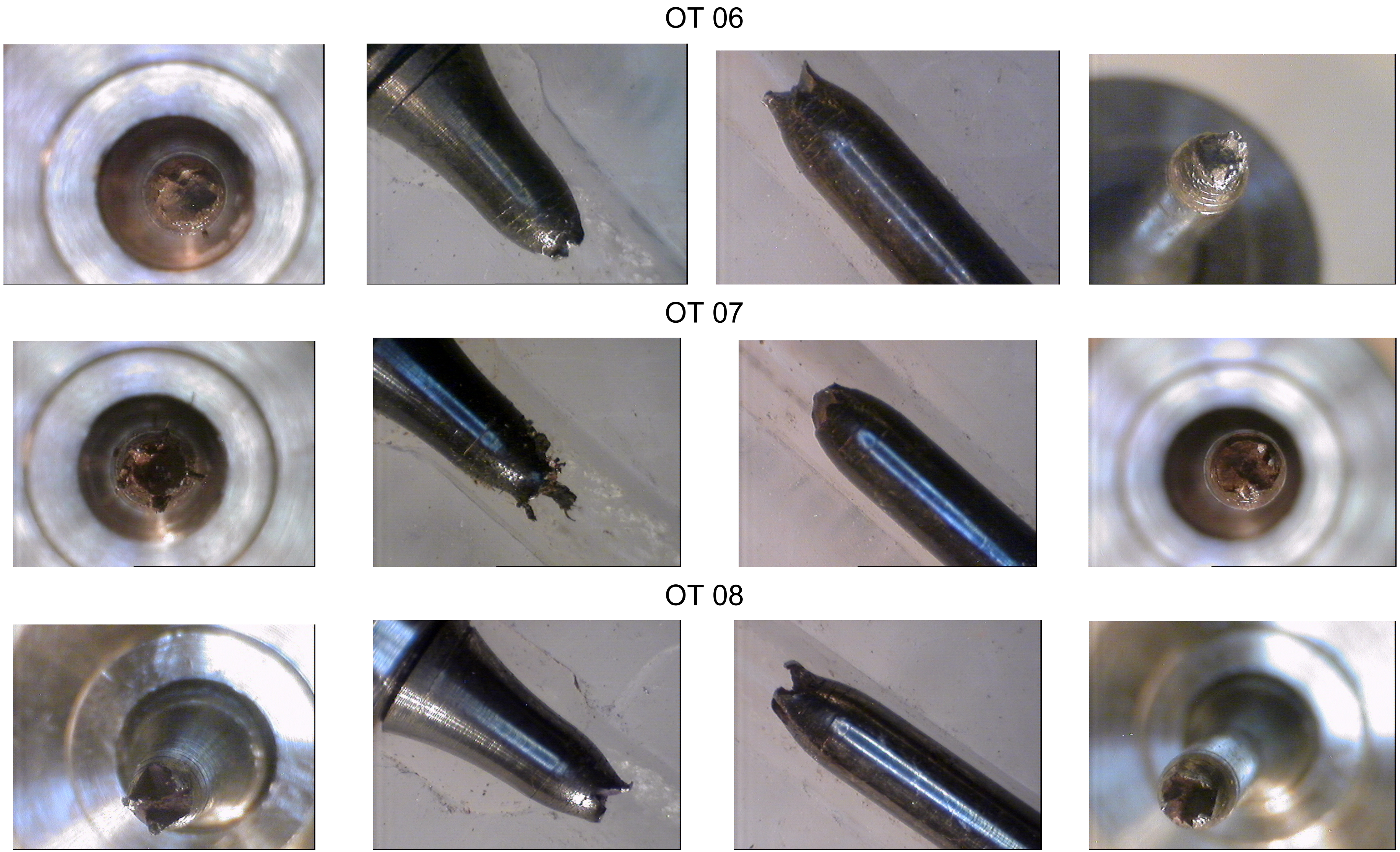

Fig. 9-13 Photographs (Macro) of the tensile tested OPTIFER IVc specimens: OT 06 (T_{test} = 250°C), OT 07 (300°C), OT 08 (350°C)

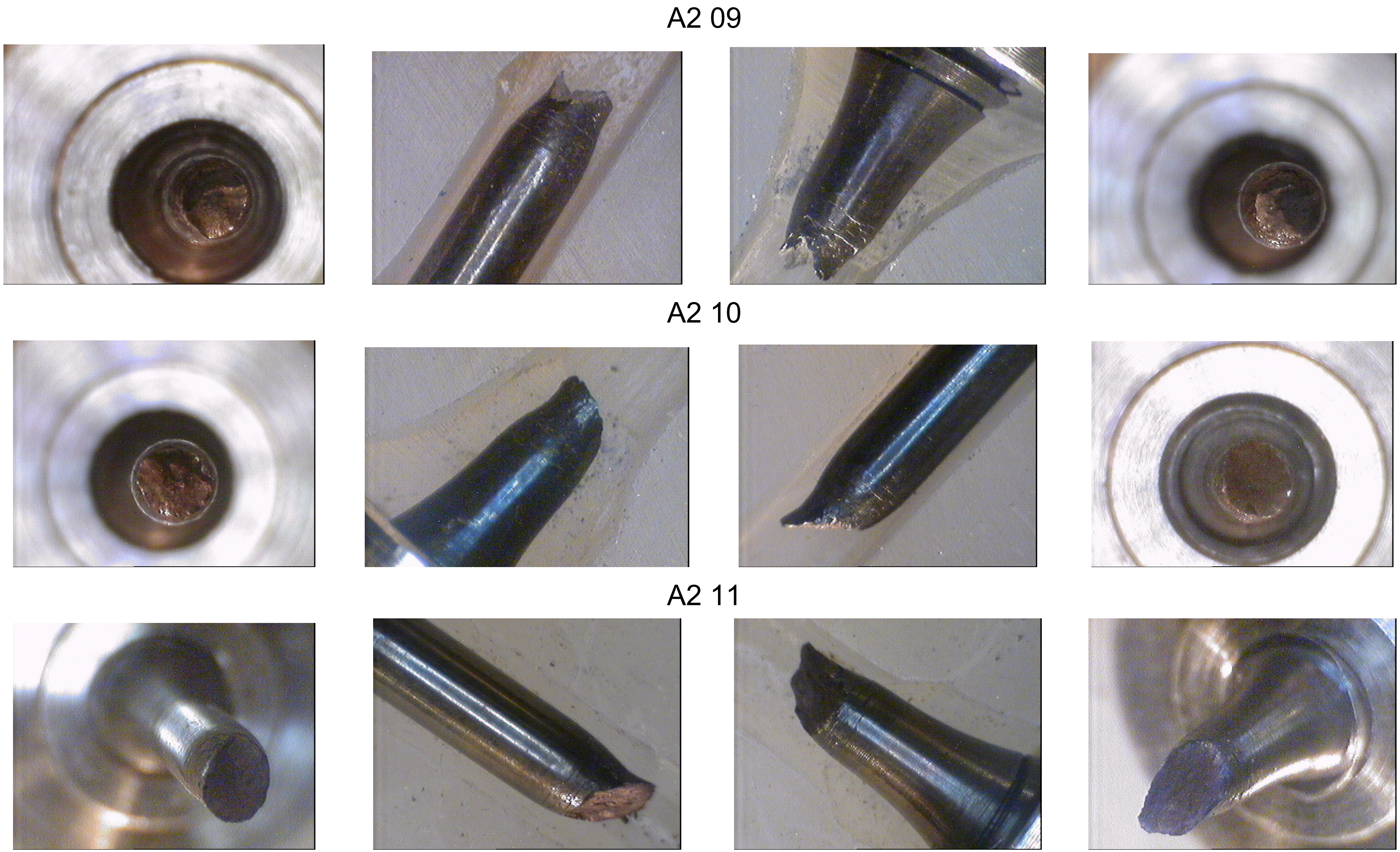

Fig. 9-14 Photographs (Macro) of the tensile tested ADS 2 specimens: A2 09 (T_{test} = 250°C), A2 10 (300°C), A2 11 (350°C)

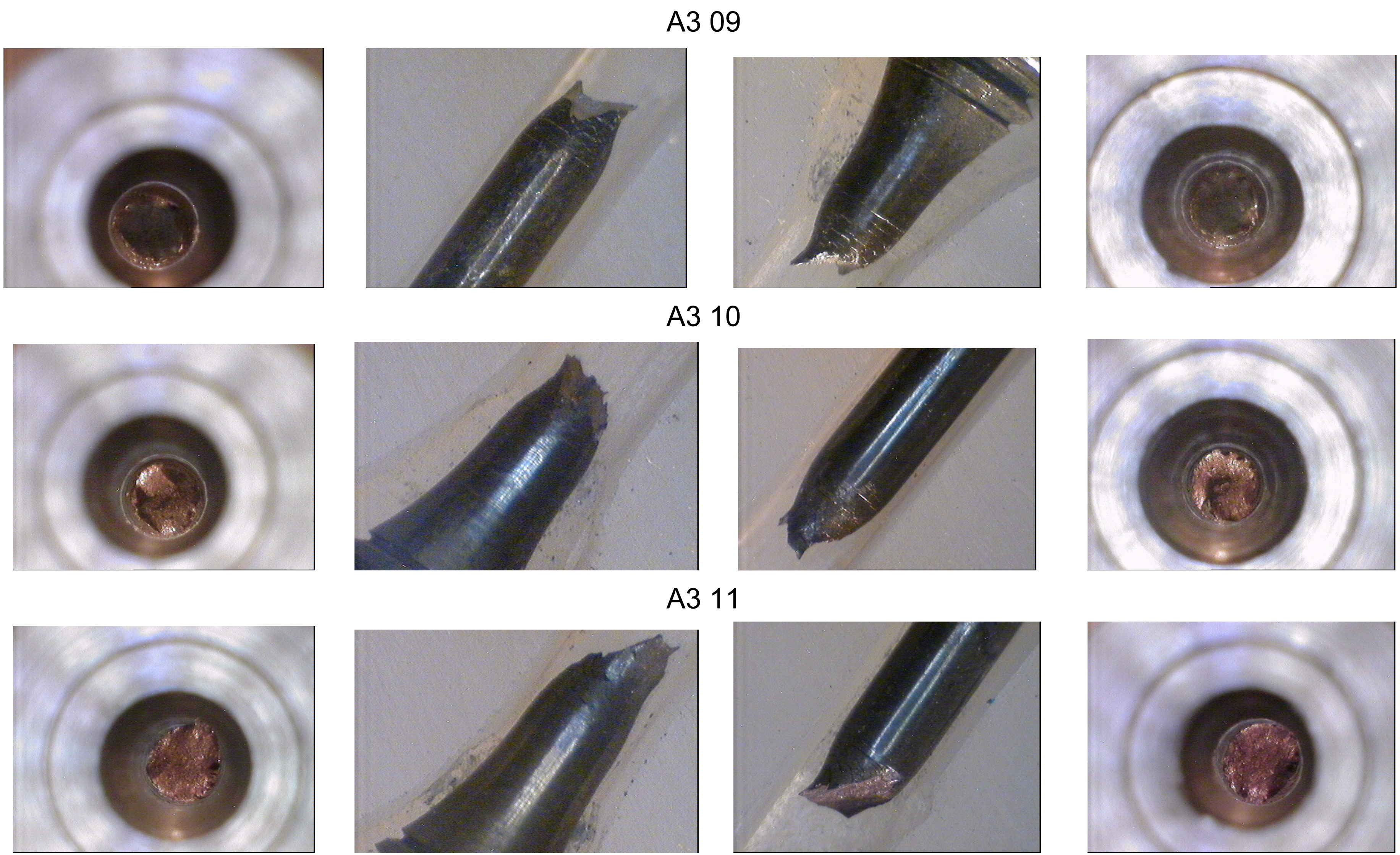

Fig. 9-15 Photographs (Macro) of the tensile tested ADS 3 specimens: A3 09 (T_{test} = 250°C), A3 10 (300°C), A3 11 (350°C)

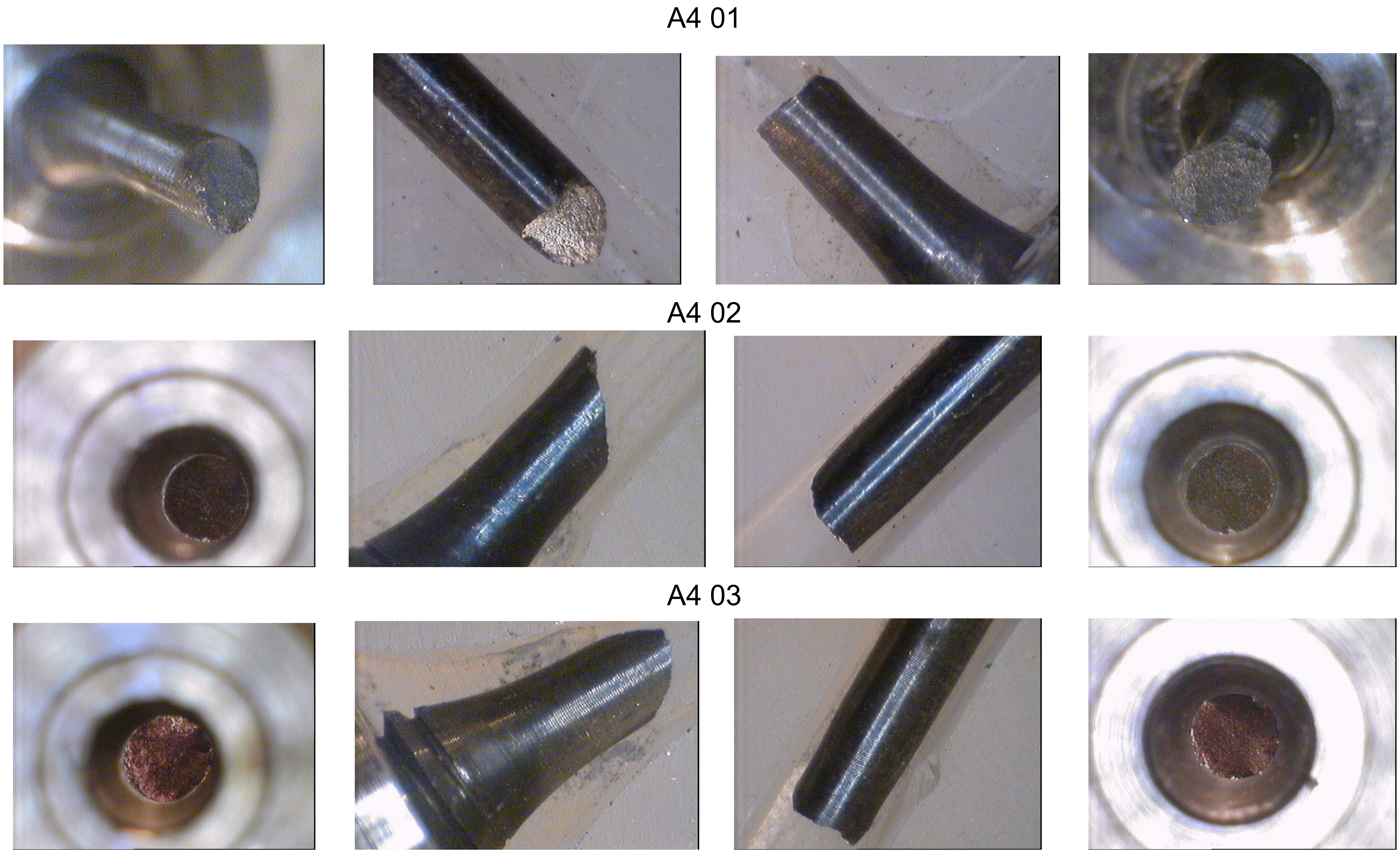

Fig. 9-16 Photographs (Macro) of the tensile tested ADS 4 specimens: A4 01 (T_{test} = 250°C), A4 02 (300°C), A4 03 (350°C)

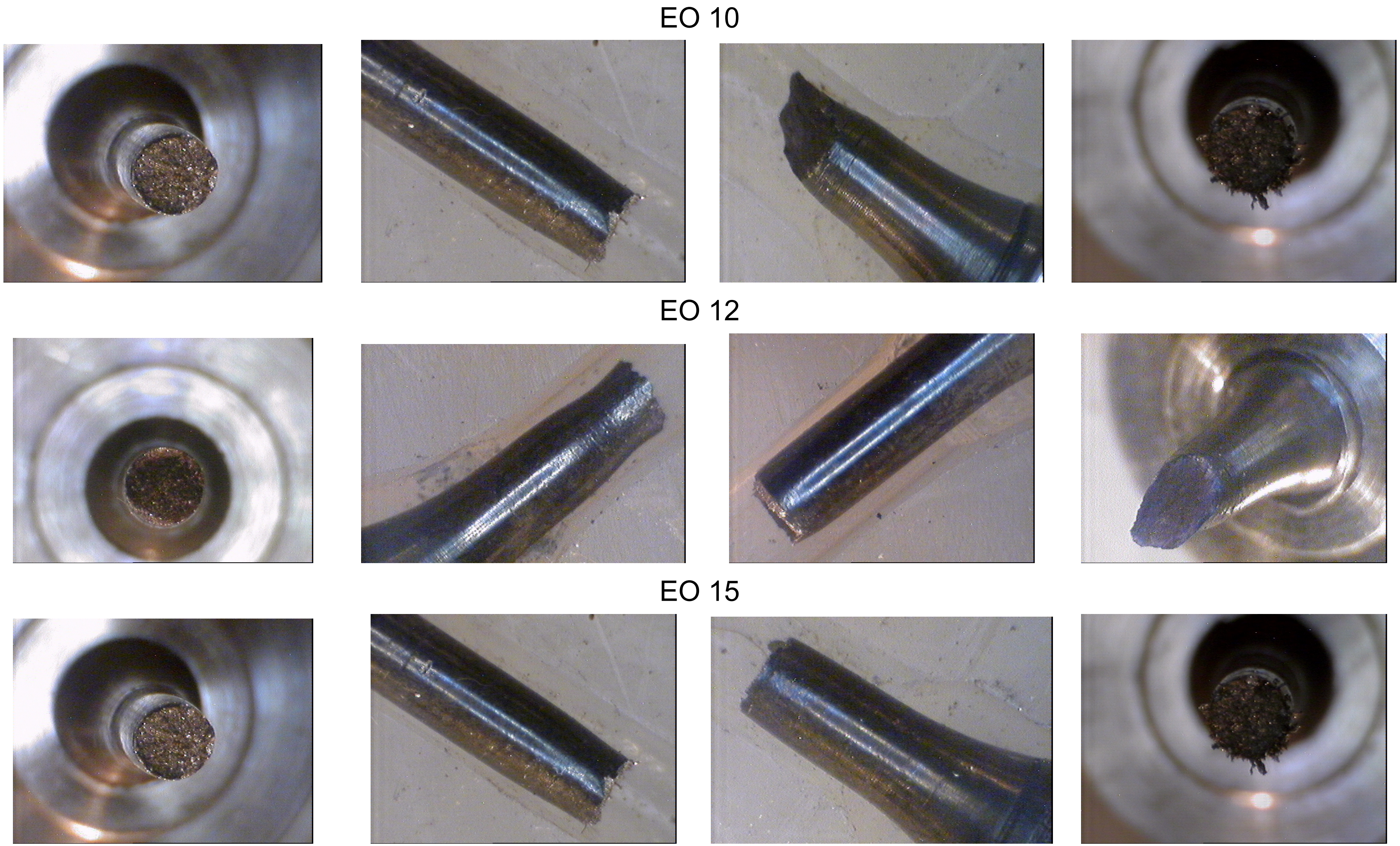

Fig. 9-17 Photographs (Macro) of the tensile tested EURODShip specimens: EO 10 (T_{test} = 250°C), EO 12 (300°C), EO 15 (350°C)

10 Annex C: LCF Tests

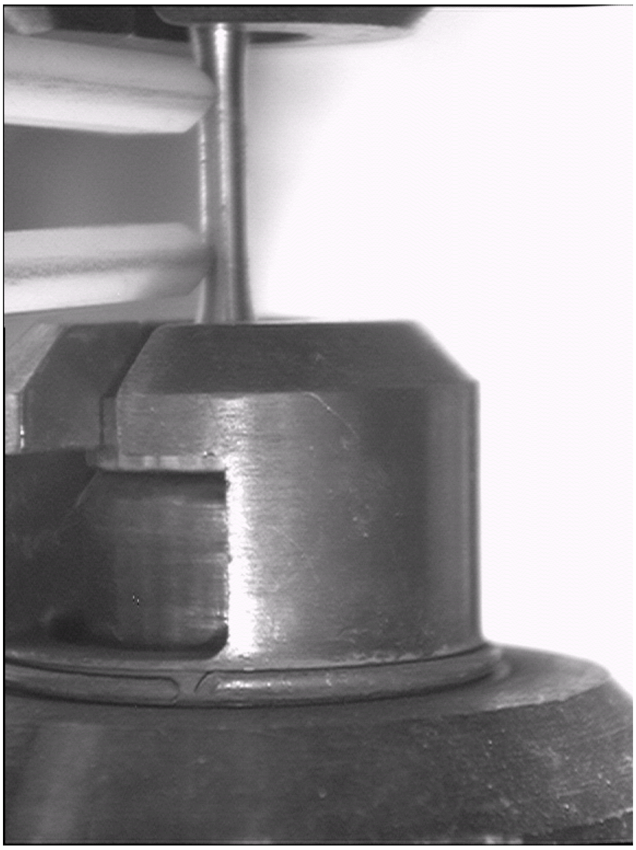

Fig. 10-1 Gripping of LCF specimen with knife ends of the strain measurement system

10.1 EUROFER 97, as received

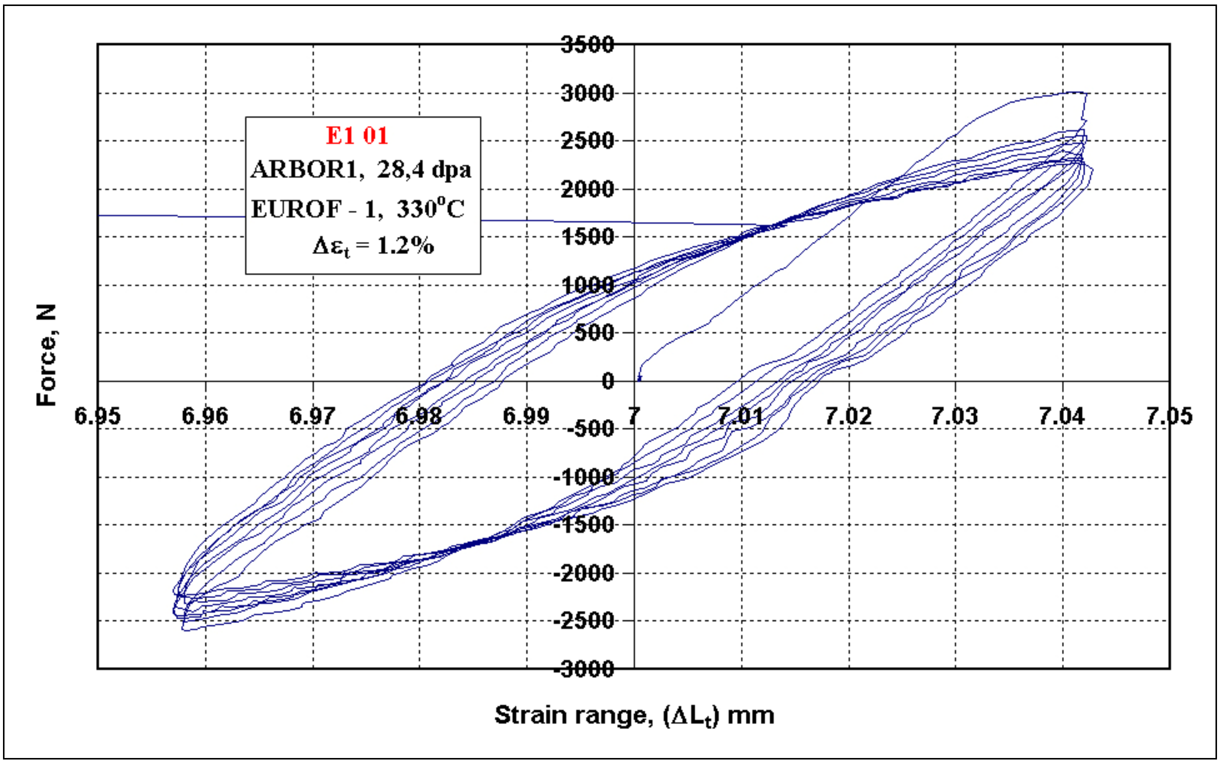

Fig. 10-2 Load vs. total strain range-diagram for the E1 01 specimen

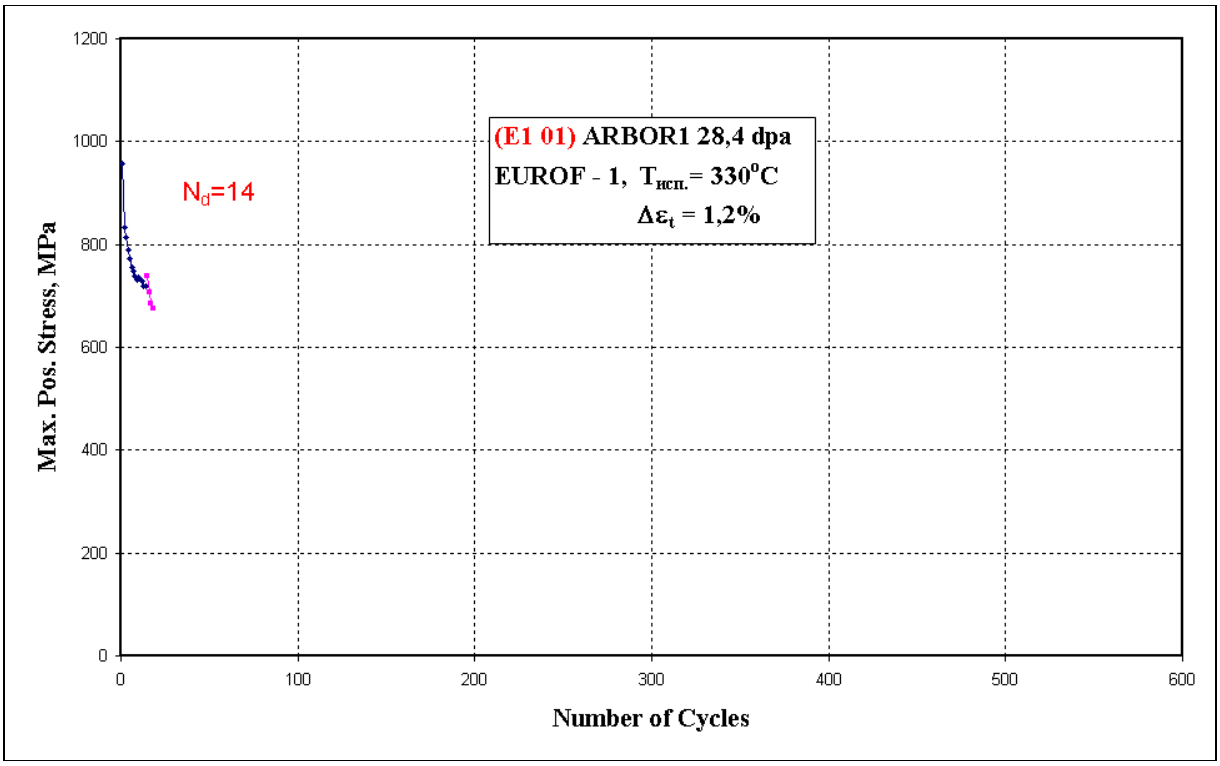

Fig. 10-3 Maximum cyclic stress vs. number of cycles-diagram for the E1 01 specimen

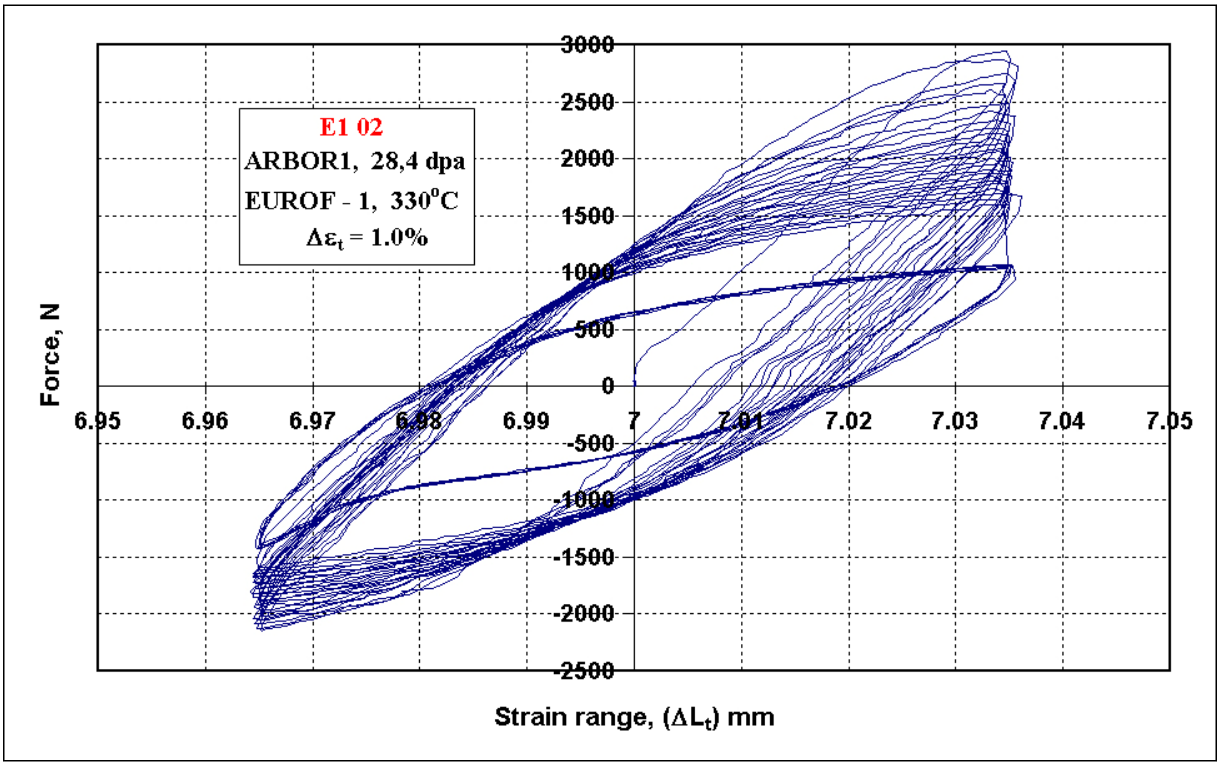

Fig. 10-4 Load vs. total strain range-diagram for the E1 02 specimen

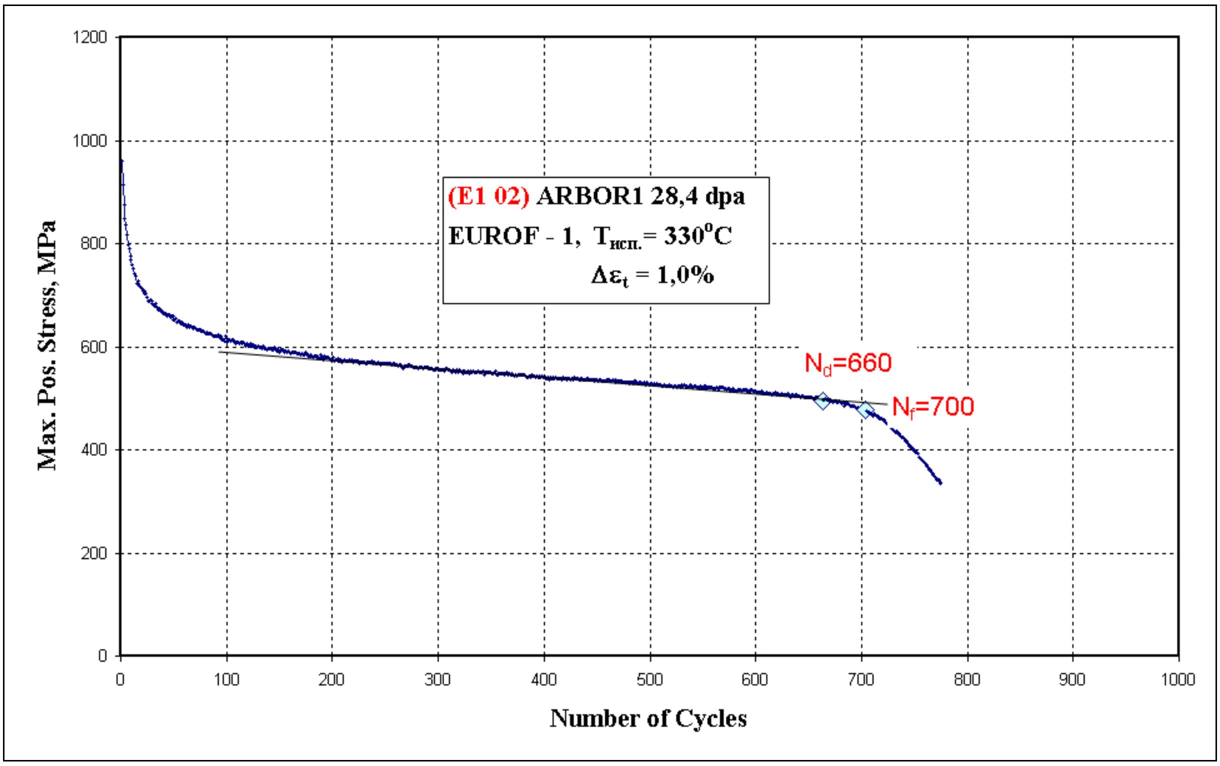

Fig. 10-5 Maximum cyclic stress vs. number of cycles-diagram for the E1 02 specimen

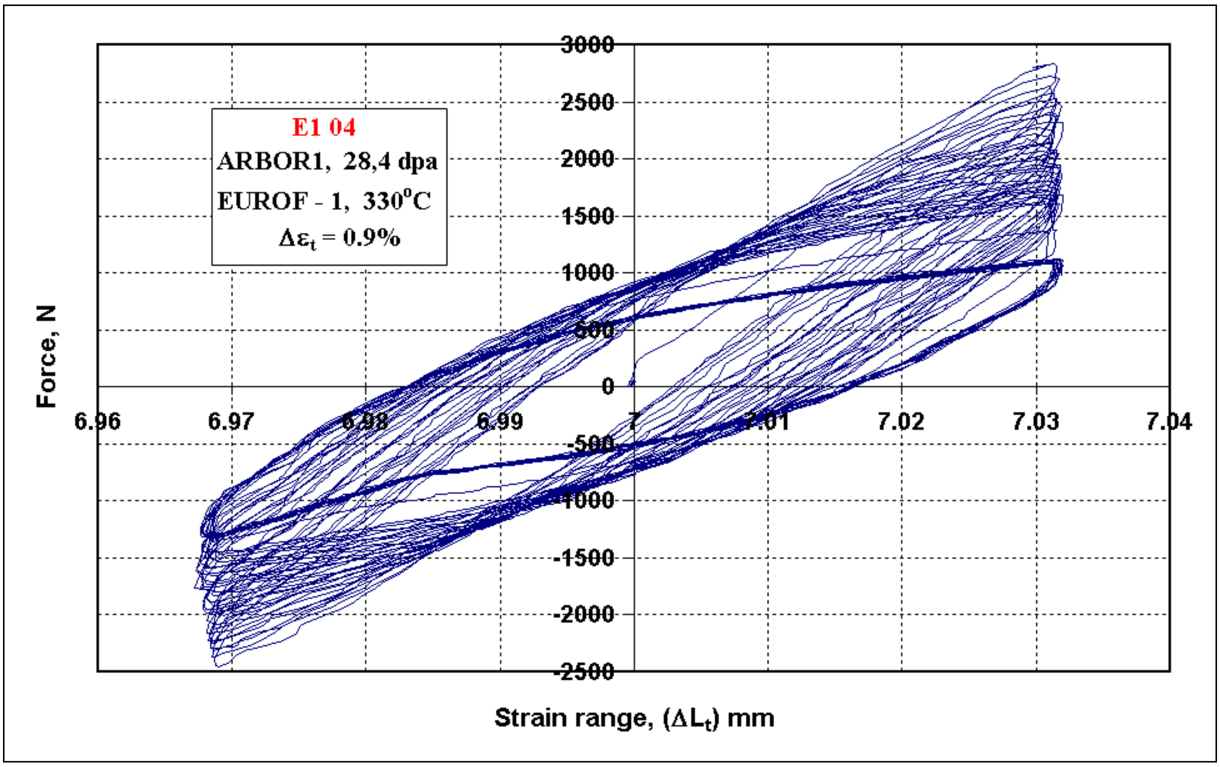

Fig. 10-6 Load vs. total strain range-diagram for the E1 04 specimen

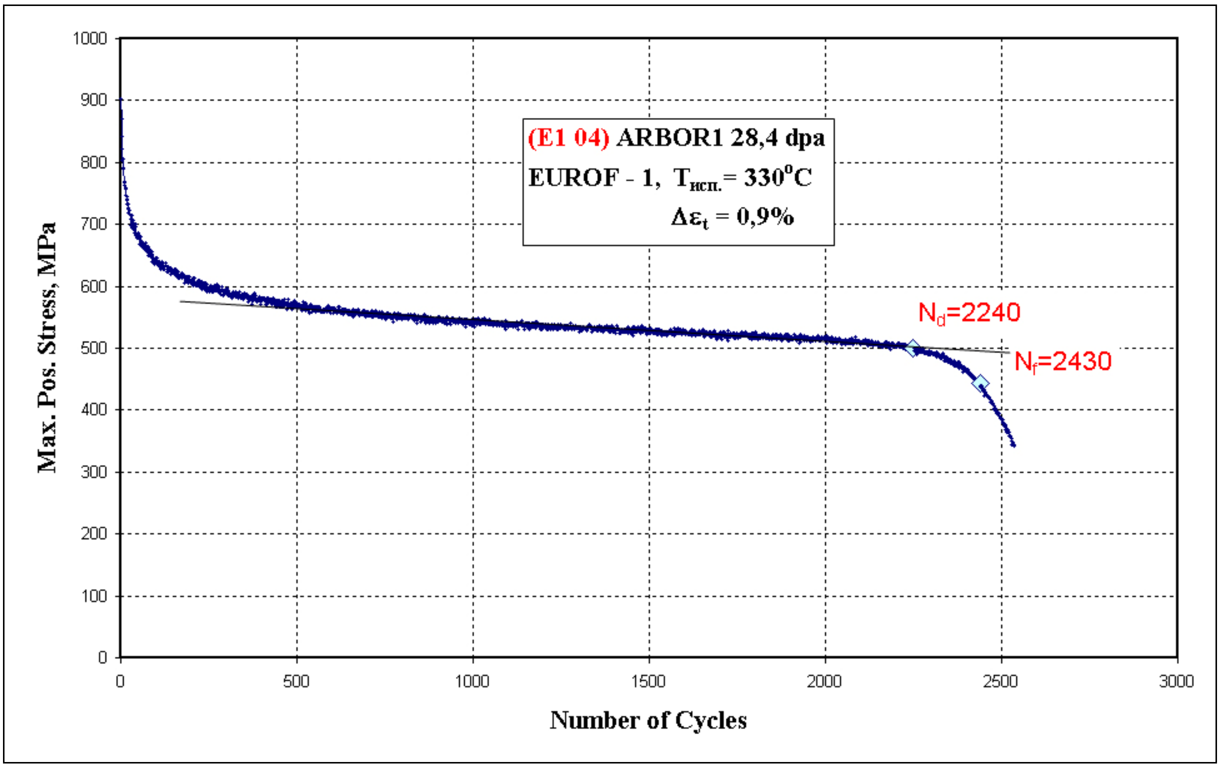

Fig. 10-7 Maximum cyclic stress vs. number of cycles-diagram for the E1 04 specimen

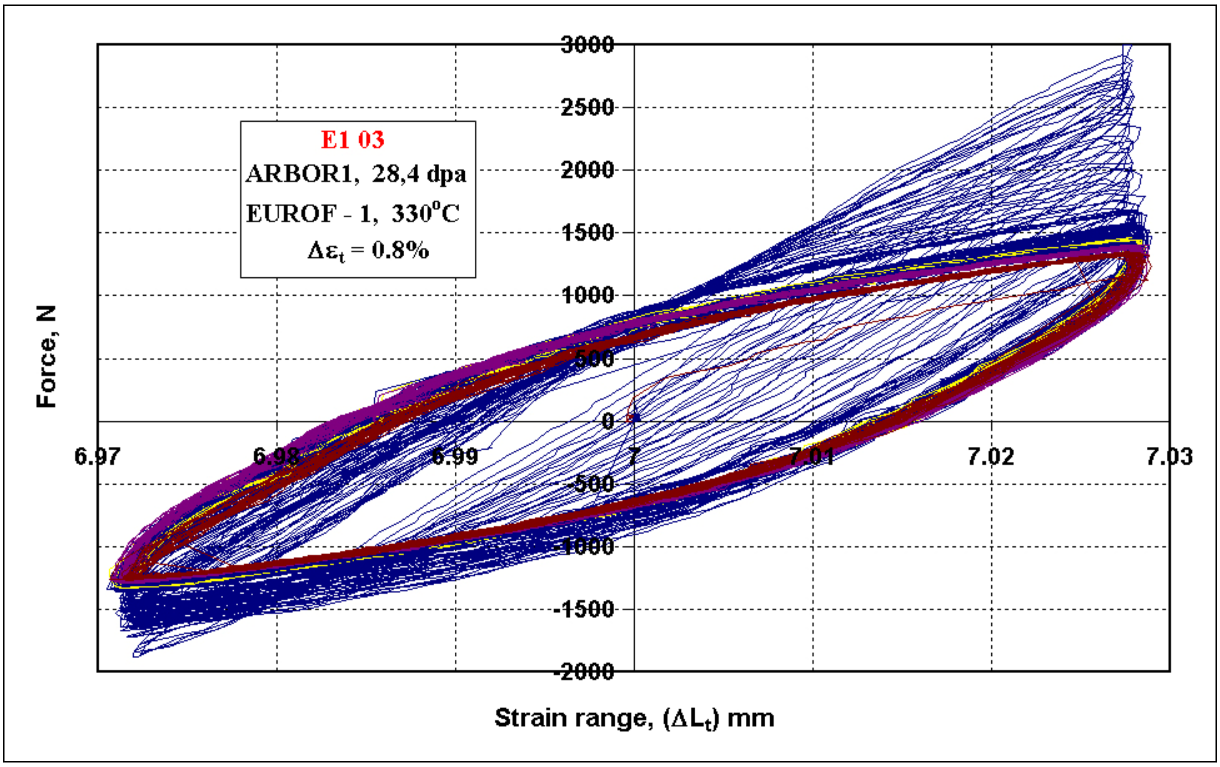

Fig. 10-8 Load vs. total strain range-diagram for the E1 03 specimen

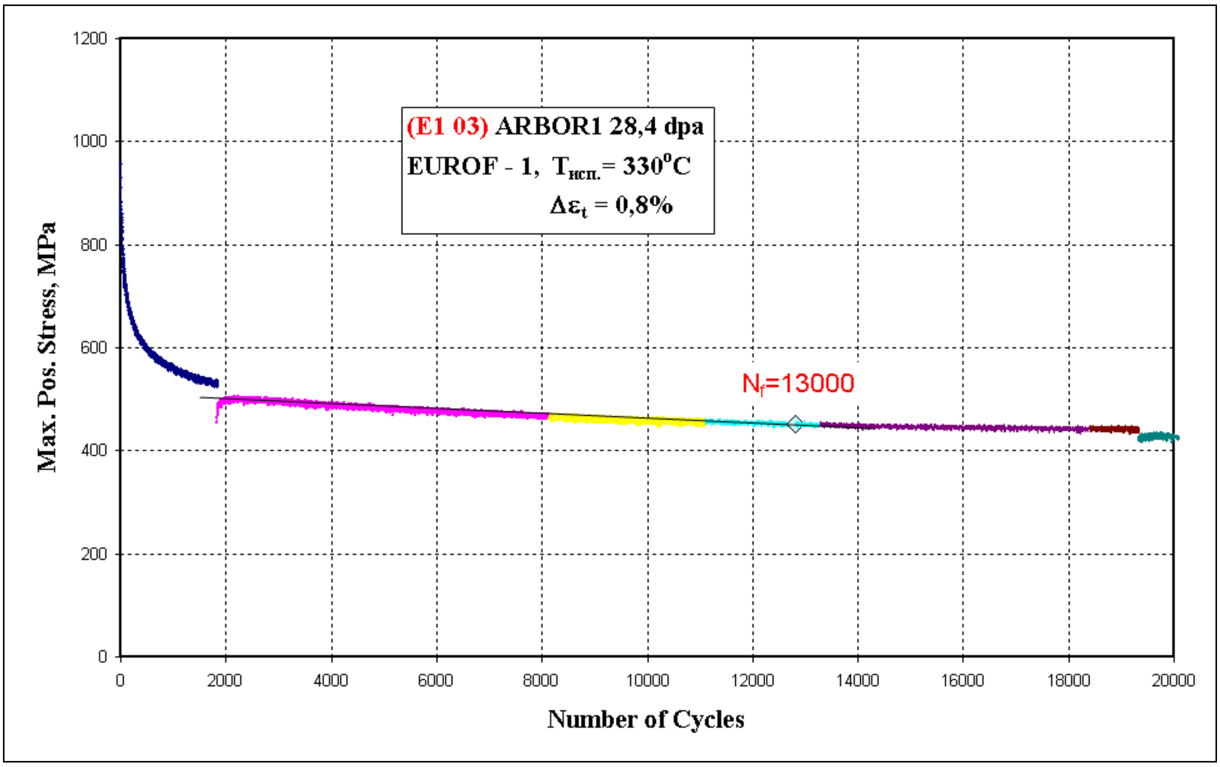

Fig. 10-9 Maximum cyclic stress vs. number of cycles-diagram for the E1 03 specimen

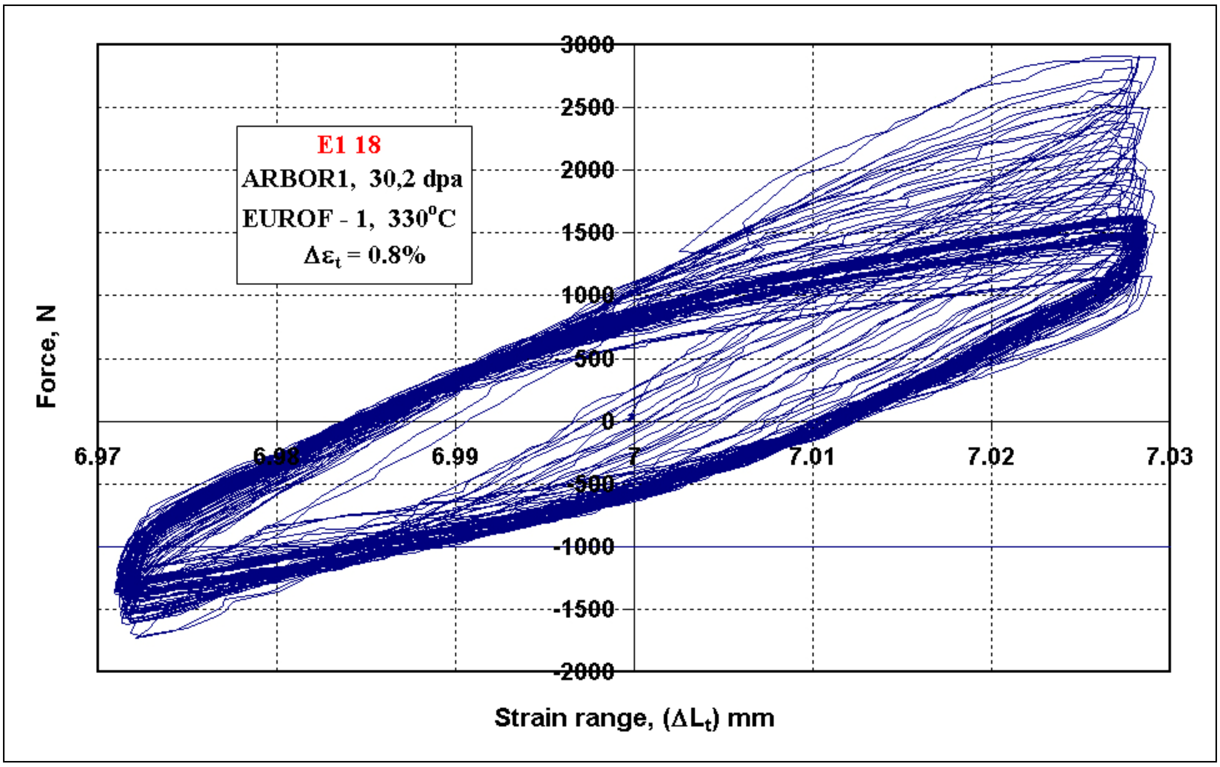

Fig. 10-10 Load vs. total strain range-diagram for the E1 18 specimen

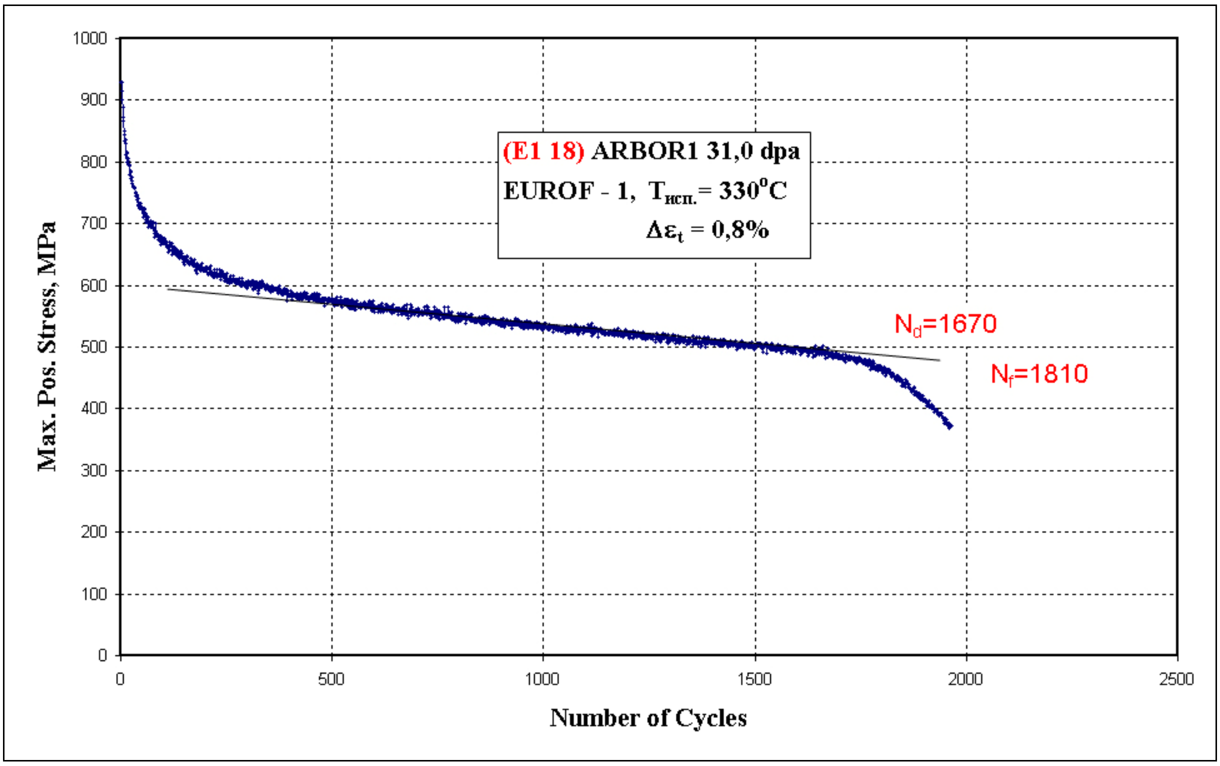

Fig. 10-11 Maximum cyclic stress vs. number of cycles-diagram for the E1 18 specimen

10.2 EUROFER 97, heat treated

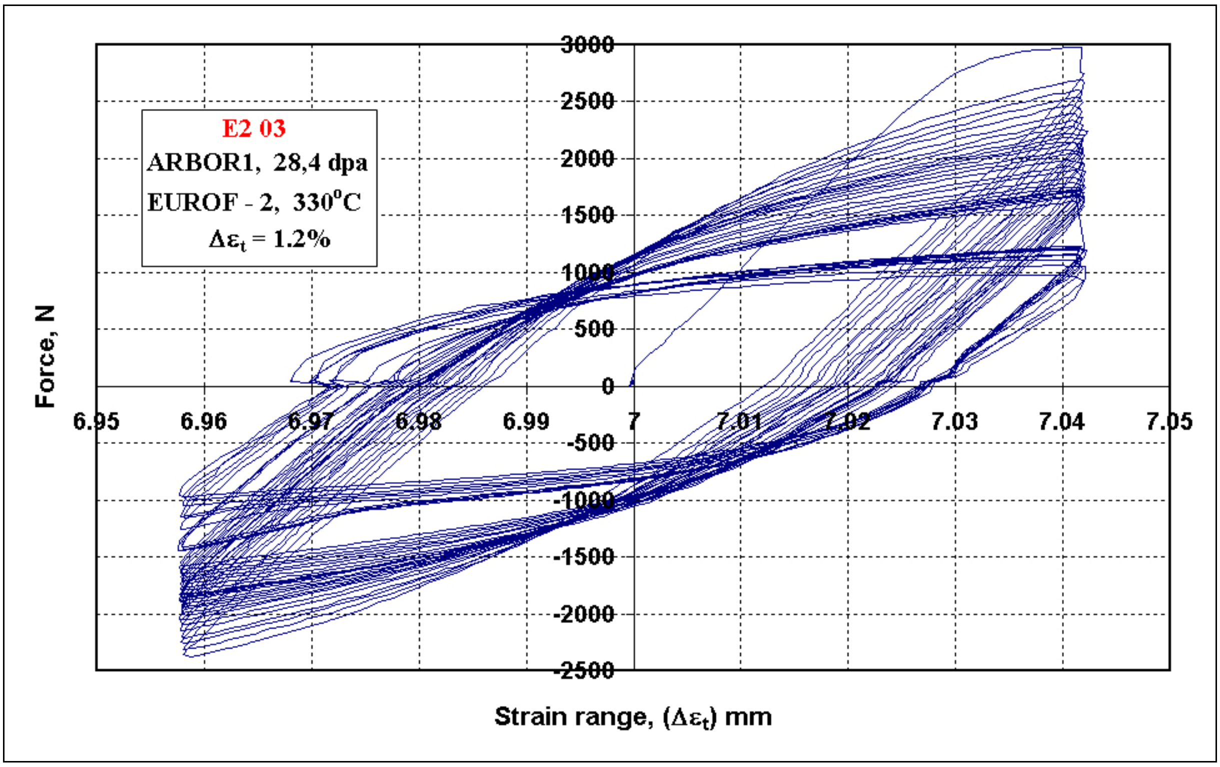

Fig. 10-12 Load vs. total strain range-diagram for the E2 03 specimen

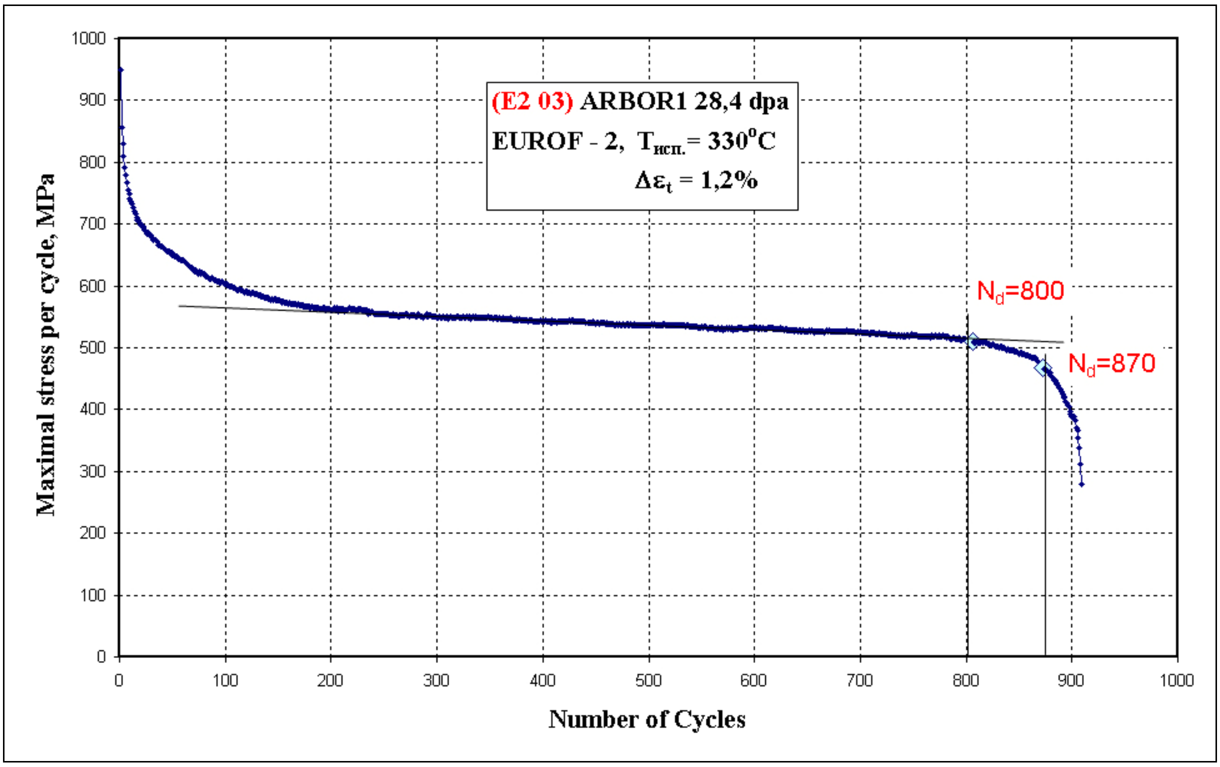

Fig. 10-13 Maximum cyclic stress vs. number of cycles-diagram for the E2 03 specimen

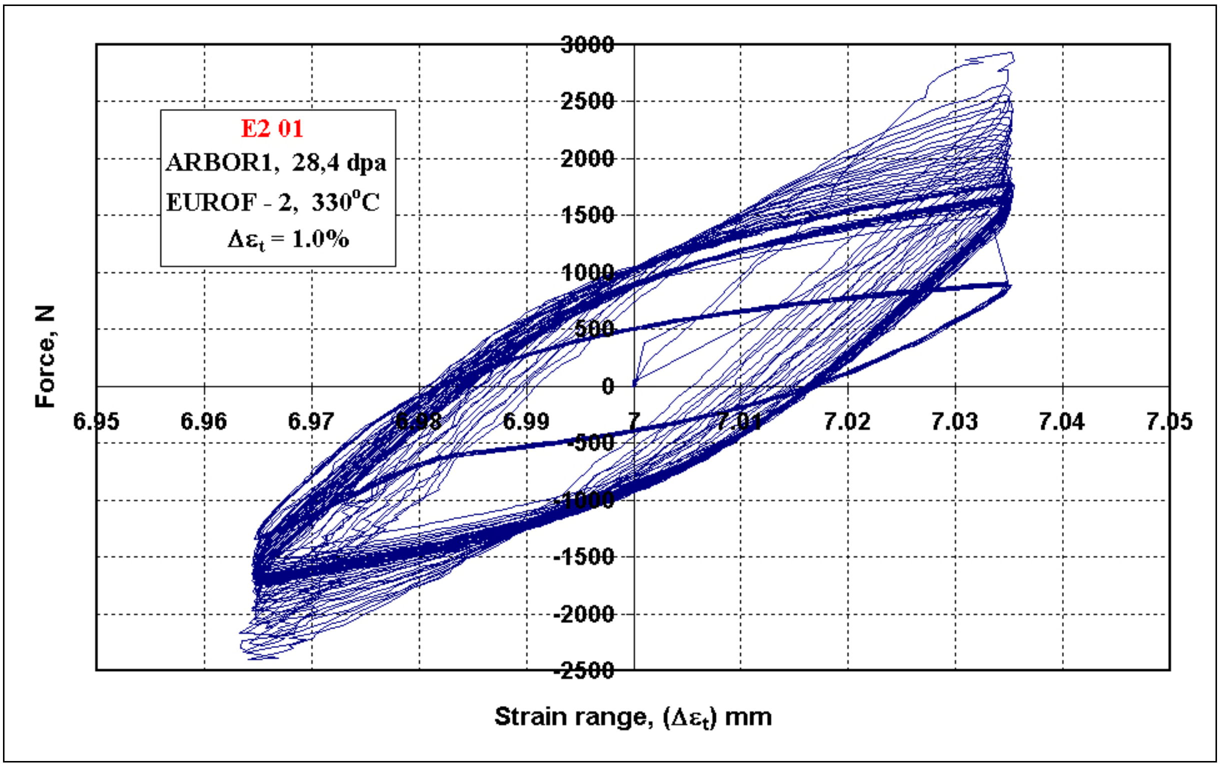

Fig. 10-14 Load vs. total strain range-diagram for the E2 01 specimen

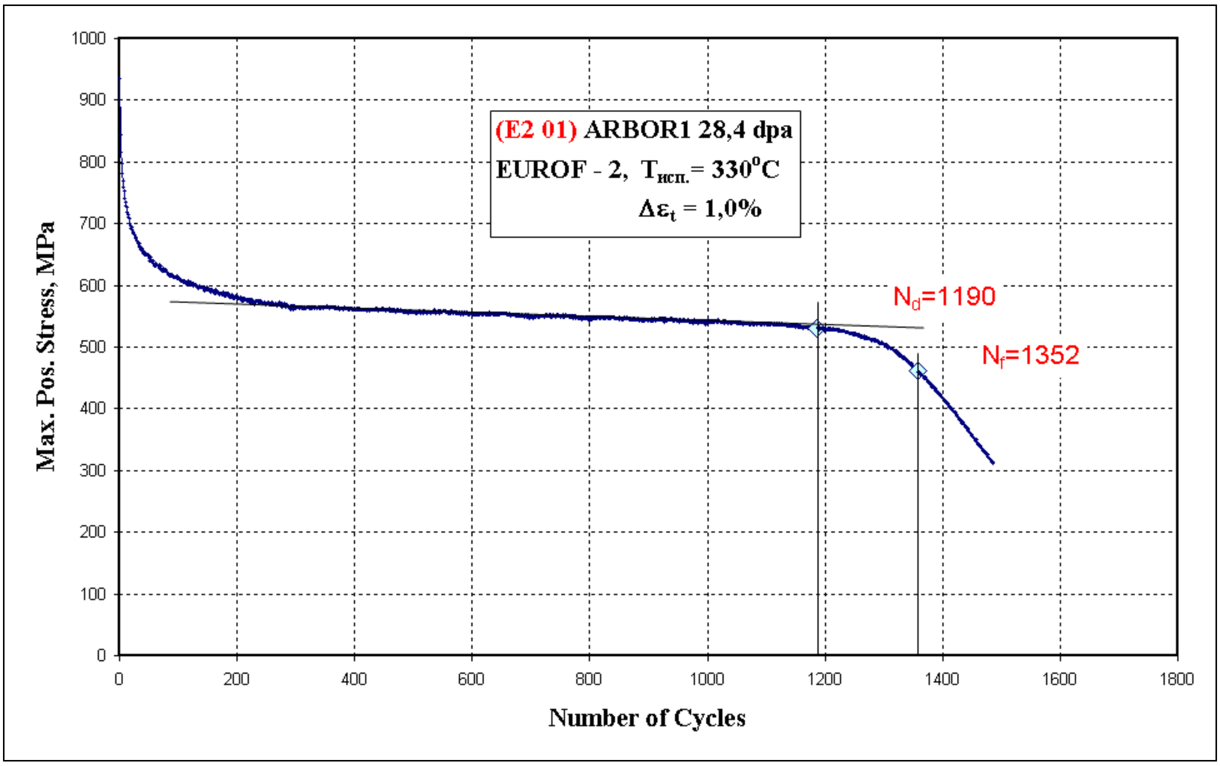

Fig. 10-15 Maximum cyclic stress vs. number of cycles-diagram for the E2 01 specimen

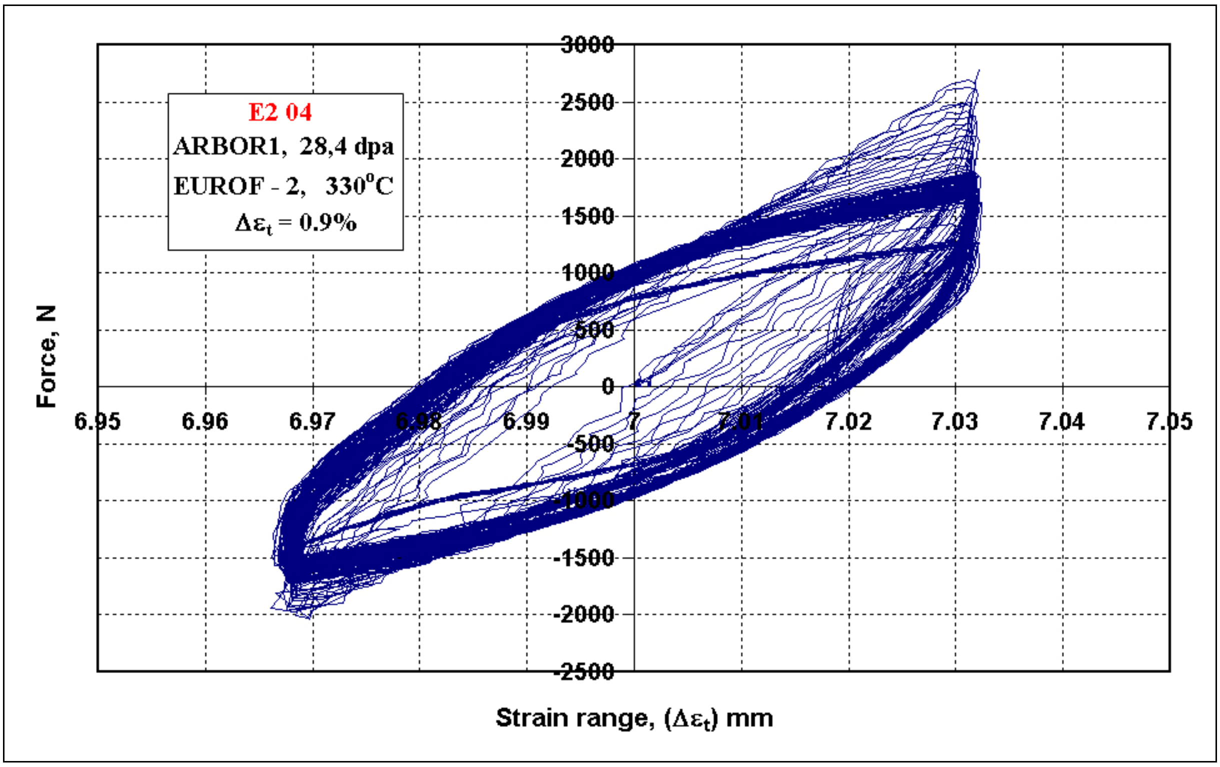

Fig. 10-16 Load vs. total strain range-diagram for the E2 04 specimen

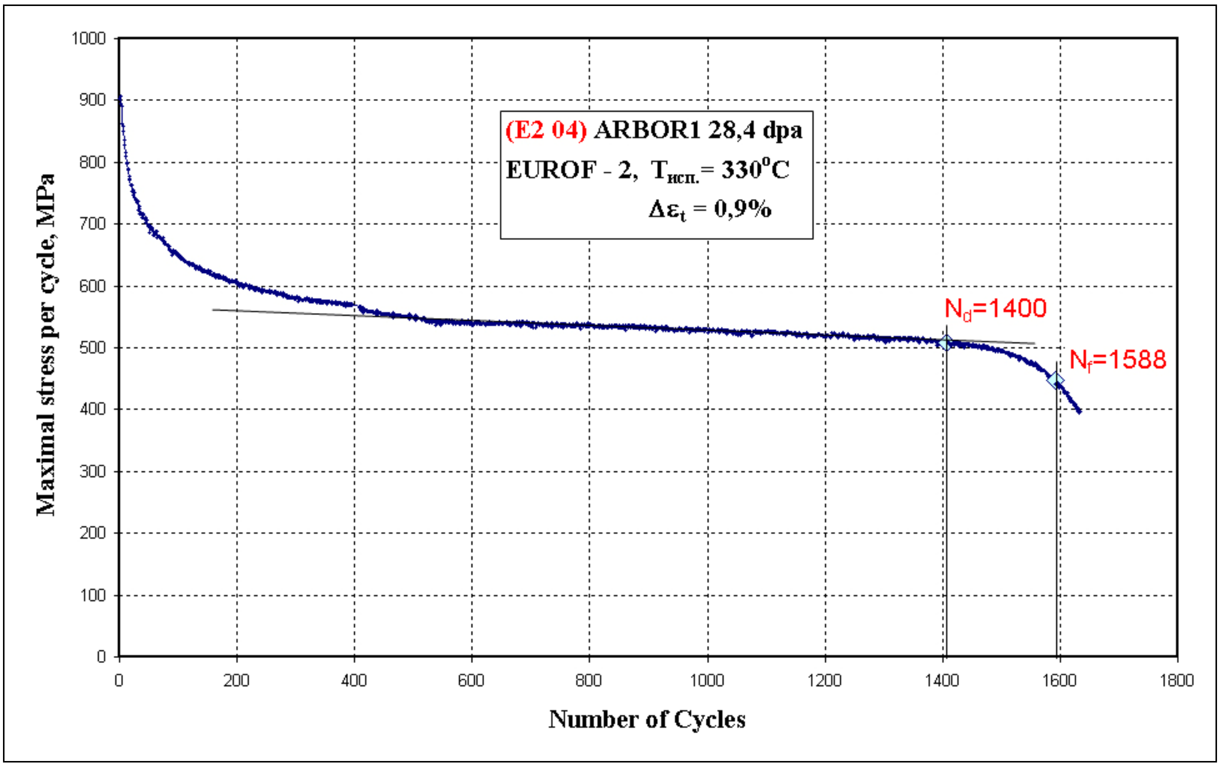

Fig. 10-17 Maximum cyclic stress vs. number of cycles-diagram for the E2 04 specimen

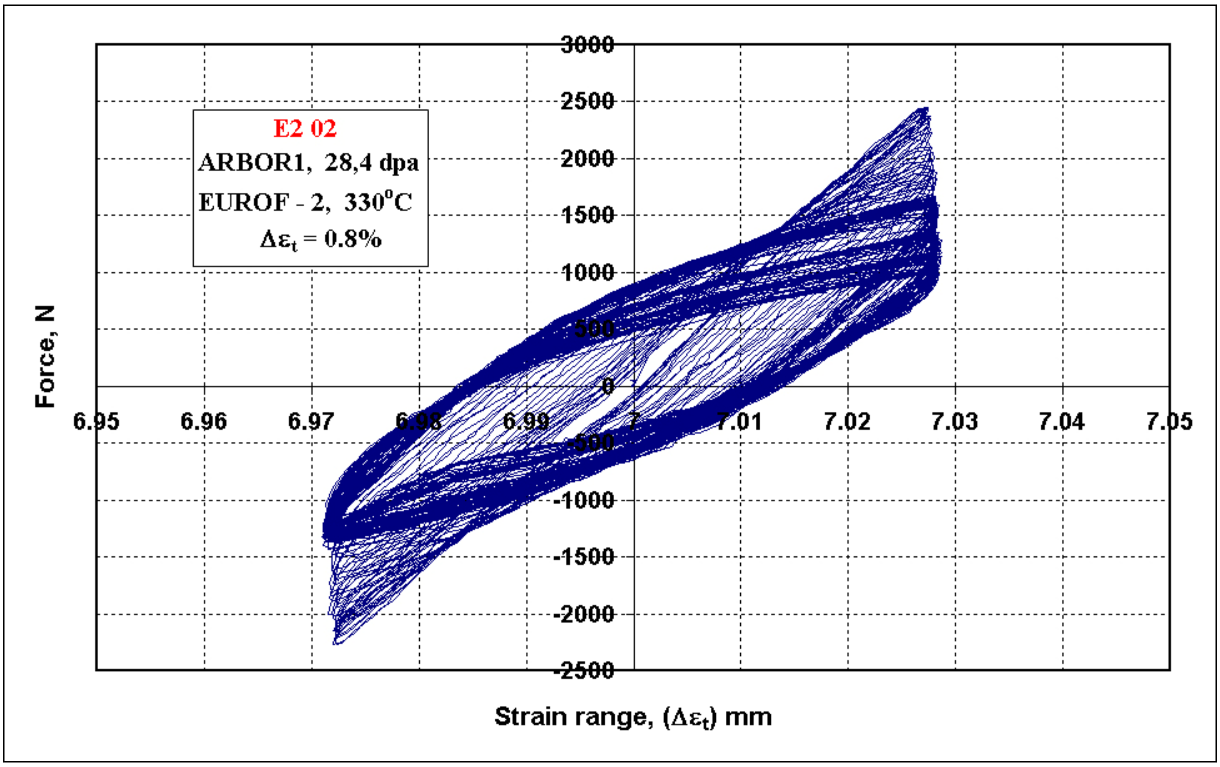

Fig. 10-18 Load vs. total strain range-diagram for the E2 02 specimen

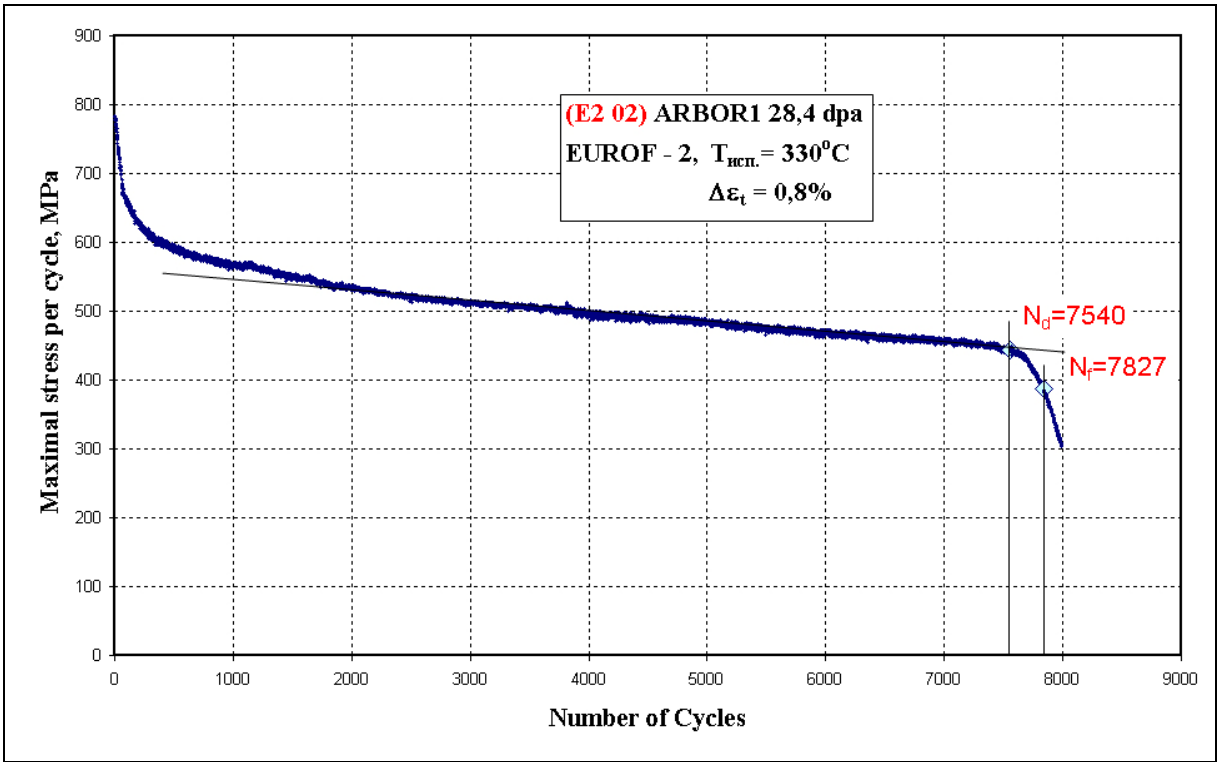

Fig. 10-19 Maximum cyclic stress vs. number of cycles-diagram for the E2 02 specimen

10.3 F82H mod.

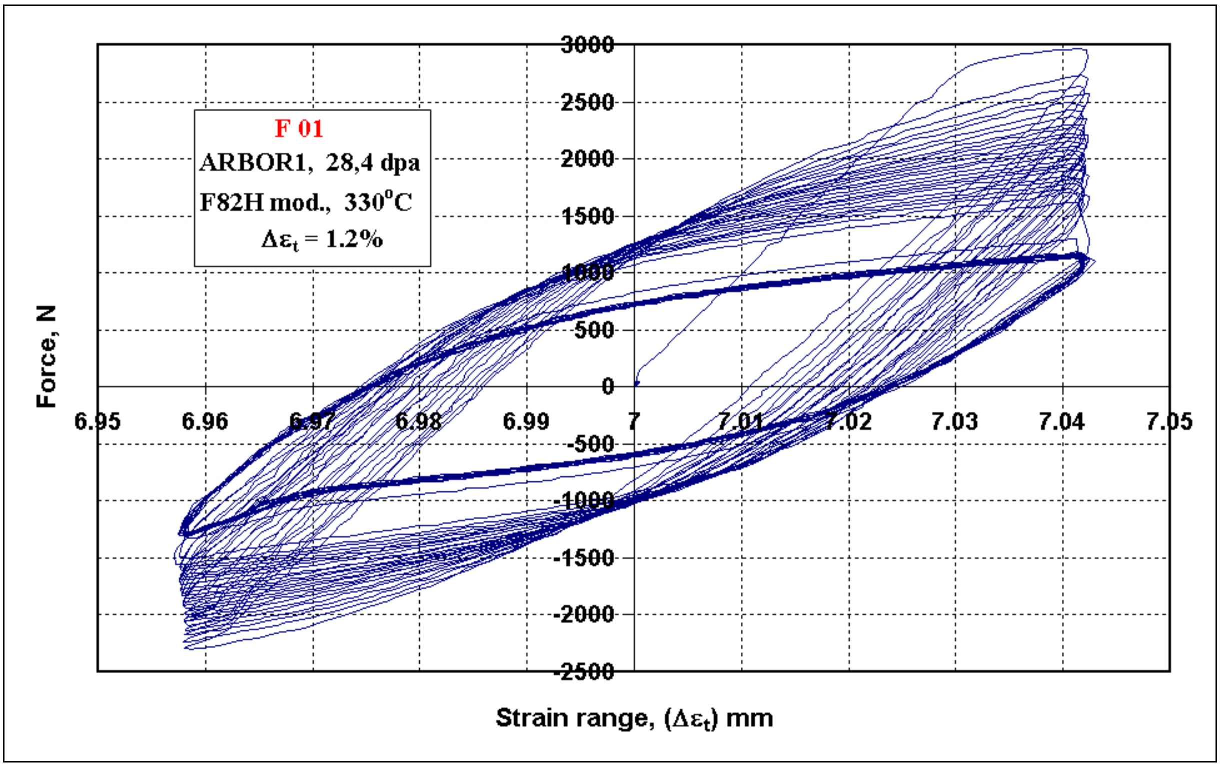

Fig. 10-20 Load vs. total strain range-diagram for the F 01 specimen

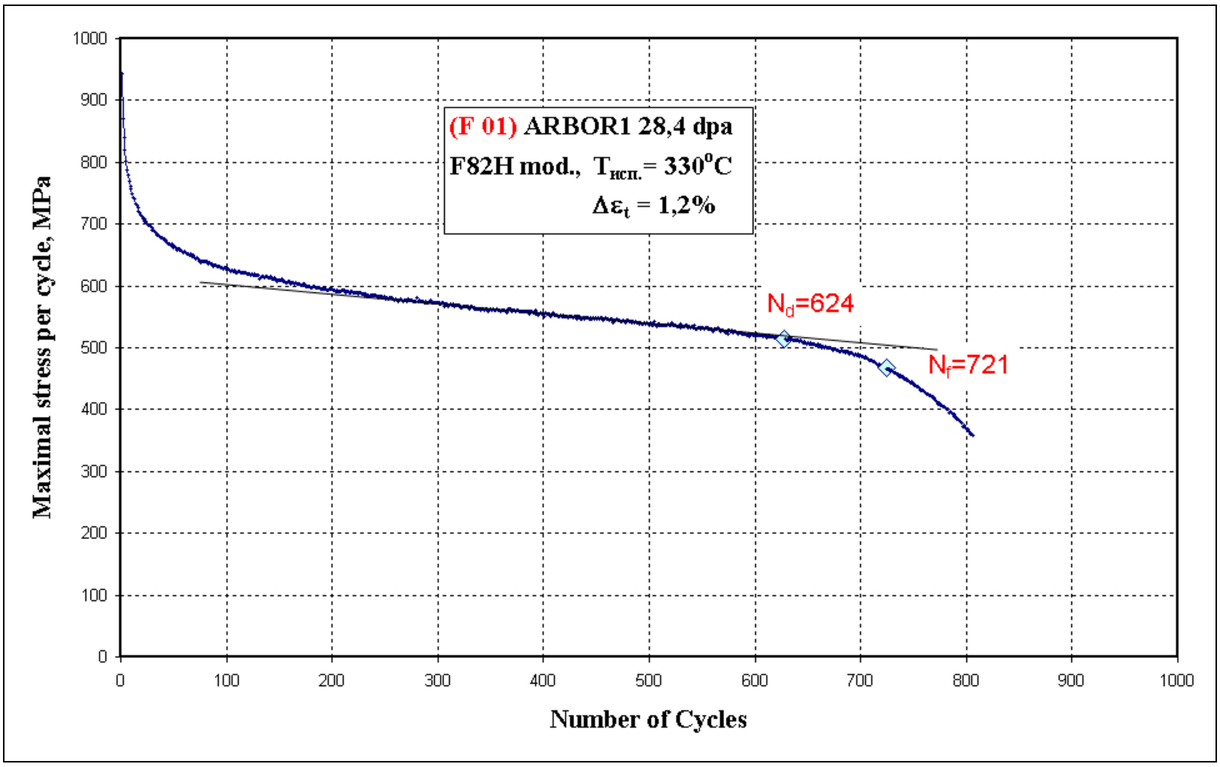

Fig. 10-21 Maximum cyclic stress vs. number of cycles-diagram for the F 01 specimen

F 01

F 02

F 04

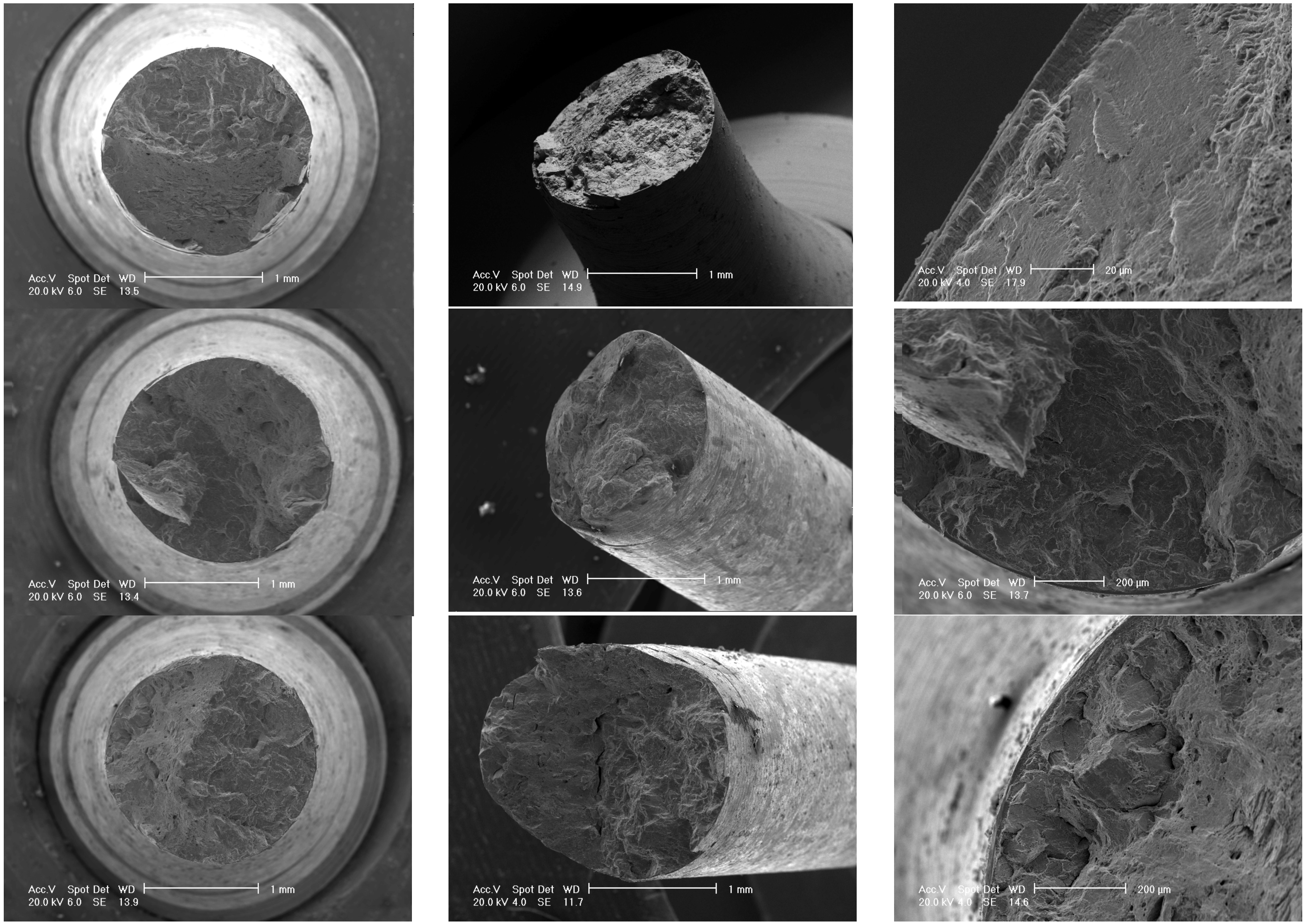

Fig. 10-22 SEM photographs of LCF tested F82H mod. specimens F 01, F 02 and F 04 after complete breaking

F 05

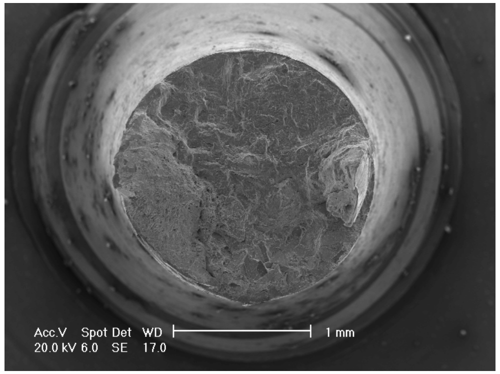

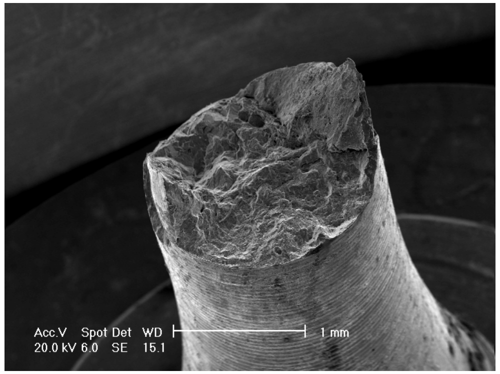

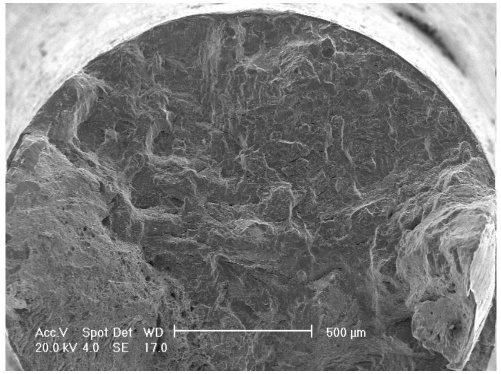

Fig. 10-23 SEM photographs of LCF tested F82H mod. specimen F 05 after complete breaking

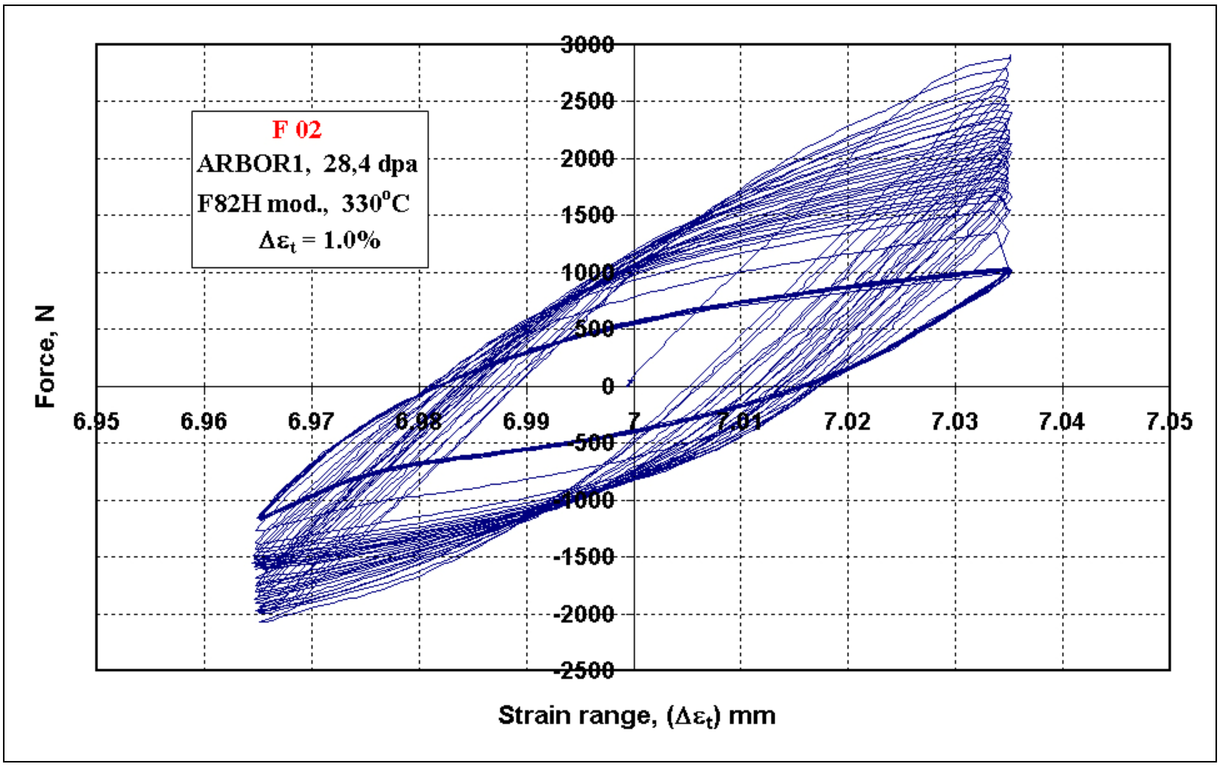

Fig. 10-24 Load vs. total strain range-diagram for the F 02 specimen

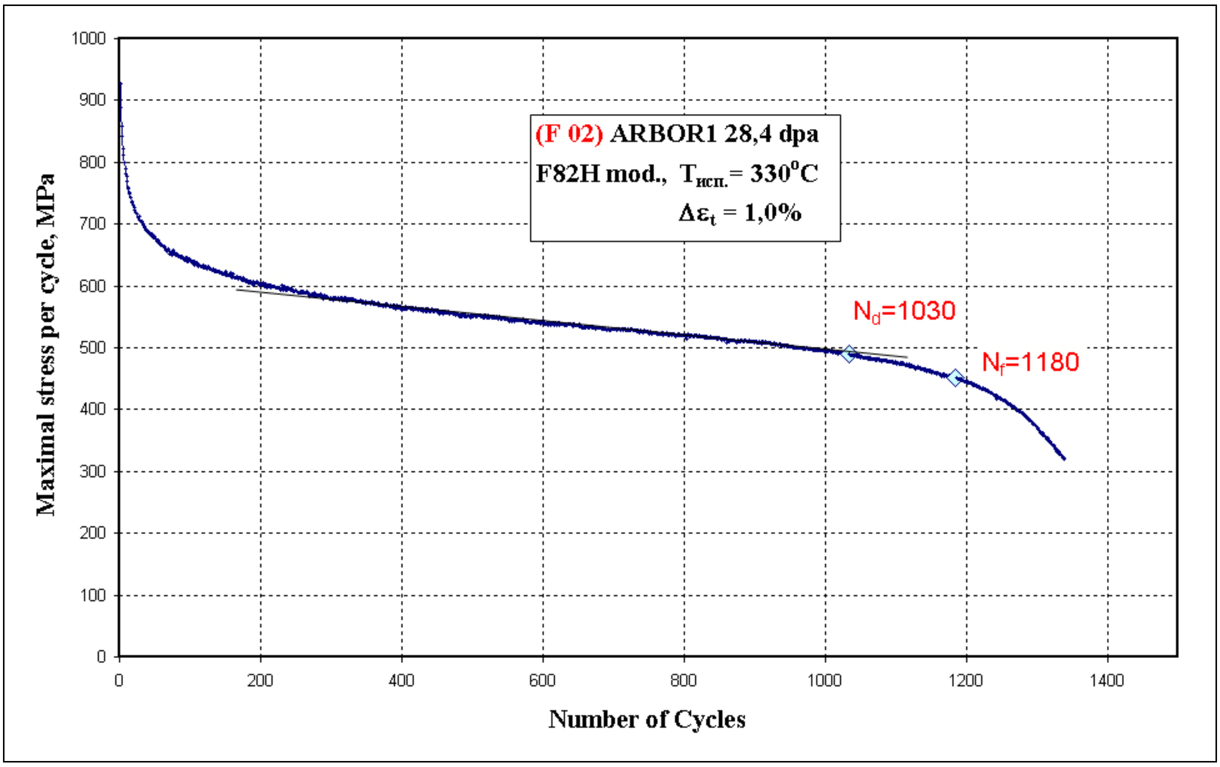

Fig. 10-25 Maximum cyclic stress vs. number of cycles-diagram for the F 02 specimen

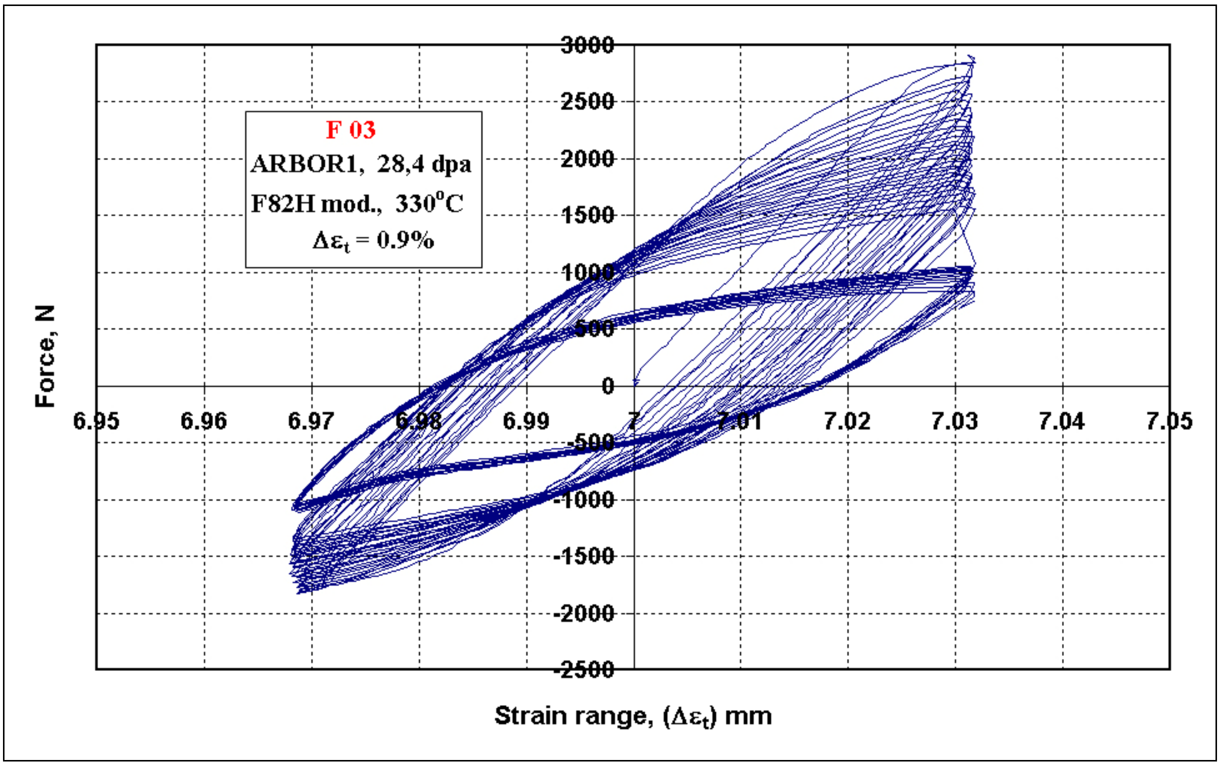

Fig. 10-26 Load vs. total strain range-diagram for the F 03 specimen

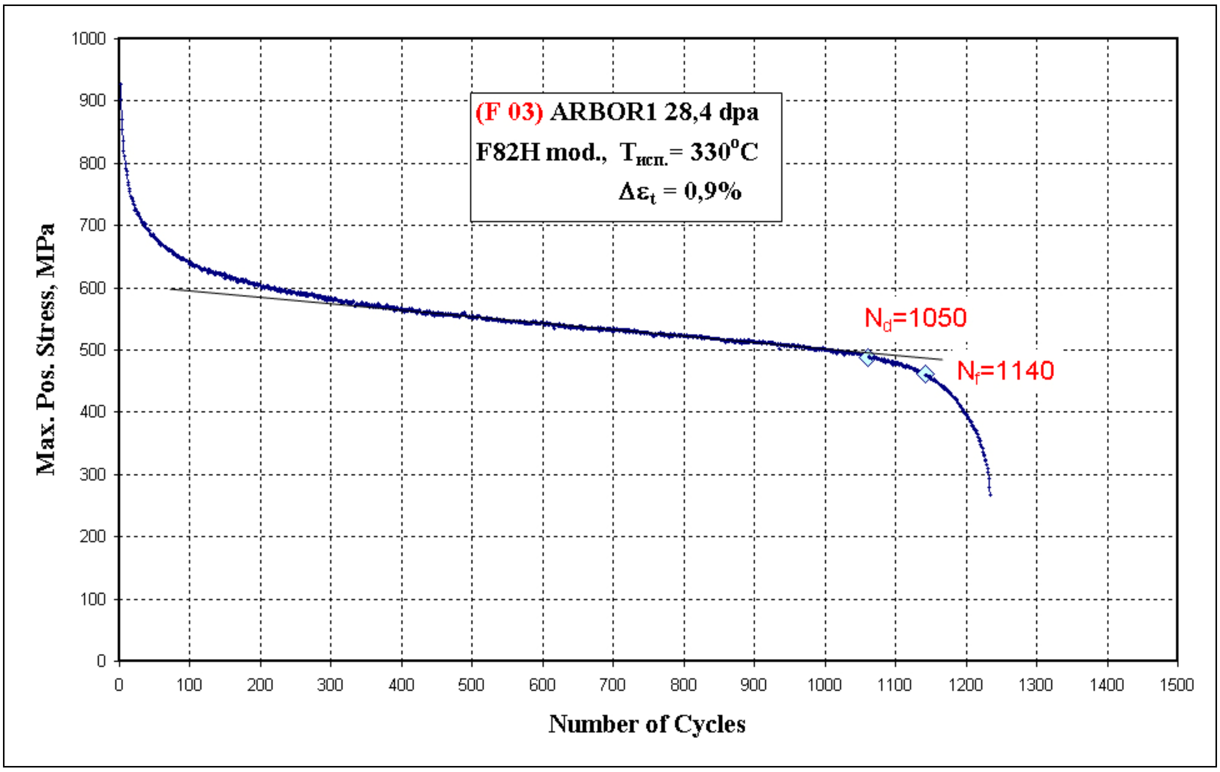

Fig. 10-27 Maximum cyclic stress vs. number of cycles-diagram for the F 03 specimen

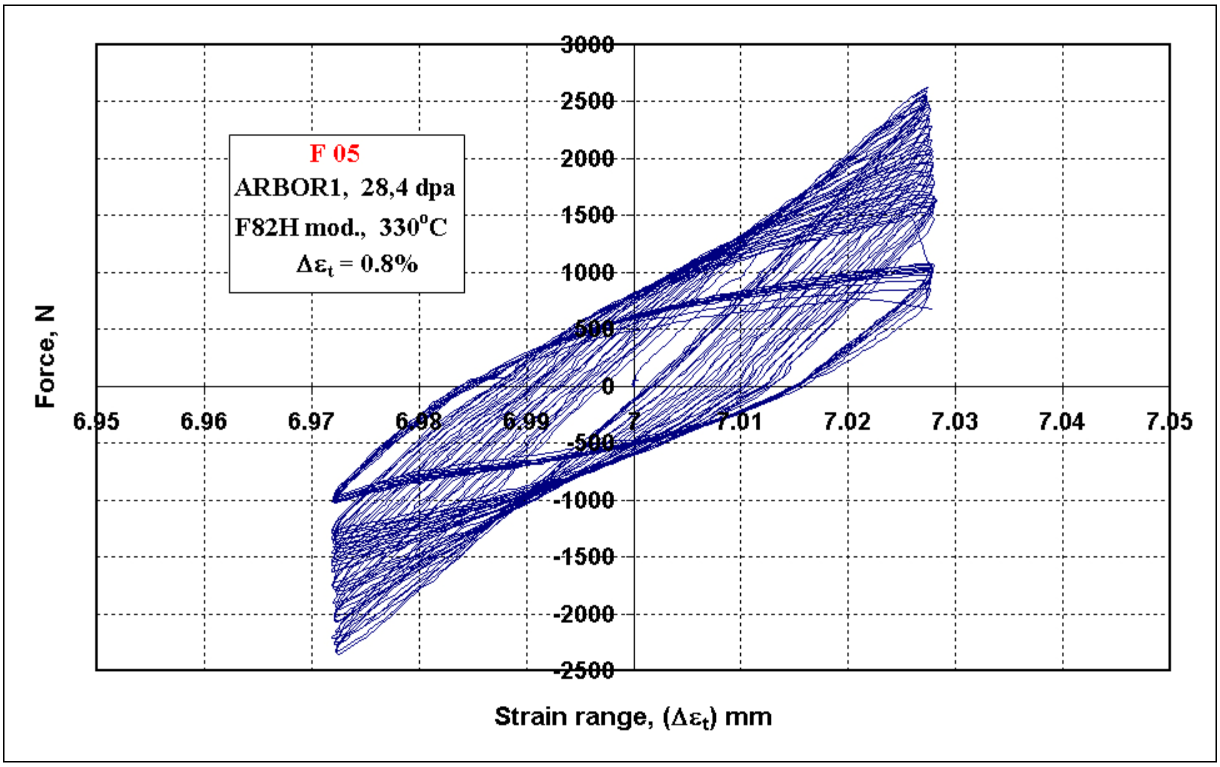

Fig. 10-28 Load vs. total strain range-diagram for the F 05 specimen

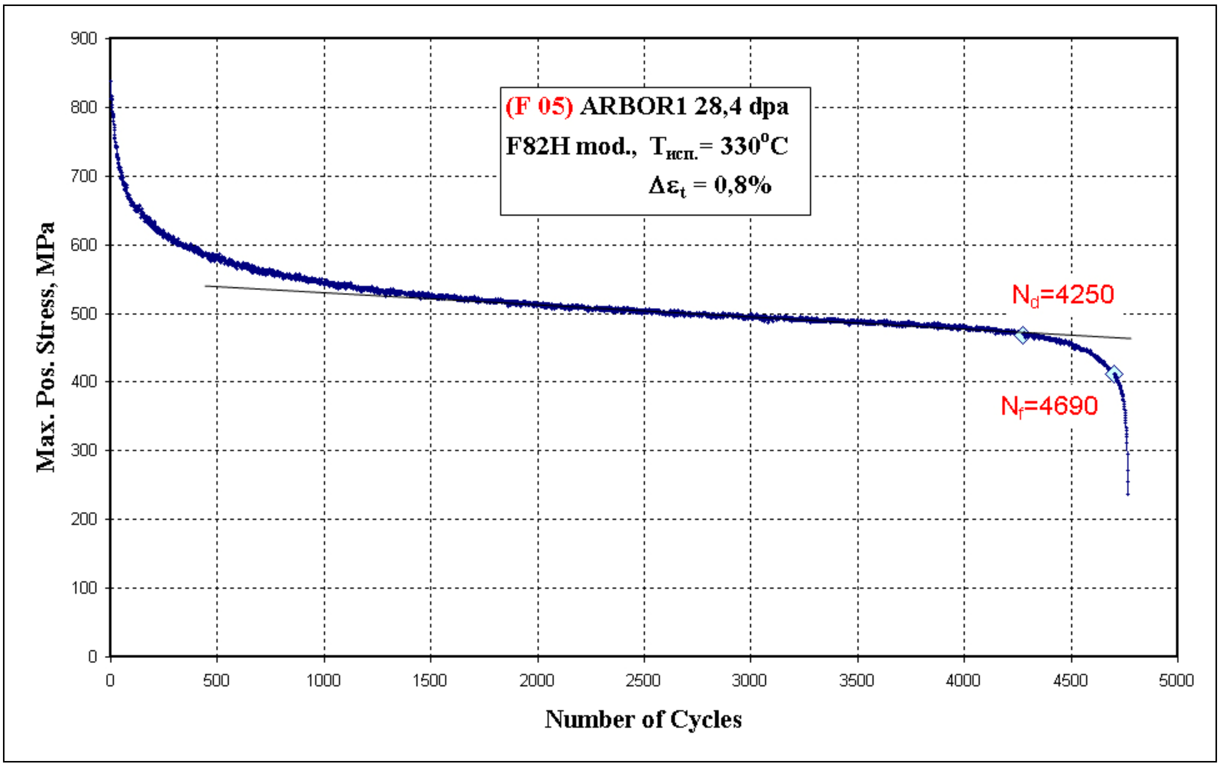

Fig. 10-29 Maximum cyclic stress vs. number of cycles-diagram for the F 05 specimen

10.4 ODS-EUROFER, 0.5 % Y_2O_3

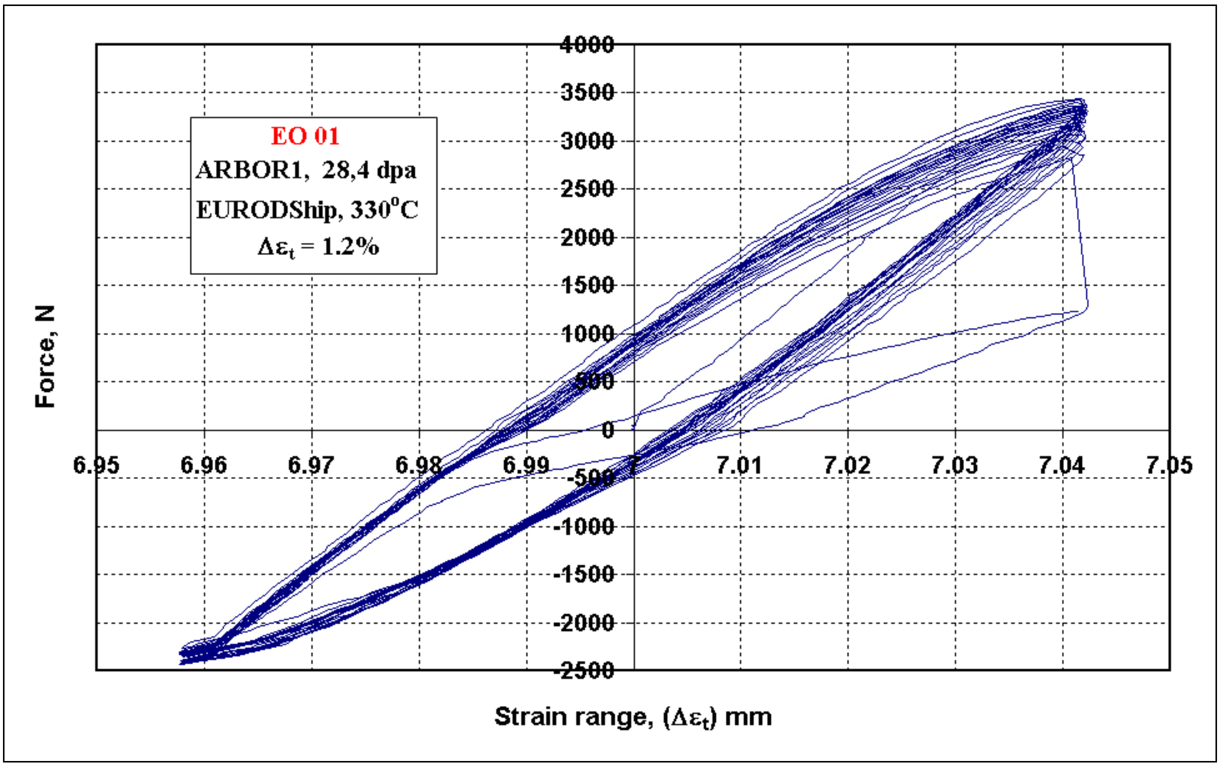

Fig. 10-30 Load vs. total strain range-diagram for the EO 01 specimen

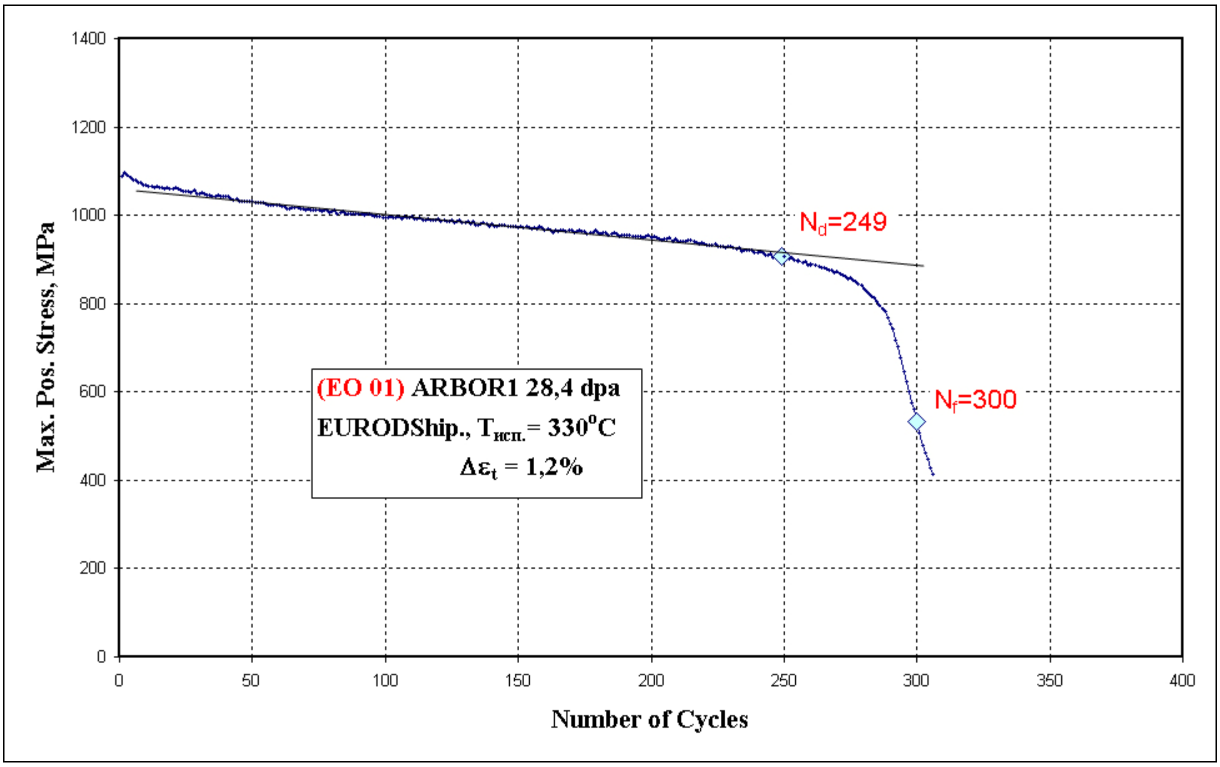

Fig. 10-31 Maximum cyclic stress vs. number of cycles-diagram for the EO 01 specimen

EO01

EO03

EO06

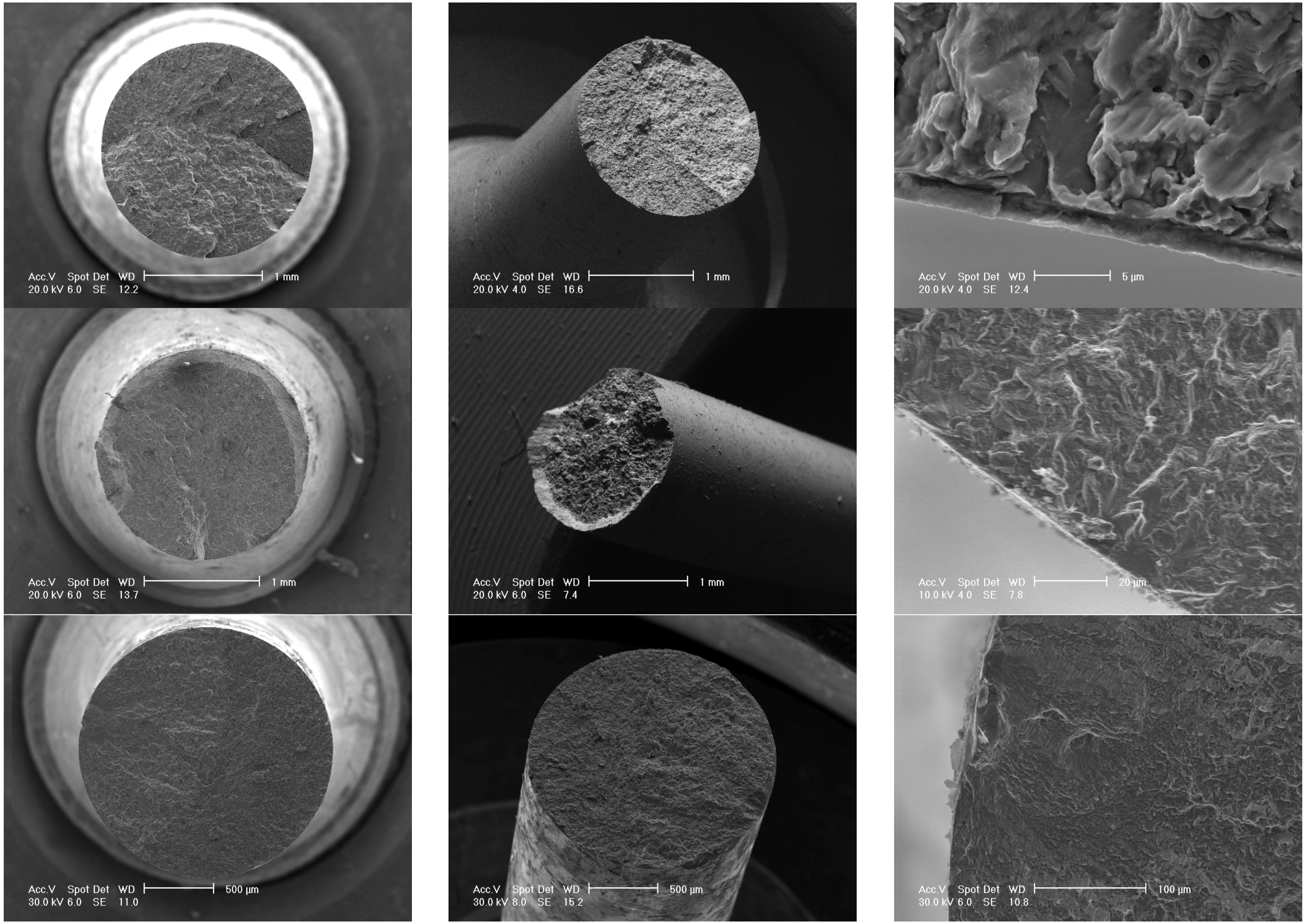

Fig. 10-32 SEM photographs of LCF tested F82H mod. specimens EO01, EO03 and EO06 after complete breaking

EO08

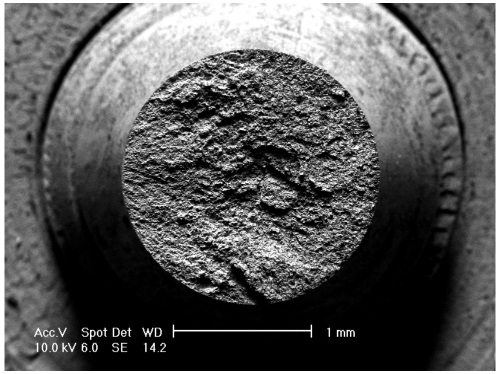

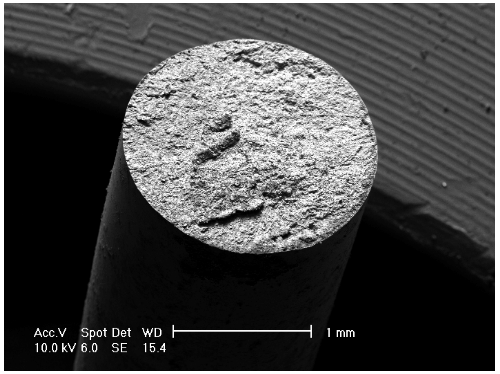

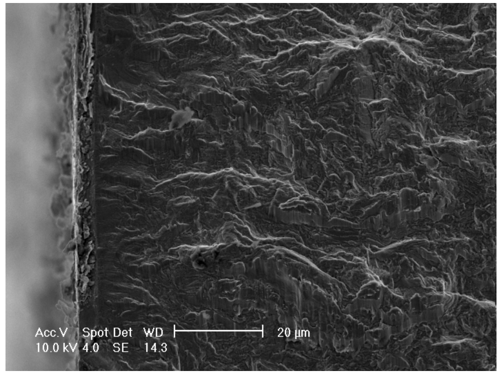

Fig. 10-33 SEM photographs of LCF tested F82H mod. specimen EO08 after complete breaking

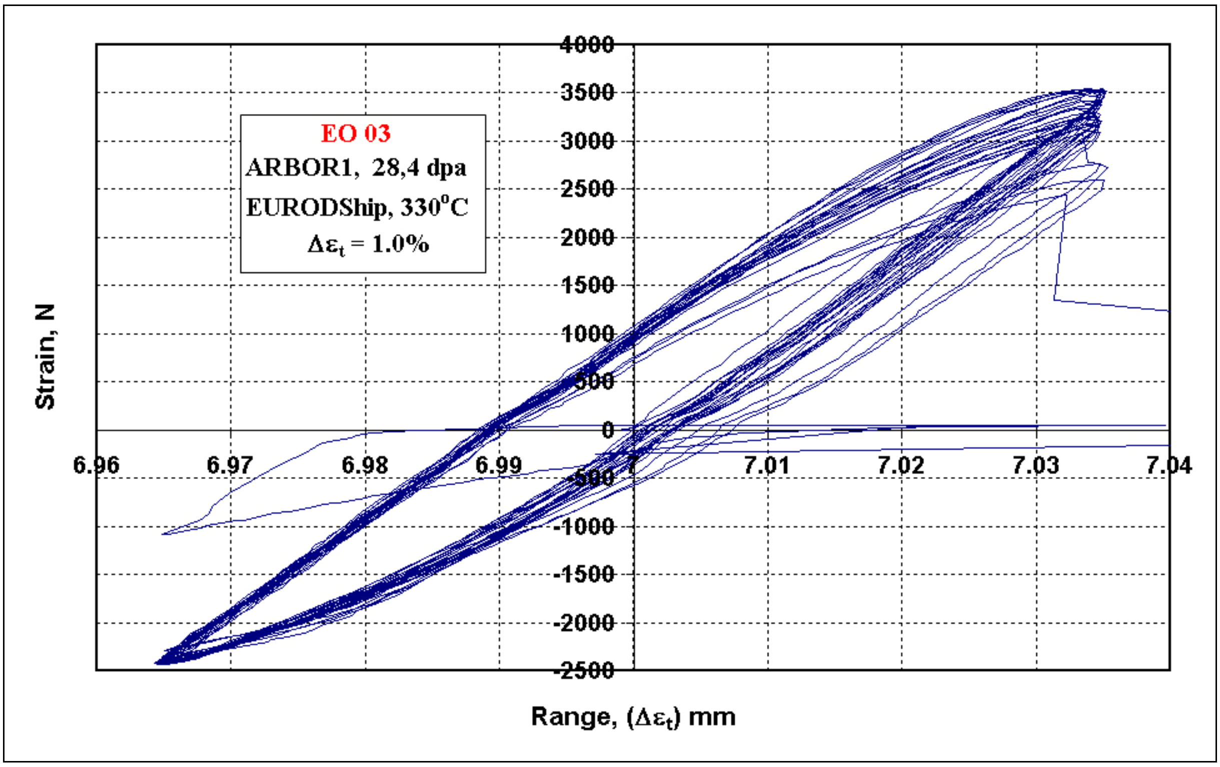

Fig. 10-34 Load vs. total strain range-diagram for the EO 03 specimen

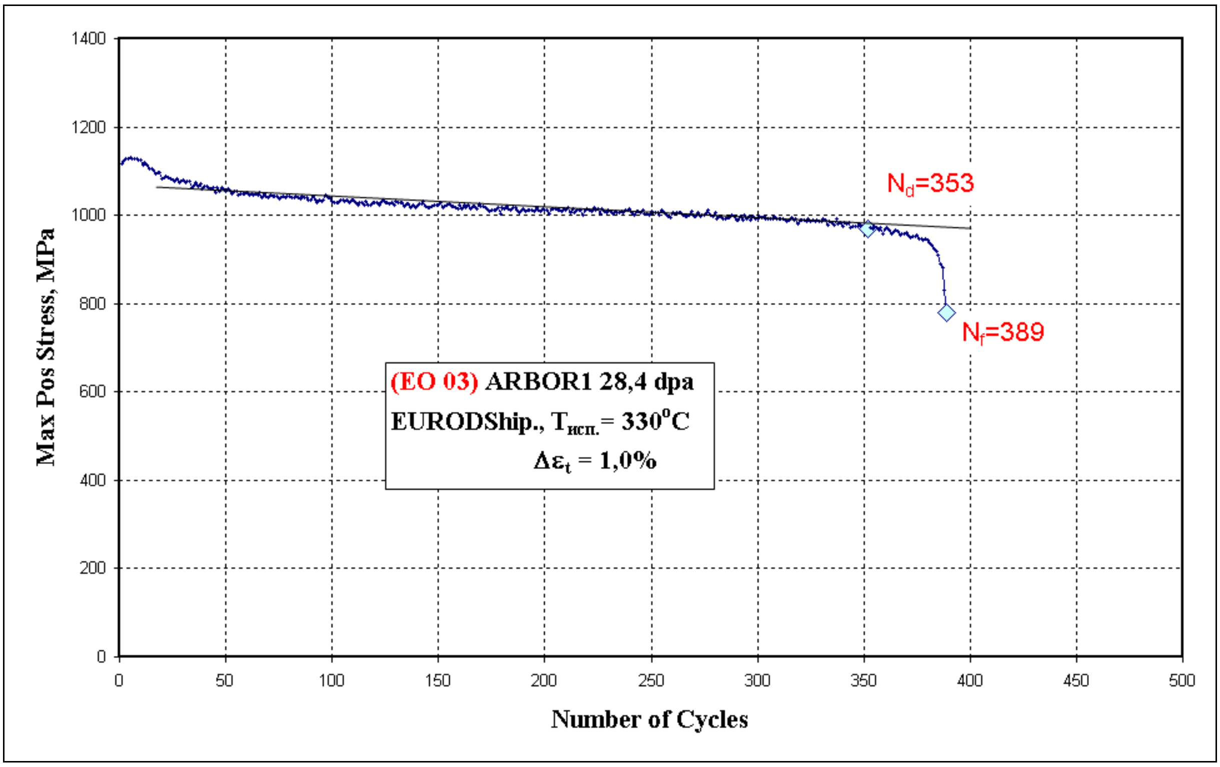

Fig. 10-35 Maximum cyclic stress vs. number of cycles-diagram for the EO 03 specimen

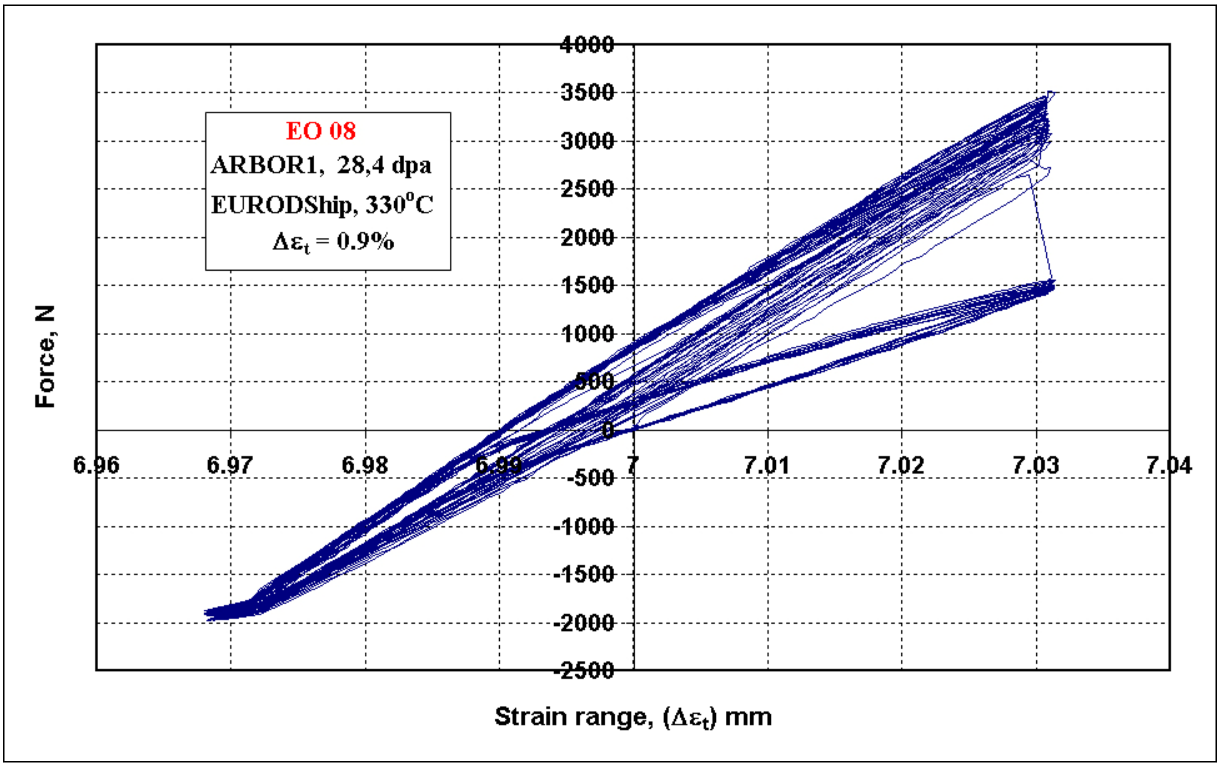

Fig. 10-36 Load vs. total strain range-diagram for the EO 08 specimen

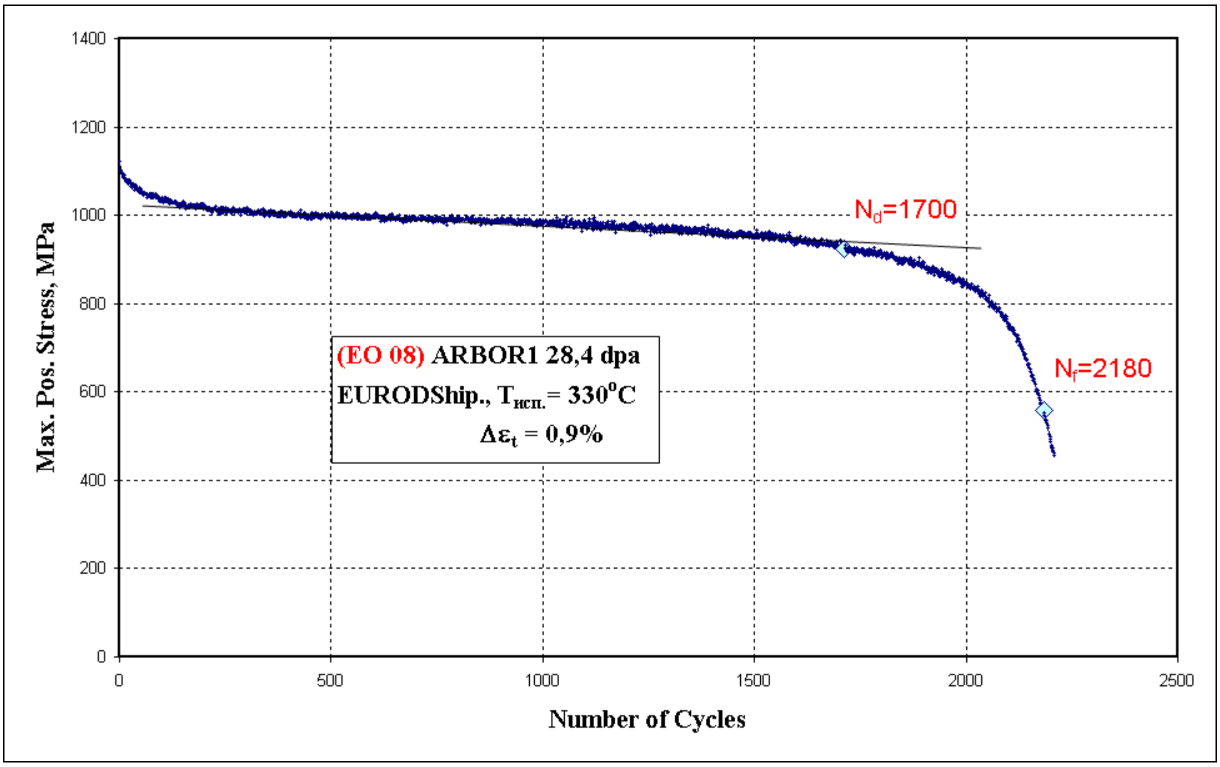

Fig. 10-37 Maximum cyclic stress vs. number of cycles-diagram for the EO 08 specimen

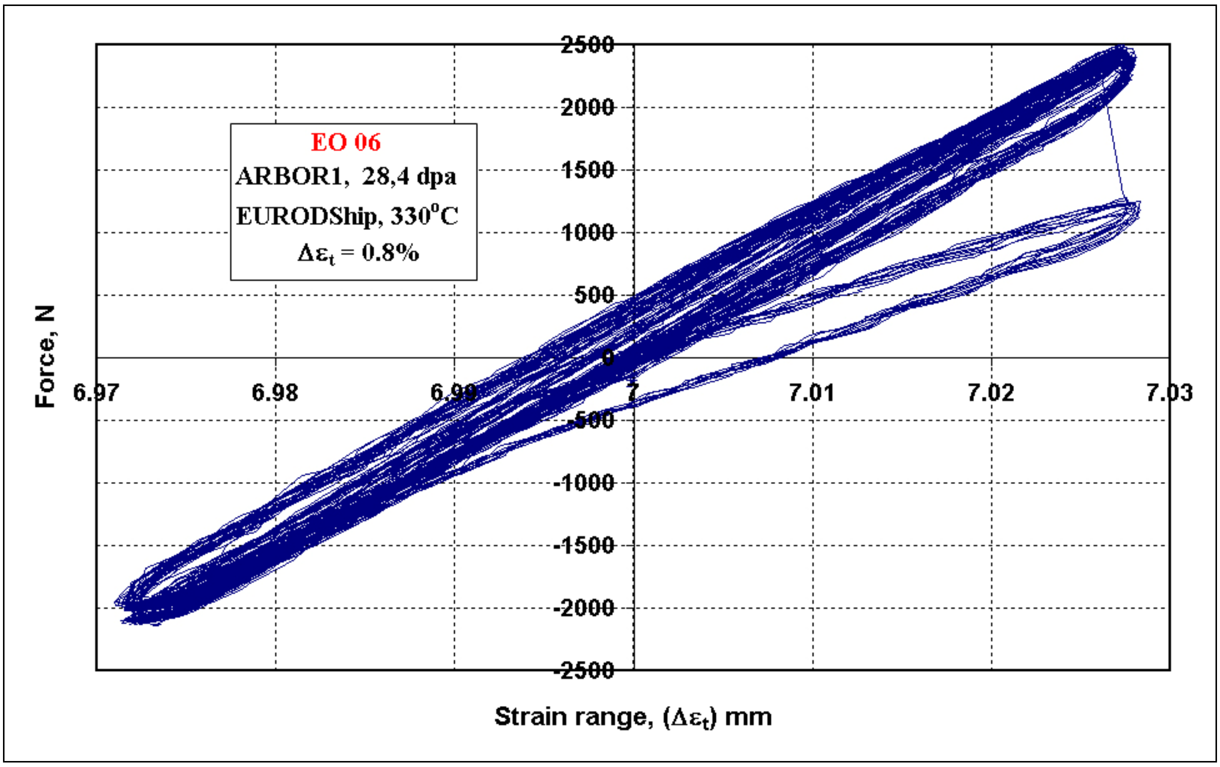

Fig. 10-38 Load vs. total strain range-diagram for the EO 06 specimen

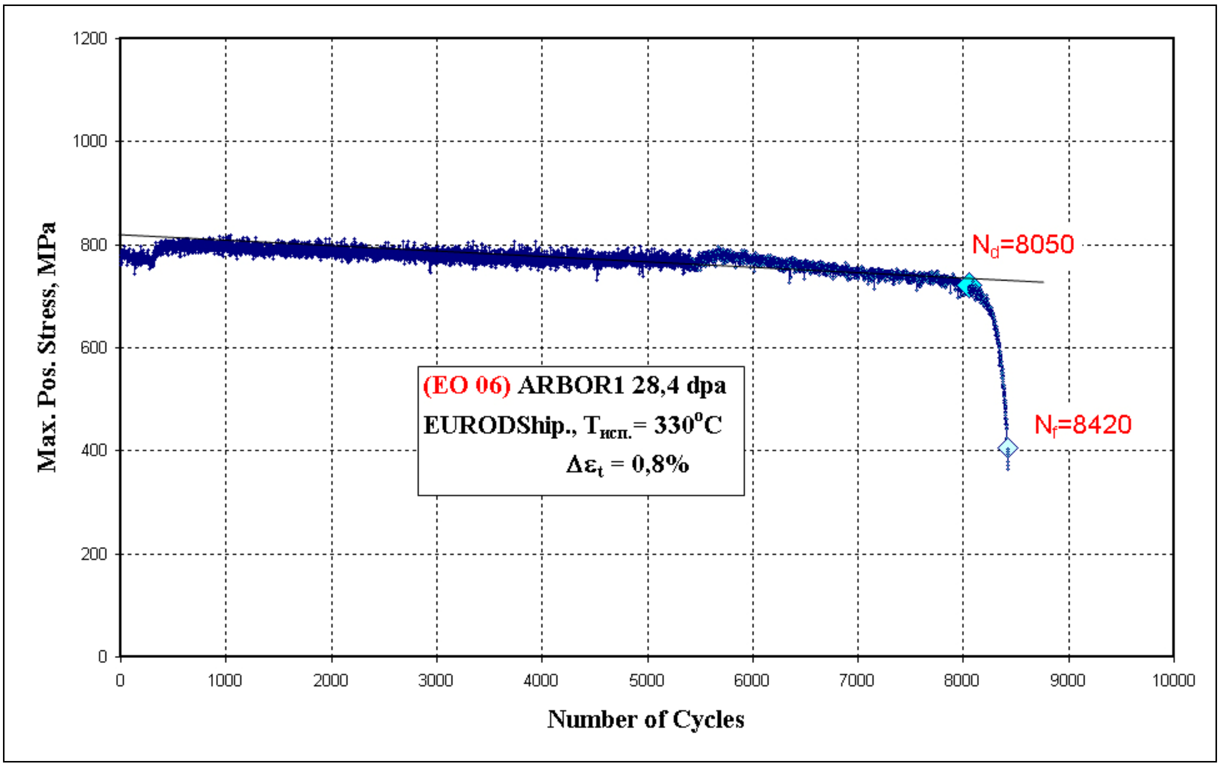

Fig. 10-39 Maximum cyclic stress vs. number of cycles-diagram for the EO 06 specimen

10.5 EUROFER 97, EB welded and PWHT

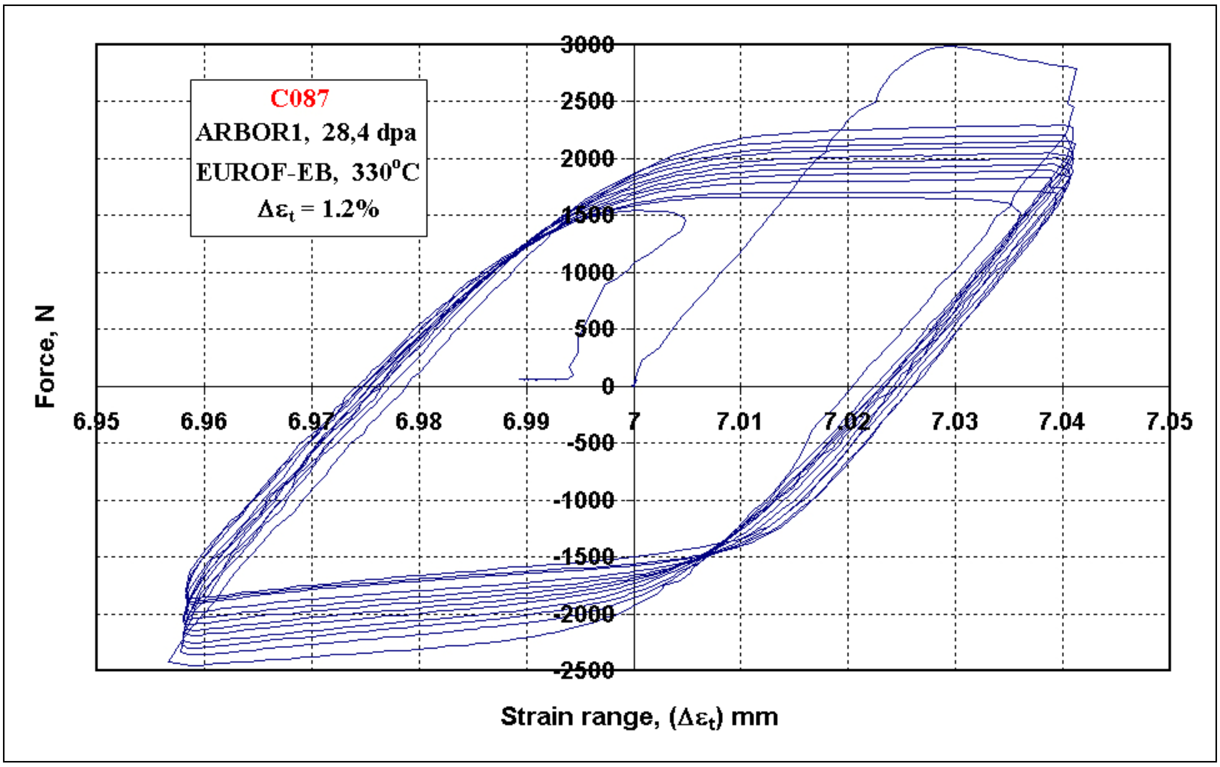

Fig. 10-40 Load vs. total strain range-diagram for the C 087 specimen

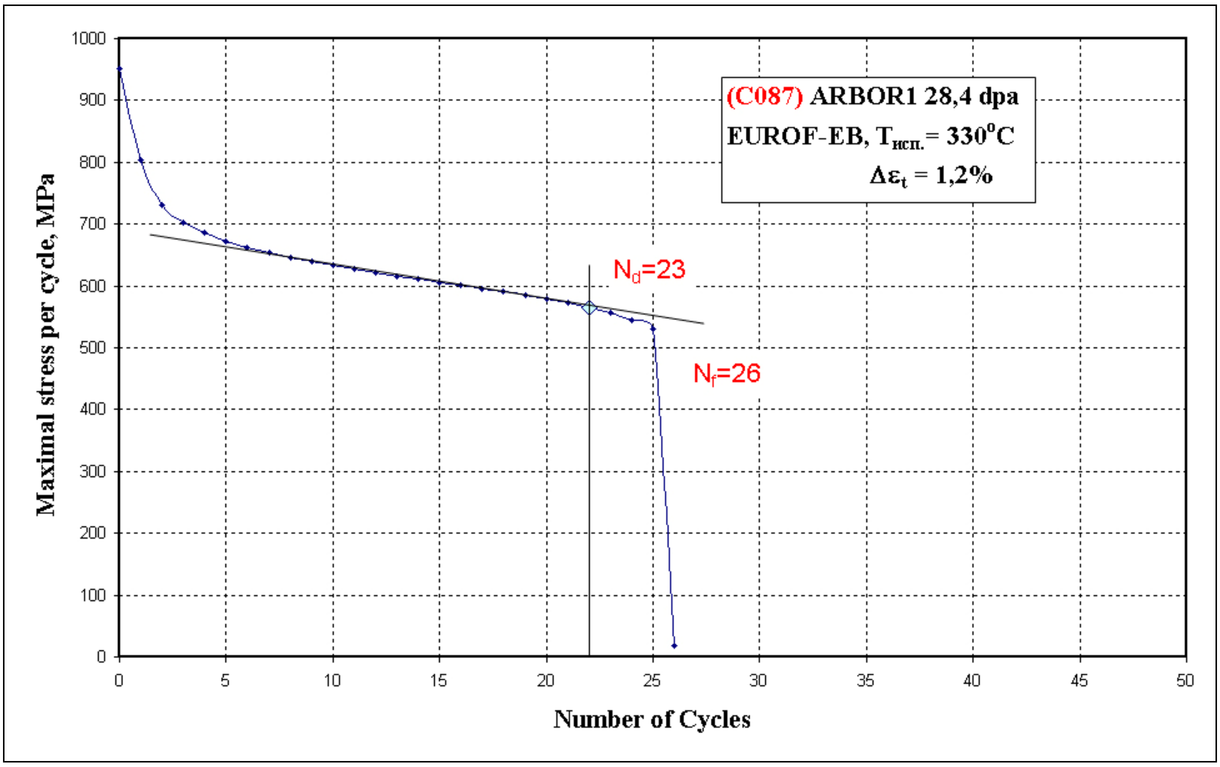

Fig. 10-41 Maximum cyclic stress vs. number of cycles-diagram for the C 087 specimen

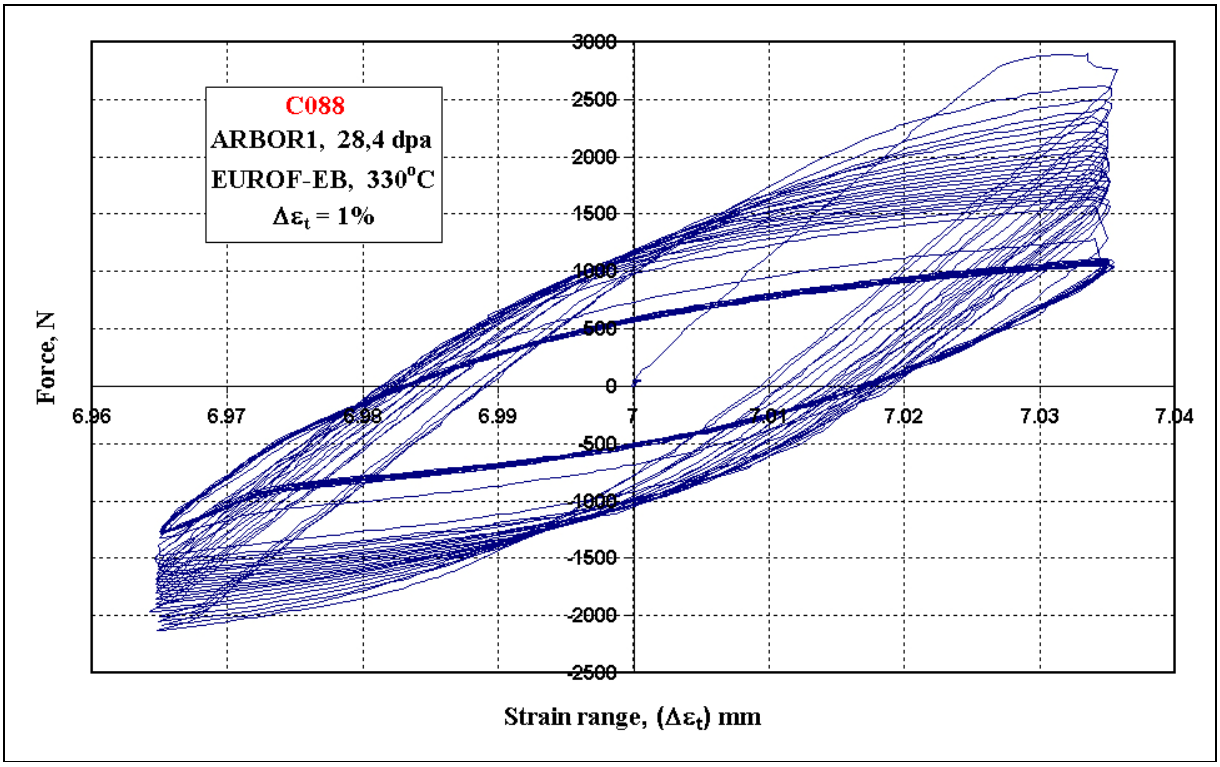

Fig. 10-42 Load vs. total strain range-diagram for the C 088 specimen

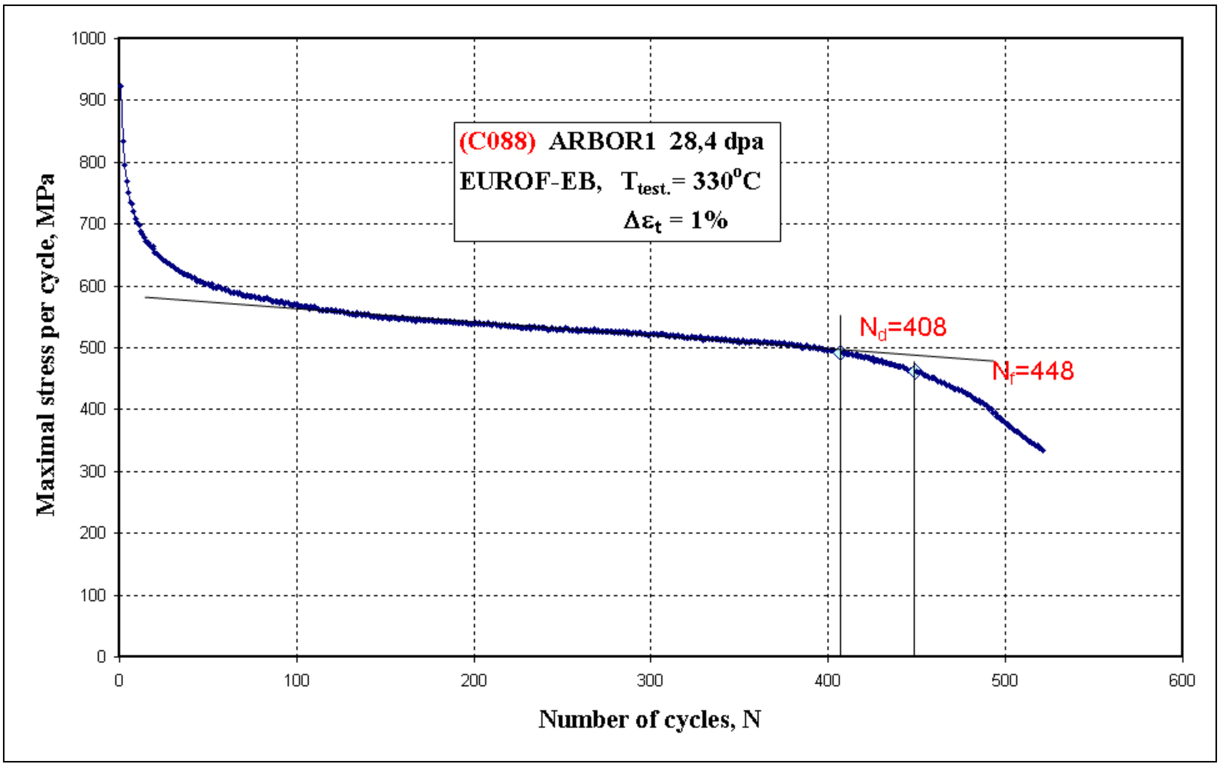

Fig. 10-43 Maximum cyclic stress vs. number of cycles-diagram for the C 088 specimen

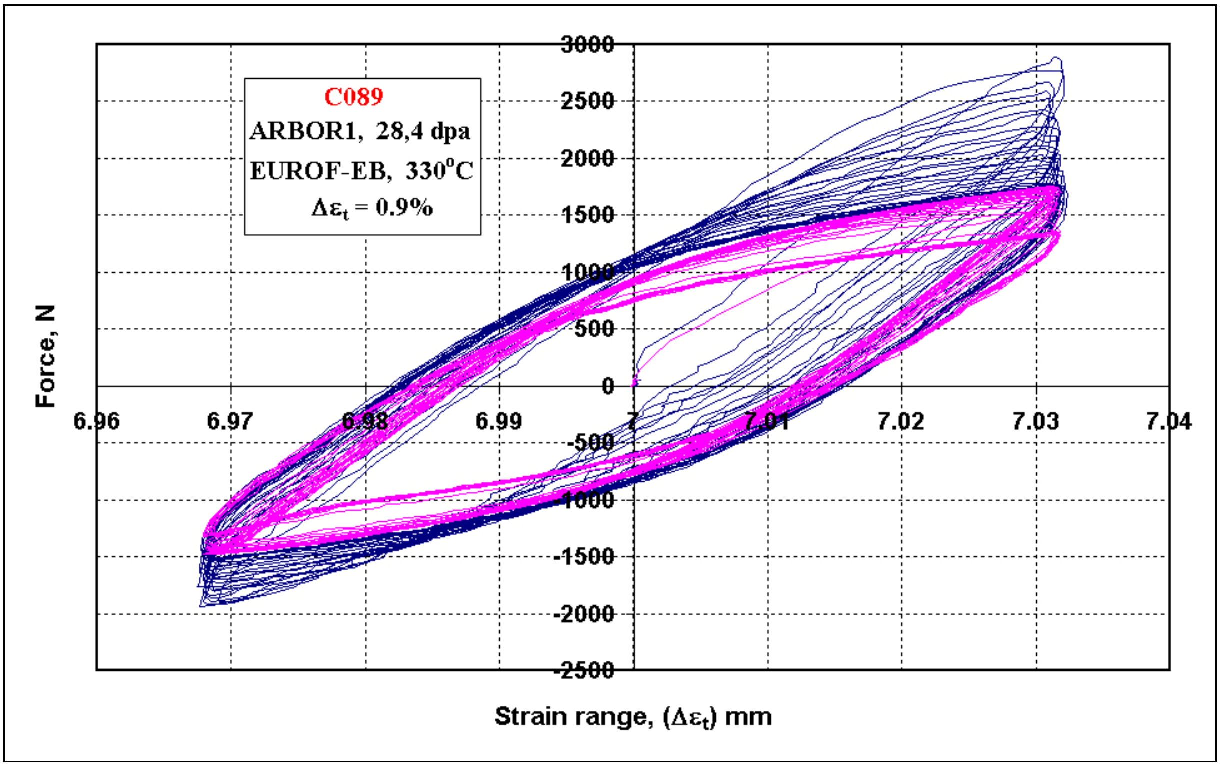

Fig. 10-44 Load vs. total strain range-diagram for the C 089 specimen

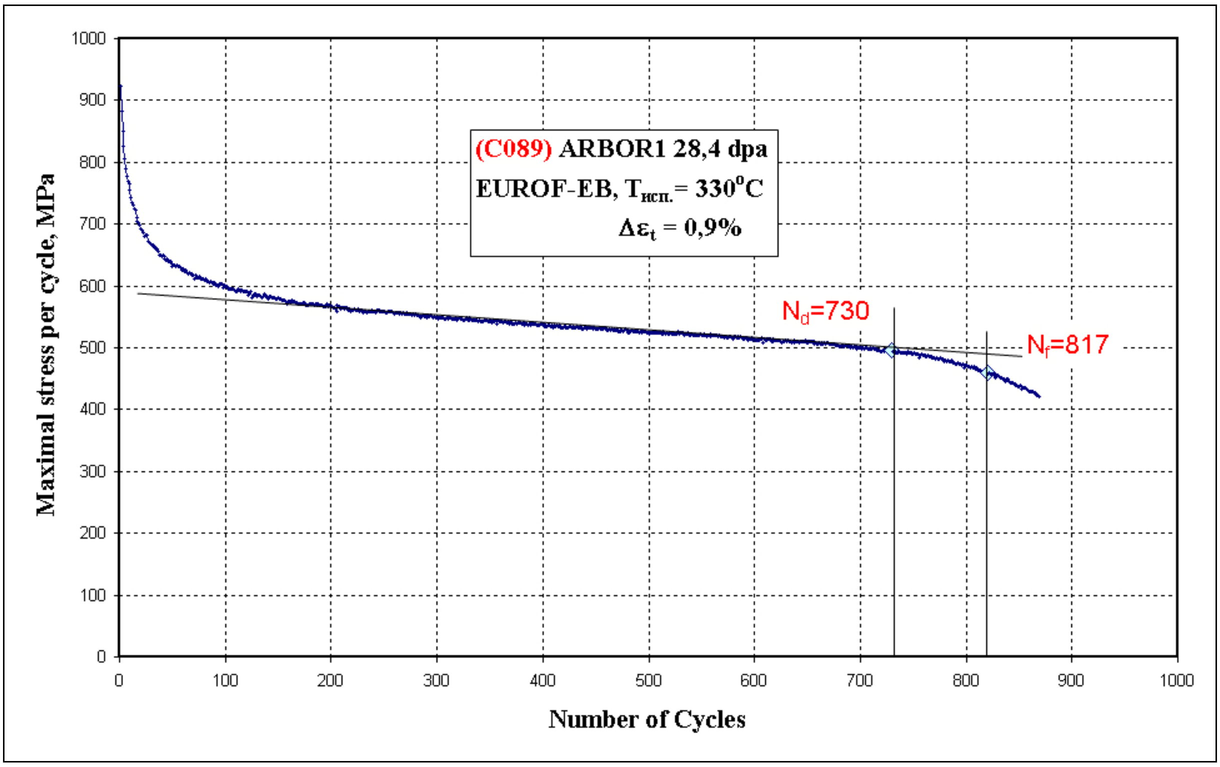

Fig. 10-45 Maximum cyclic stress vs. number of cycles-diagram for the C 089 specimen

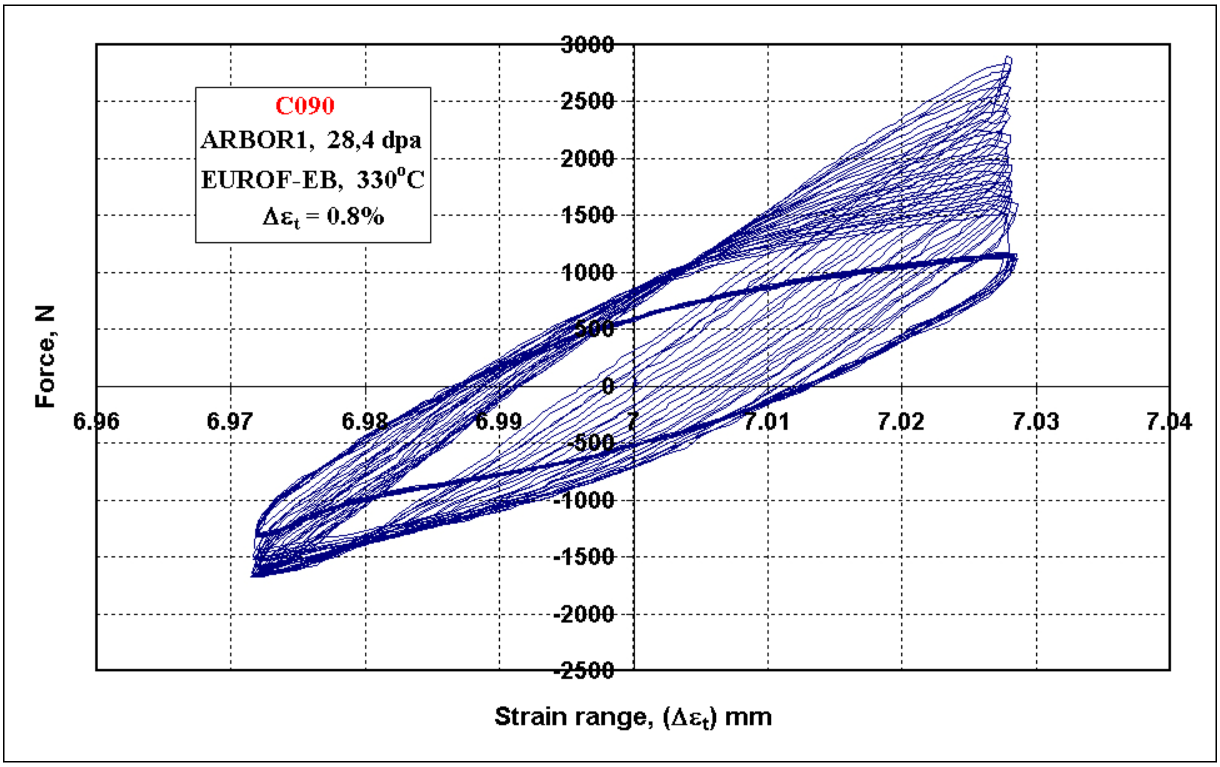

Fig. 10-46 Load vs. total strain range-diagram for the C 090 specimen

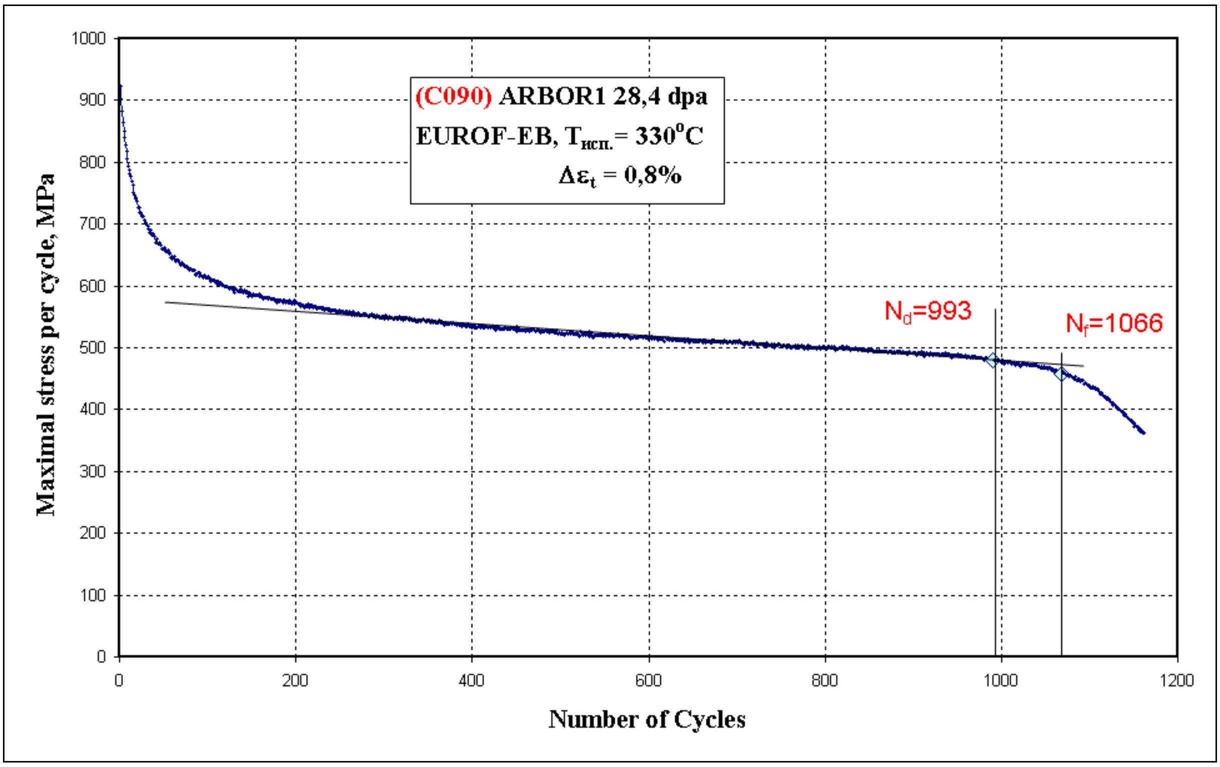

Fig. 10-47 Maximum cyclic stress vs. number of cycles-diagram for the C 090 specimen

10.6 BS-EUROFER

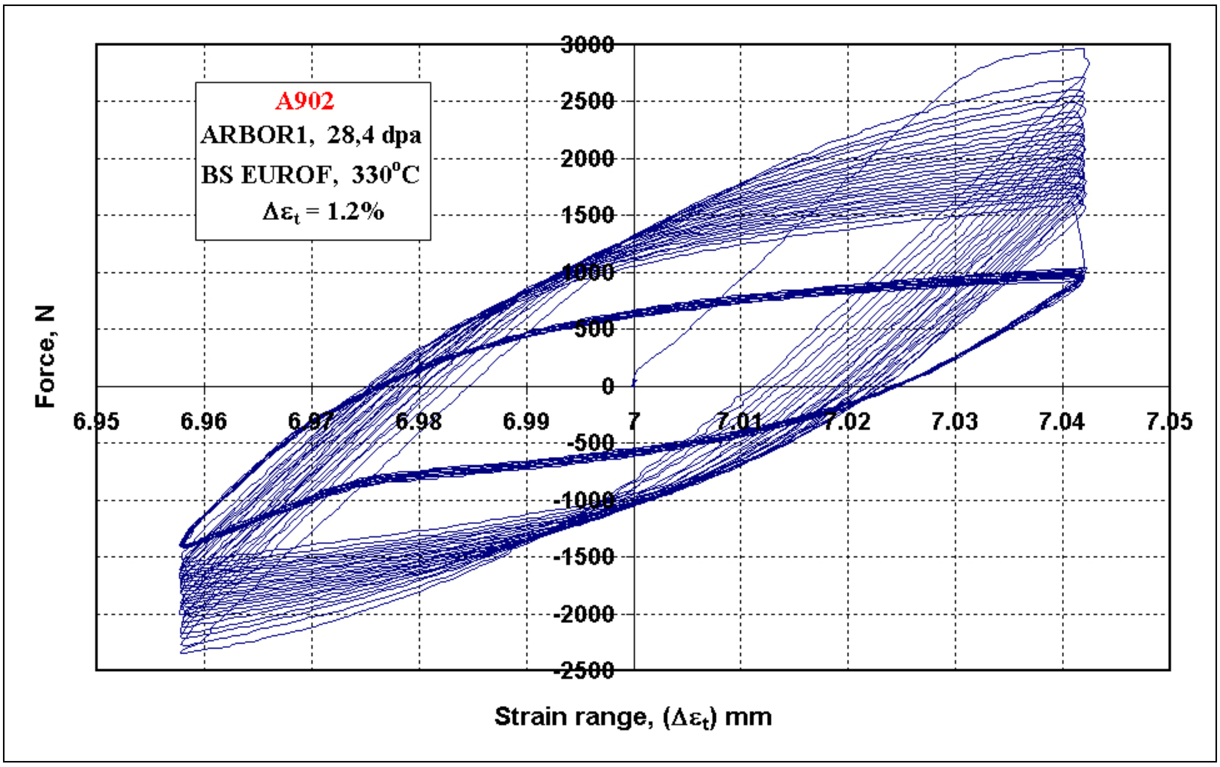

Fig. 10-48 Load vs. total strain range-diagram for the A 902 specimen

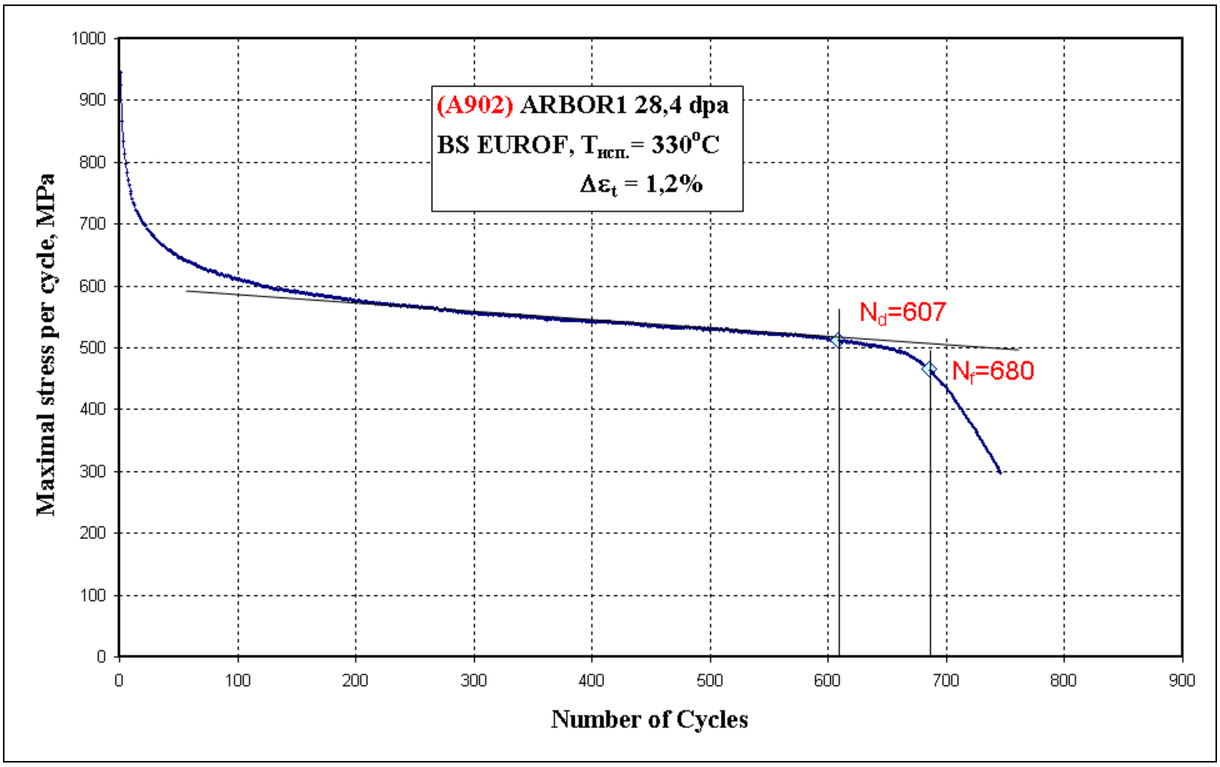

Fig. 10-49 Maximum cyclic stress vs. number of cycles-diagram for the A 902 specimen

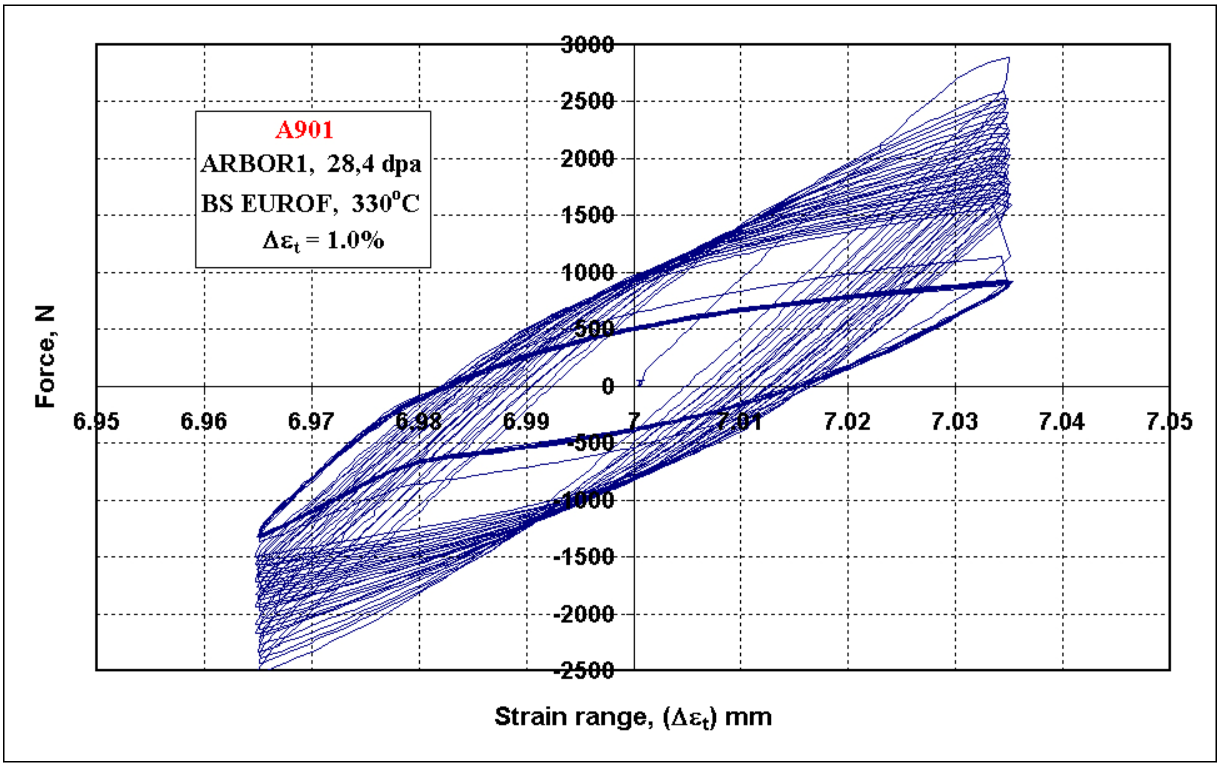

Fig. 10-50 Load vs. total strain range-diagram for the A 901 specimen

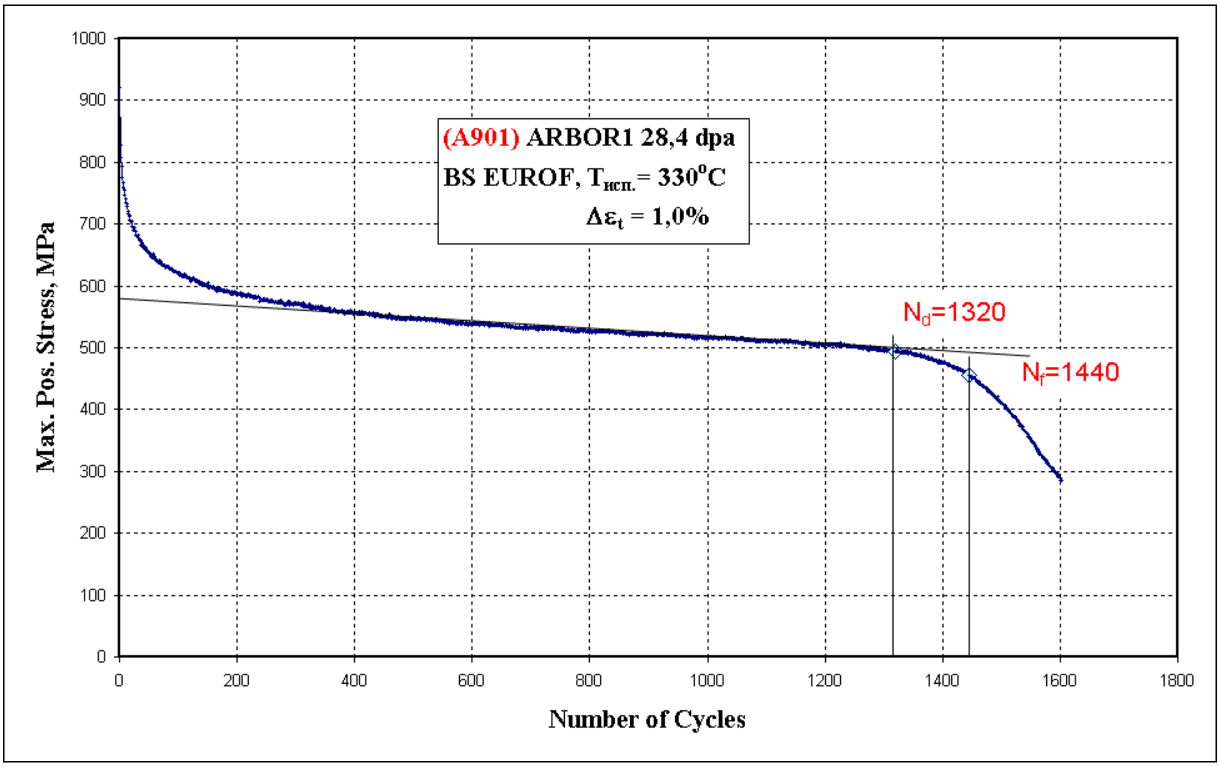

Fig. 10-51 Maximum cyclic stress vs. number of cycles-diagram for the A 901 specimen

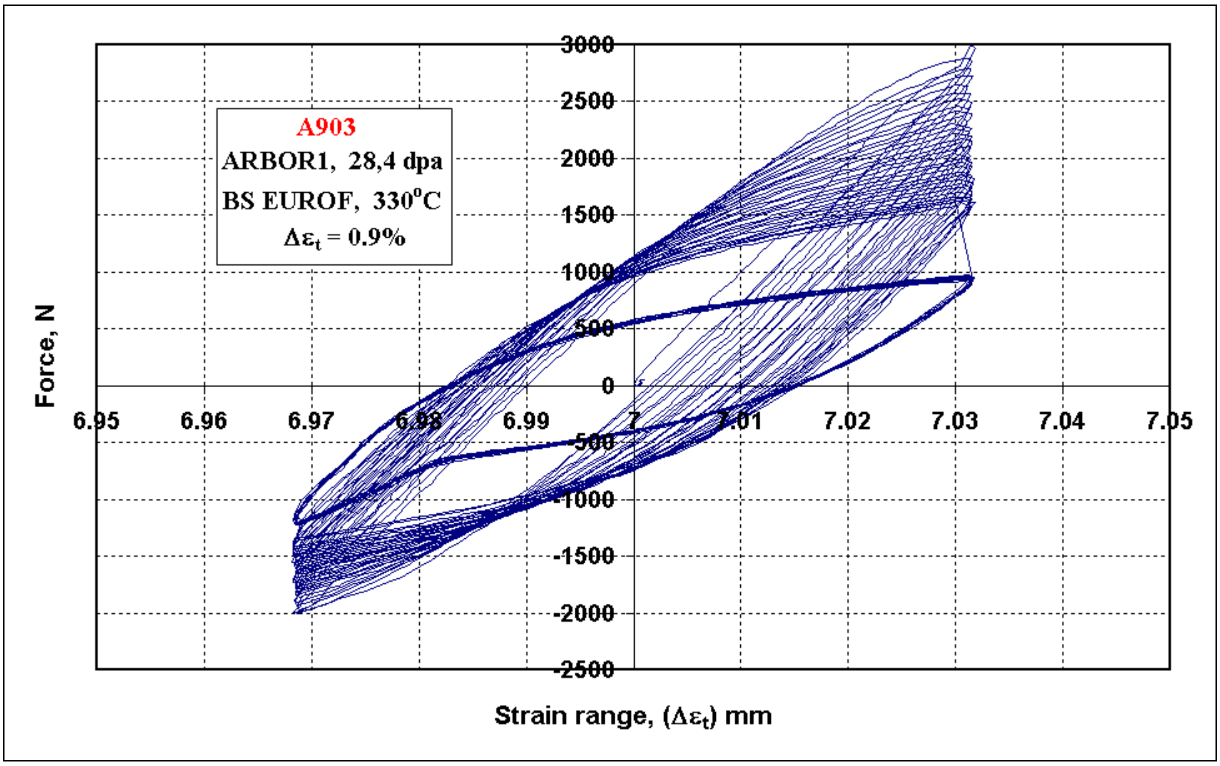

Fig. 10-52 Load vs. total strain range-diagram for the A 903 specimen

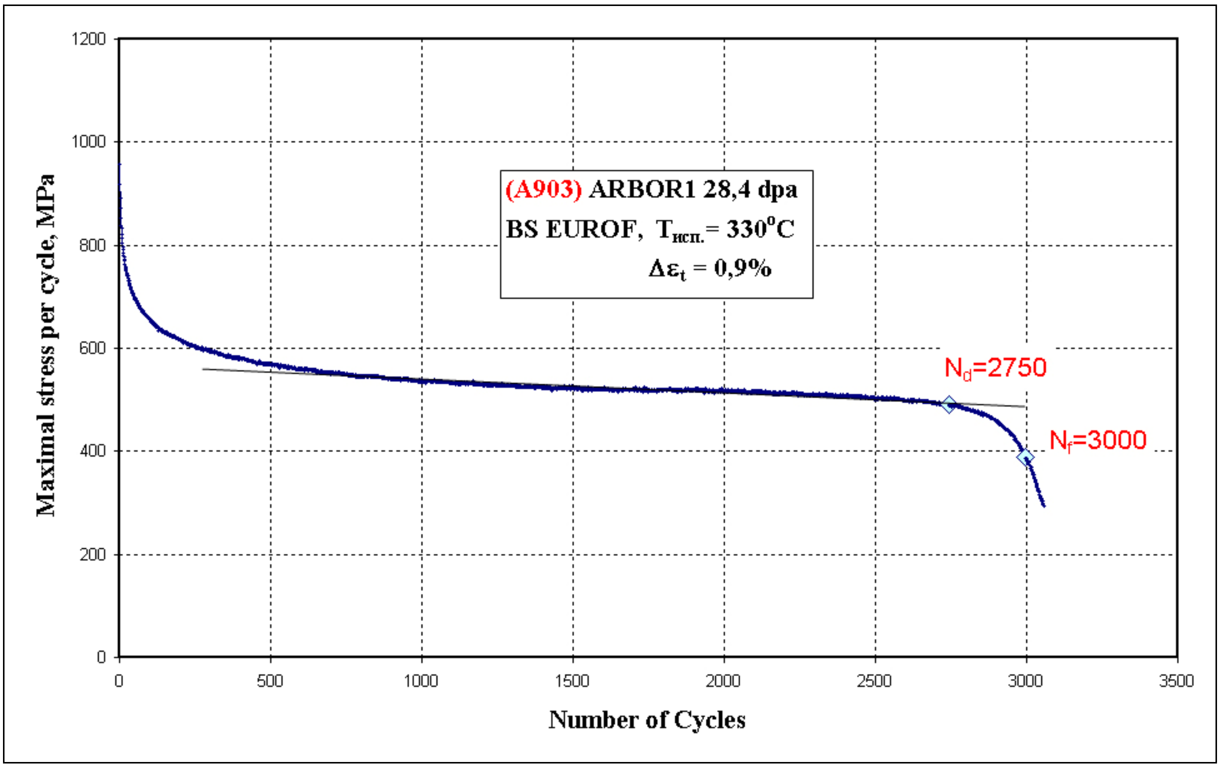

Fig. 10-53 Maximum cyclic stress vs. number of cycles-diagram for the A 903 specimen

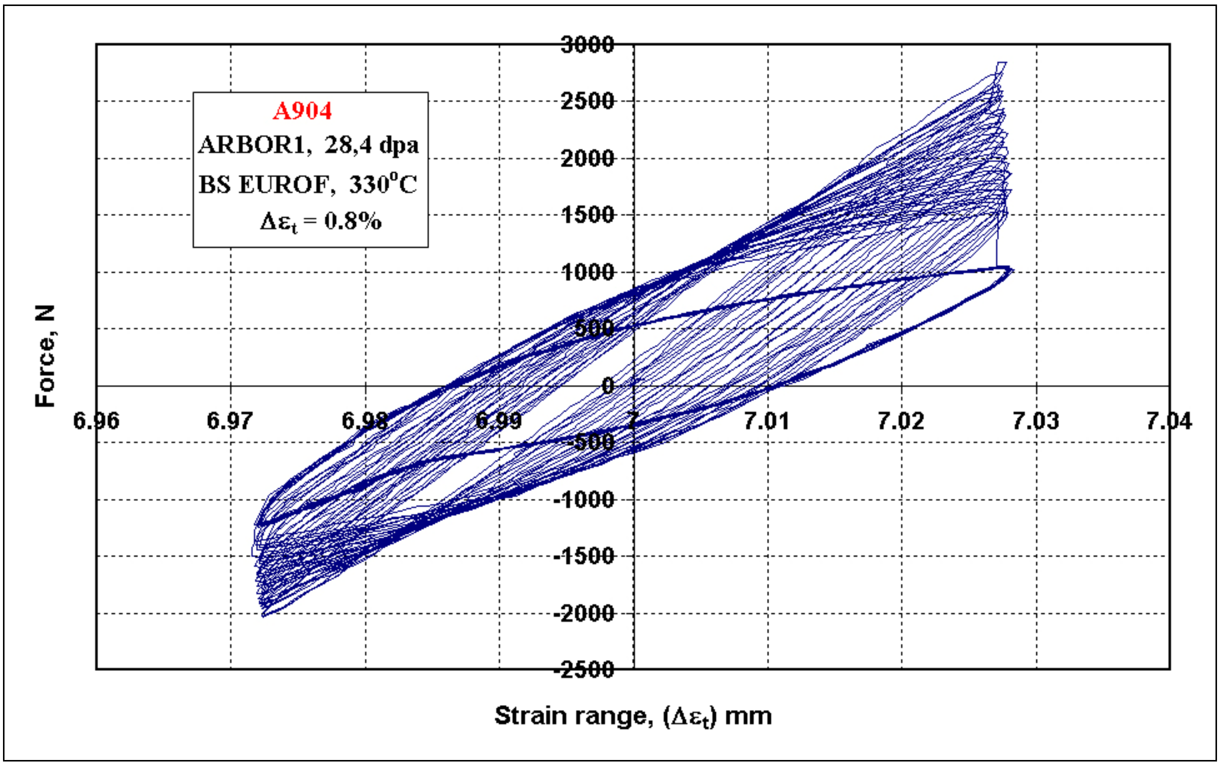

Fig. 10-54 Load vs. total strain range-diagram for the A 904 specimen

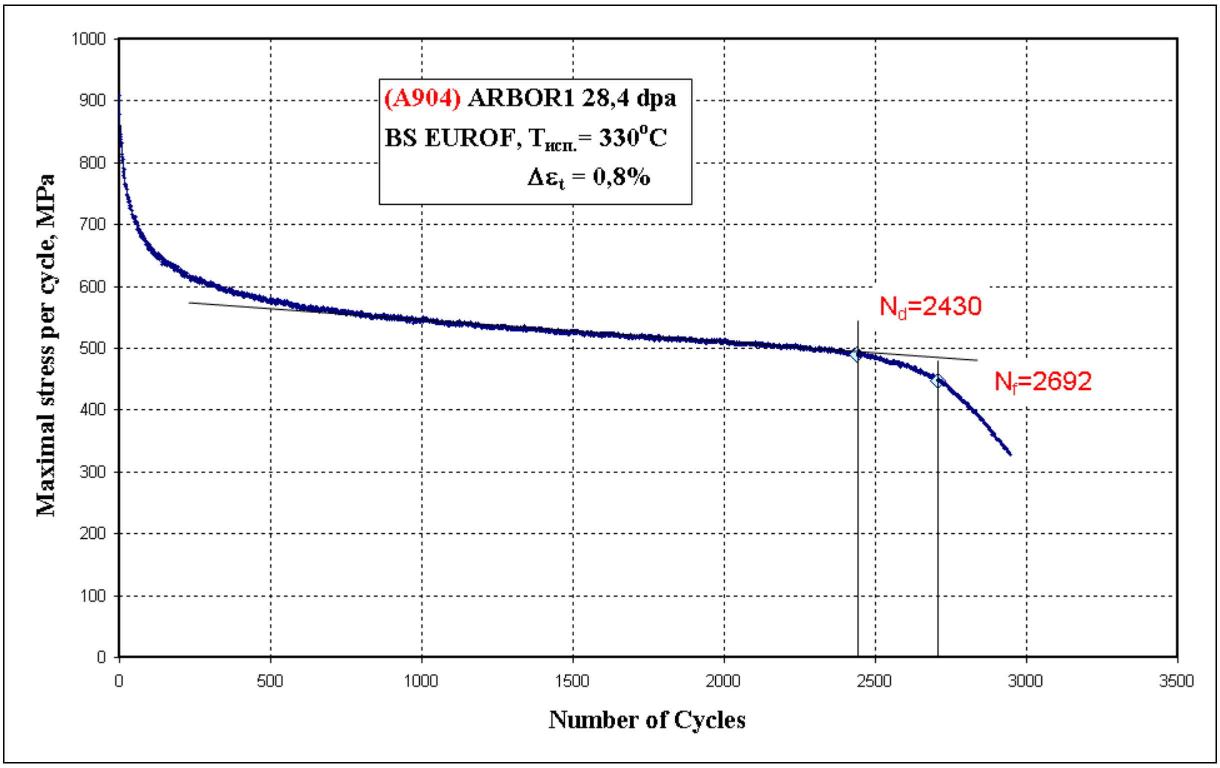

Fig. 10-55 Maximum cyclic stress vs. number of cycles-diagram for the A 904 specimen

11 Task Sheet

REPORT for TASK of the EFDA Technology Programme			
Reference:	Field: Tritium Breeding and Materials Area: Materials Development Task: TW2-TTMS-001b RAFM Steels: Metallurgical and Mechanical Characterisation Deliverable No. 9		
Document:	Post irradiation examination of RAF/M steels after fast reactor irradiation up to 33 dpa and < 340°C (ARBOR 1)		
Level of confidentiality	Free distribution ☐ Confidential ☐ Restricted distribution **X**		
Author(s):	Claus Petersen, Karlsruhe Institute of Technology, (former Forschungszentrum Karlsruhe)		
Date:	17. March 2010		
Distribution list:	Rainer Laesser (Field Co-Ordinator/) Eberhard Diegele (Responsible Officer) Enrico Lucon(Project Leader)		
Abstract:	Starting in 2003 one half of the in ARBOR 1 irradiated samples were post irradiation examined (PIE) by impact, tensile and low cycle fatigue testing under the ISTC Partner Contract #2781p in the hot cells of SSC RIAR. In the post irradiation instrumented impact tests a significant increase in the Ductile to Brittle Transition Temperature as an effect of irradiation has been detected. During tensile testing the strength values are increasing and the strain values reduced due to substantial irradiation hardening. The hardening rate is decreasing with increasing damage level, but it does not show saturation. The low cycle fatigue behaviour of all examined RAF/M - steels show at total strain amplitudes below 1 % an increase of number of cycles to failure, due to irradiation hardening. From data of these post irradiation experiments, like impact, tensile and low cycle fatigue tests, radiation induced design data, e.g. for verification of design codes, can be generated.		
Revision No: 0	Changes:		
	Written by:	Revised by:	Approved by:
	C. Petersen	Dr. J. Aktaa	Prof. Dr. O. Kraft